Regulation of Copper Homeostasis by the Ubiquitin Proteasome System

Bichao Zhang

Doctor of Philosophy

A thesis submitted for the degree of Doctor of Philosophy at
Monash University in 2021
School of Biological Sciences

Copyright notice

New page

Abstract

Copper is an essential trace element required for numerous biological processes, usually as a cofactor of cellular enzymes. As a redox-active metal, copper participates in diverse metabolic processes in living organisms, but can also generate toxic reactive oxygen species. Given the requirement for copper and the potential toxicity of copper, cellular copper concentration must be tightly controlled. The maintenance of copper homeostasis involves many molecules, including transporters which mediate uptake (CTR1) and efflux (ATP7A and ATP7B) of copper. Copper homeostasis is essential to the integrity of normal brain functions, and copper deficiency or excess is thought to contribute to diseases such as Alzheimer's disease (AD) and Parkinson's disease (PD). Recently, accumulating evidence revealed that dysregulation of ubiquitin proteasome system (UPS) is involved in the development of some neurodegenerative diseases. Intriguingly, malfunction of the UPS and copper dyshomeostasis both result in the accumulation of amyloid beta and alpha-Synuclein, the hallmarks of AD and PD respectively, suggesting that the UPS and copper homeostasis machinery function synergistically during neurodevelopment. This study aimed to exploit the molecular genetic advantages of the fruit fly *Drosophila melanogaster* to determine how the UPS and copper homeostasis interact by investigating candidate UPS component genes for their roles in regulating cellular copper levels. Based on previously described cuticular RNA interference phenotypes reminiscent of copper deficiency, the E3 ubiquitin ligase Slmb (BTRC in mammals) was first investigated and found to regulate the copper import protein Ctr1A (*Drosophila* orthologue of CTR1) through the transcription factor cnc (Nrf2 in mammals). In addition, we observed that downregulation of *Slmb* could protect larvae from copper toxicity by inhibiting copper uptake, further demonstrating that Slmb regulates intracellular copper levels through Ctr1A. Genetic screening of the fly orthologues of multiple UPS proteins shown to physically interact with mammalian ATP7A then revealed a second E3 ubiquitin complex, Vhl/EloC/Cul2, which might also influence copper homeostasis. Our results demonstrated that Vhl could regulate Ctr1A distinctly in different tissues via different transcription factors, Sima (Hif1alpha in mammals) and cnc. Furthermore, we have examined the *in vivo* requirement for an E2 ubiquitin conjugating enzyme, UBE2D2 (mammals) / UbcD1 (flies) which is a cuprotein whose conjugase activity is enhanced by copper binding *in vitro*. We showed that UbcD1 is essential for the survival of multiple epithelial and neuronal cell types in the fly and that a key copper binding residue, C111, is required for optimal UBE2D2 / UbcD1 activity. Our data suggest that UbcD1 might regulate intracellular copper levels via the copper transporters Ctr1A and ATP7 to protect cells from copper toxicity. Finally, we propose that UbcD1, Slmb and Vhl form part of complex network that controls the production of melanin, in part through the regulation of cellular copper levels and that disruption of this network can lead to extensive apoptosis *in vivo*. In conclusion, this study demonstrated that the UPS and copper homeostasis are

indeed interdependent, supporting the idea that modulation of neuronal copper levels has considerable potential in the treatment of related neurodegenerative diseases.

Publications during enrolment

- **Zhang, B.,** Binks, T., Burke, R., 2020. The E3 ubiquitin ligase Slimb/β-TrCP is required for normal copper homeostasis in Drosophila. Biochim Biophys Acta Mol Cell Res 1867, 118768.
- **Zhang, B.,** Kirn, L., Burke, R., 2021. The Vhl E3 ubiquitin ligase complex regulates melanisation via sima, cnc and the copper import protein Ctr1A. Biochim Biophys Acta Mol Cell Res 1868, 119022.

Thesis including published works declaration

I hereby declare that this thesis contains no material which has been accepted for the award of any other degree or diploma at any university or equivalent institution and that, to the best of my knowledge and belief, this thesis contains no material previously published or written by another person, except where due reference is made in the text of the thesis.

This thesis includes 2 original papers published in peer reviewed journals. The core theme of the thesis is copper homeostasis and ubiquitin proteasome system. The ideas, development and writing up of all the papers in the thesis were the principal responsibility of myself, the student, working within the School of Biological Science under the supervision of Richard Burke.

(The inclusion of co-authors reflects the fact that the work came from active collaboration between researchers and acknowledges input into team-based research.)

This thesis also includes 3 chapters which have not been submitted for publication. In the case of 5 chapters my contribution to the work involved the following:

Thesis Chapter	Publication Title	Status (published, in press, accepted or returned for revision, submitted)	Nature and % of student contribution	Co-author name(s) Nature and % of Co-author's contribution*	Co-author(s), Monash student Y/N*
Chapter 1	*Copper Homeostasis and Ubiquitin Proteasome System*	*Not submitted*	*100%. Conceptualization, Methodology, Investigation, Writing*		
Chapter 3	*The E3 ubiquitin ligase Slimb/β-TrCP is required for normal copper homeostasis in Drosophila*	*Published*	*65%. Conceptualization, Methodology, Investigation, Writing - Original Draft, Visualization*	*1) Tim Binks, input into manuscript 10%* *2) Richard Burke, Conceptualization, Investigation, Writing - original draft, Supervision, Project administration, Funding acquisition, input into manuscript 25%*	*Yes* *No*
Chapter 4	*Identification of novel ATP7 regulating proteins from candidates provided by*	*Not submitted*	*100%. Conceptualization, Methodology, Investigation, Writing*		

	the ATP7A interactome				
Chapter 5	*The Vhl E3 ubiquitin ligase complex regulates melanisation via sima, cnc and the copper import protein Ctr1A*	*Published*	*70%. Conceptualization, Methodology, Investigation, Writing - Original Draft, Visualization*	*1) Lauren Kirn, input into manuscript 5%* *2) Richard Burke, Conceptualization, Investigation, Writing - original draft, Supervision, Project administration, Funding acquisition, input into manuscript 25%*	*Yes* *No*
Chapter 6	*A copper binding site on UBE2D2 is essential for Drosophila development*	*Not submitted*	*100%. Conceptualization, Methodology, Investigation, Writing*		

*If no co-authors, leave fields blank

I have renumbered sections of submitted or published papers in order to generate a consistent presentation within the thesis.

Student name: Bichao Zhang

Student signature: **Date: 30 / 3 / 2021**

I hereby certify that the above declaration correctly reflects the nature and extent of the student's and co-authors' contributions to this work. In instances where I am not the responsible author I have consulted with the responsible author to agree on the respective contributions of the authors.

Main Supervisor name: Richard Burke

Main Supervisor signature: **Date: 30 / 3 / 2021**

Acknowledgements

Firstly, I would like to express my deepest gratitude to my main supervisor Dr. Richard Burke for his excellent supervision, mentorship and support during my PhD candidature. When I started my PhD, I was totally unfamiliar to fly work. Dr Burke was so patient and enthusiastic to teach me all the techniques that would be used in my research work. Every time when I encountered problems, he was always there to help me. I really appreciate what he has done to me, and I could not have asked for a better mentor than him. To my co-supervisor Associate Professor Robert Bryson-Richardson, he also offered me a lot of help during the course of my PhD program. Here, I sincerely thank him for his help and supervision.

I would also like to thank past and present members of Burke lab. Without their help, this thesis would not have been completed. Special thanks go to my friends Kimberly Aw and Amy Luan for their help in teaching me some experimental techniques with patience and kindness. Thank you to our research assistants Pontus Leblanc and Sebastian Judd-Mole for their hard work to keep our lab running normally. Special thanks go to my research fellows Lachlan Cauchi and Brendan Houston for their scientific insight and willingness to solve my problems.

I would also like to thank all the members of Johnson lab, in particular Travis Johnson, Daniel Bakopoulos, Monica Caggiano, Grace Jefferies and Sarah Mele for their wisdom and assistance to my research work. Thank you to my fellow PhD candidates, Avishikta Chakraborty and An Ngyuen for their motivational support in stressful times. A special thank must also got to Monash University and School of Biological Science for offering me a Faculty of Science Dean's International Postgraduate Research Scholarship and a Co-funded Monash Graduate Scholarship to pursue my PhD candidature.

I would also like to thank my amazing housemates and friends, Vera, Gavin, Nick, Kevin and Henry who have provided physical and spiritual supports to me in both good and bad times.

Last but not least, I would like to express my thanks to my girlfriend and parents. Without their support, I don't think I could live through the painful but terrific PhD time. Their unquestionable support drives me to pursue my dream and be the one I want to be. Thank you so much!

Table of contents

Abbreviations

Aβ: Amyloid-β

AD: Alzheimer's disease

α-Syn: α-Synuclein

ALS: Amyotrophic Lateral Sclerosis

APP: Amyloid precursor protein

Atx1: Antioxidant protein 1

BACE1: β-secretase

BBB: Blood-brain barrier

CCO: Cytochrome c oxidase

CCS: Copper chaperone for superoxide dismutase

Cu: Copper

Fe: Iron

GSH: Glutathione

HSP: Heat shock protein

LB: Lewy body

LN: Lewy neurite

LOX: Lysyl oxidase

MD: Menkes disease

MT: Metallothionein

NCT: Nicastrin

NFT: Neurofibrillary tangles

OHS: Occipital horn syndrome

PD: Parkinson's disease

PS: Presenilin

SCF: SKP1-CUL1-F-box-protein

SOD: Superoxide dismutase

ROS: Reactive oxygen species

TGN: *trans*-Golgi network

UPS: Ubiquitin proteasome system

WD: Wilson's disease

CHAPTER 1: COPPER HOMEOSTASIS AND THE UBIQUITIN PROTEASOME SYSTEM

Copper Homeostasis and the Ubiquitin Proteasome System

1.1 Introduction

Copper is an essential trace element that is required as a catalytic cofactor and/or structural component of several important cellular enzymes involved in numerous biological processes including energy metabolism (e.g., cytochrome c oxidase), antioxidative defence (e.g., Zn, Cu-superoxide dismutase), and iron metabolism (e.g., ceruloplasmin) (Hellman and Gitlin, 2002; Perry et al., 2010; Popovic et al., 2010). The relatively high redox potential of the Cu^{2+}/Cu^+ system is utilized for oxidation reactions, such as the generation of superoxide by superoxide dismutase (SOD) and catechols by tyrosinase (Scheiber et al., 2013). Since an excess of copper can also harm cells due to its potential to catalyze the generation of toxic reactive oxygen species (ROS) (Halliwell, 1996), transport of copper and cellular copper content are tightly controlled. One characteristic manifestation of copper dyshomeostasis is neurodegenerative diseases, such as Menkes disease, occipital horn syndrome, and Wilson's disease (Huster, 2010; Kaler, 2011; Kaler et al., 1994). The ubiquitin proteasome system (UPS) participates in the degradation of cytosolic, nuclear and transmembrane proteins and plays an important role in neurodevelopment (Dantuma and Bott, 2014; Luza et al., 2020). Multiple UPS proteins have been demonstrated to interact with the copper homeostasis machinery. In this study, we aim to investigate the mechanisms of how copper and the UPS interact.

1.2 Cellular Copper Homeostasis

The copper homeostasis system is a complex network of proteins that bind and deliver copper to copper dependent proteins and protect cells from the harmful effects of excess copper. Many of the components involved in cellular copper homeostasis have been identified, including transporters that mediate copper uptake and efflux, biomolecules that sequester and store copper, and copper chaperones that guide copper to copper-dependent enzymes (Fig.1).
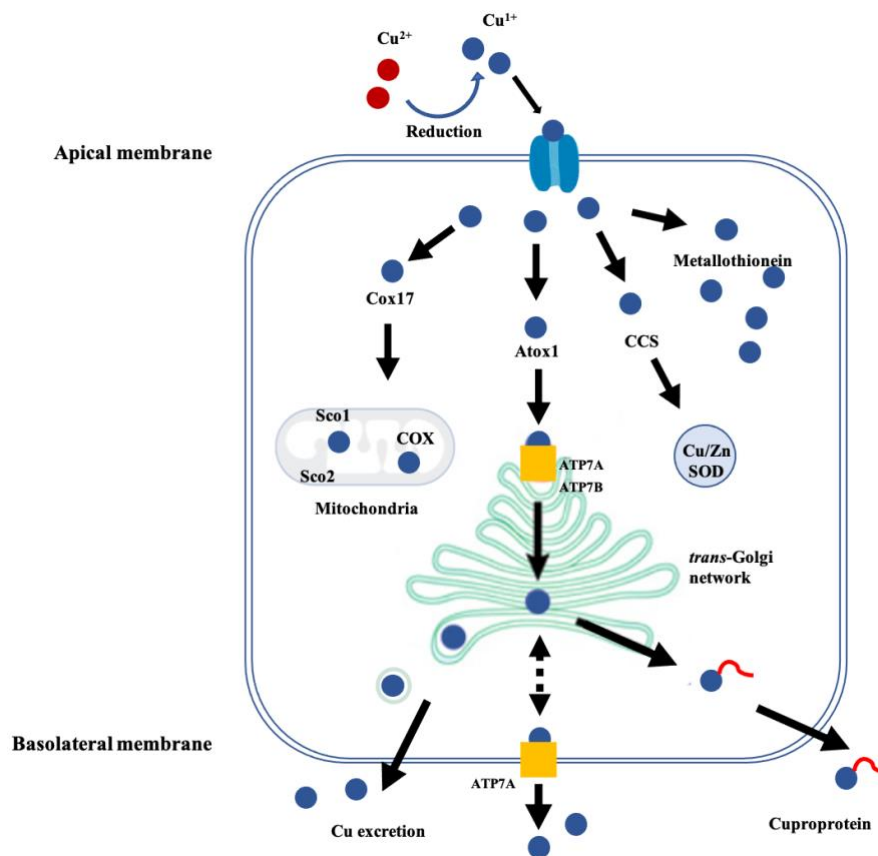
Fig.1 Model of cellular copper homeostasis (Davies et al., 2016). In mammalian cells, Cu (II) ions are reduced to Cu (I) before being imported into the cell by CTR1. Once Cu (I) ions enter cells, they are distributed to different cellular locations by copper chaperones. Some are trafficked into the mitochondria for incorporation into COX by Cox17, Sco1 and Sco2. The copper transport protein Atox1 transports copper to the ATPases, ATP7A and ATP7B, in the late Golgi. CCS delivers copper to copper/zinc superoxide dismutase (Cu/Zn SOD/SOD1). Some free copper ions are sequestered by metallothioneins for maintaining copper homeostasis.

Members of the copper transporter receptor (Ctr) family play a key role in copper uptake in eukaryotic cells (Nose et al., 2006). In vertebrates, CTR1 is expressed ubiquitously in all tissues (Zhou and Gitschier, 1997). Structural studies revealed that CTR1 molecules are arranged in a symmetrical trimer, forming a pore for the passage of copper across the lipid bilayer (Aller and Unger, 2006). In polarized intestinal enterocytes, CTR1 is observed at the apical membrane where it is responsible for copper uptake from the diet (Nose et al., 2010).

The concentration of free copper within the cell is less than one free copper ion per cell, which is maintained by binding of copper to metallothioneins (MTs) and ligands of low molecular mass such as glutathione (GSH) (Rae et al., 1999). The majority of cytosolic copper is bound

to GSH (Freedman et al., 1989), which can participate in cellular copper homeostasis by regulating the activities of the copper efflux proteins ATP7A and ATP7B via (de)glutathionylation (Singleton et al., 2010). MTs are involved in the intracellular sequestration and storage of excess copper. In patients with Wilson's disease, excess hepatic copper was found to be bound to MTs (Mulder et al., 1992). An excess of copper induces the expression of MTs (Wake and Mercer, 1985), and therefore the rise in MT levels reflects an adaptation of cells to copper overloaded conditions.

The intracellular trafficking of copper is mediated by a group of copper chaperones, including antioxidant protein 1 (Atx1), copper chaperone for superoxide dismutase (CCS), and Cox17. Atox1, the human homologue of Atx1, has been demonstrated to bind Cu(I) and transfer it to the transporters ATP7A and ATP7B, which deliver copper to cuproenzymes in the secretory pathway (Scheiber et al., 2013). CCS is primarily localized in the cytosol and its expression levels depend on cellular copper content (Culotta et al., 1997; Prohaska et al., 2003). CCS transports copper imported by CTR1 to the cytosolic copper-dependent enzymes Cu, Zn-superoxide dismutase and BACE1 (Angeletti et al., 2005; Culotta et al., 1997; Okado-Matsumoto and Fridovich, 2001; Sturtz et al., 2001). Cox17, a small, cysteine-rich, hydrophilic protein is responsible for delivering copper to mitochondrial cytochrome *c* oxidase (CCO) via Cox11, Sco1 and Sco2 (Gaggelli et al., 2006; Kim et al., 2008).

Cellular copper efflux in mammals relies on the function of two copper transporting P-type ATPases, ATP7A and ATP7B. ATP7A continuously recycles between the *trans*-Golgi network (TGN) and the plasma membrane, whereas ATP7B traffics between the TGN and a cytosolic vesicular compartment (Cater et al., 2006; Petris et al., 1996). ATP7A and ATP7B are normally localized to the TGN where they are required for transporting copper to the Golgi lumen for incorporation into copper dependent enzymes (Petris et al., 1996; Petris et al., 2000). When copper is overloaded in cells, ATP7A- and ATP7B- containing vesicles are transported to the plasma membrane for copper efflux (La Fontaine et al., 2010; La Fontaine and Mercer, 2007).

1.3 Copper Dyshomeostasis

As a redox-active metal, copper participates in diverse metabolic processes in living organisms, but can also generate toxic ROS (Halliwell and Gutteridge, 1984). In order to supply sufficient copper for the synthesis of cuproenzymes but also to prevent copper-induced oxidative stress, copper levels must be tightly regulated (Scheiber et al., 2014). Disturbance of copper

homeostasis can cause both copper deficiency disorders (e.g., Menkes disease, occipital horn syndrome, distal hereditary peripheral neuropathy) (Kaler, 2011; Kennerson et al., 2010) and copper overload disorders (Wilson's disease, copper-associated infantile cirrhosis)(Huster, 2010; Scheinberg and Sternlieb, 1996).

1.3.1 Copper deficiency disorders

Copper deficiency can occur through multiple mechanisms, such as low copper intake or high zinc intake (Horvath et al., 2010; Klevay, 2011). The clinical symptoms of acquired copper deficiency in humans are numerous, including anemia and neuropathies (Halfdanarson et al., 2008). Severe copper deficiency is a hallmark of the X-linked recessive Menkes disease (MD), which is caused by genetic defects in the ATP7A copper transporting ATPase (Kaler, 2011). MD is an incurable disorder which often leads to childhood mortality as a consequence of reduced Cu efflux from enterocytes into the bloodstream (Kim et al., 2003; Madsen and Gitlin, 2007; Menkes et al., 1962). The brain is especially sensitive to defective ATP7A protein and copper deficiency since the passage of copper across the blood-brain barrier (BBB) is mediated by ATP7A, and several cuproenzymes (e.g. Cu, Zn-superoxide dismutase) play critical roles in neuronal development (Kaler, 2011; Nelson and Prohaska, 2009; Prohaska and Broderius, 2006; Qian et al., 1997). Paradoxically, although less copper is transported to the blood and major tissues including the brain, copper accumulates in other tissues of MD patients such as the duodenum, kidney, spleen, pancreas and skeletal muscles. These patients also exhibit skeletal and connective tissue abnormalities as a result (Kodama and Murata, 1999; Møller, 2015).

Specific missense mutations in ATP7A also cause other copper deficiency disorders such as occipital horn syndrome (OHS), a connective tissue disorder resulting from lowered activity of lysyl oxidase (LOX) (Mercer, 2001) and distal hereditary motor neuropathy (Kaler et al., 1994; Kennerson et al., 2010), a degenerative motor neuron disease that will be explored in more detail later.

1.3.2 Copper overload disorders

Copper in excess is highly toxic. Wilson's disease (WD) is a serious but mostly treatable copper toxicity disorder caused by recessive mutations in ATP7B (Huster, 2010). ATP7B, structurally similar to ATP7A, is mainly restricted to the liver where it is required for exporting copper to

the bile (Linz and Lutsenko, 2007). In WD, copper accumulates in the liver, compromising hepatocyte function and leading to the unregulated release of copper, which accumulates in the central nervous system resulting in neurological abnormalities (Huster, 2010).

1.4 Copper Homeostasis and the Ubiquitin Proteasome System

1.4.1 Ubiquitin proteasome system

The ubiquitin proteasome system (UPS) is a selective proteolytic mechanism for degrading ubiquitin-conjugated substrates by the proteasome (Ciechanover, 2015). Ubiquitination also serves as a signal to control the activation of multiple intracellular signalling pathways, such as those controlling cell proliferation. Three key enzyme types participate in ubiquitination: E1 ubiquitin activating enzymes, E2 ubiquitin conjugating enzymes, and E3 ubiquitin ligases (Ciechanover, 2015). The process of ubiquitin-mediated substrate delivery to 26S proteasomes can be summarized in the simplified schematic graph in Fig.2. Ubiquitin is initially activated by an E1 in the presence of ATP and then transferred to an E2 through a thioester bond. An E3 subsequently catalyses the transfer of ubiquitin from E2 to Lys residues within specific substrates. Once the substrate is tagged with at least 4 ubiquitin molecules, it will be recognized by the 26S proteasome for degradation (Maupin-Furlow, 2011; Nandi et al., 2006).
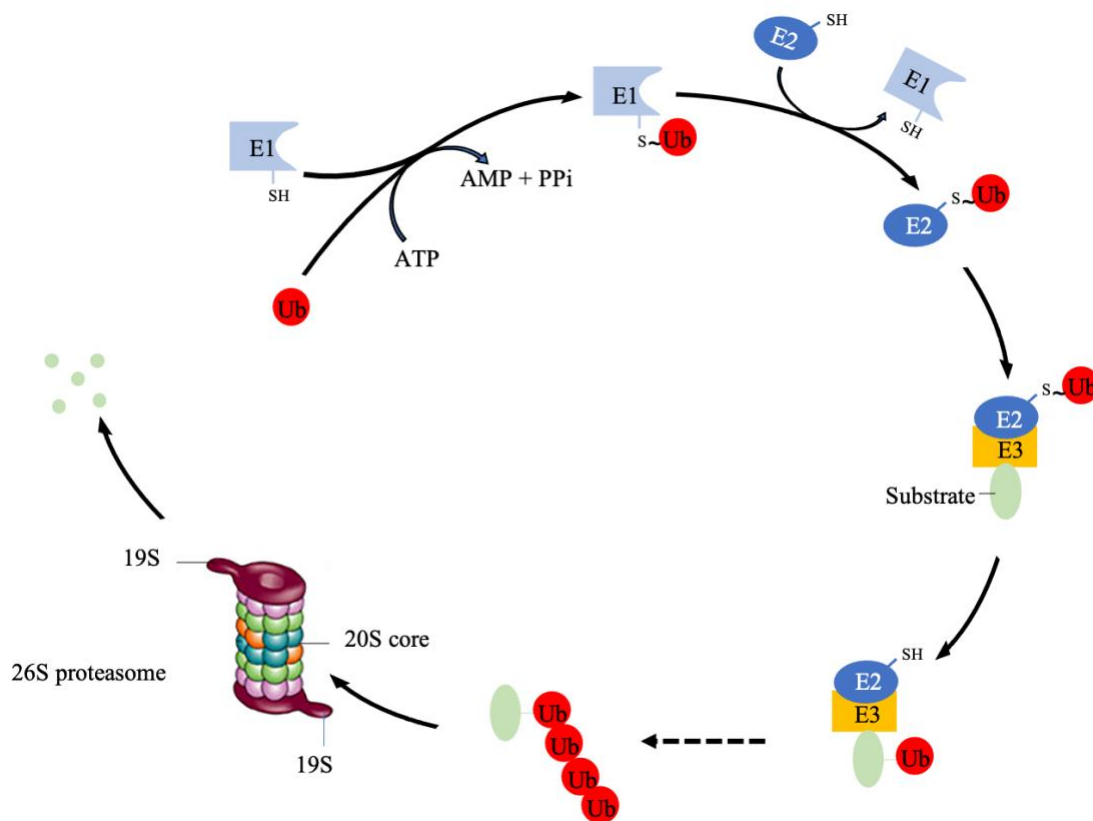
Fig.2 The signal of degradation-ubiquitination adapted from (Maupin-Furlow, 2011). Ubiquitination is a common signal for eukaryotic 26S proteasomes and involves a cascade of E1 ubiquitin-activating, E2 ubiquitin-conjugating and E3 ubiquitin ligase enzymes.

In humans, more than 40 E2s and 500 E3s have been identified to date (Nakayama and Nakayama, 2006; Valimberti et al., 2015). In contrast, the human genome encodes just a few (~9 identified to date) E1 enzymes (He et al., 2006). Importantly, E3s play a critical role in the final target selection and specificity (Nandi et al., 2006). E3s are now categorized into 4 major classes based on specific structural motifs: HECT-type, RING-finger-type, U-box-type and PHD-finger-type. RING-finger-type E3s constitute the largest family and cullin-based E3s are one of its largest subfamilies (Nakayama and Nakayama, 2006). There are seven cullin-based E3s including the SKP1-CUL1-F-box-protein (SCF) complex, which consists of three invariable components, RBX1 (a RING-finger protein), CUL1 (a scaffold protein), and SKP1 (an adaptor protein) as well as one variable component – the F-box protein (Nakayama and Nakayama, 2005). F-box protein binds to an F-box motif within SKP1 and is responsible for substrate recognition (Nakayama and Nakayama, 2006).

The UPS is involved in numerous biological process including: (i) regulation of the cell cycle (Murray, 2004); (ii) cancer and cell survival (Ciechanover and Iwai, 2004); (iii) inflammatory responses (Karin and Ben-Neriah, 2000); (iv) immune response (Kloetzel, 2004); (v) degradation of protein misfolding (McDonough and Patterson, 2003); and (vi) endogenous reticular associated degradation (Ward et al., 1995). Therefore, it is unsurprising that UPS dysregulation is heavily implicated in disease progression (Kishino et al., 1997; Staub et al., 1997) and targeted manipulation of the UPS is seen as a promising therapeutic strategy.

1.4.2 Ubiquitin proteasome system, copper homeostasis and neurodegenerative diseases

The UPS is considered a master regulator of neural development and the maintenance of brain structure and function (Luza et al., 2020) and UPS dysfunction has been linked to aging and the development of several neurodegenerative diseases, as has copper dysregulation.

1.4.2.1 The role of the UPS and copper in Alzheimer's Disease

UPS

Amyloid precursor protein (APP), a transmembrane glycoprotein, plays important roles in neuronal plasticity and brain homeostasis (Kang et al., 1987; Seabrook et al., 1999). APP can be proteolytically processed via both amyloidogenic and non-amyloidogenic pathways (Fig.3). Amyloid-β (Aβ) peptide, generated via the amyloidogenic pathway, is thought to be the causative factor of Alzheimer's disease (AD) (Hong et al., 2014). Aβ peptides are deposited in amyloid plaques, the pathological hallmark found in the central nervous system of AD patients (Olson and Shaw, 1969; Praticò, 2008; Watanabe et al., 2012). Aβ40 represents the most common amyloid species overall while Aβ42 is the most abundant species in amyloid plaques (Hung et al., 2010). Aβ42 peptides can aggregate to oligomers which mediate neurotoxicity and participate in the formation of amyloid plaques and NFTs (Lopez Salon et al., 2003; McLean et al., 1999). Recently, an increasing amount of evidence has revealed that disruption of UPS activity is implicated in the accumulation of Aβ42 peptide in AD (Harris et al., 2020).
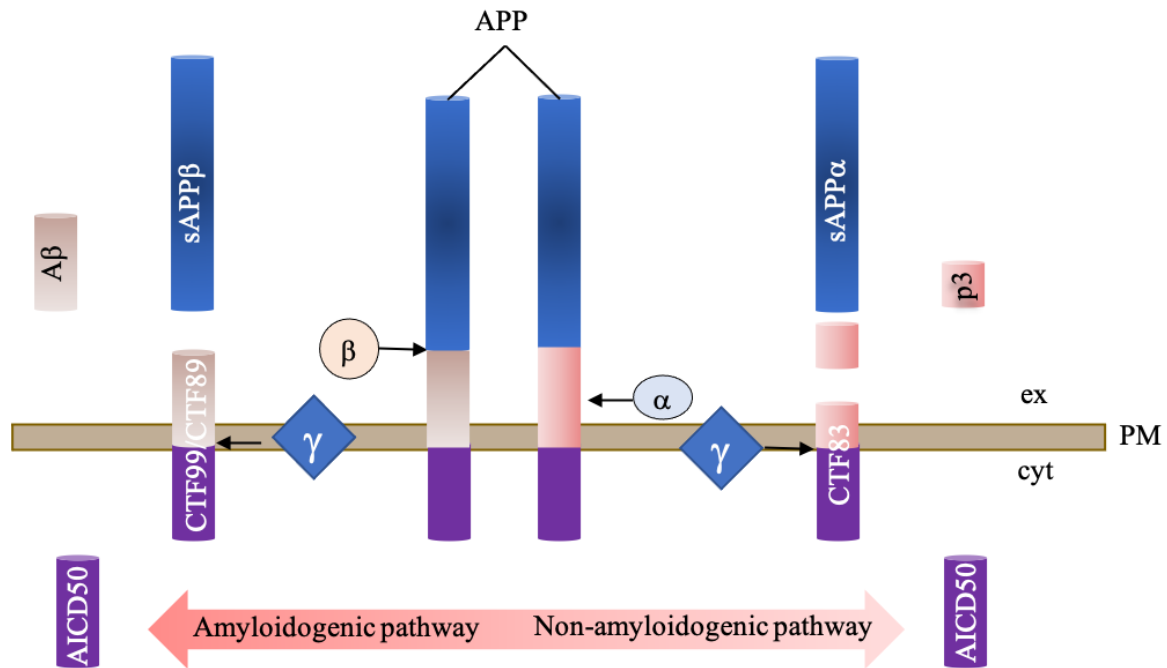
Fig.3 APP processing and cleavage products. The non-amyloidogenic pathway includes the initial cleavage of APP via α-secretase, followed by γ-secretase-mediated cleavage, finally generating a long-secreted form of APP (sAPPα) and C-terminal fragments (CTF 83, p3 and AICD50) (De Strooper et al., 1998; Esch et al., 1990; Haass et al., 1993; Sisodia, 1992; Vassar et al., 1999). In the amyloidogenic pathway, APP is sequentially cleaved by β-secretase (BACE1) and γ-secretase, which then results in the generation of a long-secreted form of APP (sAPPβ), C-terminal fragments (CTF 99 and CTF 89) and Aβs (Chow et al., 2010). Aβ fragments oligomerize and fibrillize leading to AD pathology (left and upper panel). ex - extracellular, PM - plasma membrane, cyt - cytosol.

The UPS was found to play a critical role in maintaining Aβ42 equilibrium. In primary cultures of cortical neurons and astrocytes, inhibition of 26S proteasome activity by lactacystin (a non-peptidic proteasome inhibitor) resulted in a remarkable decrease in Aβ42 degradation (Lopez Salon et al., 2003). In addition, in Aβ42-overexpressing cells treated with MG132 (a cell-permeable proteasome inhibitor), monomeric Aβ42, low-molecular weight (MW) Aβ42 oligomers, putative oligomeric 6kDa and trimeric 12kDa Aβ42 levels were dramatically elevated while the levels of high-MW Aβ42 oligomer were not significantly altered. These data suggest that the UPS preferentially removes monomeric Aβ42 and low-MW Aβ42 aggregates (Ji et al., 2018), explaining why inhibition of the UPS activity could lead to the accumulation of Aβ42.

The UPS also has the potential to regulate Aβ production via two key secretases in the amyloidogenic pathway, β-secretase (BACE1) and γ-secretase (Hong et al., 2014). BACE1 in particular plays a central role in β-amyloidogenesis (See Fig.3). Fbx2, a neuron-specific F-box protein, forms the SCF^{Fbx2}-E3 ubiquitin ligase complex by binding to the Skp1 domain of SCF (Skp1-Cullin1-F-box protein) (Hong et al., 2014). The SCF^{Fbx2}-E3 ligase binds and ubiquitinates BACE1 via the Trp 280 residue of its F-box-associated domain. In the brain of AD-model mice, BACE1 protein levels and activity were reduced by overexpressing Fbx2, resulting in a decrease in Aβ levels (Gong et al., 2010).

The second secretase involved in β-amyloidogenesis, γ-secretase, is made up of four subunits, nicastrin (NCT), presenilin (PS, two isoforms PS1 and PS2), presenilin enhancer-2 (PEN-2) and anterior pharynx defective-1 (APH-1) (He et al., 2007; Viswanathan et al., 2011). These four components are necessary and sufficient for γ-secretase activity in *Caenorhabditis elegans*, *Drosophila*, yeast and mammalian cells (He et al., 2006). High levels of ubiquitin might reduce γ-secretase activity by decreasing the formation of PS fragments and/or the levels of PEN-2 and NCT (Hong et al., 2014). Specific transcript variants of ubiquilin-1 (ubiquitin-like protein) which are genetically and functionally associated with AD, regulate proteasomal and aggresomal targeting of PS1 (Haapasalo et al., 2011; Viswanathan et al., 2011). In addition, inhibition of proteasomal degradation of APH-1 by lactacystin in N2a cells facilitated γ-secretase-mediated cleavage of APP to generate Aβ (He et al., 2006). These studies demonstrated that UPS regulates γ-secretase activity via post-translational regulation of its four components and then participates in the generation of Aβ42.

Hyperphosphorylation of the microtubule binding protein tau is also considered as a hallmark of AD. Tau phosphorylation abnormalities have been linked to misfolding and deposition of the protein in NFTs (Vega et al., 2005; Wegmann et al., 2013). Immunoblot results revealed that overexpression of the E3 ubiquitin ligase CHIP in COS7 cells induces the ubiquitination of phosphorylated tau in collaboration with E2 ubiquitin conjugating enzyme UbcH5B (Shimura et al., 2004), suggesting the importance of UPS in maintaining tau equilibrium.

Copper

Copper homeostasis is essential to the integrity of normal brain functions, and copper deficiency or excess is thought to contribute to diseases such as AD, Down Syndrome (DS), and

Parkinson's disease. The AD brain is characterized by abnormal neuronal copper distribution, with accumulation of copper in amyloid plaques (Cater et al., 2008; Lovell et al., 1998). An increasing body of evidence supports the proposition that the alteration of copper levels might cause the accumulation of Aβ42 in AD (Hung et al., 2010; James et al., 2017). In an APP/PS1 mouse model of AD, X-ray fluorescence microscopy and immunohistochemical staining showed an increase of copper levels in Aβ plaques (James et al., 2017) compared to the same tissue in wild type mice. Aggregation of Aβ42, generated by the cleavage of APP by BACE1 (Vassar et al., 1999), is fundamental to Aβ-mediated neurotoxicity. BACE1 contains a high-affinity Cu(I) binding site within its C-terminal domain (Angeletti et al., 2005), is transcriptionally upregulated by exogenous copper in PC12 cells (Lin et al., 2008), and physically interacts with the copper chaperone CCS. These results indicate that BACE1-mediated cleavage of APP may occur in a copper dependent manner (Angeletti et al., 2005). Copper was also found to directly bind to both nicastrin and presenilin, and was shown to inhibit the activity of γ-secretase in cleaving APP-C99 to form Aβ. (Gerber et al., 2017).

APP itself possesses an N-terminal copper binding region (CuBD) capable of reducing Cu(II) to Cu(I) (Hung et al., 2010). Cu(II) binding to APP could cause a conformational change, which then facilitates α-secretase-mediated cleavage but attenuates BACE1-mediated cleavage, thus promoting the non-amyloidogenic APP processing pathway (Borchardt et al., 1999). Structural analysis of the APP CuBD revealed topological similarity to the copper chaperones Atox1 and CCS (Barnham et al., 2003; Hung et al., 2010; Kong et al., 2007). In APP knockout mice, copper levels were significantly elevated in the cerebral cortex (White et al., 1999), whereas overexpressing APP in mouse brains resulted in dramatically decreased copper levels (Maynard et al., 2002), leading to the hypothesis that APP is involved in copper efflux. Copper in turn may regulate APP expression. In human fibroblast cells, copper deficiency caused by overexpressing ATP7A down-regulated *APP* gene expression and significantly reduced APP protein levels (Bellingham et al., 2004). However, the level of Aβ secretion was elevated in copper deficient conditions (Cater et al., 2008). In contrast, human fibroblasts exposed to high copper conditions increased APP levels while excess copper inhibits Aβ production (Cater et al., 2008; Crouch et al., 2009; Gerber et al., 2017; Phinney et al., 2003). These data together indicated that copper upregulates APP while at the same time inhibiting APP cleavage, possibly by its inhibition of γ-secretase (see above).

Mutations in some copper transporters have the potential to increase the occurrence of AD. Heterozygosity for ATP7B mutations has been shown to be associated with elevated risk of developing AD (Squitti et al., 2016). However, the mechanism underpinning this association remains unclear. Non-ceruloplasmin-copper (non-Cp-Cu) is toxic to the brain since it can cross the BBB, and has been found to be increased in some neurological disorders (Bandmann et al., 2015), including in AD (Squitti et al., 2017). Given that ATP7B mutants cause an altered copper loading into nascent ceruloplasmin (Squitti et al., 2013; Squitti et al., 2016; Squitti et al., 2017), we postulate that ATP7B mutants might contribute to the development of AD via increasing non-Cp-Cu. In conclusion, copper homeostasis plays a critical role in brain function and the alteration of copper levels, for instance via ATP7B mutation, might contribute to AD through elevated APP expression, even though the production of Aβ peptides is mostly inhibited by high copper.

1.4.2.2 The role of the UPS and copper in Parkinson's Disease

UPS

Parkinson's disease (PD) is a long-term neurodegenerative disorder, characterized by a selective loss of dopaminergic neurons in the *substantia nigra* region of the brain and the presence of Lewy bodies (Grubman et al., 2014). α-synuclein (α-Syn) is a natively unfolded presynaptic protein considered as a major pathogenic factor in PD due to its accumulation in Lewy bodies (LBs) or Lewy neurites (LNs) (Shults, 2006; Spillantini et al., 1997). Unbound and cytosolic α-Syn is a substrate for the proteasome while membrane-bound α-Syn is protected against proteasomal degradation (Liu et al., 2005). High levels of undegraded or poorly degraded α-Syn protein tend to self-aggregate, induce aggregation of other proteins, interfere with intracellular functions and induce cytotoxicity (Bennett et al., 2005). In *Drosophila*, exogenous expression of *α-Syn* produces adult-onset loss of dopaminergic neurons, filamentous intraneuronal inclusions and locomotor dysfunction (Feany and Bender, 2000). In mice, ablation of α-Syn alleviates the symptoms of Parkinson-like syndrome induced by the dopaminergic neurotoxin MPTP, such as neuronal loss and the formation of ubiquitin-positive inclusions (Fornai et al., 2005). Recently, the aggregation of α-Syn in PD has been found to be associated with the activity of UPS.

The E3 ubiquitin ligase Parkin has also been linked to PD. Mutations in the *parkin* gene are a major cause of early-onset autosomal recessive familial PD and isolated juvenile-onset PD (Lücking et al., 2000). Parkin may normally protect cells from premature death by degrading misfolded or damaged proteins (Pawlyk et al., 2003). Parkin has been shown to become more insoluble with age and PD caused by Parkin mutations appears to universally result from alterations in Parkin solubility and intracellular localization (Cook and Petrucelli, 2009; Pawlyk et al., 2003). In PD brains, Parkin has been found to colocalize with α-Syn in Lewy bodies, even though α-Syn is not a substrate of Parkin (Cook and Petrucelli, 2009; Schlossmacher et al., 2002). α-Syn and Parkin have been shown to associate and colocalize to cytosolic and neuritic processes in PD (Choi et al., 2001). α-Syn aggregates interfere with Parkin solubility and distribution; co-expression of α-Syn and Parkin led to a decrease in Parkin solubility while α-Syn knockdown increased Parkin solubility (Kawahara et al., 2008).

Heat shock proteins (HSPs) such as HSP70 and HSP90 also participate in the management of excess or deleterious proteins (Olanow and McNaught, 2006) and Carboxyl-terminus-of-HSP70-interacting protein (CHIP), an E3 ubiquitin ligase, can mediate the degradation of misfolded proteins associated with PD (Shin et al., 2005; Tetzlaff et al., 2008). CHIP can rescue the cytotoxicity caused by α-Syn oligomers and reduce the formation of higher molecular weight oligomeric α-Syn species (Tetzlaff et al., 2008). Bcl-2-associated athanogene 5 inhibits CHIP-mediated ubiquitination of α-Syn, and regulates the ability of CHIP to decrease the levels of α-Syn oligomeric species (Kalia et al., 2011). Since the UPS plays a critical role in removing α-Syn aggregates, understanding the associated mechanism could contribute a promising therapeutic development to PD.

Copper

In most cases, the damaging aspects of copper are seen when it is present as a free ion or linked to low molecular weight ligands. In PD, free copper is associated with increased oxidative stress, α-Syn oligomerization and Lewy body formation (Montes et al., 2014). α-Syn has high affinity for copper through two binding sites, M1-D2 and H50 (Okita et al., 2017; Rasia et al., 2005; Uversky et al., 2001). The binding of copper to α-Syn is an important event for the development of PD (Montes et al., 2014). Copper has been demonstrated to accelerate the formation of toxic oligomeric forms of α-Syn (Binolfi et al., 2010; Santner and Uversky, 2010; Wang et al., 2010; Wright et al., 2009). *In vitro* studies revealed that copper and dopamine cooperatively bind to

α-Syn at different sites and enhance the propensity of α-Syn to oligomerize (Tavassoly et al., 2014). In a human blastoma cell line, copper depletion resulted in the redistribution of α-Syn towards the plasma membrane and reduced aggregate formation (Wang et al., 2010). Quantum and molecular mechanics simulations revealed that copper binding to α-Syn could make α-Syn more susceptible to misfolding which then resulted in the formation of LBs (Rose et al., 2011). These demonstrated that copper dyshomeostasis made a contribution to the development of PD.

Some copper binding proteins are also found to be involved in the progress of PD. Ceruloplasmin, a multicopper containing glycoprotein, possesses two most prominent functions; plasma copper binding (95% of circulating copper is bound to ceruloplasmin) and regulating iron homeostasis by means of its ferroxidase activity (Montes et al., 2014). In the brain, ceruloplasmin is synthesized by astrocytes and is linked to iron efflux from the brain since ceruloplasmin promotes the oxidation of neuronal $Fe(II)$ to $Fe(III)$ which can then be exported (Boll et al., 1999; Hare et al., 2013; Montes et al., 2014; Patel and David, 1997). The ferroxidase activity of ceruloplasmin is diminished by severe copper deficiency (Montes et al., 2014). In the plasma and cerebrospinal fluid of patients with PD, copper-dependent ferroxidase activity has also been reported to be diminished. Furthermore, the postmortem basal ganglia and *substantia nigra* of PD patients both showed increased iron and decreased copper (Ayton et al., 2013; Dexter et al., 1989; Riederer et al., 1989). Ceruloplasmin-deficient mice displayed neuronal cell death in the *substantia nigra* which could be partially rescued by an iron chelator (Ayton et al., 2013). Additionally, the increase of iron in the *substantia nigra* and the dopaminergic cell death induced by MPTP were partially prevented by the peripheral administration of ceruloplasmin (Ayton et al., 2013). These suggest that the ferroxidase activity of ceruloplasmin is diminished by copper deficiency, which then causes the accumulation of iron and promotes the development of PD.

An additional link between PD and copper homeostasis is found through SOD1. Superoxide dismutases (SODs) are major antioxidant enzymes responsible for eliminating superoxide anion radicals (McCord and Fridovich, 1969), and they have consistently been found to be neuroprotective (Montes et al., 2014). Three distinct isoforms of SOD have been identified in mammals: Cu, Zn-SOD (SOD1), Mn-SOD (SOD2) and extracellular-SOD (SOD3) (Perry et al., 2010). SOD1 requires copper and zinc as cofactors, and has an important function as a copper buffer within the cells (Culotta et al., 1995; Marklund, 1982). In patients with PD, SOD1 was diminished in red blood cells which resulted in a higher concentration of hydroxyl radical

in the plasma (Ihara et al., 1999). In addition, SOD activity is reduced significantly as the disease progresses, indicating the age-dependent deterioration of the antioxidant ability of SOD1 in PD (Tórsdóttir et al., 1999).

1.4.2.3 The role of the UPS and copper in Amyotrophic Lateral Sclerosis

Amyotrophic Lateral Sclerosis (ALS) is characterized by the progressive degeneration of motor neurons in the brain and spinal cord associated with the accumulation of misfolded proteins and insoluble inclusions (Andersen and Al-Chalabi, 2011; Cleveland and Rothstein, 2001). This protein misfolding disorder can be divided into sporadic ALS and familial ALS (Andersen and Al-Chalabi, 2011). The most common genetic form of familial ALS is due to mutations in the SOD1 because they tend to be misfolded and form protease-resistant aggregates (Bento-Abreu et al., 2010; Guo et al., 2010).

Misfolded SOD1 is initially targeted for degradation by components of the UPS such as chaperones and ubiquitin ligases (Ciechanover, 2015). However, the targeted mutants tend to aggregate and escape the delivery process to proteasomes. In SOD1-G93A transgenic mice (a familial ALS mouse model), mutant SOD1 accumulates in the cytoplasm of motor neurons then proceeds to form numerous inclusions in the axons and astrocytes (Guo et al., 2010). Large inclusions are clinical hallmarks of ALS symptoms. Furthermore, intracellular inclusions containing ubiquitin and ubiquitin ligases were detected in familial ALS mutant mice, suggesting that mutant SOD1 is resistant to the UPS (Ciechanover and Kwon, 2015). Additionally, overexpressing mutant SOD1G93A in mice stimulates the formation of SOD1 aggregates and inhibits proteasome activity; the formation of SOD1 aggregates is reversible with the restoration of proteasome function (Puttaparthi et al., 2003). Moreover, it has been shown that reduced proteasomal activity can promote the accumulation of ALS protein aggregates (Ciechanover and Kwon, 2015). Inhibition of the proteasome by lactacystin causes the formation of SOD1 aggregates in SOD1 mutant-expressing cells (Hyun et al., 2003), suggesting that the UPS plays a critical role in removing misfolded SOD1 in ALS.

Copper is required for SOD activity (Forman and Fridovich, 1973). SOD1 mutant mice showed elevated concentrations of copper, suggesting that copper dyshomeostasis might facilitate the development of ALS (Tokuda et al., 2009). Overexpressing copper chaperone CCS, which delivers copper to SOD1, led to an accelerated pathology and disease progression in the SOD1 G93A mice (Son et al., 2007). Moreover, copper deficiency has been demonstrated to accelerate

aberrant hydrophobicity of both wild-type and mutated SOD1 due to partial protein unfolding, which could be reverted by the addition of Cu(II) (Gil-Bea et al., 2017). Several studies have shown that mutant SOD1 aggregates in cultured cells or SOD1 transgenic mice have a low copper content (Bourassa et al., 2014; Lelie et al., 2011; Zetterström et al., 2007). These results revealed that SOD1 mutant accumulates in a copper-deficient state even though overall copper levels may be elevated.

1.4.3 Copper homeostasis and the ubiquitin proteasome system

The disruption of both copper levels and the UPS is detected in neurodegenerative diseases such as AD, PD and ALS, resulting in the generation or aggregation of pathogenic Aβ42, α-Syn and SOD1 respectively. These commonalities suggest that the copper homeostasis machinery and the UPS may interact during the development of neurodegenerative disease. Therefore, we next review evidence for roles of the UPS in regulating copper homeostasis.

1.4.3.1 Copper transporters, chaperones and the UPS

Each copper transporter and chaperone has a distinct and well-characterized role in copper homeostasis. CTR1, for instance, plays a critical role in copper uptake, and is downregulated by intracellular copper (Song et al., 2008). In yeast, the E3 ubiquitin ligase Rsp5 participates in the proteasomal degradation of CTR1, which then decreases cellular copper levels due to the reduction of copper uptake (Liu et al., 2007). It remains to be tested whether either NEDD4 or NEDD4-L, the mammalian homologues of Rsp5, regulate the degradation of CTR1.

In humans, copper transporters ATP7A and ATP7B play a critical role in copper transport in *trans*-Golgi network and result in MD or WD respectively when mutated. The copper metabolism MURR1 domain protein 1 (COMMD1), a scaffold protein, regulates the folding, stability, ubiquitination, and proteolysis of its interaction partners, including ATP7A and ATP7B (Vonk et al., 2011; Vonk et al., 2014). *Commd1* was originally identified as the gene underlying non-Wilsonian copper toxicosis (CT) in Bedlington terriers. This disease is characterized by hepatic copper accumulation resulting in liver fibrosis and eventually cirrhosis (Owen and Ludwig, 1982; Su et al., 1982; van De Sluis et al., 2002). It has been reported that COMMD1 regulates hepatic copper export by interacting with ATP7B (de Bie et al., 2007; Miyayama et al., 2010; Tao et al., 2003) since ATP7B is responsible for exporting excess copper in the liver. Consistent with this, copper dramatically accumulated in the liver in liver-specific

Commd1 knockout mice fed with copper-enriched diet (Vonk et al., 2011). ATP7A normally resides in the TGN and translocates to the plasma membrane only when intracellular copper levels increase. Mutations in the C-terminal DKTG motif of ATP7A block this copper-induced translocation (Vonk et al., 2012). Interestingly, COMMD1 restores the expression and subcellular localization of misfolded ATP7A mutants and promotes the proteolysis of misfolded ATP7B proteins (Vonk et al., 2012), demonstrating that COMMD1 participates in regulating intracellular copper homeostasis via ATP7A and ATP7B.

X-linked inhibitor of apoptosis (XIAP) possesses E3 ubiquitin activity which regulates the ubiquitination and proteasomal degradation of COMMD1 (Burstein et al., 2004; Maine et al., 2009). An increase in cellular XIAP levels by ectopic expression results in a decrease in COMMD1 levels, while COMMD1 levels increase when XIAP levels are suppressed (Mufti et al., 2007), suggesting that XIAP regulates copper homeostasis in addition to its well-known role as a potent suppressor of apoptosis (Tsai et al., 2015). XIAP was also found to be a strong copper binding protein and the interaction between XIAP and copper leads to a conformational change of XIAP (loss of inhibitory effect to caspase3 activity) (Mufti et al., 2007). Additionally, copper chaperone CCS is responsible for delivering copper to XIAP in mammals, meanwhile it could be ubiquitinated by XIAP (Brady et al., 2010). Interestingly, ubiquitination of CCS by XIAP enhances its ability to deliver copper to SOD1 rather than triggering degradation of CCS. As shown in Fig.4, Brady *et al* proposed that interaction of copper-free CCS and XIAP results in nondegradative ubiquitination of CCS and then the ubiquitinated CCS delivers copper to SOD1; copper-bound CCS initially transfers copper to XIAP and then CCS is ubiquitinated and targeted for proteasomal degradation (Brady et al., 2010). However, the mechanism underlying why XIAP mediated ubiquitination enhances CCS ability to deliver copper to SOD1 remains to be investigated.
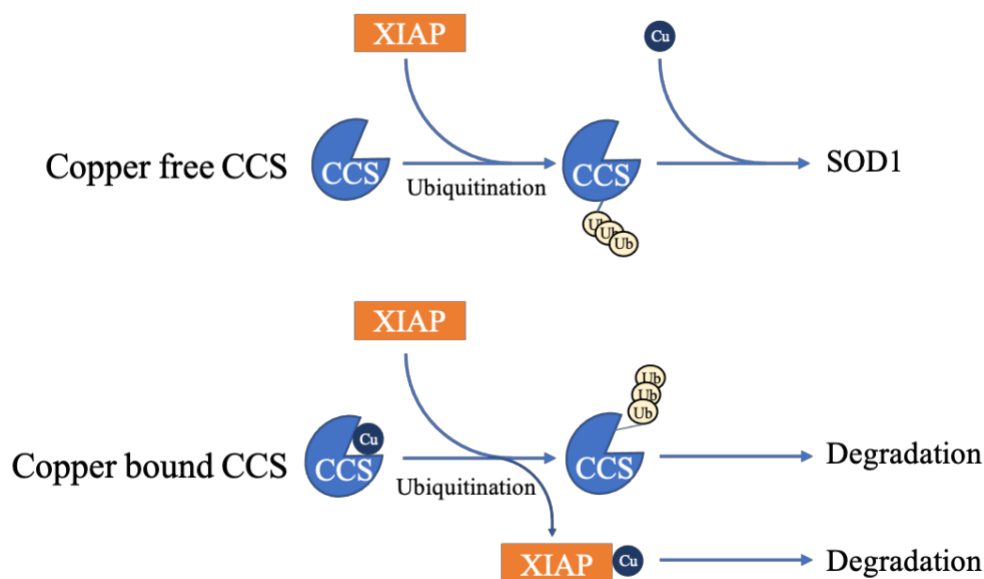
Fig.4 Regulation of copper chaperone CCS by XIAP-mediated ubiquitination. Copper-free CCS is ubiquitinated by XIAP to form the nondegradative ubiquitinated CCS, and then the ubiquitinated CCS delivers copper to SOD1. In contrast copper-bound CCS initially transfers copper to XIAP, and then CCS is ubiquitinated. Finally, ubiquitinated CCS and copper-bound XIAP are both targeted for proteasomal degradation.

COMMD1 has also been found to suppress SOD1 homodimerization, which results in a decline in SOD1 scavenging activity and consequently an induction of toxic superoxide anions (Vonk et al., 2014). Additionally, many components of the UPS have been identified to regulate SOD1 via post-translational regulation: 1) Mahogunin ring finger-1 (MGRN1, E3 ubiquitin ligase) promoted clearance of toxic mutant SOD1 inclusions (Chhangani et al., 2016); 2) Dorfin (a RING finger-type E3 ubiquitin ligase) physically bound and ubiquitinated SOD1 mutants but did not affect the stability of the wild type SOD1; 3) Cdc48 (20s proteasome complex) degraded SOD1 in a ubiquitin independent manner (Islam et al., 2020); 4) Ataxin-3 (a specific DUB) promoted mutant SOD1 aggresome formation by modifying K63-linked polyubiquitin chains (Wang et al., 2012). Given that one of SOD1's important functions is buffering copper levels, these data indirectly suggest that these UPS components are involved in regulating copper homeostasis.

1.4.3.2 The influence of copper levels on UPS activity

The UPS participates in protein quality control to prevent the accumulation of non-functional and misfolded proteins (Taylor and Dillin, 2011). Interestingly, preliminary evidence suggests

that the activity of the UPS may also be affected by copper homeostasis. For instance, we have shown that the E2 ubiquitin conjugase enzyme UBE2D2 is a cuproprotein with two putative copper binding domains, whose ubiquitinating activity is heavily dependent on allosteric conformational changes induced by the presence of copper (Opazo et al., 2021). Cu (II) ions have also been shown to target the aggregation-prone regions of ubiquitin itself, inducing self-oligomerization (Arnesano et al., 2009). Furthermore, GSH plays a central role in maintaining intracellular copper levels by sequestering and storing of excess copper (Scheiber et al., 2013) and in dopaminergic PC12 cells, a decrease in cellular GSH leads to a reduction of E1 activity, which subsequently disrupts the ubiquitin pathway (Jha et al., 2002). In addition, some evidence indicates that proteasome activity is subject to copper levels. Xiao et al demonstrated that copper ions inhibit 20S proteasome activity and induce cell death and also that the 20S proteasome is able to reduce Cu (II) to Cu (I) (Xiao et al., 2010). Copper complexes were also demonstrated to inhibit the activity of the 26S proteasome *in vitro* and *in vivo* (Daniel et al., 2004; Zhang et al., 2017).

1.5 This Study

Copper homeostasis involves many molecules such as copper transporters ATP7A/B and CTR1, copper chaperones Cox17, Atox1 and CCS. Mutations in these proteins could disrupt copper homeostasis, and then cause copper deficiency or copper overload disorder. Some neurodegenerative diseases such as AD, DS and PD have been linked to copper dyshomeostasis. Interestingly, UPS activity is also involved in the development of AD and PD. Furthermore, the disruption of copper homeostasis and UPS activity both results in the accumulation of Aβ42 (a hallmark of AD) or α-Syn (a hallmark of PD).

Recently, accumulating evidence has revealed that dysregulation of copper could affect the activity of the UPS, while multiple components of the UPS have been identified to participate in the proteasomal degradation of copper transporters and copper chaperones. Therefore, we propose that the copper homeostasis machinery and the UPS are interdependent. We hypothesize that proteasomal regulation may be a key mechanism by which cellular copper levels are sensed and controlled and that in addition, monitoring of cellular copper status by the proteasome may provide crucial checkpoints for controlling numerous critical cellular processes.

This study aims to elucidate the mechanisms by which copper and the UPS interact, using the fruit fly *Drosophila melanogaster* as the model system of choice due to its excellent gene manipulation resources. ATP7, the *Drosophila* orthologue mammalian ATP7A and ATP7B, is responsible for intracellular copper efflux in the fly while Ctr1A is the major copper uptake protein. Previous research has shown that depletion of copper in the cells that give rise to the adult cuticle results in a loss of melanin production resulting in a hypopigmentation phenotype; this is because the multicopper oxidase Laccase 2 is a copper dependent enzyme required for the final step in cuticle melanisation.

Genome-wide *RNAi* screens have shown that knockdown of numerous genes can cause pigmentation defects in *Drosophila*. Previous unpublished research in our group showed that knockdown of one such gene encoding the E3 ubiquitin ligase supernumerary limbs (Slmb) causes a cuticle hypopigmentation phenotype highly similar to that caused by *ATP7* overexpression or *Ctr1A* knockdown, suggesting that loss of Slmb might be causing cellular copper deficiency. Therefore **AIM 1** of this thesis, addressed in **Chapter 3** and published in 2020 (Zhang et al., 2020), was to investigate the role of Slmb-mediated proteasomal degradation in the regulation of cellular copper homeostasis.

Chapters 4 and 5 of this thesis are based on a proteomics study where 541 ATP7A binding proteins were identified in mammalian cells by performing immunoaffinity chromatography. Several of these proteins were involved in the ubiquitin proteasomal system (Comstra et al., 2017)*,* leading to our hypothesis that proteasomal regulation of ATP7A may play a key role in controlling copper efflux *in vivo*. Therefore **AIM 2** of this thesis, addressed in **Chapter 4**, was to interrogate the *Drosophila* orthologues of ATP7A-interacting proteasomal proteins to identify novel regulators of cellular copper homeostasis. A promising E3 ubiquitin complex, Vhl/EloC/Cul2 identified in **Chapter 4**, was selected for **AIM 3** of this thesis**,** addressed in **Chapter 5,** to investigate the mechanism by which the Vhl/EloC/Cul2 E3 complex regulates intracellular copper levels.

Identification of the E2 ubiquitin conjugase(s) working together with these E3 ubiquitin ligases is also a high priority. The E2 ubiquitin conjugase UbcD1 was reported to participate in Hedgehog signalling pathway via Slmb mediated degradation of Ci (Pan et al., 2017) and colleagues at the Florey Institute have identified UbcD1's mammalian orthologue UBE2D2 as a copper-binding protein. Therefore, **AIM 4** of this thesis, addressed in **Chapter 6**, was to examine whether UbcD1 interacts with Slmb, Vhl or other E3s in regulating copper

homeostasis. All these results in this study together demonstrated that UPS participates in copper homeostasis via proteasomal degradation of copper transporters meanwhile UPS activity is subject to copper conditions.

References:

Aller, S.G., Unger, V.M., 2006. Projection structure of the human copper transporter CTR1 at 6-A resolution reveals a compact trimer with a novel channel-like architecture. Proc Natl Acad Sci U S A 103, 3627-3632.

Andersen, P.M., Al-Chalabi, A., 2011. Clinical genetics of amyotrophic lateral sclerosis: what do we really know? Nat Rev Neurol 7, 603-615.

Angeletti, B., Waldron, K.J., Freeman, K.B., Bawagan, H., Hussain, I., Miller, C.C., Lau, K.F., Tennant, M.E., Dennison, C., Robinson, N.J., Dingwall, C., 2005. BACE1 cytoplasmic domain interacts with the copper chaperone for superoxide dismutase-1 and binds copper. J Biol Chem 280, 17930-17937.

Arnesano, F., Scintilla, S., Calò, V., Bonfrate, E., Ingrosso, C., Losacco, M., Pellegrino, T., Rizzarelli, E., Natile, G., 2009. Copper-triggered aggregation of ubiquitin. PLoS One 4, e7052.

Ayton, S., Lei, P., Duce, J.A., Wong, B.X., Sedjahtera, A., Adlard, P.A., Bush, A.I., Finkelstein, D.I., 2013. Ceruloplasmin dysfunction and therapeutic potential for Parkinson disease. Ann Neurol 73, 554-559.

Bandmann, O., Weiss, K.H., Kaler, S.G., 2015. Wilson's disease and other neurological copper disorders. The Lancet. Neurology 14, 103-113.

Barnham, K.J., McKinstry, W.J., Multhaup, G., Galatis, D., Morton, C.J., Curtain, C.C., Williamson, N.A., White, A.R., Hinds, M.G., Norton, R.S., Beyreuther, K., Masters, C.L., Parker, M.W., Cappai, R., 2003. Structure of the Alzheimer's disease amyloid precursor protein copper binding domain. A regulator of neuronal copper homeostasis. J Biol Chem 278, 17401-17407.

Bellingham, S.A., Lahiri, D.K., Maloney, B., La Fontaine, S., Multhaup, G., Camakaris, J., 2004. Copper depletion down-regulates expression of the Alzheimer's disease amyloid-beta precursor protein gene. J Biol Chem 279, 20378-20386.

Bennett, E.J., Bence, N.F., Jayakumar, R., Kopito, R.R., 2005. Global impairment of the ubiquitin-proteasome system by nuclear or cytoplasmic protein aggregates precedes inclusion body formation. Mol Cell 17, 351-365.

Bento-Abreu, A., Van Damme, P., Van Den Bosch, L., Robberecht, W., 2010. The neurobiology of amyotrophic lateral sclerosis. Eur J Neurosci 31, 2247-2265.

Binolfi, A., Rodriguez, E.E., Valensin, D., D'Amelio, N., Ippoliti, E., Obal, G., Duran, R., Magistrato, A., Pritsch, O., Zweckstetter, M., Valensin, G., Carloni, P., Quintanar, L., Griesinger, C., Fernández, C.O., 2010. Bioinorganic chemistry of Parkinson's disease: structural determinants for the copper-mediated amyloid formation of alpha-synuclein. Inorg Chem 49, 10668-10679.

Boll, M.C., Sotelo, J., Otero, E., Alcaraz-Zubeldia, M., Rios, C., 1999. Reduced ferroxidase activity in the cerebrospinal fluid from patients with Parkinson's disease. Neurosci Lett 265, 155-158.

Borchardt, T., Camakaris, J., Cappai, R., Masters, C.L., Beyreuther, K., Multhaup, G., 1999. Copper inhibits beta-amyloid production and stimulates the non-amyloidogenic pathway of amyloid-precursor-protein secretion. Biochem J 344 Pt 2, 461-467.

Bourassa, M.W., Brown, H.H., Borchelt, D.R., Vogt, S., Miller, L.M., 2014. Metal-deficient aggregates and diminished copper found in cells expressing SOD1 mutations that cause ALS. Front Aging Neurosci 6, 110.

Brady, G.F., Galban, S., Liu, X., Basrur, V., Gitlin, J.D., Elenitoba-Johnson, K.S., Wilson, T.E., Duckett, C.S., 2010. Regulation of the copper chaperone CCS by XIAP-mediated ubiquitination. Molecular and cellular biology 30, 1923-1936.

Burstein, E., Ganesh, L., Dick, R.D., van De Sluis, B., Wilkinson, J.C., Klomp, L.W., Wijmenga, C., Brewer, G.J., Nabel, G.J., Duckett, C.S., 2004. A novel role for XIAP in copper homeostasis through regulation of MURR1. EMBO J 23, 244-254.

Cater, M.A., La Fontaine, S., Shield, K., Deal, Y., Mercer, J.F., 2006. ATP7B mediates vesicular sequestration of copper: insight into biliary copper excretion. Gastroenterology 130, 493-506.

Cater, M.A., McInnes, K.T., Li, Q.X., Volitakis, I., La Fontaine, S., Mercer, J.F., Bush, A.I., 2008. Intracellular copper deficiency increases amyloid-beta secretion by diverse mechanisms. Biochem J 412, 141-152.

Chhangani, D., Endo, F., Amanullah, A., Upadhyay, A., Watanabe, S., Mishra, R., Yamanaka, K., Mishra, A., 2016. Mahogunin ring finger 1 confers cytoprotection against mutant SOD1 aggresomes and is defective in an ALS mouse model. Neurobiol Dis 86, 16-28.

Choi, P., Golts, N., Snyder, H., Chong, M., Petrucelli, L., Hardy, J., Sparkman, D., Cochran, E., Lee, J.M., Wolozin, B., 2001. Co-association of parkin and alpha-synuclein. Neuroreport 12, 2839-2843.

Chow, V.W., Mattson, M.P., Wong, P.C., Gleichmann, M., 2010. An overview of APP processing enzymes and products. Neuromolecular Med 12, 1-12.

Ciechanover, A., 2015. The unravelling of the ubiquitin system. Nat Rev Mol Cell Biol 16, 322-324.

Ciechanover, A., Iwai, K., 2004. The ubiquitin system: from basic mechanisms to the patient bed. IUBMB Life 56, 193-201.

Ciechanover, A., Kwon, Y.T., 2015. Degradation of misfolded proteins in neurodegenerative diseases: therapeutic targets and strategies. Exp Mol Med 47, e147.

Cleveland, D.W., Rothstein, J.D., 2001. From Charcot to Lou Gehrig: deciphering selective motor neuron death in ALS. Nat Rev Neurosci 2, 806-819.

Comstra, H.S., McArthy, J., Rudin-Rush, S., Hartwig, C., Gokhale, A., Zlatic, S.A., Blackburn, J.B., Werner, E., Petris, M., D'Souza, P., Panuwet, P., Barr, D.B., Lupashin, V., Vrailas-Mortimer, A., Faundez, V., 2017. The interactome of the copper transporter ATP7A belongs to a network of neurodevelopmental and neurodegeneration factors. Elife 6.

Cook, C., Petrucelli, L., 2009. A critical evaluation of the ubiquitin-proteasome system in Parkinson's disease. Biochim Biophys Acta 1792, 664-675.

Crouch, P.J., Hung, L.W., Adlard, P.A., Cortes, M., Lal, V., Filiz, G., Perez, K.A., Nurjono, M., Caragounis, A., Du, T., Laughton, K., Volitakis, I., Bush, A.I., Li, Q.X., Masters, C.L., Cappai, R., Cherny, R.A., Donnelly, P.S., White, A.R., Barnham, K.J., 2009. Increasing Cu bioavailability inhibits Abeta oligomers and tau phosphorylation. Proceedings of the National Academy of Sciences of the United States of America 106, 381-386.

Culotta, V.C., Joh, H.D., Lin, S.J., Slekar, K.H., Strain, J., 1995. A physiological role for Saccharomyces cerevisiae copper/zinc superoxide dismutase in copper buffering. J Biol Chem 270, 29991-29997.

Culotta, V.C., Klomp, L.W., Strain, J., Casareno, R.L., Krems, B., Gitlin, J.D., 1997. The copper chaperone for superoxide dismutase. J Biol Chem 272, 23469-23472.

Daniel, K.G., Gupta, P., Harbach, R.H., Guida, W.C., Dou, Q.P., 2004. Organic copper complexes as a new class of proteasome inhibitors and apoptosis inducers in human cancer cells. Biochem Pharmacol 67, 1139-1151.

Dantuma, N.P., Bott, L.C., 2014. The ubiquitin-proteasome system in neurodegenerative diseases: precipitating factor, yet part of the solution. Front Mol Neurosci 7, 70.

Davies, K.M., Mercer, J.F., Chen, N., Double, K.L., 2016. Copper dyshomoeostasis in Parkinson's disease: implications for pathogenesis and indications for novel therapeutics. Clin Sci (Lond) 130, 565-574.

de Bie, P., van de Sluis, B., Burstein, E., van de Berghe, P.V., Muller, P., Berger, R., Gitlin, J.D., Wijmenga, C., Klomp, L.W., 2007. Distinct Wilson's disease mutations in ATP7B are associated with enhanced binding to COMMD1 and reduced stability of ATP7B. Gastroenterology 133, 1316-1326.

De Strooper, B., Saftig, P., Craessaerts, K., Vanderstichele, H., Guhde, G., Annaert, W., Von Figura, K., Van Leuven, F., 1998. Deficiency of presenilin-1 inhibits the normal cleavage of amyloid precursor protein. Nature 391, 387-390.

Dexter, D.T., Wells, F.R., Lees, A.J., Agid, F., Agid, Y., Jenner, P., Marsden, C.D., 1989. Increased nigral iron content and alterations in other metal ions occurring in brain in Parkinson's disease. J Neurochem 52, 1830-1836.

Esch, F.S., Keim, P.S., Beattie, E.C., Blacher, R.W., Culwell, A.R., Oltersdorf, T., McClure, D., Ward, P.J., 1990. Cleavage of amyloid beta peptide during constitutive processing of its precursor. Science 248, 1122-1124.

Feany, M.B., Bender, W.W., 2000. A Drosophila model of Parkinson's disease. Nature 404, 394-398.

Forman, H.J., Fridovich, I., 1973. On the stability of bovine superoxide dismutase. The effects of metals. J Biol Chem 248, 2645-2649.

Fornai, F., Schlüter, O.M., Lenzi, P., Gesi, M., Ruffoli, R., Ferrucci, M., Lazzeri, G., Busceti, C.L., Pontarelli, F., Battaglia, G., Pellegrini, A., Nicoletti, F., Ruggieri, S., Paparelli, A., Südhof, T.C., 2005. Parkinson-like syndrome induced by continuous MPTP infusion: convergent roles of the ubiquitin-proteasome system and alpha-synuclein. Proc Natl Acad Sci U S A 102, 3413-3418.

Freedman, J.H., Ciriolo, M.R., Peisach, J., 1989. The role of glutathione in copper metabolism and toxicity. The Journal of biological chemistry 264, 5598-5605.

Gaggelli, E., Kozlowski, H., Valensin, D., Valensin, G., 2006. Copper homeostasis and neurodegenerative disorders (Alzheimer's, prion, and Parkinson's diseases and amyotrophic lateral sclerosis). Chem Rev 106, 1995-2044.

Gerber, H., Wu, F., Dimitrov, M., Garcia Osuna, G.M., Fraering, P.C., 2017. Zinc and Copper Differentially Modulate Amyloid Precursor Protein Processing by γ-Secretase and Amyloid-β Peptide Production. J Biol Chem 292, 3751-3767.

Gil-Bea, F.J., Aldanondo, G., Lasa-Fernández, H., López de Munain, A., Vallejo-Illarramendi, A., 2017. Insights into the mechanisms of copper dyshomeostasis in amyotrophic lateral sclerosis. Expert Rev Mol Med 19, e7.

Gong, B., Chen, F., Pan, Y., Arrieta-Cruz, I., Yoshida, Y., Haroutunian, V., Pasinetti, G.M., 2010. SCFFbx2-E3-ligase-mediated degradation of BACE1 attenuates Alzheimer's disease amyloidosis and improves synaptic function. Aging Cell 9, 1018-1031.

Grubman, A., White, A.R., Liddell, J.R., 2014. Mitochondrial metals as a potential therapeutic target in neurodegeneration. Br J Pharmacol 171, 2159-2173.

Guo, Y., Li, C., Wu, D., Wu, S., Yang, C., Liu, Y., Wu, H., Li, Z., 2010. Ultrastructural diversity of inclusions and aggregations in the lumbar spinal cord of SOD1-G93A transgenic mice. Brain Res 1353, 234-244.

Haapasalo, A., Viswanathan, J., Kurkinen, K.M., Bertram, L., Soininen, H., Dantuma, N.P., Tanzi, R.E., Hiltunen, M., 2011. Involvement of ubiquilin-1 transcript variants in protein degradation and accumulation. Commun Integr Biol 4, 428-432.

Haass, C., Hung, A.Y., Schlossmacher, M.G., Teplow, D.B., Selkoe, D.J., 1993. beta-Amyloid peptide and a 3-kDa fragment are derived by distinct cellular mechanisms. J Biol Chem 268, 3021-3024.

Halfdanarson, T.R., Kumar, N., Li, C.Y., Phyliky, R.L., Hogan, W.J., 2008. Hematological manifestations of copper deficiency: a retrospective review. Eur J Haematol 80, 523-531.

Halliwell, B., 1996. Antioxidants in human health and disease. Annu Rev Nutr 16, 33-50.

Halliwell, B., Gutteridge, J.M., 1984. Oxygen toxicity, oxygen radicals, transition metals and disease. Biochem J 219, 1-14.

Hare, D., Ayton, S., Bush, A., Lei, P., 2013. A delicate balance: Iron metabolism and diseases of the brain. Front Aging Neurosci 5, 34.

Harris, L.D., Jasem, S., Licchesi, J.D.F., 2020. The Ubiquitin System in Alzheimer's Disease. Adv Exp Med Biol 1233, 195-221.

He, G., Qing, H., Cai, F., Kwok, C., Xu, H., Yu, G., Bernstein, A., Song, W., 2006. Ubiquitin-proteasome pathway mediates degradation of APH-1. J Neurochem 99, 1403-1412.

He, G., Qing, H., Tong, Y., Cai, F., Ishiura, S., Song, W., 2007. Degradation of nicastrin involves both proteasome and lysosome. J Neurochem 101, 982-992.

Hellman, N.E., Gitlin, J.D., 2002. Ceruloplasmin metabolism and function. Annu Rev Nutr 22, 439-458.

Hong, L., Huang, H.C., Jiang, Z.F., 2014. Relationship between amyloid-beta and the ubiquitin-proteasome system in Alzheimer's disease. Neurol Res 36, 276-282.

Horvath, J., Beris, P., Giostra, E., Martin, P.Y., Burkhard, P.R., 2010. Zinc-induced copper deficiency in Wilson disease. J Neurol Neurosurg Psychiatry 81, 1410-1411.

Hung, Y.H., Bush, A.I., Cherny, R.A., 2010. Copper in the brain and Alzheimer's disease. J Biol Inorg Chem 15, 61-76.

Huster, D., 2010. Wilson disease. Best Pract Res Clin Gastroenterol 24, 531-539.

Hyun, D.H., Lee, M., Halliwell, B., Jenner, P., 2003. Proteasomal inhibition causes the formation of protein aggregates containing a wide range of proteins, including nitrated proteins. J Neurochem 86, 363-373.

Ihara, Y., Chuda, M., Kuroda, S., Hayabara, T., 1999. Hydroxyl radical and superoxide dismutase in blood of patients with Parkinson's disease: relationship to clinical data. J Neurol Sci 170, 90-95.

Islam, M.T., Ogura, T., Esaki, M., 2020. The Cdc48-20S proteasome degrades a class of endogenous proteins in a ubiquitin-independent manner. Biochem Biophys Res Commun 523, 835-840.

James, S.A., Churches, Q.I., de Jonge, M.D., Birchall, I.E., Streltsov, V., McColl, G., Adlard, P.A., Hare, D.J., 2017. Iron, Copper, and Zinc Concentration in Aβ Plaques in the APP/PS1 Mouse Model of Alzheimer's Disease Correlates with Metal Levels in the Surrounding Neuropil. ACS Chem Neurosci 8, 629-637.

Jha, N., Kumar, M.J., Boonplueang, R., Andersen, J.K., 2002. Glutathione decreases in dopaminergic PC12 cells interfere with the ubiquitin protein degradation pathway: relevance for Parkinson's disease? J Neurochem 80, 555-561.

Ji, X.R., Cheng, K.C., Chen, Y.R., Lin, T.Y., Cheung, C.H.A., Wu, C.L., Chiang, H.C., 2018. Dysfunction of different cellular degradation pathways contributes to specific β-amyloid42-induced pathologies. FASEB J 32, 1375-1387.

Kaler, S.G., 2011. ATP7A-related copper transport diseases-emerging concepts and future trends. Nature reviews. Neurology 7, 15-29.

Kaler, S.G., Gallo, L.K., Proud, V.K., Percy, A.K., Mark, Y., Segal, N.A., Goldstein, D.S., Holmes, C.S., Gahl, W.A., 1994. Occipital horn syndrome and a mild Menkes phenotype associated with splice site mutations at the MNK locus. Nat Genet 8, 195-202.

Kalia, L.V., Kalia, S.K., Chau, H., Lozano, A.M., Hyman, B.T., McLean, P.J., 2011. Ubiquitinylation of α-synuclein by carboxyl terminus Hsp70-interacting protein (CHIP) is regulated by Bcl-2-associated athanogene 5 (BAG5). PLoS One 6, e14695.

Kang, J., Lemaire, H.G., Unterbeck, A., Salbaum, J.M., Masters, C.L., Grzeschik, K.H., Multhaup, G., Beyreuther, K., Müller-Hill, B., 1987. The precursor of Alzheimer's disease amyloid A4 protein resembles a cell-surface receptor. Nature 325, 733-736.

Karin, M., Ben-Neriah, Y., 2000. Phosphorylation meets ubiquitination: the control of NF-[kappa]B activity. Annu Rev Immunol 18, 621-663.

Kawahara, K., Hashimoto, M., Bar-On, P., Ho, G.J., Crews, L., Mizuno, H., Rockenstein, E., Imam, S.Z., Masliah, E., 2008. alpha-Synuclein aggregates interfere with Parkin solubility and distribution: role in the pathogenesis of Parkinson disease. J Biol Chem 283, 6979-6987.

Kennerson, M.L., Nicholson, G.A., Kaler, S.G., Kowalski, B., Mercer, J.F., Tang, J., Llanos, R.M., Chu, S., Takata, R.I., Speck-Martins, C.E., Baets, J., Almeida-Souza, L., Fischer, D., Timmerman, V., Taylor, P.E., Scherer, S.S., Ferguson, T.A., Bird, T.D., De Jonghe, P., Feely, S.M., Shy, M.E., Garbern, J.Y., 2010. Missense mutations in the copper transporter gene ATP7A cause X-linked distal hereditary motor neuropathy. Am J Hum Genet 86, 343-352.

Kim, B.E., Nevitt, T., Thiele, D.J., 2008. Mechanisms for copper acquisition, distribution and regulation. Nat Chem Biol 4, 176-185.

Kim, B.E., Smith, K., Petris, M.J., 2003. A copper treatable Menkes disease mutation associated with defective trafficking of a functional Menkes copper ATPase. J Med Genet 40, 290-295.

Kishino, T., Lalande, M., Wagstaff, J., 1997. UBE3A/E6-AP mutations cause Angelman syndrome. Nat Genet 15, 70-73.

Klevay, L.M., 2011. Is the Western diet adequate in copper? J Trace Elem Med Biol 25, 204-212.

Kloetzel, P.M., 2004. The proteasome and MHC class I antigen processing. Biochim Biophys Acta 1695, 225-233.

Kodama, H., Murata, Y., 1999. Molecular genetics and pathophysiology of Menkes disease. Pediatr Int 41, 430-435.

Kong, G.K., Adams, J.J., Cappai, R., Parker, M.W., 2007. Structure of Alzheimer's disease amyloid precursor protein copper-binding domain at atomic resolution. Acta Crystallogr Sect F Struct Biol Cryst Commun 63, 819-824.

La Fontaine, S., Ackland, M.L., Mercer, J.F., 2010. Mammalian copper-transporting P-type ATPases, ATP7A and ATP7B: emerging roles. Int J Biochem Cell Biol 42, 206-209.

La Fontaine, S., Mercer, J.F., 2007. Trafficking of the copper-ATPases, ATP7A and ATP7B: role in copper homeostasis. Arch Biochem Biophys 463, 149-167.

Lelie, H.L., Liba, A., Bourassa, M.W., Chattopadhyay, M., Chan, P.K., Gralla, E.B., Miller, L.M., Borchelt, D.R., Valentine, J.S., Whitelegge, J.P., 2011. Copper and zinc metallation status of

copper-zinc superoxide dismutase from amyotrophic lateral sclerosis transgenic mice. J Biol Chem 286, 2795-2806.

Lin, R., Chen, X., Li, W., Han, Y., Liu, P., Pi, R., 2008. Exposure to metal ions regulates mRNA levels of APP and BACE1 in PC12 cells: blockage by curcumin. Neurosci Lett 440, 344-347.

Linz, R., Lutsenko, S., 2007. Copper-transporting ATPases ATP7A and ATP7B: cousins, not twins. J Bioenerg Biomembr 39, 403-407.

Liu, C.W., Giasson, B.I., Lewis, K.A., Lee, V.M., Demartino, G.N., Thomas, P.J., 2005. A precipitating role for truncated alpha-synuclein and the proteasome in alpha-synuclein aggregation: implications for pathogenesis of Parkinson disease. J Biol Chem 280, 22670-22678.

Liu, J., Sitaram, A., Burd, C.G., 2007. Regulation of copper-dependent endocytosis and vacuolar degradation of the yeast copper transporter, Ctr1p, by the Rsp5 ubiquitin ligase. Traffic 8, 1375-1384.

Lopez Salon, M., Pasquini, L., Besio Moreno, M., Pasquini, J.M., Soto, E., 2003. Relationship between beta-amyloid degradation and the 26S proteasome in neural cells. Exp Neurol 180, 131-143.

Lovell, M.A., Robertson, J.D., Teesdale, W.J., Campbell, J.L., Markesbery, W.R., 1998. Copper, iron and zinc in Alzheimer's disease senile plaques. Journal of the neurological sciences 158, 47-52.

Lücking, C.B., Dürr, A., Bonifati, V., Vaughan, J., De Michele, G., Gasser, T., Harhangi, B.S., Meco, G., Denèfle, P., Wood, N.W., Agid, Y., Brice, A., Group, F.P.s.D.G.S., Disease, E.C.o.G.S.i.P.s., 2000. Association between early-onset Parkinson's disease and mutations in the parkin gene. N Engl J Med 342, 1560-1567.

Luza, S., Opazo, C.M., Bousman, C.A., Pantelis, C., Bush, A.I., Everall, I.P., 2020. The ubiquitin proteasome system and schizophrenia. Lancet Psychiatry 7, 528-537.

Madsen, E., Gitlin, J.D., 2007. Copper and iron disorders of the brain. Annu Rev Neurosci 30, 317-337.

Maine, G.N., Mao, X., Muller, P.A., Komarck, C.M., Klomp, L.W., Burstein, E., 2009. COMMD1 expression is controlled by critical residues that determine XIAP binding. Biochem J 417, 601-609.

Marklund, S.L., 1982. Human copper-containing superoxide dismutase of high molecular weight. Proc Natl Acad Sci U S A 79, 7634-7638.

Maupin-Furlow, J., 2011. Proteasomes and protein conjugation across domains of life. Nat Rev Microbiol 10, 100-111.

Maynard, C.J., Cappai, R., Volitakis, I., Cherny, R.A., White, A.R., Beyreuther, K., Masters, C.L., Bush, A.I., Li, Q.X., 2002. Overexpression of Alzheimer's disease amyloid-beta opposes the age-dependent elevations of brain copper and iron. J Biol Chem 277, 44670-44676.

McCord, J.M., Fridovich, I., 1969. Superoxide dismutase. An enzymic function for erythrocuprein (hemocuprein). J Biol Chem 244, 6049-6055.

McDonough, H., Patterson, C., 2003. CHIP: a link between the chaperone and proteasome systems. Cell Stress Chaperones 8, 303-308.

McLean, C.A., Cherny, R.A., Fraser, F.W., Fuller, S.J., Smith, M.J., Beyreuther, K., Bush, A.I., Masters, C.L., 1999. Soluble pool of Abeta amyloid as a determinant of severity of neurodegeneration in Alzheimer's disease. Ann Neurol 46, 860-866.

Menkes, J.H., Alter, M., Steigleder, G.K., Weakley, D.R., Sung, J.H., 1962. A sex-linked recessive disorder with retardation of growth, peculiar hair, and focal cerebral and cerebellar degeneration. Pediatrics 29, 764-779.

Mercer, J.F., 2001. The molecular basis of copper-transport diseases. Trends Mol Med 7, 64-69.

Miyayama, T., Hiraoka, D., Kawaji, F., Nakamura, E., Suzuki, N., Ogra, Y., 2010. Roles of COMM-domain-containing 1 in stability and recruitment of the copper-transporting ATPase in a mouse hepatoma cell line. Biochem J 429, 53-61.

Møller, L.B., 2015. Small amounts of functional ATP7A protein permit mild phenotype. J Trace Elem Med Biol 31, 173-177.

Montes, S., Rivera-Mancia, S., Diaz-Ruiz, A., Tristan-Lopez, L., Rios, C., 2014. Copper and copper proteins in Parkinson's disease. Oxid Med Cell Longev 2014, 147251.

Mufti, A.R., Burstein, E., Duckett, C.S., 2007. XIAP: cell death regulation meets copper homeostasis. Arch Biochem Biophys 463, 168-174.

Mulder, T.P., Janssens, A.R., Verspaget, H.W., van Hattum, J., Lamers, C.B., 1992. Metallothionein concentration in the liver of patients with Wilson's disease, primary biliary cirrhosis, and liver metastasis of colorectal cancer. J Hepatol 16, 346-350.

Murray, A.W., 2004. Recycling the cell cycle: cyclins revisited. Cell 116, 221-234.

Nakayama, K.I., Nakayama, K., 2005. Regulation of the cell cycle by SCF-type ubiquitin ligases. Semin Cell Dev Biol 16, 323-333.

Nakayama, K.I., Nakayama, K., 2006. Ubiquitin ligases: cell-cycle control and cancer. Nat Rev Cancer 6, 369-381.

Nandi, D., Tahiliani, P., Kumar, A., Chandu, D., 2006. The ubiquitin-proteasome system. J Biosci 31, 137-155.

Nelson, K.T., Prohaska, J.R., 2009. Copper deficiency in rodents alters dopamine beta-mono-oxygenase activity, mRNA and protein level. Br J Nutr 102, 18-28.

Nose, Y., Kim, B.E., Thiele, D.J., 2006. Ctr1 drives intestinal copper absorption and is essential for growth, iron metabolism, and neonatal cardiac function. Cell Metab 4, 235-244.

Nose, Y., Wood, L.K., Kim, B.E., Prohaska, J.R., Fry, R.S., Spears, J.W., Thiele, D.J., 2010. Ctr1 is an apical copper transporter in mammalian intestinal epithelial cells in vivo that is controlled at the level of protein stability. J Biol Chem 285, 32385-32392.

Okado-Matsumoto, A., Fridovich, I., 2001. Subcellular distribution of superoxide dismutases (SOD) in rat liver: Cu,Zn-SOD in mitochondria. J Biol Chem 276, 38388-38393.

Okita, Y., Rcom-H'cheo-Gauthier, A.N., Goulding, M., Chung, R.S., Faller, P., Pountney, D.L., 2017. Metallothionein, Copper and Alpha-Synuclein in Alpha-Synucleinopathies. Front Neurosci 11, 114.

Olanow, C.W., McNaught, K.S., 2006. Ubiquitin-proteasome system and Parkinson's disease. Mov Disord 21, 1806-1823.

Olson, M.I., Shaw, C.M., 1969. Presenile dementia and Alzheimer's disease in mongolism. Brain 92, 147-156.

Opazo, C.M., Lotan, A., Xiao, Z., Zhang, B., Greenough, M.A., Lim, C.M., Trytell, H., Ramirez, A., Ukuwela, A.A., Mawal, C.H., McKenna, J., Saunders, D.N., Burke, R., Gooley, P.R., Bush, A.I., 2021. Copper singaling promotes proteostasis and animal development via allosteric activation of ubiquitin E2 conjugates. bioExiv, doi.org/10.1101/2021.1102.1115.431211.

Owen, C.A., Ludwig, J., 1982. Inherited copper toxicosis in Bedlington terriers: Wilson's disease (hepatolenticular degeneration). Am J Pathol 106, 432-434.

Pan, C., Xiong, Y., Lv, X., Xia, Y., Zhang, S., Chen, H., Fan, J., Wu, W., Liu, F., Wu, H., Zhou, Z., Zhang, L., Zhao, Y., 2017. UbcD1 regulates Hedgehog signaling by directly modulating Ci ubiquitination and processing. EMBO Rep 18, 1922-1934.

Patel, B.N., David, S., 1997. A novel glycosylphosphatidylinositol-anchored form of ceruloplasmin is expressed by mammalian astrocytes. J Biol Chem 272, 20185-20190.

Pawlyk, A.C., Giasson, B.I., Sampathu, D.M., Perez, F.A., Lim, K.L., Dawson, V.L., Dawson, T.M., Palmiter, R.D., Trojanowski, J.Q., Lee, V.M., 2003. Novel monoclonal antibodies demonstrate biochemical variation of brain parkin with age. J Biol Chem 278, 48120-48128.

Perry, J.J., Shin, D.S., Getzoff, E.D., Tainer, J.A., 2010. The structural biochemistry of the superoxide dismutases. Biochim Biophys Acta 1804, 245-262.

Petris, M.J., Mercer, J.F., Culvenor, J.G., Lockhart, P., Gleeson, P.A., Camakaris, J., 1996. Ligand-regulated transport of the Menkes copper P-type ATPase efflux pump from the Golgi apparatus to the plasma membrane: a novel mechanism of regulated trafficking. Embo J 15, 6084-6095.

Petris, M.J., Strausak, D., Mercer, J.F., 2000. The Menkes copper transporter is required for the activation of tyrosinase. Hum Mol Genet 9, 2845-2851.

Phinney, A.L., Drisaldi, B., Schmidt, S.D., Lugowski, S., Coronado, V., Liang, Y., Horne, P., Yang, J., Sekoulidis, J., Coomaraswamy, J., Chishti, M.A., Cox, D.W., Mathews, P.M., Nixon, R.A., Carlson, G.A., St George-Hyslop, P., Westaway, D., 2003. In vivo reduction of amyloid-beta by a mutant copper transporter. Proc Natl Acad Sci U S A 100, 14193-14198.

Popovic, D.M., Leontyev, I.V., Beech, D.G., Stuchebrukhov, A.A., 2010. Similarity of cytochrome c oxidases in different organisms. Proteins 78, 2691-2698.

Praticò, D., 2008. Evidence of oxidative stress in Alzheimer's disease brain and antioxidant therapy: lights and shadows. Ann N Y Acad Sci 1147, 70-78.

Prohaska, J.R., Broderius, M., 2006. Plasma peptidylglycine alpha-amidating monooxygenase (PAM) and ceruloplasmin are affected by age and copper status in rats and mice. Comp Biochem Physiol B Biochem Mol Biol 143, 360-366.

Prohaska, J.R., Broderius, M., Brokate, B., 2003. Metallochaperone for Cu,Zn-superoxide dismutase (CCS) protein but not mRNA is higher in organs from copper-deficient mice and rats. Arch Biochem Biophys 417, 227-234.

Puttaparthi, K., Wojcik, C., Rajendran, B., DeMartino, G.N., Elliott, J.L., 2003. Aggregate formation in the spinal cord of mutant SOD1 transgenic mice is reversible and mediated by proteasomes. J Neurochem 87, 851-860.

Qian, Y., Tiffany-Castiglioni, E., Harris, E.D., 1997. A Menkes P-type ATPase involved in copper homeostasis in the central nervous system of the rat. Brain Res Mol Brain Res 48, 60-66.

Rae, T.D., Schmidt, P.J., Pufahl, R.A., Culotta, V.C., O'Halloran, T.V., 1999. Undetectable intracellular free copper: the requirement of a copper chaperone for superoxide dismutase. Science 284, 805-808.

Rasia, R.M., Bertoncini, C.W., Marsh, D., Hoyer, W., Cherny, D., Zweckstetter, M., Griesinger, C., Jovin, T.M., Fernández, C.O., 2005. Structural characterization of copper(II) binding to alpha-synuclein: Insights into the bioinorganic chemistry of Parkinson's disease. Proc Natl Acad Sci U S A 102, 4294-4299.

Riederer, P., Sofic, E., Rausch, W.D., Schmidt, B., Reynolds, G.P., Jellinger, K., Youdim, M.B., 1989. Transition metals, ferritin, glutathione, and ascorbic acid in parkinsonian brains. J Neurochem 52, 515-520.

Rose, F., Hodak, M., Bernholc, J., 2011. Mechanism of copper(II)-induced misfolding of Parkinson's disease protein. Sci Rep 1, 11.

Santner, A., Uversky, V.N., 2010. Metalloproteomics and metal toxicology of α-synuclein. Metallomics 2, 378-392.

Scheiber, I., Dringen, R., Mercer, J.F., 2013. Copper: effects of deficiency and overload. Met Ions Life Sci 13, 359-387.

Scheiber, I.F., Mercer, J.F., Dringen, R., 2014. Metabolism and functions of copper in brain. Prog Neurobiol 116, 33-57.

Scheinberg, I.H., Sternlieb, I., 1996. Wilson disease and idiopathic copper toxicosis. Am J Clin Nutr 63, 842S-845S.

Schlossmacher, M.G., Frosch, M.P., Gai, W.P., Medina, M., Sharma, N., Forno, L., Ochiishi, T., Shimura, H., Sharon, R., Hattori, N., Langston, J.W., Mizuno, Y., Hyman, B.T., Selkoe, D.J., Kosik, K.S., 2002. Parkin localizes to the Lewy bodies of Parkinson disease and dementia with Lewy bodies. Am J Pathol 160, 1655-1667.

Seabrook, G.R., Smith, D.W., Bowery, B.J., Easter, A., Reynolds, T., Fitzjohn, S.M., Morton, R.A., Zheng, H., Dawson, G.R., Sirinathsinghji, D.J., Davies, C.H., Collingridge, G.L., Hill, R.G., 1999. Mechanisms contributing to the deficits in hippocampal synaptic plasticity in mice lacking amyloid precursor protein. Neuropharmacology 38, 349-359.

Shimura, H., Schwartz, D., Gygi, S.P., Kosik, K.S., 2004. CHIP-Hsc70 complex ubiquitinates phosphorylated tau and enhances cell survival. J Biol Chem 279, 4869-4876.

Shin, Y., Klucken, J., Patterson, C., Hyman, B.T., McLean, P.J., 2005. The co-chaperone carboxyl terminus of Hsp70-interacting protein (CHIP) mediates alpha-synuclein degradation decisions between proteasomal and lysosomal pathways. J Biol Chem 280, 23727-23734.

Shults, C.W., 2006. Lewy bodies. Proc Natl Acad Sci U S A 103, 1661-1668.

Singleton, W.C., McInnes, K.T., Cater, M.A., Winnall, W.R., McKirdy, R., Yu, Y., Taylor, P.E., Ke, B.X., Richardson, D.R., Mercer, J.F., La Fontaine, S., 2010. Role of glutaredoxin1 and glutathione in regulating the activity of the copper-transporting P-type ATPases, ATP7A and ATP7B. The Journal of biological chemistry 285, 27111-27121.

Sisodia, S.S., 1992. Beta-amyloid precursor protein cleavage by a membrane-bound protease. Proc Natl Acad Sci U S A 89, 6075-6079.

Son, M., Puttaparthi, K., Kawamata, H., Rajendran, B., Boyer, P.J., Manfredi, G., Elliott, J.L., 2007. Overexpression of CCS in G93A-SOD1 mice leads to accelerated neurological deficits with severe mitochondrial pathology. Proc Natl Acad Sci U S A 104, 6072-6077.

Song, I.S., Chen, H.H., Aiba, I., Hossain, A., Liang, Z.D., Klomp, L.W., Kuo, M.T., 2008. Transcription factor Sp1 plays an important role in the regulation of copper homeostasis in mammalian cells. Mol Pharmacol 74, 705-713.

Spillantini, M.G., Schmidt, M.L., Lee, V.M., Trojanowski, J.Q., Jakes, R., Goedert, M., 1997. Alpha-synuclein in Lewy bodies. Nature 388, 839-840.

Squitti, R., Polimanti, R., Siotto, M., Bucossi, S., Ventriglia, M., Mariani, S., Vernieri, F., Scrascia, F., Trotta, L., Rossini, P.M., 2013. ATP7B variants as modulators of copper dyshomeostasis in Alzheimer's disease. Neuromolecular Med 15, 515-522.

Squitti, R., Siotto, M., Arciello, M., Rossi, L., 2016. Non-ceruloplasmin bound copper and ATP7B gene variants in Alzheimer's disease. Metallomics 8, 863-873.

Squitti, R., Ventriglia, M., Gennarelli, M., Colabufo, N.A., El Idrissi, I.G., Bucossi, S., Mariani, S., Rongioletti, M., Zanetti, O., Congiu, C., Rossini, P.M., Bonvicini, C., 2017. Non-Ceruloplasmin Copper Distincts Subtypes in Alzheimer's Disease: a Genetic Study of ATP7B Frequency. Mol Neurobiol 54, 671-681.

Staub, O., Gautschi, I., Ishikawa, T., Breitschopf, K., Ciechanover, A., Schild, L., Rotin, D., 1997. Regulation of stability and function of the epithelial Na+ channel (ENaC) by ubiquitination. EMBO J 16, 6325-6336.

Sturtz, L.A., Diekert, K., Jensen, L.T., Lill, R., Culotta, V.C., 2001. A fraction of yeast Cu,Zn-superoxide dismutase and its metallochaperone, CCS, localize to the intermembrane space of mitochondria. A physiological role for SOD1 in guarding against mitochondrial oxidative damage. J Biol Chem 276, 38084-38089.

Su, L.C., Ravanshad, S., Owen, C.A., McCall, J.T., Zollman, P.E., Hardy, R.M., 1982. A comparison of copper-loading disease in Bedlington terriers and Wilson's disease in humans. Am J Physiol 243, G226-230.

Tao, T.Y., Liu, F., Klomp, L., Wijmenga, C., Gitlin, J.D., 2003. The copper toxicosis gene product Murr1 directly interacts with the Wilson disease protein. J Biol Chem 278, 41593-41596.

Tavassoly, O., Nokhrin, S., Dmitriev, O.Y., Lee, J.S., 2014. Cu(II) and dopamine bind to α-synuclein and cause large conformational changes. FEBS J 281, 2738-2753.

Taylor, R.C., Dillin, A., 2011. Aging as an event of proteostasis collapse. Cold Spring Harb Perspect Biol 3.

Tetzlaff, J.E., Putcha, P., Outeiro, T.F., Ivanov, A., Berezovska, O., Hyman, B.T., McLean, P.J., 2008. CHIP targets toxic alpha-Synuclein oligomers for degradation. J Biol Chem 283, 17962-17968.

Tokuda, E., Okawa, E., Ono, S., 2009. Dysregulation of intracellular copper trafficking pathway in a mouse model of mutant copper/zinc superoxide dismutase-linked familial amyotrophic lateral sclerosis. J Neurochem 111, 181-191.

Tórsdóttir, G., Kristinsson, J., Sveinbjörnsdóttir, S., Snaedal, J., Jóhannesson, T., 1999. Copper, ceruloplasmin, superoxide dismutase and iron parameters in Parkinson's disease. Pharmacol Toxicol 85, 239-243.

Tsai, C.Y., Liebig, J.K., Tsigelny, I.F., Howell, S.B., 2015. The copper transporter 1 (CTR1) is required to maintain the stability of copper transporter 2 (CTR2). Metallomics 7, 1477-1487.

Uversky, V.N., Li, J., Fink, A.L., 2001. Metal-triggered structural transformations, aggregation, and fibrillation of human alpha-synuclein. A possible molecular NK between Parkinson's disease and heavy metal exposure. J Biol Chem 276, 44284-44296.

Valimberti, I., Tiberti, M., Lambrughi, M., Sarcevic, B., Papaleo, E., 2015. E2 superfamily of ubiquitin-conjugating enzymes: constitutively active or activated through phosphorylation in the catalytic cleft. Sci Rep 5, 14849.

van De Sluis, B., Rothuizen, J., Pearson, P.L., van Oost, B.A., Wijmenga, C., 2002. Identification of a new copper metabolism gene by positional cloning in a purebred dog population. Hum Mol Genet 11, 165-173.

Vassar, R., Bennett, B.D., Babu-Khan, S., Kahn, S., Mendiaz, E.A., Denis, P., Teplow, D.B., Ross, S., Amarante, P., Loeloff, R., Luo, Y., Fisher, S., Fuller, J., Edenson, S., Lile, J., Jarosinski, M.A., Biere, A.L., Curran, E., Burgess, T., Louis, J.C., Collins, F., Treanor, J., Rogers, G., Citron, M., 1999. Beta-secretase cleavage of Alzheimer's amyloid precursor protein by the transmembrane aspartic protease BACE. Science 286, 735-741.

Vega, I.E., Cui, L., Propst, J.A., Hutton, M.L., Lee, G., Yen, S.H., 2005. Increase in tau tyrosine phosphorylation correlates with the formation of tau aggregates. Brain Res Mol Brain Res 138, 135-144.

Viswanathan, J., Haapasalo, A., Böttcher, C., Miettinen, R., Kurkinen, K.M., Lu, A., Thomas, A., Maynard, C.J., Romano, D., Hyman, B.T., Berezovska, O., Bertram, L., Soininen, H., Dantuma, N.P., Tanzi, R.E., Hiltunen, M., 2011. Alzheimer's disease-associated ubiquilin-1 regulates presenilin-1 accumulation and aggresome formation. Traffic 12, 330-348.

Vonk, W.I., Bartuzi, P., de Bie, P., Kloosterhuis, N., Wichers, C.G., Berger, R., Haywood, S., Klomp, L.W., Wijmenga, C., van de Sluis, B., 2011. Liver-specific Commd1 knockout mice are susceptible to hepatic copper accumulation. PLoS One 6, e29183.

Vonk, W.I., de Bie, P., Wichers, C.G., van den Berghe, P.V., van der Plaats, R., Berger, R., Wijmenga, C., Klomp, L.W., van de Sluis, B., 2012. The copper-transporting capacity of ATP7A mutants associated with Menkes disease is ameliorated by COMMD1 as a result of improved protein expression. Cell Mol Life Sci 69, 149-163.

Vonk, W.I., Kakkar, V., Bartuzi, P., Jaarsma, D., Berger, R., Hofker, M.H., Klomp, L.W., Wijmenga, C., Kampinga, H.H., van de Sluis, B., 2014. The Copper Metabolism MURR1 domain protein 1 (COMMD1) modulates the aggregation of misfolded protein species in a client-specific manner. PLoS One 9, e92408.

Wake, S.A., Mercer, J.F., 1985. Induction of metallothionein mRNA in rat liver and kidney after copper chloride injection. Biochem J 228, 425-432.

Wang, H., Ying, Z., Wang, G., 2012. Ataxin-3 regulates aggresome formation of copper-zinc superoxide dismutase (SOD1) by editing K63-linked polyubiquitin chains. J Biol Chem 287, 28576-28585.

Wang, X., Moualla, D., Wright, J.A., Brown, D.R., 2010. Copper binding regulates intracellular alpha-synuclein localisation, aggregation and toxicity. J Neurochem 113, 704-714.

Ward, C.L., Omura, S., Kopito, R.R., 1995. Degradation of CFTR by the ubiquitin-proteasome pathway. Cell 83, 121-127.

Watanabe, T., Hikichi, Y., Willuweit, A., Shintani, Y., Horiguchi, T., 2012. FBL2 regulates amyloid precursor protein (APP) metabolism by promoting ubiquitination-dependent APP degradation and inhibition of APP endocytosis. J Neurosci 32, 3352-3365.

Wegmann, S., Medalsy, I.D., Mandelkow, E., Müller, D.J., 2013. The fuzzy coat of pathological human Tau fibrils is a two-layered polyelectrolyte brush. Proc Natl Acad Sci U S A 110, E313-321.

White, A.R., Reyes, R., Mercer, J.F., Camakaris, J., Zheng, H., Bush, A.I., Multhaup, G., Beyreuther, K., Masters, C.L., Cappai, R., 1999. Copper levels are increased in the cerebral cortex and liver of APP and APLP2 knockout mice. Brain Res 842, 439-444.

Wright, J.A., Wang, X., Brown, D.R., 2009. Unique copper-induced oligomers mediate alpha-synuclein toxicity. FASEB J 23, 2384-2393.

Xiao, Y., Chen, D.I., Zhang, X., Cui, Q., Fan, Y., Bi, C., Dou, Q.P., 2010. Molecular study on copper-mediated tumor proteasome inhibition and cell death. Int J Oncol 37, 81-87.

Zetterström, P., Stewart, H.G., Bergemalm, D., Jonsson, P.A., Graffmo, K.S., Andersen, P.M., Brännström, T., Oliveberg, M., Marklund, S.L., 2007. Soluble misfolded subfractions of mutant superoxide dismutase-1s are enriched in spinal cords throughout life in murine ALS models. Proc Natl Acad Sci U S A 104, 14157-14162.

Zhang, B., Binks, T., Burke, R., 2020. The E3 ubiquitin ligase Slimb/β-TrCP is required for normal copper homeostasis in Drosophila. Biochim Biophys Acta Mol Cell Res 1867, 118768.

Zhang, Z., Wang, H., Yan, M., Zhang, C., 2017. Novel copper complexes as potential proteasome inhibitors for cancer treatment (Review). Mol Med Rep 15, 3-11.

Zhou, B., Gitschier, J., 1997. hCTR1: a human gene for copper uptake identified by complementation in yeast. Proceedings of the National Academy of Sciences of the United States of America 94, 7481-7486.

CHAPTER 2: MATERIALS AND METHODS

2.1 Materials

2.1.1 *Drosophila melanogaster* strains

2.1.1.1 Wild type strain

A w^{1118} strain (BL3605, Bloomington Stock Centre, Indiana, USA) was applied as a wild type control in all experiments.

2.1.1.2 GAL4 strains

All GAL4 strains used are listed below: *Pannier (Pnr)-Gal4* (BL3039), *GMR-Gal4* (BL9146), *tub-Gal4*, *Mex-Gal4* (Phillips and Thomas, 2006), *HR-Gal4* (gift from P. Batterham, University of Melbourne, Australia) (Chung et al., 2007), *En-Gal4*, *Ey-Gal4*, *CCAP-Gal4* (gift from B. White, NIH, USA) (Luan et al., 2006), *Elav-Gal4* (BL458). Table 1 shows the expression pattern of different *GAL4* drivers.

	GAL4 drivers							
	Pnr-Gal4	*GMR-Gal4*	*tub-Gal4*	*Mex-Gal4*	*HR-Gal4*	*En-Gal4*	*Ey-Gal4*	*Elav-Gal4*
Expression pattern	Wing disc	Eye disc	Ubiquitous	Midgut	Midgut	Posterior Compartment of wing imaginal discs	Eye imaginal disc	All neurons

Table 1 Expression pattern of different *GAL4* drivers

2.1.1.3 Temperature sensitive strain

tubP-GAL80ts/CyO; Pnr-Gal4/TM6B (BL67060)

2.1.1.4 RNA interference strains

RNAi lines obtained from the Vienna *Drosophila* Resource Centre (VDRC) include V15303 (*EloC*), V107825 and V34274 (*Slmb*), V108127 (*cnc*), V108159 and V8315 (*ATP7*), V108920 (*Vhl*), V46757 and V46758 (*Ctr1A*). Other *RNAi* lines were purchased from Bloomington Drosophila Stock Center, including BL27030 (*Ddc*), BL34988 (*Cul2*), BL33894 (*sima*),

BL34034 and BL67915 (*Rpn9*), BL35431 (*UbcD1*), BL50727 (*Vhl*), BL65875 (*ple*) (all these stocks are TRiP lines).

2.1.1.5 Overexpression strains

Overexpression lines *UAS-Ddc* (BL37540) and *UAS-sima* (BL9582) were obtained from the Bloomington *Drosophila* Stock Center while *UAS-cnc::HA* (F000602) was purchased from FlyORF. *pUAST-ATP7::FLAG* and *pUAST-dNCtr1A::FLAG* (missing the first ~20 amino acids) has been described previously (Binks et al., 2010), and *UAS-Slmb* was a gift from Prof. François Rouyer (Institut des Neurosciences Paris Saclay, France) (Zhang et al., 2020).

2.1.1.6 Other *Drosophila* strains

Double balancer (*w; IF/CyO; MKRS/TM6B*, gift from G. Hime, University of Melbourne, Australia); *UAS-Golgi::RFP* (BL30907); *Ctr1B::eYFP* and *MtnB::eYFP* (gift from W. Schaffner, University of Zurich, Switzerland) (Selvaraj et al., 2005), *gATP7^{WT}::GFP* (Mercer et al., 2017).

2.1.1.7 ATP7 interacting protein *RNAi* screening strains

All ATP7 interacting protein *RNAi* lines were obtained from the Vienna *Drosophila* Resource Centre, and Table 2 shows the stock ID and the mammalian gene names and their *Drosophila* orthologues.

VDRC ID	CG number	Mammalian	*Drosophila*	Library	Insertion site	Notes
100483	CG8209	UBXN1	CG8209	KK stocks	30B	Used in Chapter 4 and Chapter 6
100620	CG1489	PSMC5	Rpt6	KK stocks	40D and 30B	
101467	CG5378	PSMD6	Rpn7	KK stocks	40D and 30B	
103733	CG10230	PSMD13	Rpn9	KK stocks	-	
104167	CG6235	PPP2R2A	tws	KK stocks	-	
34340				GD stocks	-	
105740	CG9291	TCEB1	EloC	KK stocks	30B	

15303				GD stocks	-	Used in Chapter 4 and Chapter 5
105483	CG1906	PPM1B	Alph	KK stocks	30B	Used in Chapter 4 and Chapter 6
32476				GD stocks	-	
105973	CG5289	PSMC1	Rpt2	KK stocks	40D	
106180	CG10417	PPM1G	CG10417	KK stocks	40D and 30B	
106328	CG5595	RNF2	Sce	KK stocks	30B	
27465				GD stocks	-	
106457	CG11888	PSMD1	Rpn2	KK stocks	-	
106971	CG7392	STRN	Cka	KK stocks	-	
35234				GD stocks	-	
107447	CG5203	STUB1	Chi	KK stocks	40D	
43934				-	-	
107621	CG4733	PPP2R5D	CG4733	KK stocks	30B	
107815	CG16983	SKP1	SkpA	KK stocks	30B	
32879				TRiP	-	
108206	CG10542	RNF20	Bre1	KK stocks	-	
108582	CG42641	PSMD3	Rpn3	KK stocks	30B	
108834	CG1341	PSMC2	Rpt1	KK stocks	30B	
109415	CG42616	CUL3	Cul3	KK stocks	30B	
25875				GD stocks	-	
109824	CG34389	BRCC3	Cv-c	KK stocks	30B	
32329				GD stocks	-	
110659	CG7619	PSMD4	Rpn10	KK stocks	30B	
34894	CG4733	PPP2R5D	CG4733	GD stocks	-	
35029	CG5659	ARIH1	Ari-1	GD stocks	-	
39591					-	
49681	CG18495	PSMA6	Prosα1	GD stocks	-	

Table 2 ATP7 interactome members possessing ubiquitin-protein transferase activity

2.1.1.8 UbcD1 substrate *RNAi* screening strains

All UbcD1 substrate *RNAi* lines were obtained from the Vienna *Drosophila* Resource Centre, and Table 3 shows the stock ID and the mammalian gene names and their *Drosophila* orthologues.

VDRC ID	CG number	Mammalian	*Drosophila*	Library	Insertion site	Notes
100392	CG16725	SMN	Smn	KK stocks	40D	Used in Chapter 6
45447				GD stocks	-	
100703	CG4904	PSMA1	Prosα6	KK stocks	30B	
26653				GD stocks	-	
102751	CG10965	Corp	Corp	KK stocks	30B	
16130				GD stocks	-	
103001	CG33336	TP53	p53	KK stocks	30B	
45138				GD stocks	-	
45139				GD stocks	-	
103575	CG3329	PSMB7	Prosβ2	KK stocks	40D	
104437	CG32446	Atox1	Atox1	KK stocks	30B	
23057				GD stocks	-	
105351	CG8293	DIAP	Diap2	KK stocks	30B	
2973				GD stocks	-	
105973	CG5289	PSMC1	Rpt2	KK stocks	40D	
107628	CG12323	ARPC3	Prosβ5	KK stocks	40D and 30B	
108296	CG14472	UBR4	poe	KK stocks	40D and 30B	
17648				GD stocks	-	
28444	CG10679	NEDD8	Nedd8	GD stocks	-	
28445				GD stocks	-	
28985	CG8892	UBXN7	CG8892	GD stocks	-	
49681	CG18495	PSMA6	Prosα1	GD stocks	-	

Table 3 UbcD1 potential substrates

2.1.2 Copper chloride and copper chelator

In order to create high copper or low copper conditions, copper chloride (CuCl$_2$; Merck, Whitehouse station, NJ, USA) or copper chelator Bathocuproine disulfonate (BCS; Sigma-Aldrich, St. Louis, MO, USA) was added to *Drosophila* media, respectively. Copper chloride was dissolved in MilliQ water to make 200 mM stock solution and stored at room temperature. The 300 µM stock solution of Bathocuproine disulfonate was prepared by dissolving in MilliQ water and stored in the dark at -20ºC.

2.1.3 *Drosophila* media

2.1.3.1 Standard media

Cooking 15 L fly food: 108 g Potassium tartrate, 6.75 g Calcium chloride, 72 g agar, 162 g yeast, 720 g dextrose and 360 g raw sugar were dissolved in 10.62 L of hot water. The mixture was boiled, followed by the addition of 900 g semolina and 2.7 L cold water. Once the mixture was boiled again, 1.8 L water, 108 ml Nipagen and 54 ml propionic acid were added. The recipe of standard medium is listed in Table 4.

Litres	15
Water (hot) (L)	10.62
Potassium tartrate (g)	108
Calcium chloride (g)	6.75
Agar (g)	72
Yeast (g)	162
Dextrose (g)	720
Sugar (raw) (g)	360
Water (cold) (L)	2.7
Semolina (g)	900
Water (L)	1.8
Nipagen (ml)	108
Propionic acid (ml)	54

Table 4 Recipe of standard medium

2.1.3.2 Copper-deficient and copper-supplemented media

Standard medium was supplemented with either 300 μM BCS or 1- or 2-mM $CuCl_2$ to make copper-deficient or copper-supplemented food medium.

2.1.3.3 Apple juice agar

4.5% w/v agar, 25% v/v apple juice, 1.25% w/v sucrose.

1 L apple juice agar: 45 g agar and 12.5 g sucrose were weighed and added in 500 ml MilliQ water and mixed thoroughly. After the addition of 250 ml apple juice, MilliQ water was then added up to 1 L. The mixture was aliquoted into 5 bottles (200 ml each), and stored at room temperature after autoclaving.

2.1.4 Buffers and solutions

$1\times$ PBS (Phosphate-buffered saline): 7.5 mM Na_2HPO_4, 2.5 mM NaH_2PO_4, 145 mM NaCl, pH7.4. MilliQ water to 1 L

$1\times$ PBT (Phosphate-buffered saline with Trition-X100): $1\times$ PBS, 0.1% or 0.5% Triton-X100

$10\times$ SDS page buffer: 288.6 g Glycine, 60.6 g Tris Base, 20 g SDS (Sodium dodecyl sulfate), MilliQ water to 2 L

$1\times$ Transfer buffer (semidry transfer): 11.64 g Tris Base, 5.86 g Glycine, 7.5 ml 10% SDS, 400 ml Methanol, MilliQ water to 2 L.

$1\times$ Low salt Tween 20-Tris Base Sodium (LSTTBS): 24.2 g Tris Base, 87.66 g NaCl, 5 g Tween 20, MilliQ water to 2 L, pH7.5.

5% Skim milk buffer: 5 g skim milk powder dissolved in $1\times$ LSTTBS to 1 ml.

2.1.5 DNA and RNA purification kits

Wizard®Plus SV Miniprep kit (PAA1460, Promega, Madison, WI, USA)

Wizard®DNA Clean Up kit (PAA9341, Promega)

Trizol plus RNA purification kit (12183555, Invitrogen, Carlsbad, CA, USA)

Note: all kits used as per manufacturer's instructions.

2.1.6 cDNA synthesis kit

Tetro cDNA Synthesis Kit (BIO-65042, Invitrogen)

2.1.7 Primers for real-time PCR

Gene name	Forward primer	Reverse primer
Rpl23	GACAACACCGGAGCCAAGAACC	GTTTGCGCTGCCGAATAACCAC
Vhl	CGGATCAGCTGGTTGACGTA	CCGTGGATAATCCTCCGTGG
Rpn9	ATGTCCAATCCTCAGCCTAATGT	TGGTCAGCTCATTCCAGAGTTT
Ctr1A	GACCACGCCCATCACAGTG	GATCAGGTCGAACATGGAAGC
MtnB	GGTTTGCAAGGGGTTGTGGAA	CAGTTGTCCCCGCACTTTTG
Sima	GCCCCAAAAACCAATCTCACG	CAGCCGAGAGTTCCATGAATATC
cnc	CTGCATCGTCATGTCTTCCAGT	AGCAAGTAGACGGAGCCAT

Table 5 Sequences of primers used for real-time PCR

2.2 Methods

2.2.1 Fly maintenance

All *Drosophila* strains and crosses were maintained on standard medium in the dark under variable humidity at 25°C, unless stated otherwise.

2.2.2 Basic *Drosophila* crosses

Each cross for investigating genetic interactions consisted of 1-3 males and 6-8 virgin females. All crosses were cultured at 25°C unless otherwise stated and transferred to fresh vials every three days.

2.2.3 Microscopy

2.2.3.1 Phenotypic analysis

Microscopy was used for recording the phenotypic defects produced by knockdown or overexpression of candidate genes. Specific procedures are listed as follows. Adult flies were anaesthetized using CO_2, then mounted directly onto white plasticine and monitored with a Leica MZ6 stereomicroscope. All images of adult fly phenotypes were recorded with a Leica DFC295 digital camera using Leica Application Suite (LAS) software. All adult fly images are representative of > 10 individuals of that genotype / temperature, unless stated otherwise. Where mild variation existed between individuals of a particular genotype, images were chosen to represent the intermediate phenotype. Where considerable variation presented, examples of mild, moderate and severe phenotypes are all provided. All adult flies were imaged between 24 and 72 hours of age.

2.2.3.2 Imaging Ctr1B::eYFP or MtnB::eYFP expression in the midgut

In order to detect the alteration of copper levels after knockdown or overexpression of our genes of interest, midgut microscopy was performed by using reporter genes *Ctr1B::eYFP* or *MtnB::eYFP*. The expression level of reporter genes could indirectly indicate the change of copper levels. Specific procedures are listed as follows. Wandering 3rd instar larvae were inverted in cold PBS, and then fixed with 4% PFA for 30 min on ice. Afterwards, larvae were dissected and directly mounted on slides with PermaFluor (Thermo Scienti!c, Fremont, CA, USA) for fluorescence microscopy using either a Leica M165 FC Fluorescent Stereo Microscope with a Leica DFC450 C digital camera or a CV1000 laser confocal microscope (CellVoyager CV1000, Yokogawa, Tokyo, Japan). The grey values of Ctr1B::eYFP or MtnB::eYFP intensity in the copper cell region were obtained by ImageJ (version: 2.0.o-rc-65/1.52a), and then divided by each copper cell region area to get average grey values for statistical analysis. The copper cell region is the area in the middle midgut defined by an extremely low pH (pH < 3) and the place where copper ions are absorbed from the diet (Strand and Micchelli, 2011).

2.2.3.3 Protein localization studies

Protein localization techniques were used for detecting whether modifying our genes of interest could affect ATP7 intracellular localization in the midgut, using a transgenic reporter gene *gATP7^{WT}::GFP*. Specific procedures are listed as follows. Whole midguts from wandering 3rd instar larvae were dissected in cold PBS, and then fixed for 30 min in 4% paraformaldehyde (PFA, v/v, fisher scientific) on ice. Tissues were stained with 1× DAPI (4′,6-diamidino-2-phenylindole, 1 μg / ml, Bio-Rad, diluted in MilliQ water) for 15 min at RT. Finally, midguts were mounted onto slides. Monitoring and recording GFP or RFP was performed within 1 h of dissection/ mounting for optimal fluorescent signal using a CV1000 confocal microscope.

2.2.4 Western blot analysis

10 adult heads per sample were lysed in 50 μl of 1% Triton X-100 lysis buffer (50 mM Tris-HCl (pH 7.5), 100 mM NaCl, 1 mM EDTA, 1% Triton-X, 10% glycerol, complete EDTA-free protease inhibitor mixture (Roche Applied Science)). Equal volumes of lysates were separated by SDS-PAGE (Mini-PROTEAN® TGXTM Precast Gels Any kDTM, Bio-Rad). ATP7::Flag and Ctr1A::Flag were detected using mouse anti-Flag primary antibody (1:5000; Sigma-Aldrich, St. Louis, MO, USA) and HRP-conjugated anti-mouse secondary antibody (1:5000; Southern Biotech, Birmingham, AL, USA). Immunoblots were developed using ECL Prime (GE Healthcare, Chicago, IL, USA) and imaged using a chemiluminescence detector (Vilber Lourmat). Image J was used to quantify the grey value of each western blot band; in cases where the bands 'frowned' (i.e. were not straight), the entire band-containing region was included for quantification. Relative grey values were then calculated by dividing the grey value for each anti-Flag band by the grey value for the corresponding loading control (anti-Tubulin).

2.2.5 *Drosophila* survival experiments

Drosophila survival experiments were performed to test whether copper levels could affect the survival rate of adult flies after modifying our genes of interest. Specific procedures are listed as follows. In all survival experiments, crosses were set up in a cage with > 50 virgin females and 20–25 males. To assess adult survival, 50 1st instar larvae (=1 replicate) for each group were transferred onto standard medium or medium supplemented with 1 or 2 mM CuCl$_2$ or 300 μM BCS. Successful adult survival was classified as the ability of the adults to emerge from

their pupal cases. The survival of each genotype was calculated as percentage of expected. n ≥ 4 for each genotype / food type combination.

2.2.6 Temporal control of gene manipulation

Temperature shift experiments were used to examine the phenotypic defects generated by manipulation of genes which caused lethality after up- or down- regulation. In this study, the *tubP-GAL80ts/CyO; Pnr-Gal4/TM6B* (BL67060) stock was used to perform temperature shift experiments to test phenotypic defects caused by overexpression of *sima* and *cnc*. *Pnr-Gal4* activity was suppressed at low temperature (22°C) and switched on at high temperature (29°C). All crosses were maintained at 22°C and transferred to a new vial every day in the afternoon. When progeny developed to early pupal stages, fly vials were transferred to 29°C. The phenotypic defects caused by *sima* and *cnc* overexpression were assessed in surviving adults.

2.2.7 Real-time PCR

Total RNA was extracted using the Trizol plus RNA purification kit (Invitrogen), including DNase treatment. cDNA was transcribed from 1 µg of total RNA in a 20 µl reaction by using AMV Reverse Transcriptase (Invitrogen). Primers for real-time PCR were designed using Primer3 software; primer sequences are listed in Table 5.

QuantStudio 3 Real-Time PCR System (Applied Biosystems, Foster City, CA, USA) was applied to perform real-time PCR. cDNA was amplified in a 10 µl reaction containing 1 µM of each primer and 5 µl of 2×SYBR Select Master Mix (Applied Biosystems, A25742). The amount of gene product in each sample was determined using ΔCT method. *Rpl23* was used as a housekeeping gene. The amount of gene product for each gene of interest was expressed relative to that of *Rpl23* to normalize for differences in total cDNA between samples.

2.2.8 Sequence alignment

Sequence alignment is a way of arranging the sequences of DNA, RNA, or protein to identify regions of similarity between the sequences. In this study, we aligned two amino acid sequences (obtained from the NCBI protein database) by using the National Center for Biotechnology Information's (NCBI) Protein BLAST function.

2.2.9 Statistical analysis

All data were presented as mean ± S.E.M. An independent Student's t-test was applied using GraphPad Prism 7.0b (GraphPad, San Diego, CA, USA). P < 0.05 was considered as a statistically significant difference.

References:

Binks, T., Lye, J.C., Camakaris, J., Burke, R., 2010. Tissue-specific interplay between copper uptake and efflux in Drosophila. J Biol Inorg Chem 15, 621-628.

Chung, H., Bogwitz, M.R., McCart, C., Andrianopoulos, A., Ffrench-Constant, R.H., Batterham, P., Daborn, P.J., 2007. Cis-regulatory elements in the Accord retrotransposon result in tissue-specific expression of the Drosophila melanogaster insecticide resistance gene Cyp6g1. Genetics 175, 1071-1077.

Luan, H., Lemon, W.C., Peabody, N.C., Pohl, J.B., Zelensky, P.K., Wang, D., Nitabach, M.N., Holmes, T.C., White, B.H., 2006. Functional dissection of a neuronal network required for cuticle tanning and wing expansion in Drosophila. J Neurosci 26, 573-584.

Mercer, S.W., Wang, J., Burke, R., 2017. In Vivo Modeling of the Pathogenic Effect of Copper Transporter Mutations That Cause Menkes and Wilson Diseases, Motor Neuropathy, and Susceptibility to Alzheimer's Disease. J Biol Chem 292, 4113-4122.

Phillips, M.D., Thomas, G.H., 2006. Brush border spectrin is required for early endosome recycling in Drosophila. J Cell Sci 119, 1361-1370.

Selvaraj, A., Balamurugan, K., Yepiskoposyan, H., Zhou, H., Egli, D., Georgiev, O., Thiele, D.J., Schaffner, W., 2005. Metal-responsive transcription factor (MTF-1) handles both extremes, copper load and copper starvation, by activating different genes. Genes Dev 19, 891-896.

Strand, M., Micchelli, C.A., 2011. Quiescent gastric stem cells maintain the adult Drosophila stomach. Proc Natl Acad Sci U S A 108, 17696-17701.

Zhang, B., Binks, T., Burke, R., 2020. The E3 ubiquitin ligase Slimb/β-TrCP is required for normal copper homeostasis in Drosophila. Biochim Biophys Acta Mol Cell Res 1867, 118768.

CHAPTER 3: THE E3 UBIQUITIN LIGASE Slmb/β-TrCP IS REQUIRED FOR NORMAL COPPER HOMEOSTASIS IN DROSOPHILA

The E3 ubiquitin ligase Slimb/β-TrCP is required for normal copper homeostasis in *Drosophila*

Bichao Zhang, Tim Binks, Richard Burke*

School of Biological Sciences, Monash University, Wellington Rd, Clayton 3800, VIC, Australia

ARTICLE INFO

Keywords:
Slmb
β-TrCP
E3 ubiquitin ligase
Copper
CTR1
ATP7

ABSTRACT

The *Drosophila Slimb* (*Slmb*) gene encodes a Skp1-Cul1-F-box (SCP) E3 ubiquitin ligase orthologous to the human β-TrCP/BTRC protein. Slmb and/or BTRC play regulatory roles in numerous biological processes by ubiquitinating several substrate proteins which are then targeted for proteasomal degradation. Here, we demonstrate an additional role for Slmb in maintaining cellular copper homeostasis. In the thorax, midgut and eye, *Slmb* knockdown causes copper deficiency phenotypes which can be rescued by increasing cellular copper levels via decreased efflux or increased uptake. Furthermore, *Slmb* knockdown results in decreased levels of the copper transporters Ctr1A and ATP7, indicating Slmb is required to regulate copper homeostasis. We also present evidence that the transcription factor Cap-n-Collar (Nrf2 in mammals), a known substrate of Slmb/BTRC, mediates Slmb's regulatory effect on Ctr1A in a post-transcriptional manner.

1. Introduction

Copper is an essential dietary trace element required for the enzymatic activity of cuproenzymes such as Cu, Zn superoxide dismutase, Cytochrome C oxidase, Lysyl oxidase and Tyrosinase [1]. At the cellular level, copper flux is controlled by regulated import via the CTR1 proteins and efflux via the ATP7A and ATP7B transmembrane ATPases [1]. Within cells, copper distribution is tightly regulated to ensure adequate cuproenzyme supply while also avoiding the high cytotoxicity caused by free copper, which can participate in the Fenton reaction to generate superoxide radicals. Copper chaperones such as CCS, ATOX1 and SCO1 guide incoming copper to the cytosol, Golgi and mitochondria respectively while Metallothionein proteins act to sequester excess cytosolic copper for detoxification or storage [1]. Glutathione is another key molecule in copper homeostasis, binding copper upon import and facilitating exchange of copper between ATOX1 and ATP7A/B at the Golgi membrane [2].

The essentiality of copper is illustrated by male infants suffering the copper deficiency disorder Menkes disease, caused by mutations in the X-linked *ATP7A* gene. Menkes sufferers die in early childhood, exhibiting a range of symptoms including connective tissue and profound neurological defects [3]. Loss of ATP7A reduces copper supply by blocking efflux from intestinal enterocytes into the circulation and

preventing transport of copper across the blood brain barrier. *CTR1* knockout mice die during early embryogenesis, providing further evidence of the importance of copper [4].

Excess copper is also damaging to animals. Humans and mice with loss of ATP7B/Atp7b function exhibit symptoms of Wilson disease, a copper-toxicity disorder caused by the failure of hepatocytes to remove excess bodily copper into the bile [5]. In addition to hepatitis-like liver damage, untreated Wilson disease patients can experience neurological symptoms including Parkinson-like tremors [5].

To maintain cellular and organismal health, copper levels must be maintained in the safe zone between deficiency and excess. Such control could be achieved at either the local or systemic level and may involve regulated uptake, efflux, distribution or sequestration. For instance, copper exposure induces the clathrin-mediated endocytosis of hCTR1, followed by slow recycling through the Rab11 pathway upon copper withdrawal, to protect cells against excess copper [6]. In *Saccharomyces cerevisiae*, copper regulates turnover of the CTR1 orthologue Ctr1p by stimulating Rsp5p-dependent endocytosis, ubiquitylation and degradation of Ctr1p in the vacuole [7].

Drosophila melanogaster has proved to be a useful animal model for studying copper regulation. The fruit fly has functional orthologues of all the major copper homeostasis genes, with uptake proteins (Ctr1A and Ctr1B), a single efflux protein (ATP7), chaperones (CCS, Atox1,

Sco1) and several metallothioneins (MtnA to E) [8].

To further investigate mechanisms of copper transport regulation, we sought genes that cause knockdown phenotypes reminiscent of those induced by copper deficiency, and that encode proteins with potential roles in protein regulation. Copper deficiency in the adult *Drosophila* thorax/abdomen causes a striking combination of hypo-pigmentation, sensory bristle loss and cleft in the notum [9]. A genome wide RNAi screen reported numerous genes showing morphological and/or pigmentation defects when knocked down in the thorax/abdomen [10]. One such gene, *Slmb*, encodes a Skp1-Cul1-F-box (SCP) E3 ubiquitin ligase orthologous to mammalian BTRC/β-TrCP.

Drosophila Slmb and its mammalian orthologue BTRC have been shown to ubiquitinate and/or regulate a wide array of substrate proteins in a range of biological contexts. For instance, Slmb targets for degradation the Hh-responsive transcription factor Ci/Gli3 [11–14] and the intracellular WNT signaling component Arm/beta-catenin [11,15–17]. In these contexts, Homeodomain interacting protein kinase (Hipk) negatively regulates Slmb action via inhibitory phosphorylation. Slmb is also a negative regulator of components of the Hippo signaling pathway including Expanded/FRMD1 [18,19], dSmurf/SMURF1,2 [20] and YAP1 [21].

Given the role of copper in reactive oxygen species generation and defense, it is noteworthy that Slmb/BTRC inhibits the master transcriptional regulator of oxidative stress, Cap-n-collar (cnc)/NRF2 [22] as well as other oxidative stress responsive genes such as ASK1/Ask1 [23] and Sra/RCAN1 [24]. Additional Slmb/BTRC substrates include Akt1/AKT1-3 [25], PAR-1/MARK1-4 [26] and Nerfin 1/NSM1 [27] (neuronal differentiation, axon and dendrite pruning), SAK/PLK4 [28] (centriole duplication), CAP-H2 [29] (chromosome compaction and pairing), Sif/Tiam1 [30] and Corp/MDM2 [31] (DNA damage-induced apoptosis), BimEL [32], BOK/Bax/Debcl [33](apoptosis), Cactus/NFKBIA [34] (metastasis), Prickle/PRICKLE1,2 [35] (planar cell polarity) and Lpin/Lpin1 [36] (lipid metabolism). The remarkable diversity in function of this E3 ubiquitin ligase raises the question of how a single protein is itself regulated in order to perform different roles in different cellular and developmental contexts.

Given the key role of the Ubiquitin Proteasomal System in regulating protein degradation and/or localisation, Slmb was a promising candidate to participate in copper homeostasis. Here, we present evidence that Slmb activity is needed for copper uptake and efflux, acting as a positive regulator of CTR1 and ATP7 activity.

2. Materials and methods

2.1. Drosophila strains and maintenance

2.1.1. Drosophila stocks

The following fly stocks were used: w^{1118} (BL (Bloomington *Drosophila* Stock Center, Bloomington, IN, USA) 3605), *Pannier (Pnr)-Gal4* (BL3039), *GMR-Gal4* (BL9146), *HR-Gal4* (gift from P. Batterham, University of Melbourne, Australia) [37], *Mex-Gal4* [38], *UAS-Golgi::RFP* (BL30907), *Ctr1B::eYFP* and *MtnB::eYFP* (gift from W. Schaffner, University of Zurich, Switzerland) [39], Double balancer (*w; IF/CyO; MKRS/TM6β*, gift from G. Hime, University of Melbourne, Australia), and *gATP7^{WT}::GFP* [40]. *RNAi* lines obtained from the Vienna *Drosophila* Resource Center include *V108159* and *V8315* (*ATP7*), *V107825* and *V34274* (*Slmb*), *V46757* and *V46758* (*Ctr1A*), and *V108127* (*cnc*). Overexpression lines *pUAST-ATP7*, *pUAST-dNCtr1A* (missing the first ~20 amino acids) have been described previously [9,41] and *UAS-Slmb* was a gift from Prof. François Rouyer (Institut des Neurosciences Paris-Saclay, France). *UAS-cnc::HA* (*F000602*) was purchased from FlyORF Zurich ORFeome Project.

2.1.2. Drosophila maintenance

All *Drosophila* strains and crosses were maintained on standard medium at 25 °C unless stated otherwise. Standard medium was supplemented with either 300 μM bathocuproine disulfonate (BCS; Sigma-Aldrich, St. Louis, MO, USA) or 1 or 2 mM copper chloride (CuCl₂; Merck, Whitehouse station, NJ, USA) to make copper-deficient or copper supplemented food medium.

2.1.3. Drosophila survival experiments

In all survival experiments, crosses were set up in a cage with > 50 virgin females and 20–25 males. To assess adult survival, 50 1st instar larvae (=1 replicate) for each group were transferred onto standard medium or medium supplemented with 1 or 2 mM CuCl₂ or 300 μM BCS. Successful adult survival was classified as the ability of the adults to emerge from their pupal cases. The survival of each genotype was calculated as percentage of expected. $n \geq 4$ for each genotype/food type combination.

2.2. Immunohistochemistry and microscopy

2.2.1. Immunohistochemistry

Wandering 3rd instar larvae were inverted, and directly fixed for 30 min (min) in 4% paraformaldehyde (PFA) at room temperature (RT). After three × five-minute washes in phosphate-buffered saline (PBS), samples were rinsed with 0.5% Triton X-100 containing PBS (PBT) three times (20 min per time), followed by blocking with 5% goat serum in PBT at RT for 1 h (hr). They were incubated with polyclonal Rabbit anti-Caspase 3 (1:200; Cell Signaling Technology, Danvers, MA, USA) or polyclonal Rabbit anti-PH3 (1:200; Abcam, Cambridge, UK) overnight at 4 °C. anti-Rabbit 488 (1:500; Invitrogen, Carlsbad, CA, USA) secondary antibody was used to detect primary antibodies. After DAPI staining (1 μg/ml, Bio-Rad, Hercules, CA, USA), larval wing discs were dissected and mounted in PermaFluor (Thermo Scientific, Fremont, CA, USA) for confocal microscopy (CellVoyager CV1000, Yokogawa, Tokyo, Japan).

2.2.2. Microscopy

For phenotypic analysis, adult flies were anaesthetized using CO₂, then mounted directly onto white plasticine and monitored with a Leica MZ6 stereomicroscope. All images of adult fly phenotypes were recorded with a Leica DFC295 digital camera using Leica Application Suite (LAS) software.

For observing *Ctr1B::eYFP* or *MtnB::eYFP* expression in the midgut, wandering 3rd instar larvae were inverted in cold PBS, and then fixed with 4% PFA for 30 min on ice. Afterwards, larvae were dissected and directly mounted on slides for fluorescence microscopy using either a Leica M165 FC Fluorescent Stereo Microscope with a Leica DFC450 C digital camera or a CV1000 laser confocal microscope. The gray values of Ctr1B::eYFP or MtnB::eYFP intensity in the copper cell region were obtained by ImageJ (version: 2.0.o-rc-65/1.52a), and then divided by each copper cell region area to get average gray values for statistical analysis.

For localization studies, whole midguts from wandering 3rd instar larvae were dissected in cold PBS, and then fixed for 30 min in 4% PFA on ice. Tissues were stained with 1× DAPI (1 μg/ml, Bio-Rad) for 15 min at RT. Finally, midguts were mounted onto slides. Monitoring and recording GFP or RFP was performed within 1 h of dissection/mounting for optimal fluorescent signal using a CV1000 confocal microscope.

2.3. Western blot analysis

10 adult heads per sample were lysed in 50 μl of 1% Triton X-100 lysis buffer (50 mM Tris-HCl (pH 7.5), 100 mM NaCl, 1 mM EDTA, 1% Triton-X, 10% glycerol, complete EDTA-free protease inhibitor mixture (Roche Applied Science)). Equal volumes of lysates were separated by SDS-PAGE (Mini-PROTEAN® TGX™ Precast Gels Any kD™, Bio-Rad). ATP7::Flag and Ctr1A::Flag were detected using mouse anti-Flag primary antibody (1:5000; Sigma-Aldrich, St. Louis, MO, USA) and HRP-

conjugated anti-mouse secondary antibody (1:5000; Southern Biotech, Birmingham, AL, USA). Immunoblots were developed using ECL Prime (GE Healthcare, Chicago, IL, USA) and imaged using a chemiluminescence detector (Vilber Lourmat). Image J was used to quantify the gray value of each western blot band; in cases where the bands 'frowned' (i.e. were not straight), the entire band-containing region was included for quantification. Relative gray values were then calculated by dividing the gray value for each anti-Flag band by the gray value for the corresponding loading control (anti-Tubulin).

2.4. Statistical analysis

All data were presented as mean ± S.E.M. An independent Student's *t*-test was applied using GraphPad Prism 7.0b (GraphPad, San Diego, CA, USA). $P < 0.05$ was considered as a statistically significant difference. For the adult eye necrosis phenotype (Fig. 2), each data point represents the average number of progeny of appropriate genotype (from a single genetic cross) that show necrosis in one or both eyes.

3. Results

3.1. Knockdown of Slmb causes copper deficiency phenotypes in the Drosophila thorax and eye

In order to investigate potential roles of *Slmb* in regulating copper transport, we tested various UAS overexpression and RNAi knockdown constructs under the control of the *Pannier* (*Pnr*)-*Gal4* line, which drives expression in a broad stripe down the midline of the developing thorax and abdomen (Fig. 1A) and *GMR-Gal4* which drives expression in the developing and adult eye. Unless stated otherwise, all phenotypes described below were fully penetrant with at least 10 individuals assessed for each genotype.

Knockdown of *Slmb* under *Pnr-Gal4* control resulted in either moderate thoracic cleft (weaker (w) *RNAi* line V107825, Fig. 1B, F) or severe thoracic cleft (strong (st) *RNAi* line V34274, Fig. 1C, G), coupled with hypopigmentation on the abdomen. In the eye, strong *Slmb* knockdown caused necrosis at the posterior margin of the eye in ~80% of flies (Fig. 1K). Overexpression of *Slmb* had no effect in the thorax/abdomen (Fig. 1D, H) or eye (Fig. 1L) but was able to fully rescue the *Slmb* knockdown thoracic defects (Supp. Fig. 1).

The thoracic and abdominal phenotypes caused by *Slmb* knockdown were strongly reminiscent of those previously shown by overexpression of the copper efflux protein ATP7; loss of pigmentation on the adult abdomen, loss of sensory micro and macrochaetae and a mild thoracic cleft (Fig. 2C) [41]. RNAi-mediated knockdown of *ATP7* (*RNAi* line V108159) in contrast, caused a strong hypopigmentation phenotype on the thorax and abdomen (Fig. 2B) [41].

Manipulation of *Slmb* and *ATP7* were examined in various combinations to investigate potential genetic interactions between the E3 ubiquitin ligase and copper efflux. The thoracic cleft caused by strong *Slmb* knockdown was rescued by knockdown of *ATP7* (Fig. 2F), but hypopigmentation remained. Co-expression of *ATP7* exacerbated the *Slmb* knockdown defects, causing larval death (not shown). Overexpression of *Slmb* did not have any effect on the defects caused by *ATP7* knockdown (Fig. 2G) or overexpression (Fig. 2H).

In the adult eye, *ATP7* knockdown (Fig. 2J) or overexpression alone (Fig. 2K) had no phenotypic effect as shown previously [41], but *ATP7* knockdown completely rescued the posterior necrosis caused by strong *Slmb* knockdown (Fig. 2N, Q), just as it rescued the *Slmb* knockdown thoracic cleft.

Reduction of copper uptake by *Ctr1A* knockdown also caused thoracic and abdominal hypopigmentation (Fig. 3C, D) and thoracic cleft (Fig. 3D) as published [41]. Combining *Slmb* knockdown with *Ctr1A* overexpression (Fig. 3F) or knockdown (Fig. 3G, weak) gave the same phenotype as *Slmb* knockdown alone while *Slmb* overexpression

had no impact on thoracic *Ctr1A* knockdown phenotypes.

Ctr1A overexpression in the adult fly eye had no phenotypic effect (Fig. 3K) but two copies of this transgene were able to partially rescue the *Slmb* knockdown necrotic eye phenotype (Fig. 3O and P).

ATP7 overexpression and *Ctr1A* knockdown are predicted to both cause copper deficiency, by increased export and decreased import respectively. Therefore, we postulated that *Slmb* may normally be required to maintain copper levels. This hypothesis was supported by the finding that increased copper uptake (*Ctr1A* overexpression) or decreased copper efflux (*ATP7* knockdown) both suppressed the *Slmb* knockdown eye necrosis while reduced *ATP7* also rescued the *Slmb* knockdown thoracic cleft.

A promising candidate for mediating Slmb's influence on copper transport is the transcription factor Cap-n-Collar (cnc, Nrf2 in mammals). cnc/Nrf2 is negatively regulated by Slmb/BTRC, which targets it for proteasomal degradation [22] and cnc is considered to be the master regulator of cellular oxidative stress response. Knockdown of *cnc* (*RNAi* line V108127) had no phenotypic effect in the thorax (Fig. 4B) or eye (Fig. 4F) and had no impact on the thoracic/abdominal *Slmb* knockdown phenotypes (Fig. 4D). However, *cnc* knockdown did rescue *Slmb* knockdown defects in the eyes (Fig. 4I, N) to a greater extent than two copies of *Ctr1A* (Fig. 3). Strikingly, the necrotic spots generated by *Slmb* knockdown were completely rescued by the combination of *cnc* knockdown and *Ctr1A* overexpression (Fig. 4J, N). *cnc* overexpression was lethal under *Pnr-Gal4* control (not shown) and caused a smaller eye with central necrosis under *GMR-Gal4* (Fig. 4K).

3.2. Slmb is required for maintenance of ATP7 and CTR1 levels

The genetic interaction results presented above showed that *Slmb* might interact via *cnc* with either *Ctr1A* or *ATP7* to regulate copper homeostasis. Next, we investigated by western blot whether *Slmb* could influence Ctr1A/B or ATP7 protein levels.

We first assessed ATP7 expression after *Slmb* knockdown using a *UAS-ATP7::Flag* transgene under the control of *GMR-Gal4* (Fig. 5A). In lysates from homogenized adult heads, an anti-Flag antibody detected two clear bands in ATP7::Flag expressing flies. A dramatic decrease in ATP7::Flag was detected after *Slmb* knockdown, demonstrating that *Slmb* regulates the expression of ATP7 in the eye. *Slmb* overexpression and *cnc* knockdown had no effect but *cnc* overexpression also caused a decrease in ATP7 levels.

A *UAS-Ctr1A::Flag* transgene was similarly applied to assess Ctr1A expression (Fig. 5B). Knockdown of *Slmb* caused a decrease in Ctr1A::Flag expression, as did *cnc* overexpression. *cnc* knockdown had no impact on Ctr1A levels while a mild increase in Ctr1A was detected after *Slmb* overexpression. As two copies of Ctr1A::Flag had a much greater rescue effect on *Slmb* knockdown in the eye than a single copy, this combination was also tested by western blot and found to result in significantly higher Ctr1A levels (Fig. 5C). Finally, the restorative combination of *Ctr1A* overexpression and *cnc* knockdown on the *Slmb* knockdown eye necrosis was also confirmed by western blot which showed elevated Ctr1A levels (Fig. 5D).

These results revealed that Slmb is required for the post-transcriptional maintenance of ATP7 and Ctr1A protein levels and that this regulatory effect may be indirect, via the cnc transcription factor.

3.3. Knockdown of Slmb causes copper deficiency in the larval midgut

ATP7 has been shown to have a copper efflux function [41,42], and *Ctr1A* was reported to play critical roles in copper uptake [43–45]. Due to the relationship between *Slmb*, *ATP7* and *Ctr1A* described above, we assayed copper levels in the larval midgut after knockdown of *Slmb* using a reporter gene, *Ctr1B::eYFP* which is induced in a copper deficient environment [39,46]. We focused on the copper cell region of the midgut (indicated by the white arrows in Figs. 6A and B, 7A and B) where copper is thought to be absorbed [40]. Expression of *Ctr1B::eYFP*
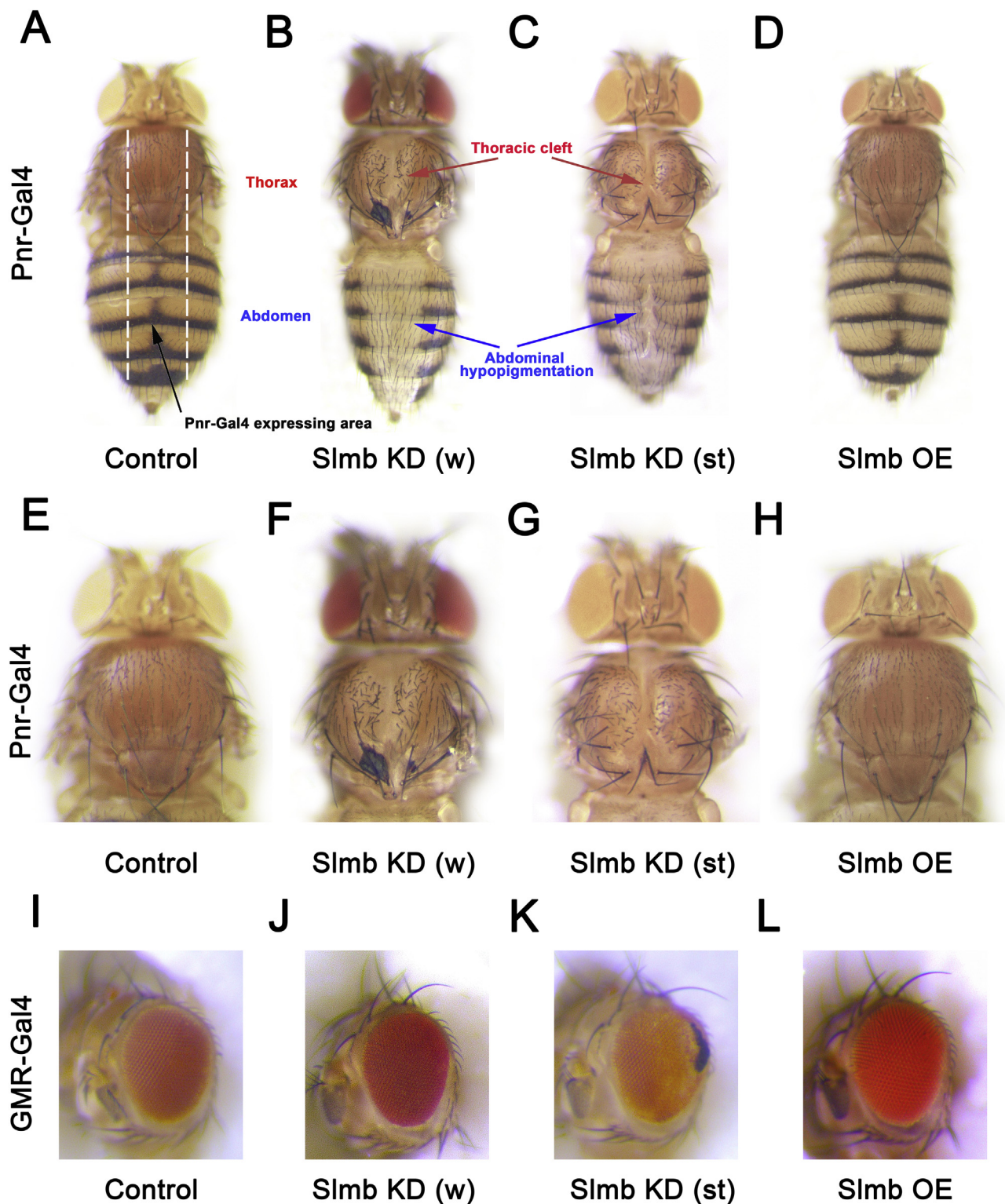
Fig. 1. Targeted knockdown of *Slmb* causes copper deficiency phenotypes. A–D) Dorsal views of adult female *Drosophila* containing the *Pnr-Gal4* driver together with the following transgenes: A) no transgene (*w[1118]*); B) *UAS-Slmb[wRNAi]*; C) *UAS-Slmb[stRNAi]*; D) *UAS-Slmb*. The white dotted lines in A indicate the *Pnr-Gal4* expression domain. Both weak (w) and strong (st) *Slmb RNAi* lines produced thoracic (red arrows) and abdominal (blue arrows) hypopigmentation and a thoracic cleft. Images were captured using the 3.2× objective lens. E–H) Higher-magnification images of A–D respectively highlighting thoracic defects. I–L) Eyes of adult female *Drosophila*, all with *GMR-Gal4*, anterior to the left: I) no transgene (*w[1118]*); J) *UAS-Slmb[wRNAi]*; K) *UAS-Slmb[stRNAi]*; L) *UAS-Slmb*. Under the control of *GMR-Gal4*, the strong *Slmb RNAi* line generated necrosis (dark spots at the posterior edge of eyes) in ~80% of flies. E–L were captured using the 4.0× objective lens. Abbreviations: w, weak; st, strong; KD, knockdown; OE, overexpression. *n* > 10 for each genotype.
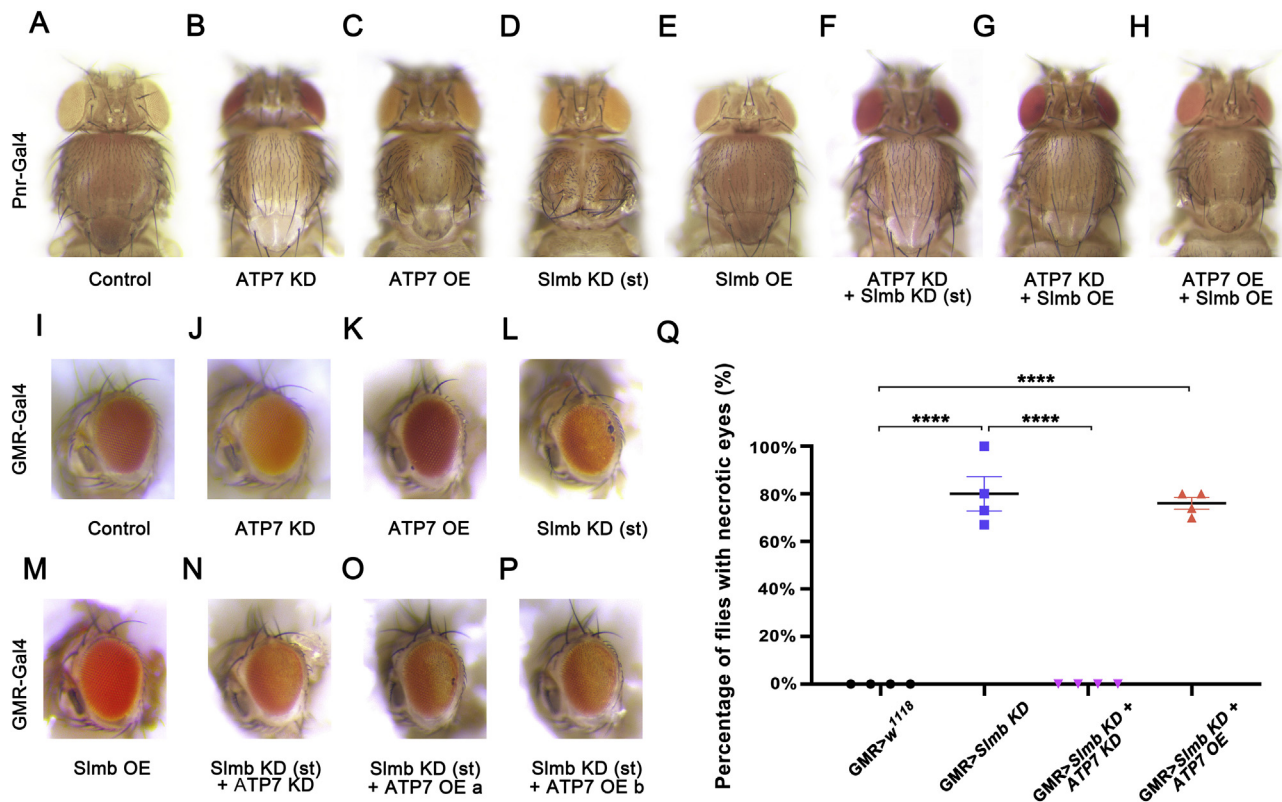
Fig. 2. Decreased copper efflux rescues *Slmb* knockdown phenotypes. A–H) Dorsal views of adult female *Drosophila* containing the *Pnr-Gal4* driver together with the following transgenes: A) no transgene (*w1118*); B) *UAS-ATP7RNAi*; C) *UAS-ATP7FLAG*; D) *UAS-SlmbstRNAi*; E) *UAS-Slmb*; F) *UAS-SlmbstRNAi + UAS-ATP7RNAi*; G) *UAS-ATP7RNAi + UAS-Slmb*; H) *UAS-ATP7FLAG + UAS-Slmb*. Both *ATP7* knockdown (B) and overexpression (C) produced copper deficiency defects (hypopigmentation (both) and thoracic cleft (overexpression only)). The thoracic cleft caused by the strong *Slmb* RNAi line was rescued by *ATP7* knockdown (F). When combined with *ATP7* overexpression, *Slmb* knockdown caused death during pupal development. *Slmb* overexpression did not have any effect on *ATP7* knockdown (G) or overexpression (H). The rescue effect of *ATP7* knockdown on *Slmb* knockdown was also observed in the eyes. I–P) Adult female *Drosophila* eyes, all with *GMR-Gal4*, shown anterior to the left: I) no transgene (*w1118*); J) *UAS-ATP7RNAi*; K) *UAS-ATP7FLAG*; L) *UAS-SlmbstRNAi*; M) *UAS-Slmb*; N) *UAS-SlmbstRNAi + UAS-ATP7RNAi*; O) *UAS-SlmbstRNAi + UAS-ATP7FLAG a* (with necrosis); P) *UAS-SlmbstRNAi + UAS-ATP7FLAG b* (without necrosis). Q) Quantification of the proportion of flies of each genotype showing necrotic eyes. ~80% of *Slmb* knockdown flies have necrotic eye defects and these defects were completely rescued by *ATP7* knockdown. Abbreviations: st, strong; KD, knockdown; OE, overexpression. All images were captured using a 4× objective lens and are representative of $n > 20$ for each genotype. ****$p < 0.0001$.

in the region of the copper cells is strikingly elevated in BCS-supplemented food (low copper) compared to expression in larvae raised on normal food (Fig. 6A and B). Under low dietary copper conditions (control Fig. 6C), over-expression of *ATP7* caused a significant increase in *Ctr1B::eYFP* expression (Fig. 6E and H) while *ATP7* knockdown had the opposite effect (Fig. 6D and H). However, *Ctr1B::eYFP* expression was reduced after *Slmb* knockdown (Fig. 6F and H) and increased after *Slmb* overexpression (Fig. 6G and H) an unexpected result since *Slmb* knockdown in the thorax caused a typical copper deficiency phenotype.

To further investigate copper levels in the midgut, a second reporter gene, *MtnB::eYFP* was utilized. In contrast to *Ctr1B::eYFP*, *MtnB::eYFP* is elevated in high dietary copper conditions. We confirmed that *MtnB::eYFP* expression was upregulated in CuCl₂-supplemented food (Fig. 7A and B). *ATP7* knockdown increased *MtnB::eYFP* expression (Fig. 7 D and G) while the combination of *ATP7* overexpression and high dietary copper was lethal (see Fig. 8). When *Slmb* was knocked down, expression of *MtnB::eYFP* significantly decreased (Fig. 7E and G), demonstrating, in contrast to the *Ctr1B::eYFP* results, that *Slmb* knockdown could decrease copper levels. However, Slmb overexpression also caused downregulation of *MtnB::eYFP*. As discussed later, we believe that the *Slmb* knockdown/*Ctr1B::eYFP* decrease (Fig. 6) is due to the fact that *Ctr1B::eYFP* contains some of the Ctr1B N terminus which is degraded in the absence of *Slmb*.

In order to further investigate the functional consequences of midgut *Slmb* activity, adult survival experiments were performed on

flies raised from 1st larval instar on normal media or media supplemented with CuCl₂ or BCS. Using the midgut-specific driver *Mex-Gal4*, *ATP7* and *Slmb* were manipulated. Overexpression of *ATP7* caused a moderate increase in survival on normal food but resulted in dramatically decreased survival on 1 mM and 2 mM CuCl₂-supplemented food (Fig. 8). No changes in survival rate were observed on 300 μM BCS-supplemented food after *ATP7* overexpression. *Slmb* knockdown significantly increased the survival rate on basal, 1 mM and 2 mM CuCl₂-containing medium, but had no effect on survival rate in 300 μM BCS medium (Fig. 8), indicating that *Slmb* knockdown could protect larvae from copper toxicity. *Slmb* overexpression had a mildly protective effect on normal food but otherwise showed no influence on survival.

3.4. Slmb knockdown affects ATP7 intracellular localization

Both our phenotypic and western blot results showed that *Slmb* interacts genetically with *ATP7*. Therefore, we next assessed ATP7 intracellular localization after *Slmb* knockdown. A genomic *gATP7::GFP* transgene, which can functionally replace endogenous *ATP7* activity [40], was introduced to detect ATP7 localization after *Slmb* knockdown under the control of midgut specific-driver *Mex-Gal4*.

In mammalian cells, the ATP7 orthologue ATP7A is normally localized to the *trans*-Golgi network, and can translocate to the outer plasma membrane in a copper overloaded environment in order to export excess copper [47,48]. However, trafficking of ATP7 between the Golgi
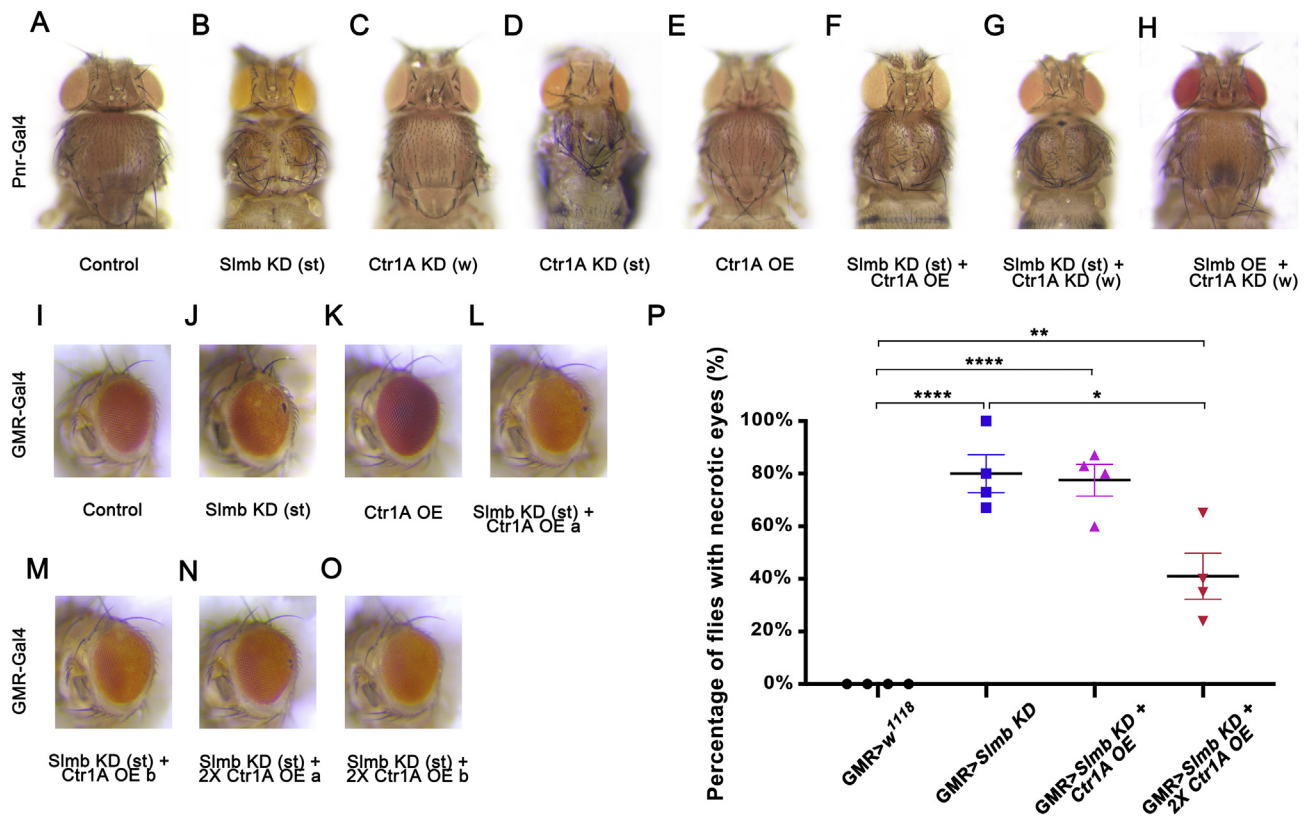
Fig. 3. Increased copper uptake also rescues *Slmb* knockdown phenotypes. A–H) Dorsal views of adult female *Drosophila* (except D, male) containing the *Pnr-Gal4* driver together with the following transgenes: A) no transgene (*w*^1118^); B) *UAS-Slmb*^stRNAi^; C) *UAS-Ctr1A*^wRNAi^; D) *UAS-Ctr1A*^stRNAi^; E) *UAS-dNCtr1A*^FLAG^; F) *UAS-Slmb*^stRNAi^ + *UAS-dNCtr1A*^FLAG^; G) *UAS-Slmb*^stRNAi^ + *UAS-Ctr1A*^wRNAi^; H) *UAS-Ctr1A*^wRNAi^ + *UAS-Slmb*. C) Weak *Ctr1A* knockdown produced a mild thoracic hypopigmentation typical of copper deficiency. D) Strong *Ctr1A* knockdown caused death at the pharate adult stage; extracted adults displayed severe thoracic cleft and abdominal hypopigmentation. *Ctr1A* overexpression or knockdown had no apparent impact on *Slmb* knockdown defects in the thorax or abdomen. However, *Ctr1A* overexpression partially rescued the *Slmb* knockdown necrotic eye phenotype. I–O) Adult female *Drosophila* eyes, all with *GMR-Gal4*, shown anterior to the left: I) no transgene (*w*^1118^); J) *UAS-Slmb*^stRNAi^; K) *UAS-dNCtr1A*^FLAG^; L) *UAS-Slmb*^stRNAi^ + *UAS-dNCtr1A*^FLAG^ *a* (with necrosis); M) *UAS-Slmb*^stRNAi^ + *UAS-dNCtr1A*^FLAG^ *b* (without necrosis); N) *UAS-Slmb*^stRNAi^ + 2× *UAS-dNCtr1A*^FLAG^ *a* (with necrosis); O) *UAS-Slmb*^stRNAi^ + 2× *UAS-dNCtr1A*^FLAG^ *b* (without necrosis). P) Quantification of the proportion of flies of each genotype showing necrotic eyes. Two copies of the *Ctr1A*^FLAG^ transgene decreased the percentage of flies with necrosis caused by *Slmb*^stRNAi^ knockdown. Abbreviations: w, weak; st, strong; KD, knockdown; OE, overexpression. All images were captured using a 4 X objective lens and are representative of n > 20 for each genotype. *$p < 0.05$, **$p < 0.01$, ****$p < 0.0001$.

and the plasma membrane has never been observed in *Drosophila* cells. Thus, we first tested whether ATP7 cellular localization could be affected by surrounding copper conditions. In the copper cells of the larval midgut, the majority of ATP7::GFP localized to the plasma membrane and a small amount co-localized with a Golgi::RFP marker in both peri-nuclear and peripheral (sub-plasma membrane) cellular locations (Fig. 9A–D) in larvae raised on normal food. Under copper-deficient conditions (BCS-supplemented media), the amount of ATP7::GFP at the cytoplasmic membrane was reduced but peri-nuclear Golgi levels remained stable (Fig. 9E–H). Therefore, for the first time, we have demonstrated that ATP7 intracellular localization can be affected by surrounding copper conditions. The amount of ATP7::GFP at the plasma membrane was significantly reduced after *Slmb* knockdown in larvae raised on normal food, closely resembling the ATP7::GFP levels seen in control larvae raised on copper-deficient media (Fig. 9I–L). Slmb overexpression had no detectable impact on ATP7::GFP localisation (Supp. Fig. 2).

4. Discussion

ATP7 has been reported to play critical roles in copper trafficking and efflux of excess copper [49], while Ctr1A has been shown to function in cellular copper uptake [9], with Ctr1B complementing Ctr1A's action in certain cell types. We have previously proposed that cuticle hypopigmentation can be caused by lack of the copper required

for cuproenzyme laccase 2, the fly equivalent of Tyrosinase [9]. In our working model, *ATP7* knockdown causes hypopigmentation by blocking copper transport to the Golgi, where laccase 2/Tyrosinase is copper-loaded. In contrast, cytosolic copper levels are elevated in *ATP7* knockdown cells due to reduced copper efflux; this is seen here in the midgut where *ATP7* knockdown results in decreased Ctr1B::eYFP, indicating increased copper levels. *ATP7* overexpression is postulated to cause excessive copper efflux, leading to both Golgi and cytosolic copper deficiency. We believe the additional thoracic cleft caused by *ATP7* over expression is due to the lack of cytosolic copper. Reduced copper import caused by *Ctr1A/Ctr1B* knockdown results in hypopigmentation either alone or in combination with thoracic cleft, depending on the severity of the copper deficiency.

Here, we show that knockdown of *Slmb* causes phenotypes reminiscent of copper deficiency; cuticle hypopigmentation, thoracic cleft and decreased midgut MtnB::eYFP expression. Knockdown of *Slmb* in the midgut also protects growing larvae from copper toxicity. In the eye, *Slmb* knockdown induces a mild posterior necrosis that is less severe than the small, flat eye phenotype caused by *Ctr1A* knockdown [9]. In both the thorax and the eye, *Slmb* knockdown defects are rescued by manipulations predicted to increase cytosolic copper levels. *ATP7* knockdown completely rescues both the thoracic cleft (hypopigmentation cannot be rescued by *ATP7* knockdown because ATP7 is required for Golgi copper accumulation) and eye necrosis. *Ctr1A* overexpression partially rescues the *Slmb* knockdown eye necrosis but notably has no
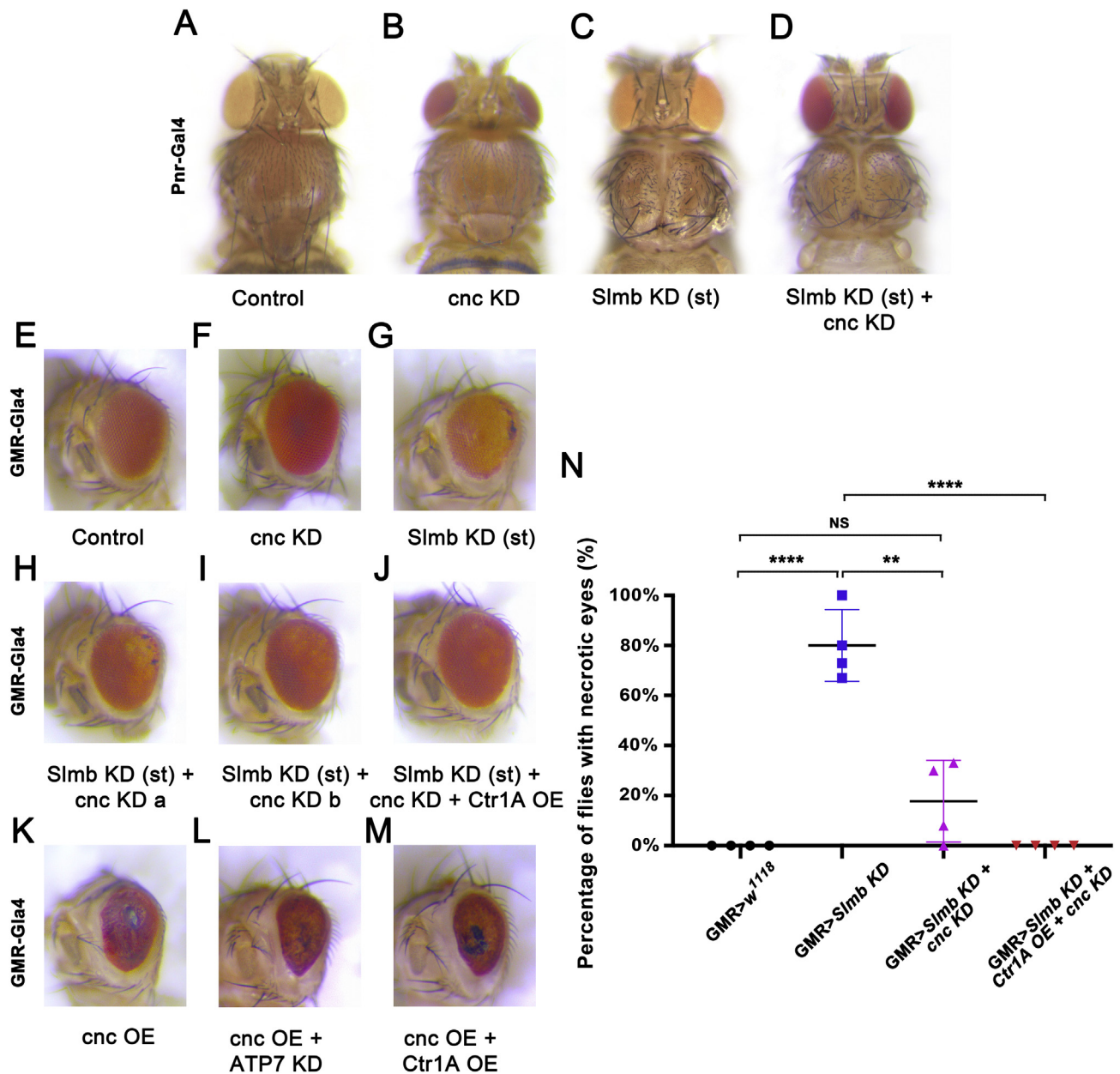
Fig. 4. Cnc may mediate Slmb's role in copper homeostasis. A–D) Dorsal views of adult female *Drosophila* containing the *Pnr-Gal4* driver together with the following transgenes: A) no transgene (*w^1118*); B) *UAS-cnc^RNAi*; C) *UAS-Slmb^stRNAi*; D) *UAS-Slmb^stRNAi + UAS-cnc^RNAi*. E–N) Adult female *Drosophila* eyes, all with *GMR-Gal4*, shown anterior to the left with the following transgenes: E) no transgene (*w^1118*); F) *UAS-cnc^RNAi*; G) *UAS-Slmb^stRNAi*; H) *UAS-Slmb^stRNAi + UAS-cnc^RNAi* a (with necrosis); I) *UAS-Slmb^stRNAi + UAS-cnc^RNAi* b (without necrosis); J) *UAS-Slmb^stRNAi + UAS-cnc^RNAi + UAS-dNCtr1A^FLAG*; K) *UAS-cnc^HA*; L) *UAS-cnc^HA + UAS-ATP7^RNAi*; M) *UAS-cnc^HA + UAS-dNCtr1A^FLAG*. N) Quantification of the proportion of flies of each genotype showing necrotic eyes. *cnc* knockdown resulted in a decrease in the percentage of *Slmb^stRNAi* flies with necrosis. When combined with *Ctr1A^FLAG* overexpression, *cnc^RNAi* knockdown completely rescued the eye necrosis produced by *Slmb* knockdown. *cnc* overexpression produced severe necrosis in the eyes which could not be rescued by *ATP7* knockdown or *Ctr1A* overexpression. Abbreviations: st, strong; KD, knockdown; OE, overexpression; NS, not significant. All images were captured using a 4× objective lens and are representative of n > 20 for each genotype. **p < 0.01, ****p < 0.0001, NS > 0.05.

impact on the cuticle hypopigmentation or thoracic cleft. These results imply that *Slmb* knockdown is influencing copper transport.

Our western blot analysis shows that *Slmb* knockdown dramatically decreases the levels of both ATP7 and Ctr1A protein, indicating that Slmb is a positive regulator of both proteins. Since ATP7 and Ctr1A were both expressed exogenously using the Gal4/UAS system, this positive regulation must be at the post-transcriptional level. We were unable to detect Ctr1B expression in the eye. However, *Slmb* knockdown caused a seemingly counterintuitive downregulation of Ctr1B::eYFP in the larval midgut. Normally, reduced Ctr1B::eYFP is indicative of elevated cytosolic copper levels [39] whereas all our other

data indicates that *Slmb* knockdown causes reduced cytosolic copper. However, Ctr1B::eYFP contains a portion of the Ctr1B N-terminus fused to eYFP [39]. Therefore, we propose that the downregulation of Ctr1B::eYFP actually reflects a requirement for Slmb activity in maintaining Ctr1B protein levels, as we have shown for Ctr1A and ATP7.

With its known role as the master regulator of oxidative stress response, we thought that the Slmb substrate cnc was a prime candidate to be mediating Slmb's regulatory effect on the copper transport proteins. Excess copper is a potent contributor to oxidative stress and can promote the production of superoxide free radicals through the Fenton reaction. Two pieces of evidence support an involvement of cnc in
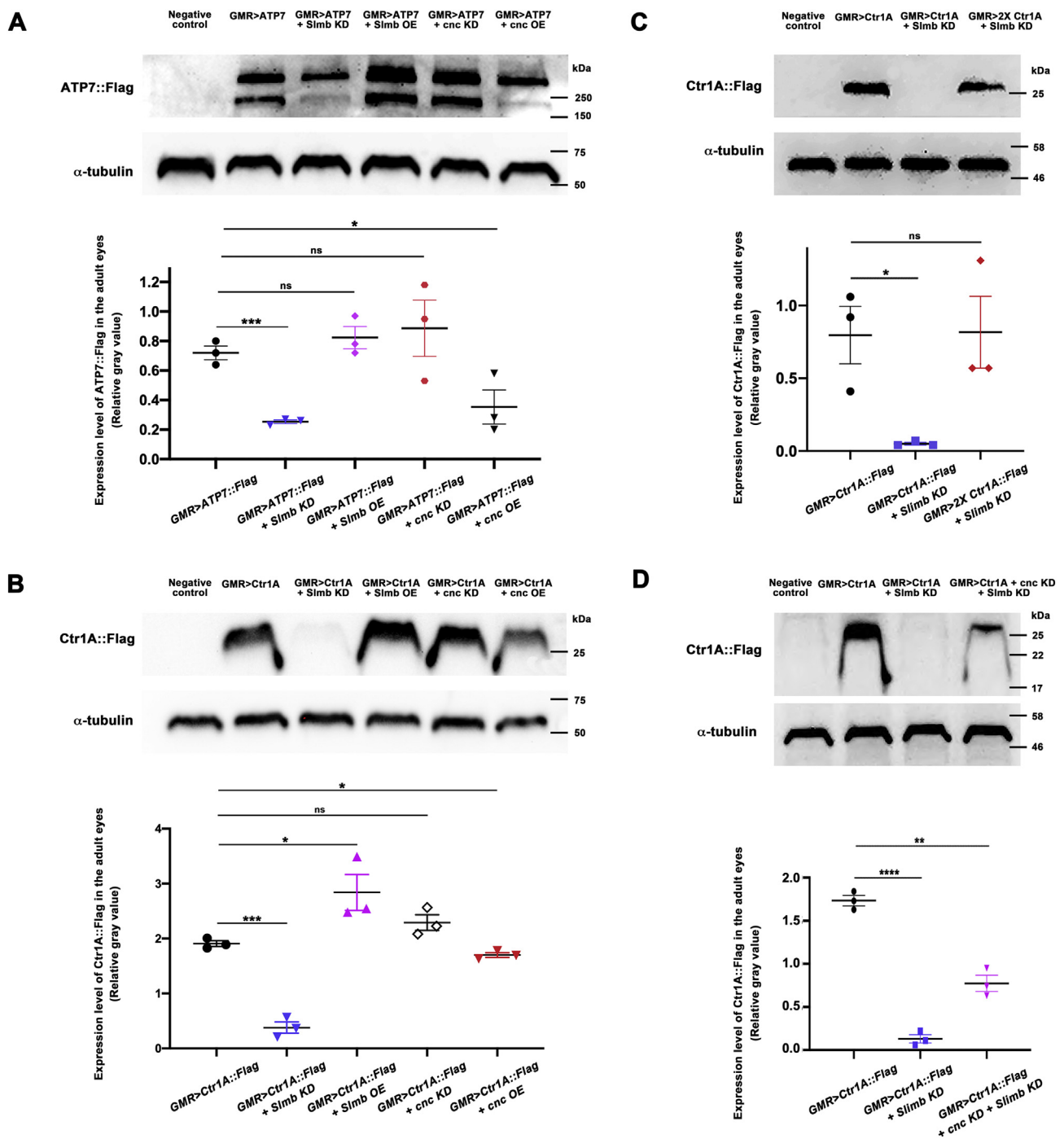
Fig. 5. *Slmb* and *cnc* are required for the maintenance of ATP7 and Ctr1A protein levels. Western blots against the Flag epitope to detect ATP7::Flag or Ctr1A::Flag expression. A–D) ATP7::Flag (A) and Ctr1A::Flag (B–D) expression in adult heads after manipulating *Slmb* and *cnc*. A) ATP7::Flag is predicted to have a MW of 195 kDa and therefore the bottom band in A is our target band. *Slmb* knockdown and *cnc* overexpression decreased ATP7 levels while no changes were detected after *Slmb* overexpression or *cnc* knockdown. B) *Slmb* knockdown and *cnc* overexpression both caused a decrease in Ctr1A::Flag (predicted MW ~25 kDa) levels, especially *Slmb* knockdown where Ctr1A was undetectable. A mild yet significant increase in Ctr1A expression was detected after *Slmb* overexpression, but *cnc* knockdown had no significant effect on Ctr1A levels. C) By introducing two copies of Ctr1A::Flag, Ctr1A expression under *Slmb* knockdown could be detected. D) The decrease of Ctr1A levels caused by *Slmb* knockdown was relieved by *cnc* knockdown. All western blot images are representative of ≥3 independent experiments. Abbreviations: st, strong; KD, knockdown; OE, overexpression, NS, no significance. $*p < 0.05$, $**p < 0.01$, $***p < 0.001$, $****p < 0.0001$.

copper regulation. First, *cnc* knockdown strongly suppressed the *Slmb* knockdown eye necrosis phenotype, as did *Ctr1A* overexpression. Second, *cnc* knockdown alleviated the ablation of Ctr1A expression caused by *Slmb* knockdown whereas cnc overexpression alone decreased both Ctr1A and ATP7 levels. We hypothesize that cnc may downregulate Ctr1A under conditions of oxidative stress, reducing copper import as one means of minimizing free radical production. In

midgut cells, the parallel downregulation of ATP7 would boost this effect by simultaneously reducing copper release into the circulation.

Cnc encodes a transcription factor. But the effect we observe of cnc on Ctr1A and ATP7 occurs post-transcriptionally. Therefore, we propose that cnc's regulation of copper homeostasis is indirect. Interestingly, identification of Nrf2 (cnc) target genes in the fly and humans found "Proteasome" to be the top KEGG pathway and
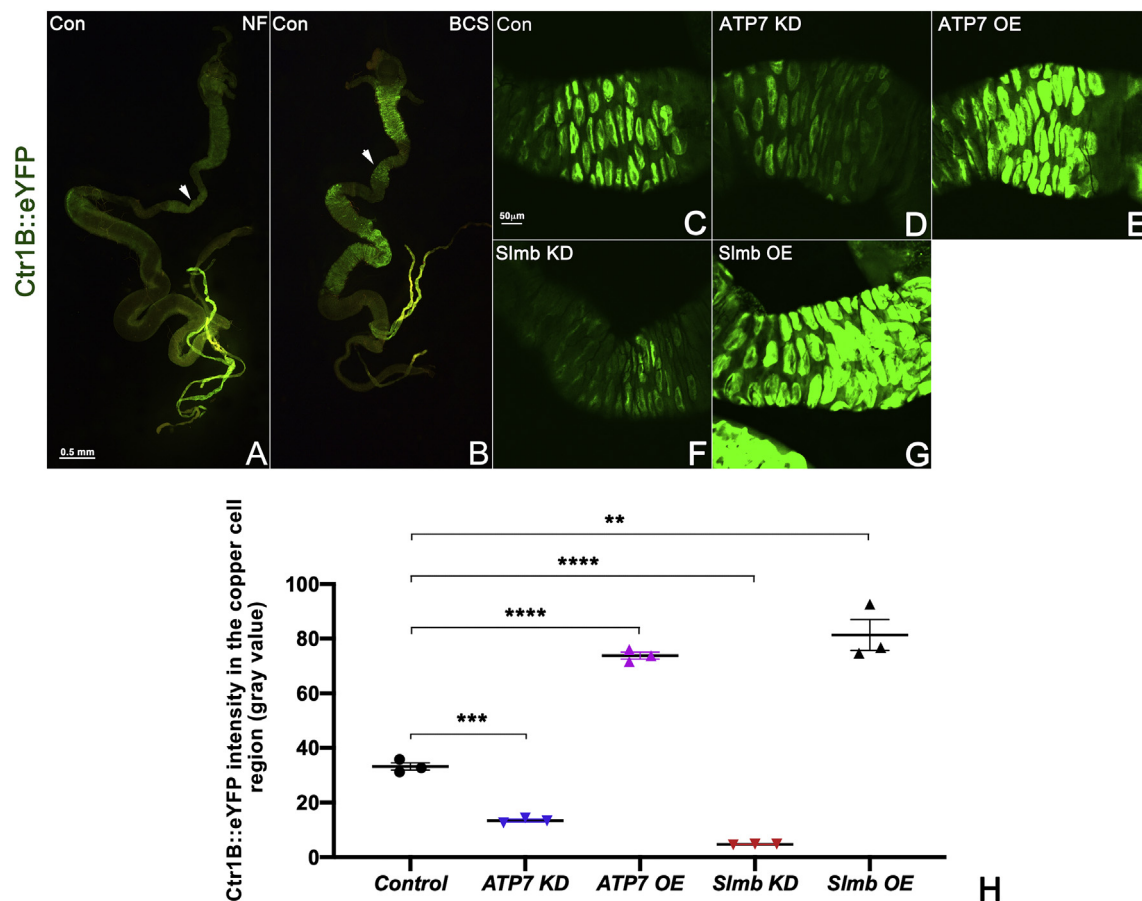
Fig. 6. Midgut Ctr1B reporter gene levels after manipulating *ATP7* and *Slmb*. Reporter gene *Ctr1B::eYFP* was used to assess copper levels under control of candidate gene modification in a dietary copper-deficient environment. A, B) Overview of control midguts raised on normal and copper-deficient (300 μm BCS-supplemented) medium respectively. White arrows point to the copper cell region. C–G) The midgut copper cell region of larvae raised under copper-deficient conditions with the following genotypes, all containing *HR-Gal4*: C) control group (w^{1118}); D) *UAS-ATP7^{RNAi}*; E) *UAS-ATP7^{Flag}*; F) *UAS-Slmb^{stRNAi}*; G) *UAS-Slmb*. H) Quantification of Ctr1B::eYFP levels based on the gray values of C–G. $n \geq 3$ for each genotype. Abbreviation: st, strong; KD, knockdown; OE, overexpression; Con, control group; NF, normal food. $**p < 0.01$, $***p < 0.001$, $****p < 0.0001$. Scale bar: 0.5 mm in A and B, 50 μm in C–G.

"Proteolysis" to be the most representative GO category [50]. Analysis of the most stringent Nrf2 (cnc) targets [50] reveals obvious candidates for Ctr1A and ATP7 regulation: GCLC (a rate limiting component of glutathione production), KEAP1 (an E3 ubiquitin ligase that inhibits cnc in parallel with Slmb), UBE2D2 (an E2 ubiquitin conjugase known to interact with Slmb), PSMA3 (a UBE2D2 substrate) and PSMD4 and 6 (proteasomal and ATP7A-binding [51] proteins). Future research will probe whether any of these cnc targets are involved in Ctr1A or ATP7 maintenance.

Given the number and diversity of known Slmb/BTRC targets described in the introduction, it is perhaps surprising to find that in the tissues we have examined, *Slmb* knockdown appears to chiefly result in copper deficiency via downregulation of Ctr1A/B. ATP7 could either be an additional target of Slmb and cnc, or could simply be responding to the decreased cellular copper levels caused by *Slmb* knockdown and cnc upregulation. We favour the latter possibility because knockdown of *ATP7* counteracts *Slmb* knockdown, presumably by trapping available copper in affected cells and minimizing damage caused by insufficient copper uptake.

We consider two possibilities to explain the data we have presented. The first is that Ctr1A and B are the major secondary targets of several of the primary Slmb targets listed in the introduction i.e. that Slmb downregulates Ci/Arm/Expanded etc. in order to maintain Ctr1A and B expression. We find this model highly unlikely given the multitude of Slmb targets. Alternatively, we postulate that cellular copper levels, modulated by Ctr1A- and Ctr1B-mediated import, are important in maintaining Slmb activity in a positive feedback loop: Slmb positively regulates Ctr1A/B expression which in turn is needed for Slmb activity. We speculate that this mechanism could be used to ensure that cells are "copper competent" and have sufficient essential copper to allow the processes regulated by other Slmb targets, such as proliferation and differentiation, to proceed. Insufficient copper - signalled through Slmb - would conversely induce apoptosis. Thus, we propose a model summarising the possible relationship between *Slmb*, *cnc*, *Ctr1A/B*, *ATP7* and copper homeostasis (Fig. 10). As a known negative regulator of Slmb, HipK may be mediating copper's influence on Slmb through inhibitory phosphorylation.

We have yet to provide any evidence regarding the nature of Ctr1A and B regulation by Slmb via cnc. Examination of Ctr1A's ubiquitination status under *Slmb* knockdown/*cnc* overexpression conditions will be the first step in determining whether this is via proteasomal degradation.

Cnc may not be the only means by which Slmb regulates copper homeostasis; other Slmb targets also have known copper associations. For instance, addition of copper to cells inhibits ubiquitin-mediated degradation of IκBα, leading to inhibition of NFkB pathways induced by multiple independent stimuli [52]. The ASK1/2-MKK7-JNK and ASK1/2-MKK3/6-p38 signaling pathways are required to mediate copper-induced apoptosis in the *C. elegans* germline [53], a role consistent with ASK1's function in responding to reactive oxygen species.

AKT proteins, negatively regulated by Slmb, have also been heavily implicated in copper homeostasis. Increasing bioavailable copper inhibits GSK3beta through activation of an Akt signaling pathway [54].
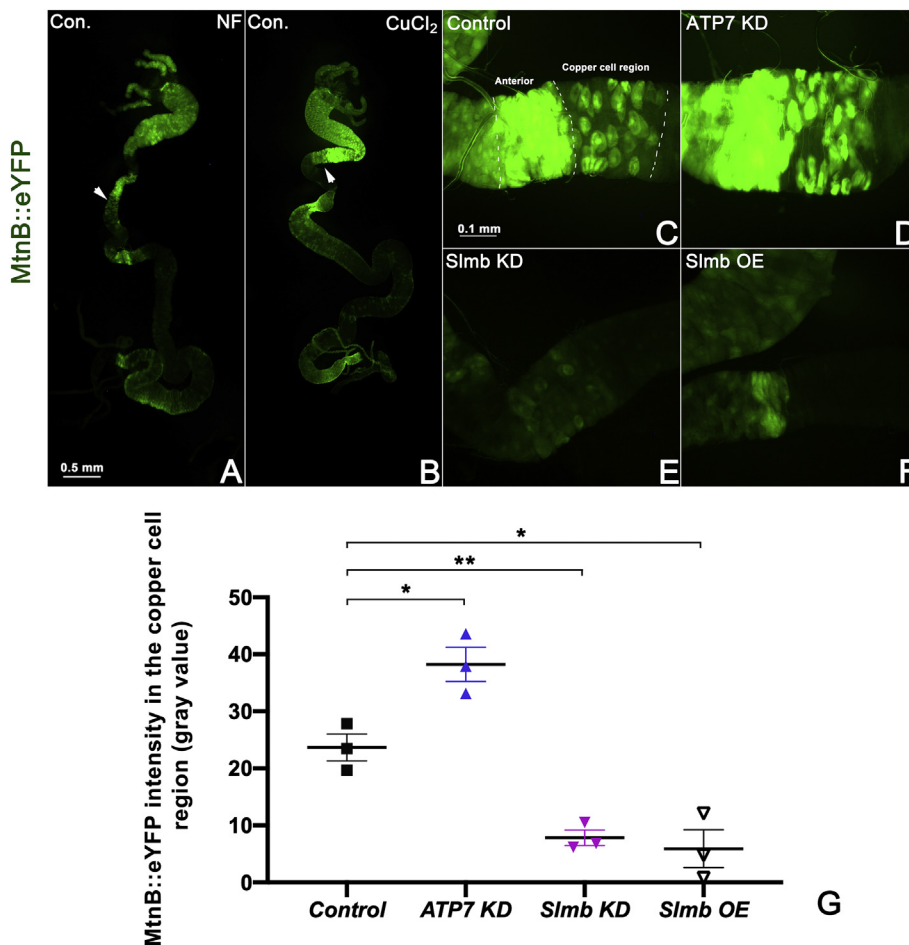
9

Fig. 7. *Slmb* knockdown causes reduced copper levels in the larval midgut. The *MtnB::eYFP* reporter gene was used to assess copper levels in high dietary copper conditions (1 mM CuCl$_2$-supplemented food). A, B) Overview of control midguts raised on normal and high copper medium respectively. White arrows point to the copper cell region. C–F) The midgut copper cell region of larvae raised under copper-supplemented conditions with the following genotypes, all containing *Mex-Gal4*: C) control group (*w^{1118}*); D) *UAS-ATP7^{RNAi}*; E) *UAS-Slmb^{stRNAi}*; F) *UAS-Slmb*. *UAS-ATP7^{FLAG}* overexpression larvae are inviable when raised on 1 mM CuCl$_2$ medium. G) Quantification of MtnB::eYFP levels based on the gray values of C–F in copper cell region. n ≥ 3 for each genotype. Abbreviations: st, strong; Con, control group; KD, knockdown: NF, normal food. *$p < 0.05$, **$p < 0.01$. Scale bar: 0.5 mm in A and B, 0.1 mm in C–F.

AKT2 has been shown to play an important role in ATP7A protein stabilization and translocation to the plasma membrane in vascular smooth muscle cells; this in turn facilitates activation of vascular SOD3, which protects against endothelial dysfunction in Type 2 diabetes mellitus [55]. Exposure to copper stimulates the phosphorylation of AKT and its transcription factor targets FoxO1a and FoxO3a, resulting in the nuclear exclusion of FoxO1a in a process apparently independent of the Insulin growth factor receptors IR and IGF1R [56]. Ctr1-mediated copper import is needed for both Erk1/2 and AKT phosphorylation, indicating the presence of a copper-dependent step upstream of Ras MAPK induced by RTKs including FGF, PDGF and EGF [57]. And activation of Erk in both flies and mammals is via copper binding to Mek1 which promotes the physical association between Mek1 and Erk [58].

The examples provided above highlight known/candidate Slmb targets (IκBα, ASK1, Nrf2, Akt) that are implicated in copper homeostasis and could therefore be regulating Ctr1 activity in mammalian and *Drosophila* cells. The next step will be to investigate Ctr1 and ATP7 levels upon perturbation of these targets and determine if/how copper in turn regulates Slmb.

Supplementary data to this article can be found online at https://doi.org/10.1016/j.bbamcr.2020.118768.

CRediT authorship contribution statement

Bichao Zhang: Conceptualization, Methodology, Investigation, Writing - original draft, Visualization. **Tim Binks:** Methodology,
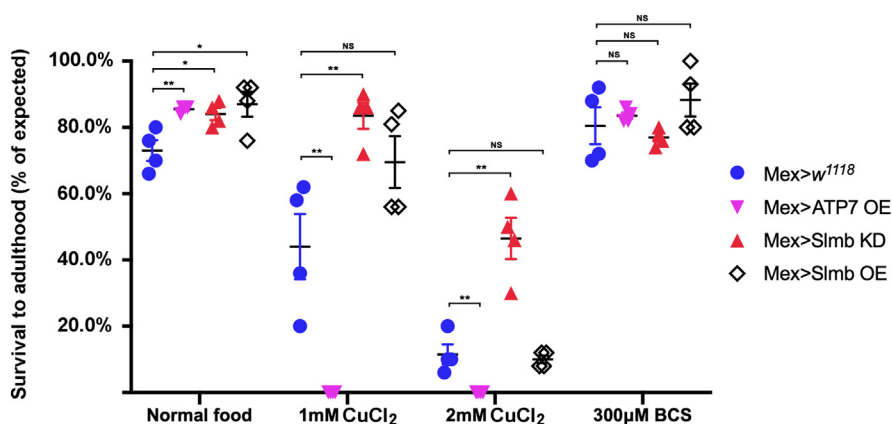

Fig. 8. *Slmb* knockdown protects larvae from copper toxicity. Percentage survival from 1st instar larval stage to adulthood was assessed for each genotype on normal, 1 mM CuCl$_2$, 2 mM CuCl$_2$ and 300 μm BCS-supplemented food. Error bars represent mean ± S.E.M. Genotypes tested were *w^{1118}*, *UAS-ATP7^{FLAG}*, *UAS-Slmb^{stRNAi}* and *UAS-Slmb* under the control of *Mex-Gal4*. *Slmb* knockdown was able to provide significant rescue compared with other genotypes on 1 mM or 2 mM CuCl$_2$ supplemented medium. *ATP7* overexpression resulted in 100% lethality on copper-supplemented food. Abbreviations: st, strong; OE, Overexpression; KD, knockdown, NS, no significance; NF, normal food. n = 4 for each genotype, *$p < 0.05$, **$p < 0.01$, NS > 0.05.
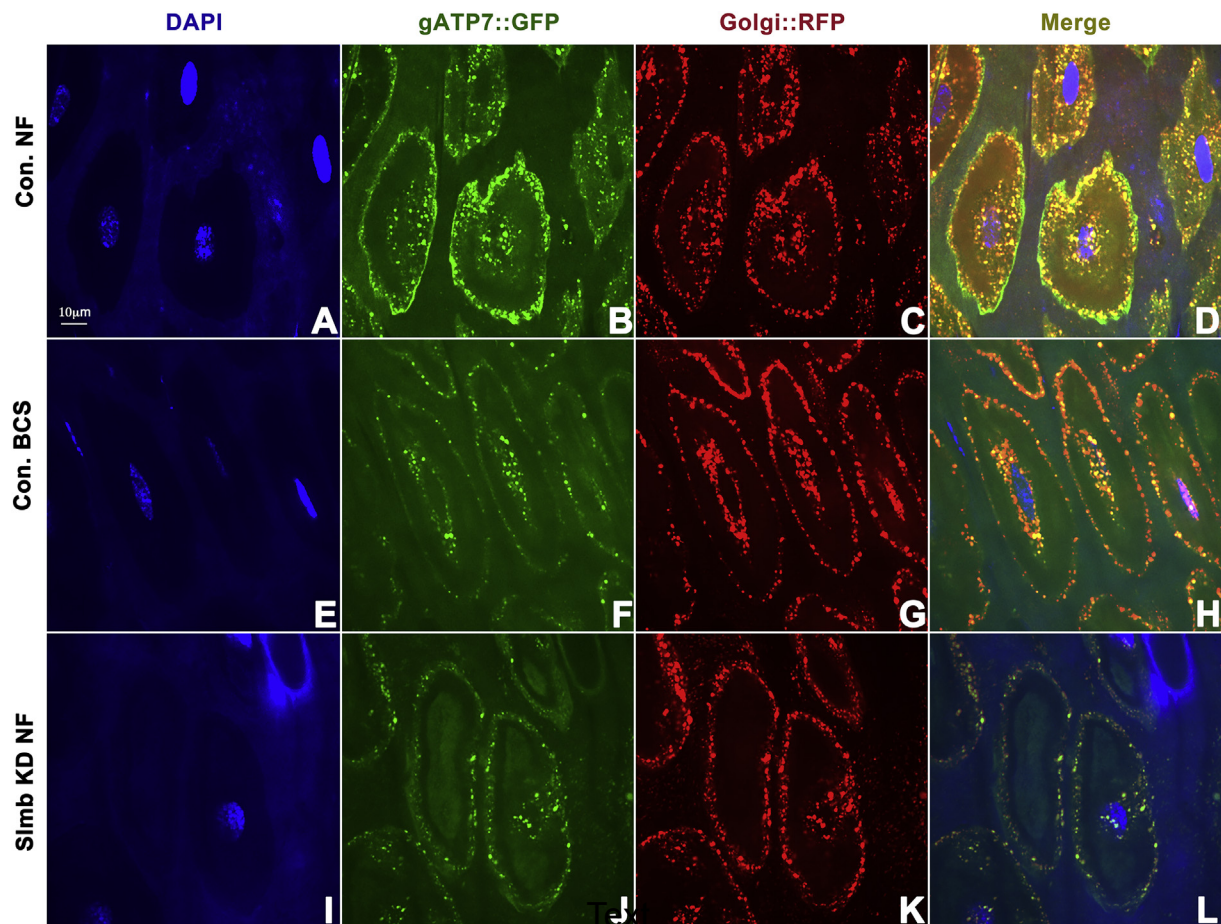
Fig. 9. *Slmb* knockdown mimics the effect of copper deficiency on ATP7 localisation. A–L) Copper cells of wandering 3rd instar larvae showing localization of nuclei (blue in A, E and I), gATP7::GFP (green in B, F and J), and Golgi::RFP (red in C, G and K) with merged image shown in D, H and L. A–H) Control larvae (*Mex-Gal4 > w[1118]*) raised on normal (NF, A-D) or BCS-supplemented (E–H) media. I–L) *Mex-Gal4 > Slmb[stRNAi]* larvae raised on normal food (NF). Each image is representative of *n* > 10 larvae per genotype/diet combination. Scale bar = 10 μm.
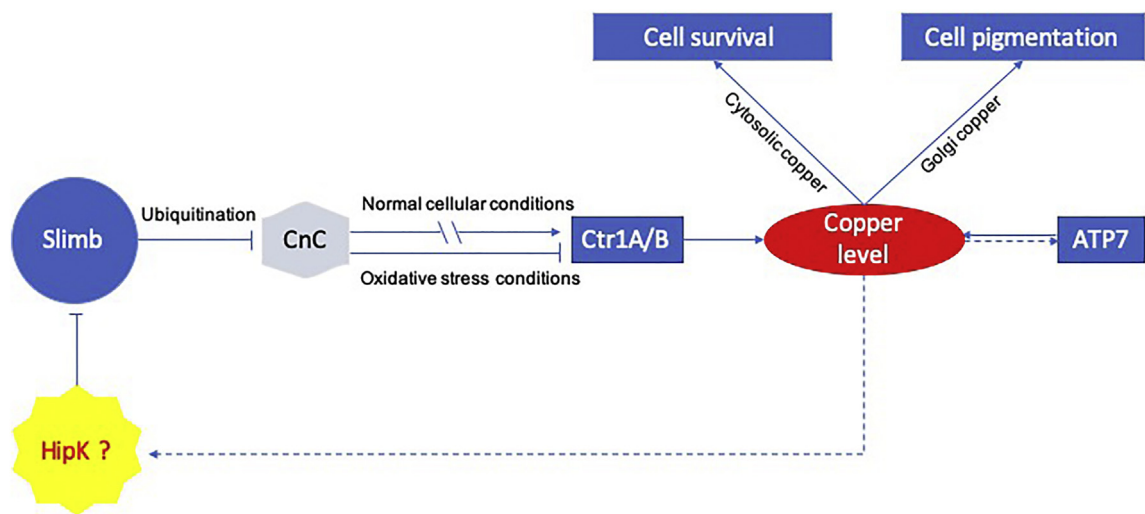

Fig. 10. Model summarising the possible relationship between Slmb and the copper homeostasis machinery.

Investigation, Writing - review & editing. **Richard Burke:** Conceptualization, Investigation, Writing - original draft, Supervision, Project administration, Funding acquisition.

Declaration of competing interest

11

Acknowledgments

The Australian *Drosophila* Biomedical Research Support Facility assisted in the importation and quarantine of fly strains used in this research. All transgenic *Drosophila* experiments carried out in this research were performed with the approval of the Monash University Institutional Biosafety Committee. Transgenic fly stocks were obtained from the Vienna Drosophila Resource Center (VDRC, www.vdrc.at) and Bloomington Drosophila Stock Centre (https://bdsc.indiana.edu/).

Funding

This work was supported by the Australian National Health and Medical Research Council (Project Grant number 606609).

References

[1] S. Lutsenko, Human copper homeostasis: a network of interconnected pathways, Curr. Opin. Chem. Biol. 14 (2010) 211–217.

[2] Z. Xiao, S. La Fontaine, A.I. Bush, A.G. Wedd, Molecular mechanisms of glutaredoxin enzymes: versatile hubs for thiol-disulfide exchange between protein thiols and glutathione, J. Mol. Biol. 431 (2019) 158–177.

[3] J.H. Menkes, M. Alter, G.K. Steigleder, D.R. Weakley, J.H. Sung, A sex-linked recessive disorder with retardation of growth, peculiar hair, and focal cerebral and cerebellar degeneration, Pediatrics 29 (1962) 764–779.

[4] P.A. Sharp, Ctr1 and its role in body copper homeostasis, Int. J. Biochem. Cell Biol. 35 (2003) 288–291.

[5] S. Lutsenko, Modifying factors and phenotypic diversity in Wilson's disease, Ann. N. Y. Acad. Sci. 1315 (2014) 56–63.

[6] R.J. Clifford, E.B. Maryon, J.H. Kaplan, Dynamic internalization and recycling of a metal ion transporter: Cu homeostasis and CTR1, the human Cu(+) uptake system, J. Cell Sci. 129 (2016) 1711–1721.

[7] J. Liu, A. Sitaram, C.G. Burd, Regulation of copper-dependent endocytosis and vacuolar degradation of the yeast copper transporter, Ctr1p, by the Rsp5 ubiquitin ligase, Traffic 8 (2007) 1375–1384.

[8] A. Southon, R. Burke, J. Camakaris, What can flies tell us about copper homeostasis? Metallomics 5 (2013) 1346–1356.

[9] T. Binks, J.C. Lye, J. Camakaris, R. Burke, Tissue-specific interplay between copper uptake and efflux in Drosophila, J. Biol. Inorg. Chem. 15 (2010) 621–628.

[10] J.L. Mummery-Widmer, M. Yamazaki, T. Stoeger, M. Novatchkova, S. Bhalerao, D. Chen, G. Dietzl, B.J. Dickson, J.A. Knoblich, Genome-wide analysis of Notch signalling in Drosophila by transgenic RNAi, Nature 458 (2009) 987–992.

[11] S. Swarup, E.M. Verheyen, Drosophila homeodomain-interacting protein kinase inhibits the Skp1-Cul1-F-box E3 ligase complex to dually promote Wingless and Hedgehog signaling, Proc. Natl. Acad. Sci. U. S. A. 108 (2011) 9887–9892.

[12] C. Pan, Y. Xiong, X. Lv, Y. Xia, S. Zhang, H. Chen, J. Fan, W. Wu, F. Liu, H. Wu, Z. Zhou, L. Zhang, Y. Zhao, UbcD1 regulates Hedgehog signaling by directly modulating Ci ubiquitination and processing, EMBO Rep. 18 (2017) 1922–1934.

[13] Z. Zhou, X. Yao, S. Li, Y. Xiong, X. Dong, Y. Zhao, J. Jiang, Q. Zhang, Deubiquitination of Ci/Gli by Usp7/HAUSP regulates hedgehog signaling, Dev. Cell 34 (2015) 58–72.

[14] Z. Zhang, X. Lv, W.C. Yin, X. Zhang, J. Feng, W. Wu, C.C. Hui, L. Zhang, Y. Zhao, Ter94 ATPase complex targets k11-linked ubiquitinated ci to proteasomes for partial degradation, Dev. Cell 25 (2013) 636–644.

[15] C. Gao, G. Chen, G. Romero, S. Moschos, X. Xu, J. Hu, Induction of Gsk3beta-beta-TrCP interaction is required for late phase stabilization of beta-catenin in canonical Wnt signaling, J. Biol. Chem. 289 (2014) 7099–7108.

[16] G. Reim, M. Hruzova, S. Goetze, K. Basler, Protection of armadillo/beta-Catenin by armless, a novel positive regulator of wingless signaling, PLoS Biol. 12 (2014) e1001988.

[17] E.M. Verheyen, S. Swarup, W. Lee, Hipk proteins dually regulate Wnt/Wingless signal transduction, Fly 6 (2012) 126–131.

[18] P. Ribeiro, M. Holder, D. Frith, A.P. Snijders, N. Tapon, Crumbs promotes expanded recognition and degradation by the SCF(Slimb/beta-TrCP) ubiquitin ligase, Proc. Natl. Acad. Sci. U. S. A. 111 (2014) E1980–E1989.

[19] X. Wang, Y. Zhang, S.S. Blair, Fat-regulated adaptor protein Dlish binds the growth suppressor expanded and controls its stability and ubiquitination, Proc. Natl. Acad. Sci. U. S. A. 116 (2019) 1319–1324.

[20] L. Hu, P. Wang, R. Zhao, S. Li, F. Wang, C. Li, L. Cao, S. Wu, The Drosophila F-box protein Slimb controls dSmurf protein turnover to regulate the Hippo pathway, Biochem. Biophys. Res. Commun. 482 (2017) 317–322.

[21] X. Hong, H.T. Nguyen, Q. Chen, R. Zhang, Z. Hagman, P.M. Voorhoeve, S.M. Cohen, Opposing activities of the Ras and Hippo pathways converge on regulation of YAP protein turnover, EMBO J. 33 (2014) 2447–2457.

[22] J.D. Hayes, S. Chowdhry, A.T. Dinkova-Kostova, C. Sutherland, Dual regulation of transcription factor Nrf2 by Keap1 and by the combined actions of beta-TrCP and GSK-3, Biochem. Soc. Trans. 43 (2015) 611–620.

[23] R. Cheng, K. Takeda, I. Naguro, T. Hatta, S.I. Iemura, T. Natsume, H. Ichijo, K. Hattori, beta-TrCP-dependent degradation of ASK1 suppresses the induction of the apoptotic response by oxidative stress, Biochim. Biophys. Acta Gen. Subj. 2018

[24] S. Asada, A. Ikeda, R. Nagao, H. Hama, T. Sudo, A. Fukamizu, Y. Kasuya, T. Kishi, Oxidative stress-induced ubiquitination of RCAN1 mediated by SCFbeta-TrCP ubiquitin ligase, Int. J. Mol. Med. 22 (2008) 95–104.

[25] J.J. Wong, S. Li, E.K. Lim, Y. Wang, C. Wang, H. Zhang, D. Kirilly, C. Wu, Y.C. Liou, H. Wang, F. Yu, A Cullin1-based SCF E3 ubiquitin ligase targets the InR/PI3K/TOR pathway to regulate neuronal pruning, PLoS Biol. 11 (2013) e1001657.

[26] S. Lee, J.W. Wang, W. Yu, B. Lu, Phospho-dependent ubiquitination and degradation of PAR-1 regulates synaptic morphology and tau-mediated Abeta toxicity in Drosophila, Nat. Commun. 3 (2012) 1312.

[27] X. Lin, F. Wang, Y. Li, C. Zhai, G. Wang, X. Zhang, Y. Gao, T. Yi, D. Sun, S. Wu, The SCF ubiquitin ligase Slimb controls Nerfin-1 turnover in Drosophila, Biochem. Biophys. Res. Commun. 495 (2018) 629–633.

[28] S. Li, C. Wang, E. Sandanaraj, S.S. Aw, C.T. Koe, J.J. Wong, F. Yu, B.T. Ang, C. Tang, H. Wang, The SCFSlimb E3 ligase complex regulates asymmetric division to inhibit neuroblast overgrowth, EMBO Rep. 15 (2014) 165–174.

[29] H.Q. Nguyen, J. Nye, D.W. Buster, J.E. Klebba, G.C. Rogers, G. Bosco, Drosophila casein kinase I alpha regulates homolog pairing and genome organization by modulating condensin II subunit Cap-H2 levels, PLoS Genet. 11 (2015) e1005014.

[30] G. Zhu, Z. Fan, M. Ding, L. Mu, J. Liang, Y. Ding, Y. Fu, B. Huang, W. Wu, DNA damage induces the accumulation of Tiam1 by blocking beta-TrCP-dependent degradation, J. Biol. Chem. 289 (2014) 15482–15494.

[31] H. Inuzuka, A. Tseng, D. Gao, B. Zhai, Q. Zhang, S. Shaik, L. Wan, X.L. Ang, C. Mock, H. Yin, J.M. Stommel, S. Gygi, G. Lahav, J. Asara, Z.X. Xiao, W.G. Kaelin Jr., J.W. Harper, W. Wei, Phosphorylation by casein kinase I promotes the turnover of the Mdm2 oncoprotein via the SCF(beta-TRCP) ubiquitin ligase, Cancer Cell 18 (2010) 147–159.

[32] A. Hay-Koren, S. Bialik, V. Levin-Salomon, A. Kimchi, Changes in cIAP2, survivin and BimEL expression characterize the switch from autophagy to apoptosis in prolonged starvation, J. Intern. Med. 281 (2017) 458–470.

[33] J. Colin, J. Garibal, A. Clavier, A. Rincheval-Arnold, S. Gaumer, B. Mignotte, I. Guenal, The drosophila Bcl-2 family protein Debcl is targeted to the proteasome by the beta-TrCP homologue slimb, Apoptosis 19 (2014) 1444–1456.

[34] B. Zhang, Z. Zhang, L. Li, Y.R. Qin, H. Liu, C. Jiang, T.T. Zeng, M.Q. Li, D. Xie, Y. Li, X.Y. Guan, Y.H. Zhu, TSPAN15 interacts with BTRC to promote oesophageal squamous cell carcinoma metastasis via activating NF-kappaB signaling, Nat. Commun. 9 (2018) 1423.

[35] B. Cho, G. Pierre-Louis, A. Sagner, S. Eaton, J.D. Axelrod, Clustering and negative feedback by endocytosis in planar cell polarity signaling is modulated by ubiquitinylation of prickle, PLoS Genet. 11 (2015) e1005259.

[36] K. Shimizu, H. Fukushima, K. Ogura, E.C. Lien, N.T. Nihira, J. Zhang, B.J. North, A. Guo, K. Nagashima, T. Nakagawa, S. Hoshikawa, A. Watahiki, K. Okabe, A. Yamada, A. Toker, J.M. Asara, S. Fukumoto, K.I. Nakayama, K. Nakayama, H. Inuzuka, W. Wei, The SCFbeta-TRCP E3 ubiquitin ligase complex targets Lipin1 for ubiquitination and degradation to promote hepatic lipogenesis, Sci. Signal. 10 (2017).

[37] H. Chung, M.R. Bogwitz, C. McCart, A. Andrianopoulos, R.H. Ffrench-Constant, P. Batterham, P.J. Daborn, Cis-regulatory elements in the Accord retrotransposon result in tissue-specific expression of the Drosophila melanogaster insecticide resistance gene Cyp6g1, Genetics 175 (2007) 1071–1077.

[38] M.D. Phillips, G.H. Thomas, Brush border spectrin is required for early endosome recycling in Drosophila, J. Cell Sci. 119 (2006) 1361–1370.

[39] A. Selvaraj, K. Balamurugan, H. Yepiskoposyan, H. Zhou, D. Egli, O. Georgiev, D.J. Thiele, W. Schaffner, Metal-responsive transcription factor (MTF-1) handles both extremes, copper load and copper starvation, by activating different genes, Genes Dev. 19 (2005) 891–896.

[40] S.W. Mercer, J. Wang, R. Burke, In vivo modeling of the pathogenic effect of copper transporter mutations that cause Menkes and Wilson diseases, motor neuropathy, and susceptibility to Alzheimer's disease, J. Biol. Chem. 292 (2017) 4113–4122.

[41] M. Norgate, E. Lee, A. Southon, A. Farlow, P. Batterham, J. Camakaris, R. Burke, Essential roles in development and pigmentation for the Drosophila copper transporter DmATP7, Mol. Biol. Cell 17 (2006) 475–484.

[42] A. Southon, N. Palstra, N. Veldhuis, A. Gaeth, C. Robin, R. Burke, J. Camakaris, Conservation of copper-transporting P(IB)-type ATPase function, Biometals 23 (2010) 681–694.

[43] H. Zhou, K.M. Cadigan, D.J. Thiele, A copper-regulated transporter required for copper acquisition, pigmentation, and specific stages of development in Drosophila melanogaster, J. Biol. Chem. 278 (2003) 48210–48218.

[44] A. Southon, R. Burke, M. Norgate, P. Batterham, J. Camakaris, Copper homoeostasis in Drosophila melanogaster S2 cells, Biochem. J. 383 (2004) 303–309.

[45] M.L. Turski, D.J. Thiele, Drosophila Ctr1A functions as a copper transporter essential for development, J. Biol. Chem. 282 (2007) 24017–24026.

[46] K. Balamurugan, D. Egli, H. Hua, R. Rajaram, G. Seisenbacher, O. Georgiev, W. Schaffner, Copper homeostasis in Drosophila by complex interplay of import, storage and behavioral avoidance, EMBO J. 26 (2007) 1035–1044.

[47] M.J. Petris, J.F. Mercer, J.G. Culvenor, P. Lockhart, P.A. Gleeson, J. Camakaris, Ligand-regulated transport of the Menkes copper P-type ATPase efflux pump from the Golgi apparatus to the plasma membrane: a novel mechanism of regulated trafficking, EMBO J. 15 (1996) 6084–6095.

[48] P. Calap-Quintana, J. Gonzalez-Fernandez, N. Sebastia-Ortega, J.V. Llorens, M.D. Molto, *Drosophila melanogaster* models of metal-related human diseases and metal toxicity, Int. J. Mol. Sci. 18 (2017).

[49] R. Burke, E. Commons, J. Camakaris, Expression and localisation of the essential copper transporter DmATP7 in Drosophila neuronal and intestinal tissues, Int. J. Biochem. Cell Biol. 40 (2008) 1850–1860.

[50] S.E. Lacher, J.S. Lee, X. Wang, M.R. Campbell, D.A. Bell, M. Slattery, Beyond

12

antioxidant genes in the ancient Nrf2 regulatory network, Free Radic. Biol. Med. 88 (2015) 452–465.

[51] H.S. Comstra, J. McArthy, S. Rudin-Rush, C. Hartwig, A. Gokhale, S.A. Zlatic, J.B. Blackburn, E. Werner, M. Petris, P. D'Souza, P. Panuwet, D.B. Barr, V. Lupashin, A. Vrailas-Mortimer, V. Faundez, The interactome of the copper transporter ATP7A belongs to a network of neurodevelopmental and neurodegeneration factors, Elife 6 (2017).

[52] N.S. Kenneth, G.E. Hucks Jr., A.J. Kocab, A.L. McCollom, C.S. Duckett, Copper is a potent inhibitor of both the canonical and non-canonical NFkappaB pathways, Cell Cycle 13 (2014) 1006–1014.

[53] S. Wang, L. Wu, Y. Wang, X. Luo, Y. Lu, Copper-induced germline apoptosis in Caenorhabditis elegans: the independent roles of DNA damage response signaling and the dependent roles of MAPK cascades, Chem. Biol. Interact. 180 (2009) 151–157.

[54] P.J. Crouch, L.W. Hung, P.A. Adlard, M. Cortes, V. Lal, G. Filiz, K.A. Perez, M. Nurjono, A. Caragounis, T. Du, K. Laughton, I. Volitakis, A.I. Bush, Q.X. Li, C.L. Masters, R. Cappai, R.A. Cherny, P.S. Donnelly, A.R. White, K.J. Barnham, Increasing Cu bioavailability inhibits Abeta oligomers and tau phosphorylation, Proc. Natl. Acad. Sci. U. S. A. 106 (2009) 381–386.

[55] V. Sudhahar, M.N. Okur, Z. Bagi, J.P. O'Bryan, N. Hay, A. Makino, V.S. Patel, S.A. Phillips, D. Stepp, M. Ushio-Fukai, T. Fukai, Akt2 (protein kinase B beta) stabilizes ATP7A, a copper transporter for extracellular superoxide dismutase, in vascular smooth muscle: novel mechanism to limit endothelial dysfunction in type 2 diabetes mellitus, Arterioscler. Thromb. Vasc. Biol. 38 (2018) 529–541.

[56] I. Hamann, K. Petroll, L. Grimm, A. Hartwig, L.O. Klotz, Insulin-like modulation of Akt/FoxO signaling by copper ions is independent of insulin receptor, Arch. Biochem. Biophys. 558 (2014) 42–50.

[57] C.Y. Tsai, J.C. Finley, S.S. Ali, H.H. Patel, S.B. Howell, Copper influx transporter 1 is required for FGF, PDGF and EGF-induced MAPK signaling, Biochem. Pharmacol. 84 (2012) 1007–1013.

[58] M.L. Turski, D.C. Brady, H.J. Kim, B.E. Kim, Y. Nose, C.M. Counter, D.R. Winge, D.J. Thiele, A novel role for copper in Ras/mitogen-activated protein kinase signaling, Mol. Cell. Biol. 32 (2012) 1284–1295.

Zhang et al., Supplementary material

Supp Fig. 1 *Slmb* overexpression line rescues phenotypic defects caused by weak *Slmb* RNAi line. A-C) Dorsal views of adult *Drosophila* containing the *Pnr-Gal4* driver together with the following transgenes: A) no transgene (*w^{1118}*); B) *UAS-Slmb^{wRNAi}*; C) *UAS-Slmb*; D) *UAS-Slmb^{wRNAi}* + *UAS-Slmb*. All images were acquired with a 3.2X objective lens. Abbreviations: w, weak; KD, knockdown; OE, overexpression. n>10 for each genotype.

Supp Fig. 2 *Slmb* overexpression does not affect ATP7 intracellular localization A-H) Copper cells of wandering 3rd instar larvae showing the localization of the nucleus (blue in A, and E), gATP7::GFP (green in B, and F), and Golgi::RFP (red in C, and G) with merged image shown in D, and H. A-D) Control (*Mex-Gal4>w^{1118}*) larvae raised on normal food. E-H) *Mex-Gal4>UAS-Slmb*larvae raised on normal food (NF). Scale bar = 10 µm.

The thoracic cleft caused by copper deficiency is due to apoptosis

Our phenotypic analysis revealed that manipulation of *ATP7*, *Ctr1A*, and *Slmb* all could generate thoracic clefts under the control of *Pnr-Gal4* driver. These thoracic clefts could be due either to inhibition of cell proliferation or induction of cell death. Immunostaining against PH3 was performed to investigate whether *Slmb* knockdown could inhibit cell proliferation. As shown in Supp Fig. 3A, PH3 positive cells were observed throughout the entire wing disc in control larvae. No changes in PH3 signal were detected after *Slmb* knockdown (Supp Fig. 3B), indicating that Slmb is not involved in regulating cell proliferation. In contrast, elevated numbers of apoptotic active Caspase 3-positive cells were detected in the *Pnr-Gal4* expressing area of wing imaginal discs with *Slmb* knockdown (Supp Fig.3G-I and S). Therefore, we propose that *Slmb* knockdown induces apoptosis but does not affect cell proliferation in larval wing discs. A similar increase in the number of apoptotic cells was observed with *Ctr1A* knockdown (Supp Fig. 3J-L, S) but not with *ATP7* knockdown (Supp Fig. 3M-O, S) or overexpression (Supp Fig. 3P-S).

Supp Fig. 3 *Slmb* knockdown induces apoptosis but does not affect cell proliferation in wing imaginal discs. Immunostaining against PH3 (A-B) and active Caspase3 (C-R) was performed to detect cell proliferation and death after manipulating *Slmb*, *ATP7*, and *Ctr1A*. A-B) PH3 (green) and DAPI (blue) staining in control (*w^{1118}*) (A), and *Slmb* knockdown (B) discs. C) Overview of larval wing discs with DAPI (blue), anti-Caspase3 (green) and Golgi::RFP (red) in control; red area is the *Pnr-Gal4* expressing region. D-R) The *Pnr-Gal4* expressing region of larval wing discs with the following genotypes: D-F) control group G-I), *UAS-Slmb^{stRNAi}*; J-L) *UAS-Ctr1A^{stRNAi}*; M-O) *UAS-ATP7^{RNAi}*; P-R) *UAS-ATP7^{FLAG}*. S) Quantification of 'over area' fraction of active Caspase3 signal after manipulating *Slmb*, *ATP7* and *Ctr1A*. Abbreviations: OE, overexpression; KD, knockdown, NS, not significant. *p <0.05, **p <0.01. Scale bar: 50µm in A-D, 30µm in E-J.

A. Control   B. Slmb KD (w)   C. Slmb OE   D. Slmb KD (w) + Slmb OE

Pnr-Gal4
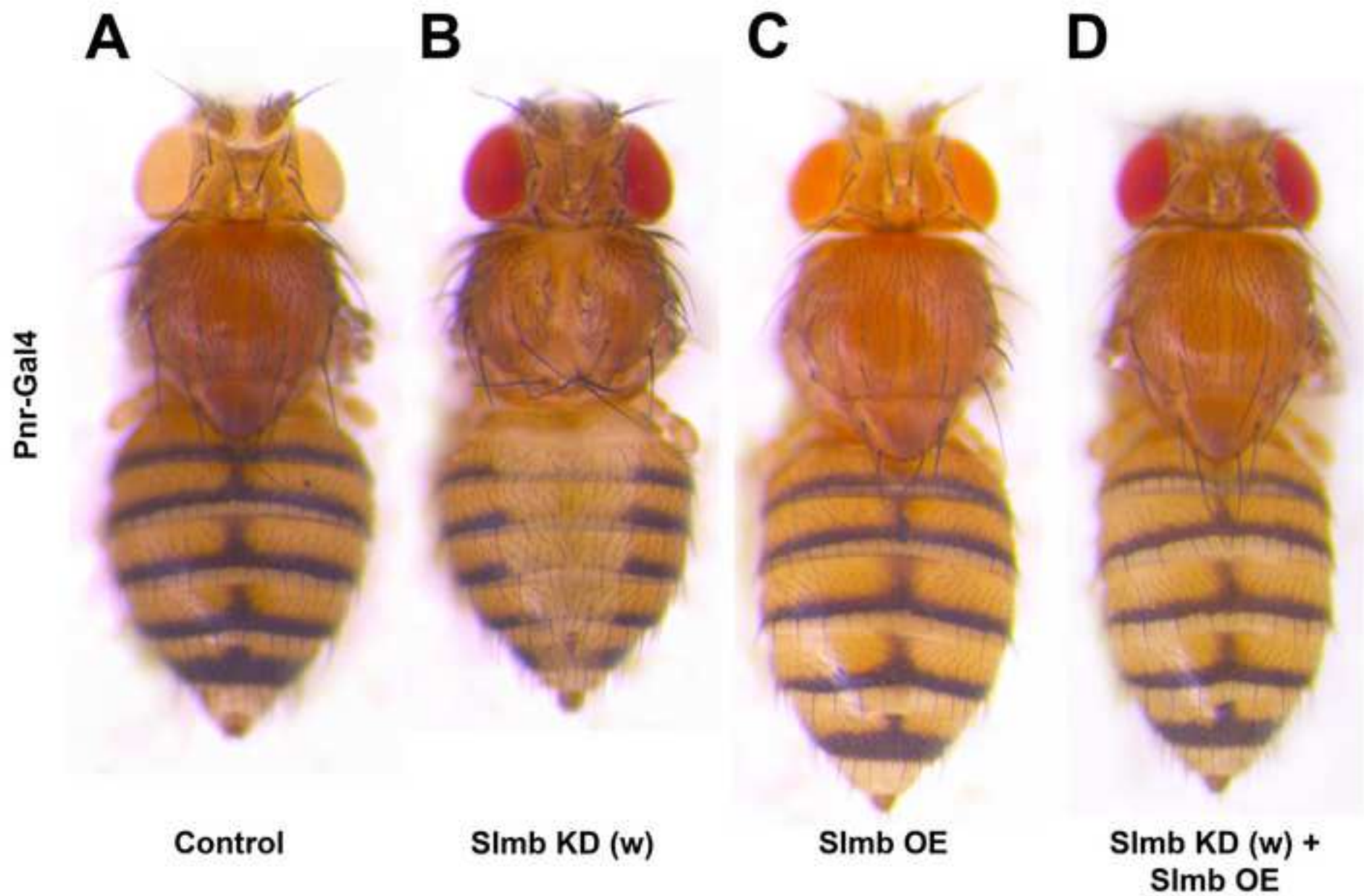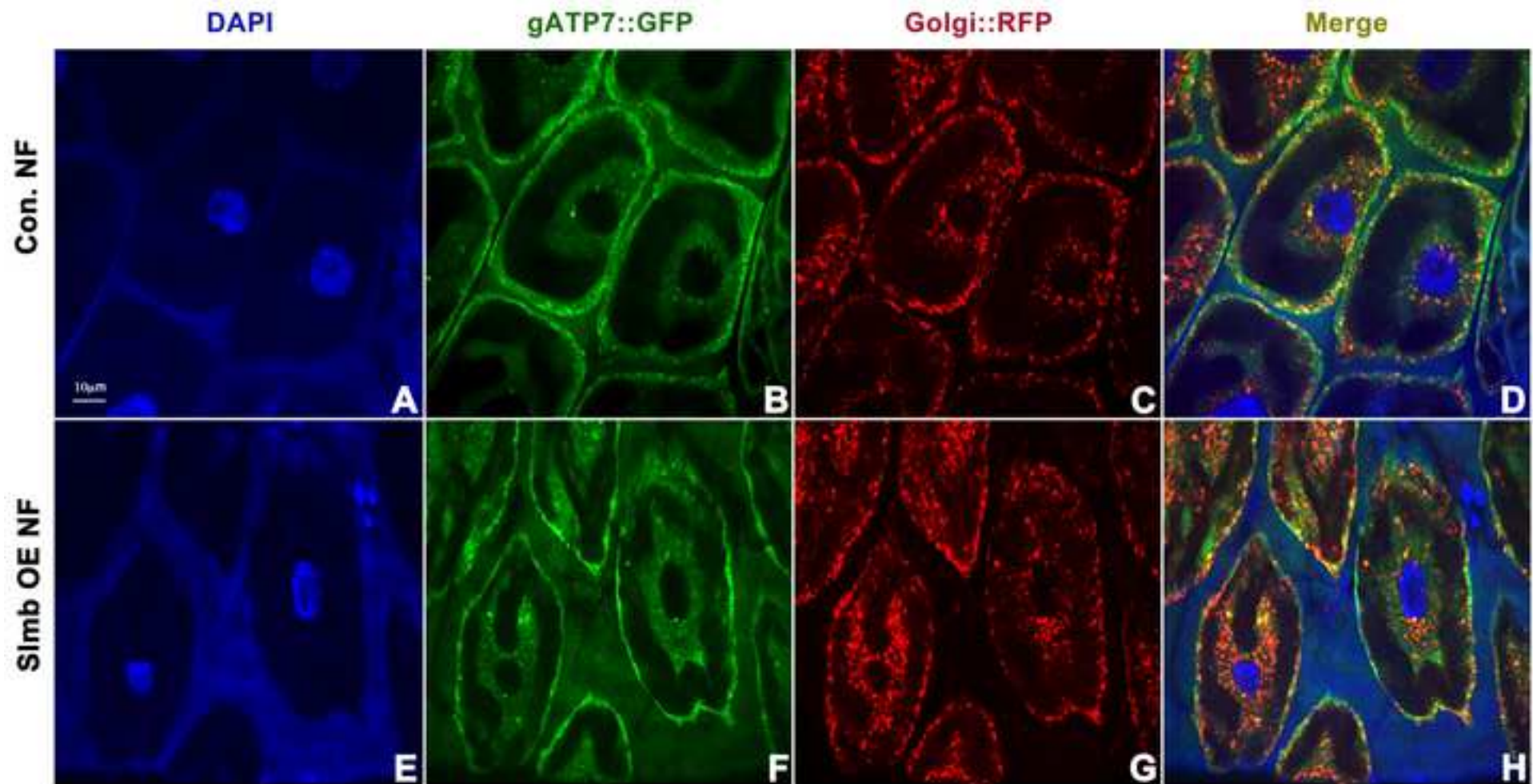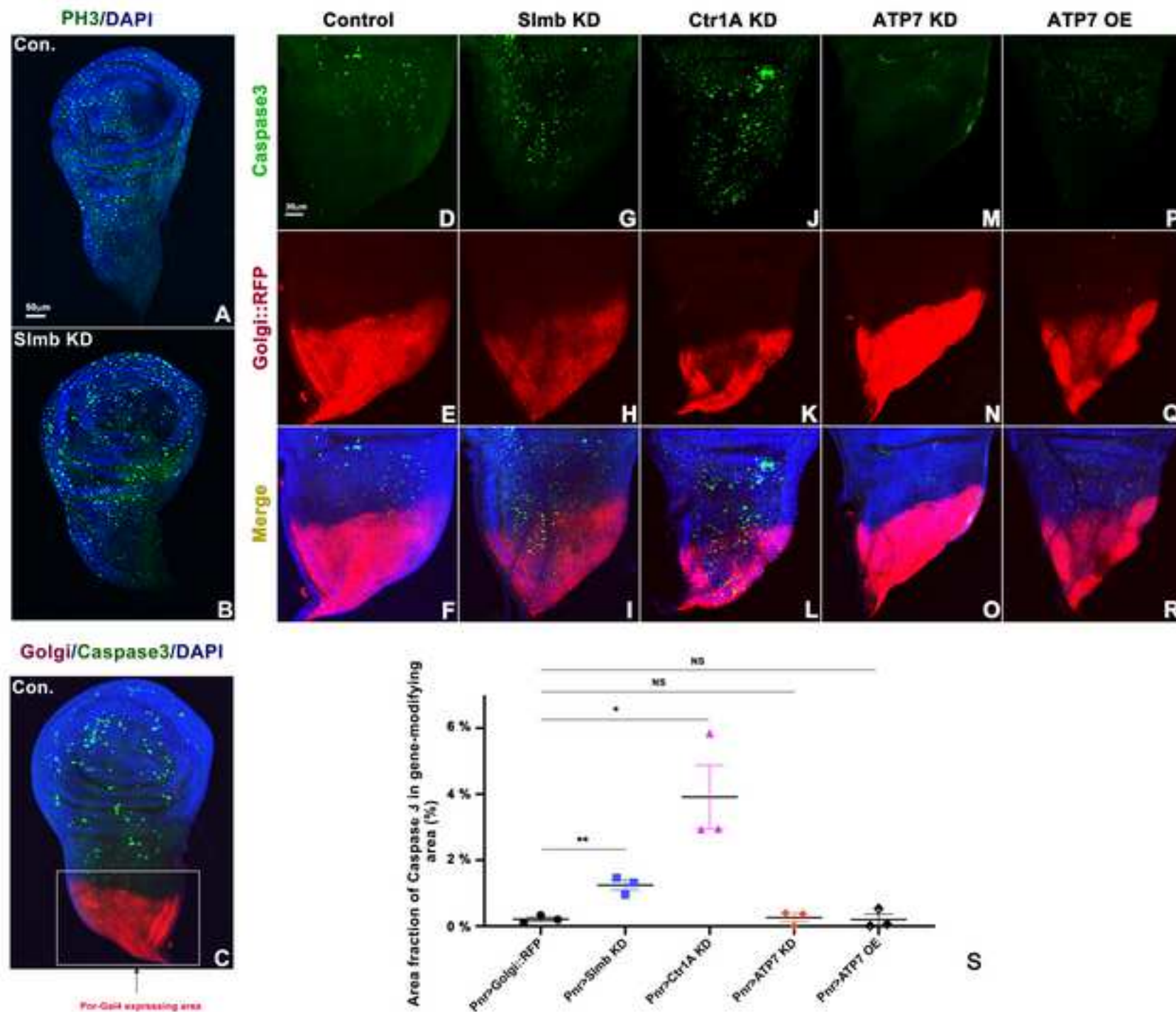
CHAPTER 4: IDENTIFICATION OF NOVEL ATP7 REGULATING PROTEINS FROM CANDIDATES PROVIDED BY THE ATP7A INTERACTOME

4.1 Background

Copper is an essential cofactor for several enzymes critically required for cellular respiration, antioxidant defence, neuronal development, and formation of connective tissue. ATP7A, a copper transporter, is normally localized to the *trans*-Golgi network (Petris et al., 1996), where it is responsible for the transport of Cu to copper-dependent enzymes such as tyrosinase (Petris et al., 2000) and lysyl oxidase (Tchaparian et al., 2000) in the lumen of the Golgi. When Cu is overloaded in cells, ATP7A-containing vesicles are transported to the plasma membrane for Cu efflux. ATP7B, structurally similar to ATP7A, is restricted to the liver where it is required to remove excess copper into the bile (Linz and Lutsenko, 2007). In humans, mutations in *ATP7A* or *ATP7B* are known to cause Menkes disease (an incurable copper deficiency disorder) (Madsen and Gitlin, 2007) or Wilson's disease (a serious copper toxicity disorder) (Squitti et al., 2016), respectively.

Our research group has demonstrated that ATP7, the sole *Drosophila* orthologue of ATP7A and ATP7B, is expressed in both the gastrointestinal tract and nervous system of the fly (Burke et al., 2008), and is required for copper transport (Norgate et al., 2006). Flies lacking ATP7 die in early larval stages from a copper deficiency. In this study, we aim to investigate how the *Drosophila* orthologues of proteins shown to interact with mammalian ATP7A may regulate ATP7 activity in the fly to modulate copper efflux.

A recent proteomics study identified 541 ATP7A-binding proteins in mammalian cells, some of which (such as COG1 and COG8) were shown to have roles in copper homeostasis (Comstra et al., 2017). COG1 and COG8 deficient HEK293 cells fail to respond to extracellular copper due to the defects in ATP7A and CTR1 surface transport mechanisms. Some of these ATP7A interactome members were known to have ubiquitin-protein transferase activity, suggesting they might be involved in regulatory degradation of ATP7A by the Ubiquitin Proteasome System (UPS). Therefore, these proteins, listed in Table 1, were selected for analysis to investigate whether they are involved in regulating copper homeostasis. In this study, the GAL4/UAS system was combined with the *RNAi* technique to investigate the role of the *Drosophila* orthologues of these ATP7A interacting proteins and screen for phenotypes suggestive of a role in regulating copper homeostasis in the fly.

4.2 Results

4.2.1 Assessing the potential role of ATP7 interacting proteins

23 *Drosophila* orthologues of mammalian ATP7A interactome members were selected to investigate their relationship with ATP7. UAS-*RNAi* transgenes targeting each candidate gene were tested under the control of the *Pnr-Gal4*, *GMR-Gal4* and *tub-Gal4* driver lines (Table 1), which drive gene expression in wing discs, eye discs and ubiquitously, respectively (Ray and Lakhotia, 2015; Wang et al., 2012; White-Cooper, 2012). The 23 genes were then classified into three groups based on the phenotypic defects caused by their knockdown under the control of *Pnr-Gal4*: Group 1 (no phenotypic defects), Group 2 (thoracic or abdominal defects), and Group 3 (lethality).

	Mammalian	*Drosophila*	VDRC ID	*Pnr-Gal4*	*GMR-Gal4*	*tub-Gal4*
Group 1	BRCC3	Cv-c	V32329	No defect	No defect	Pupal lethal
			V109824	No defect	No defect	Pupal lethal
	ARIHI	ari-1	V39591	No defect	No defect	No defect
			V35029	No defect	No defect	No defect
	PPM1B	Alph	V32476	No defect	No defect	No defect
	PPM1G	CG10417	V106180*	No defect	No defect	Pupal lethal
	PSMD13	Rpn9	V103733	No defect	No defect	Pupal lethal
	PSMC1	Rpt2	V105973*	No defect	No defect	No defect
	UBXN1	CG8209	V100483	No defect	No defect	No defect
	PPP2R5D	CG4733	V34894	No defect	No defect	Pupal lethal
			V107621	No defect	No defect	Pupal lethal
Group 2	RNF2	Sce	V27465	Abnormal thorax and wings; Lost scutellum	No defect	Pupal lethal
			106328	Abnormal thorax and wings; Lost scutellum	No defect	Pupal lethal
	TCEB1	EloC	V15303	Abnormal thorax	No defect	Larval lethal
			V105740	No defect	No defect	Larval lethal

	CUL3	Cul3	V109415	Abnormal thorax and wings	No defect	Larval lethal
			V25875	No defect	No defect	No defect
	RNF20	Bre1	V108206	Abnormal thorax	No defect	Larval lethal
	PPP2R2A	tws	V104167	Abnormal bristles on thorax	No defect	Pupal lethal
			V34340	Abnormal bristles on thorax	No defect	Pupal lethal
	PSMD4	Rpn10	V110659	Mild hypopigmentation on thorax	No defect	Pupal lethal
	STUB1	Chi	V43934	Abnormal thorax	No defect	Pupal lethal
Group 3						
	SKP1	SkpA	V32789	Larval lethal	No defect	Larval lethal
			V107815	Larval lethal	No defect	Larval lethal
	PSMA6	Prosα1	V49681	Larval lethal	shiny eye	Larval lethal
	PSMD1	Rpn2	V106457	Pupal lethal	Abnormal eyes and some pupal lethal	Larval lethal
	PSMD3	Rpn3	V108582	Larval lethal	Shiny eye	Larval lethal
	PSMD6	Rpn7	V101467*	Larval lethal	Pupal lethal	Larval lethal
	PSMC2	Rpt1	V108834	Pupal lethal	Abnormal eyes	Larval lethal
	PSMC5	Rpt6	V100620*	Pupal lethal	Abnormal eyes	Larval lethal
	STRN	Cka	V35234	Pupal lethal	No defect	Larval lethal

Table 1 *Phenotypic defects caused by knockdown of candidate ATP7 interactome genes under the control of Pnr-Gal4, GMR-Gal4 and tub-Gal4.* **"**Pupal lethal" stands for "Die at

ATP7 interacting candidates of Group 2 produced various defects under the control of *Pnr-Gal4* which drives expression in the central third of the dorsal thorax and abdomen. Knockdown of *Sce* and *Chi* both generated a severe thoracic cleft, with additional abdominal hypopigmentation was observed in *Sce RNAi*-expressing flies (Fig.1B and H). Thoracic cleft plus hyperpigmentation was caused by knockdown of *EloC* and *Cul3* (Fig.1C and D). In *Bre1* knockdown flies, a mild cleft was visualized on the dorsal midline of the thorax (Fig.1E). Additionally, *tws* knockdown was found to cause loss of bristles on the thorax (Fig.1F). Interestingly, *Rpn10* knockdown was the unique candidate in Group 2, causing the mild reduction of pigmentation in the midline of thorax and abdomen compared with surrounding tissues (Fig.1G). While we postulated that these ATP7 interactome candidates might be involved in regulating copper homeostasis, none of these defects were modified by low copper conditions (300μM BCS containing medium) or high copper conditions (1mM $CuCl_2$ containing medium) (data not shown). Four of the *RNAi* lines used in the analysis were VDRC KK lines with an additional 40A insertion site (See * in Table 1). This insertion is known to cause non-specific lethality under *tub-Gal4* but is not associated with any defects under *GMR* or *Pnr-Gal4* control.
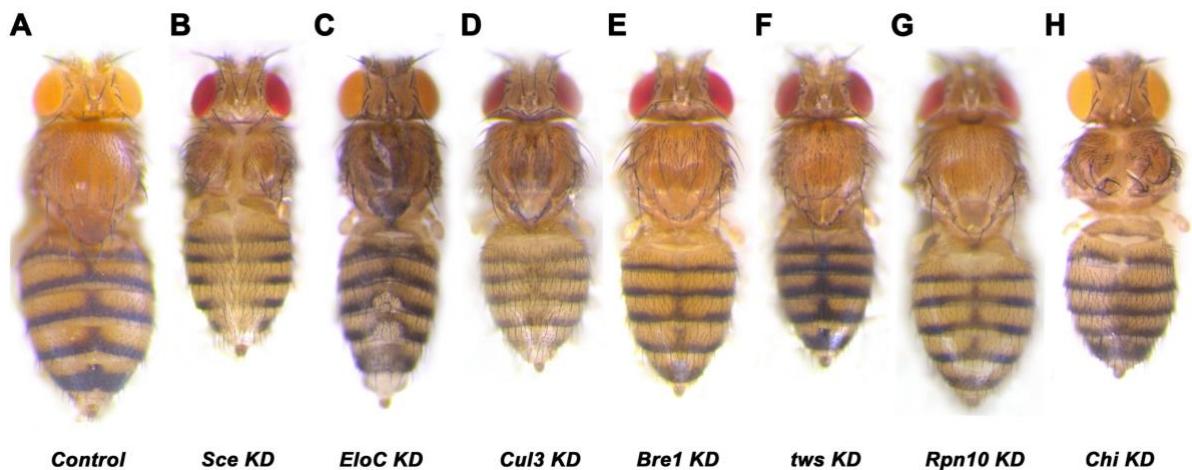

Fig.1 *Phenotypic defects caused by knockdown of ATP7 interactomes members.* A-H) Dorsal views of adult female *Drosophila* containing the *Pnr-Gal4* driver together with the following transgenes: A) no transgene (*w^1118^*); B) *UAS-Sce^RNAi^*; C) *UAS-EloC^RNAi^*; D) *UAS-Cul3^RNAi^*; E) *UAS-Bre1^RNAi^*; F) *UAS-tws^RNAi^*; G) *UAS-Rpn10^RNAi^*; H) *UAS-Chi^RNAi^*. Abbreviations: KD,

knockdown. All images were captured using a 3.2× objective lens and are representative of n >
20 for each genotype.

A fourth driver liner, *En-Gal4,* which expresses UAS transgenes in the entire posterior
compartment of the developing wing imaginal disc, was used to further characterise the Group
2 genes. Progeny were raised at 18, 22, 25 and 29°C to test different levels of knockdown; the
GAL/UAS system is temperature sensitive, with higher expression / knockdown levels achieved
at higher temperatures. Knockdown of *Sce*, *EloC* and *Chi* caused lethality at all temperatures
except 18°C, where the wings of surviving adults showed complete ablation of the posterior
compartment; *Sce* and *EloC* knockdown wings were also smaller than normal and distorted in
shape (Fig.2). At 18°C, knockdown of *Sce*, *Eloc* or *Chi* resulted in the absence of posterior
wings while *Cul3* and *tws* knockdown produced abnormal wings, but no defects were observed
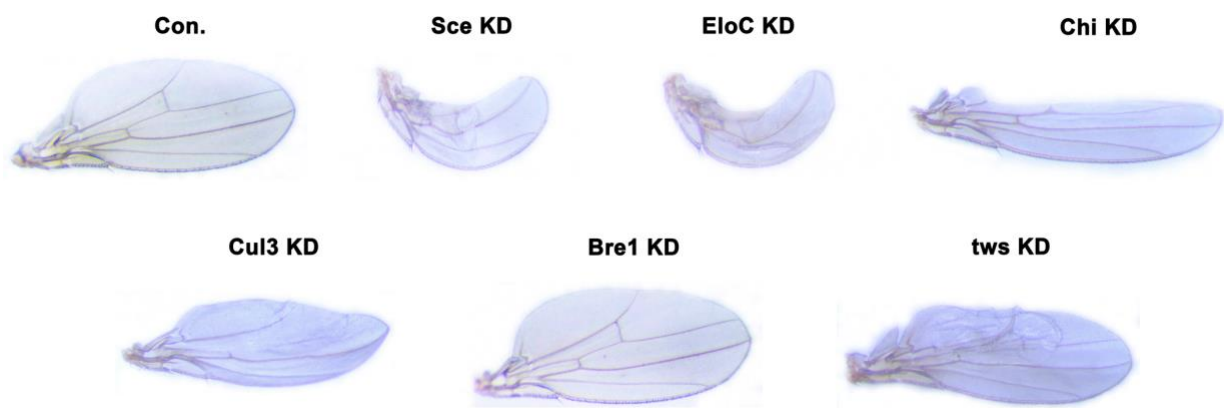after *Bre1* knockdown (Fig.2).

Fig.2 *Wing defects caused by knockdown of ATP7 interactome members*. Wing phenotype
produced by the following transgenes together with *En-Gal4*: no transgene (w^{1118}), *UAS-Sce^{RNAi}*,
UAS-EloC^{RNAi}, *UAS-Chi^{RNAi}*, *UAS-Cul3^{RNAi}*, *UAS-Bre1^{RNAi}*, *UAS-tws^{RNAi}*. All images were
captured using a 4× objective lens and are representative of n > 20 for each genotype.

The dramatic loss of posterior wing tissue seen in Fig. 2 may have been due to apoptosis of
these cells. To test this, immunostaining against active caspase 3 (a marker of apoptosis) was
performed; this revealed that only *Sce* and *EloC* knockdown-induced apoptosis in wing discs
under the control of *En-Gal4* (Fig.3). Therefore, Sce and EloC were subsequently selected for
investigating their relationship with ATP7. Since both Sce and EloC are E3 ubiquitin ligase, we
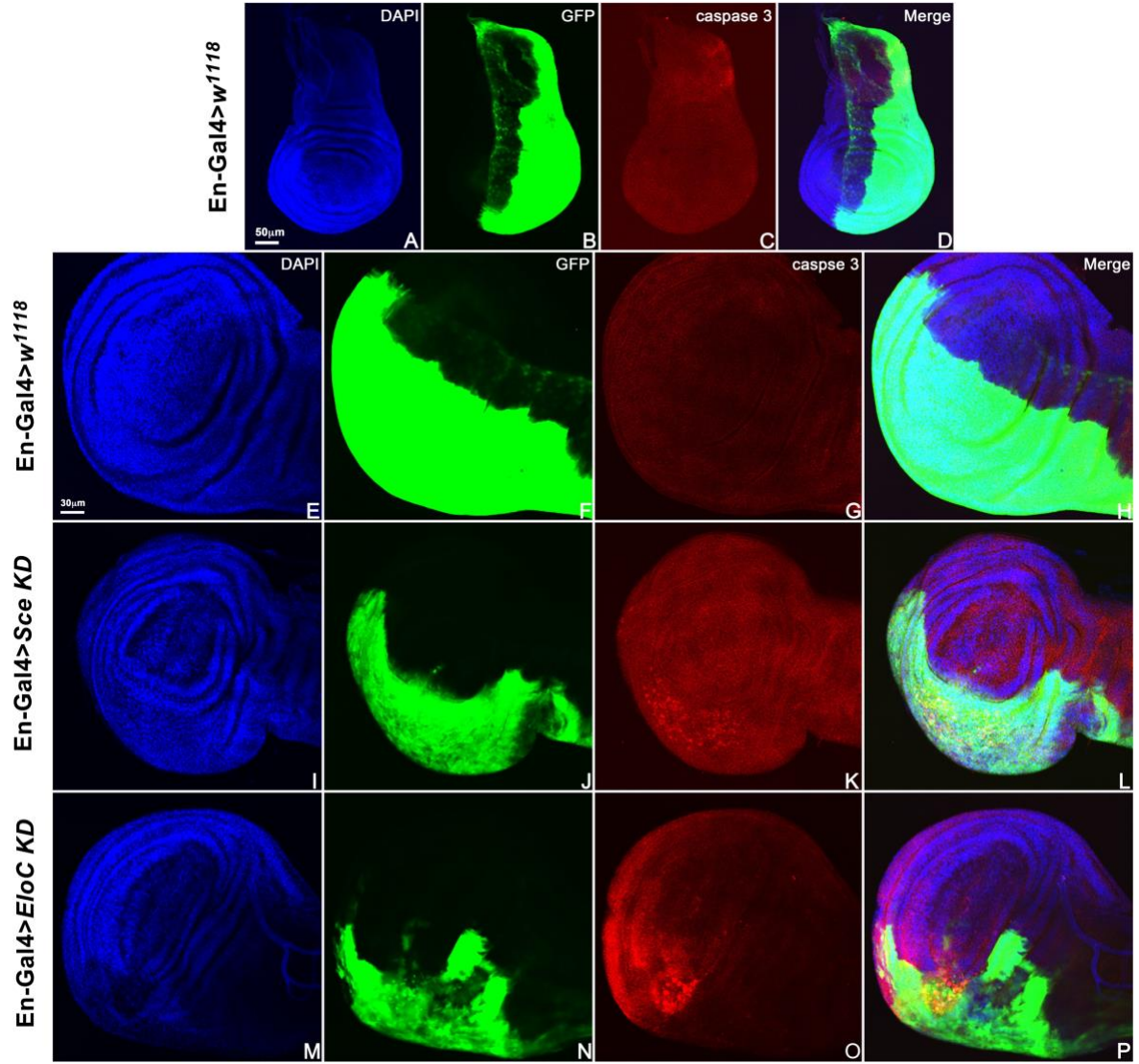postulated that they might participate in the posttranslational regulation of ATP7.

Fig.3 *Suppression of Sce and EloC induced apoptosis on wing discs.* Immunostaining against active caspase 3 (A-P) was performed to detect cell death after knockdown of *Sce* and *EloC*. A-D) Overview of larval wing discs with DAPI (blue), GFP (green), anti-caspase 3 (red) and merge in control (*w^1118*); green area is the *En-Gal4*-expressing region. E-P) The *En-Gal4*-expressing region of larval wing discs with the following genotypes: E-H) control group (*w^1118*); I-L) *UAS-Sce^RNAi*; M-P) *UAS-EloC^RNAi*. Abbreviations: KD, knockdown. Scale bar: 50μm in A-D, 30μm in E-P.

4.2.2 Investigating the relationship of Sce and EloC with ATP7/Ctr1A

In order to characterize the interaction between Sce/EloC with ATP7, *ATP7* knockdown was applied to rescue the defects caused by the suppression of *Sce* and *EloC* since our previous results revealed that knockdown of *ATP7* partially rescued the thoracic clefts of *Slmb RNAi*-

expressing flies (an E3 ubiquitin ligase) (Zhang et al., 2020). Unfortunately, *ATP7* knockdown failed to show a rescue effect to the defects produced by *Sce* knockdown (Fig.4E). However, the thoracic hyperpigmentation in *EloC* knockdown-expressing flies was abolished by *ATP7* knockdown (Fig.4F). In addition, copper transporter Ctr1A (responsible for copper uptake) is regulated by Slmb (Zhang et al., 2020). Therefore, we investigated the relationship of Sce and EloC with Ctr1A. As shown in Fig.4H, the abdominal hypopigmentation caused by *Sce* knockdown was partially rescued by *Ctr1A* overexpression, whereas no rescue effect was observed in *EloC* knockdown-expressing flies (Fig.4H and I).
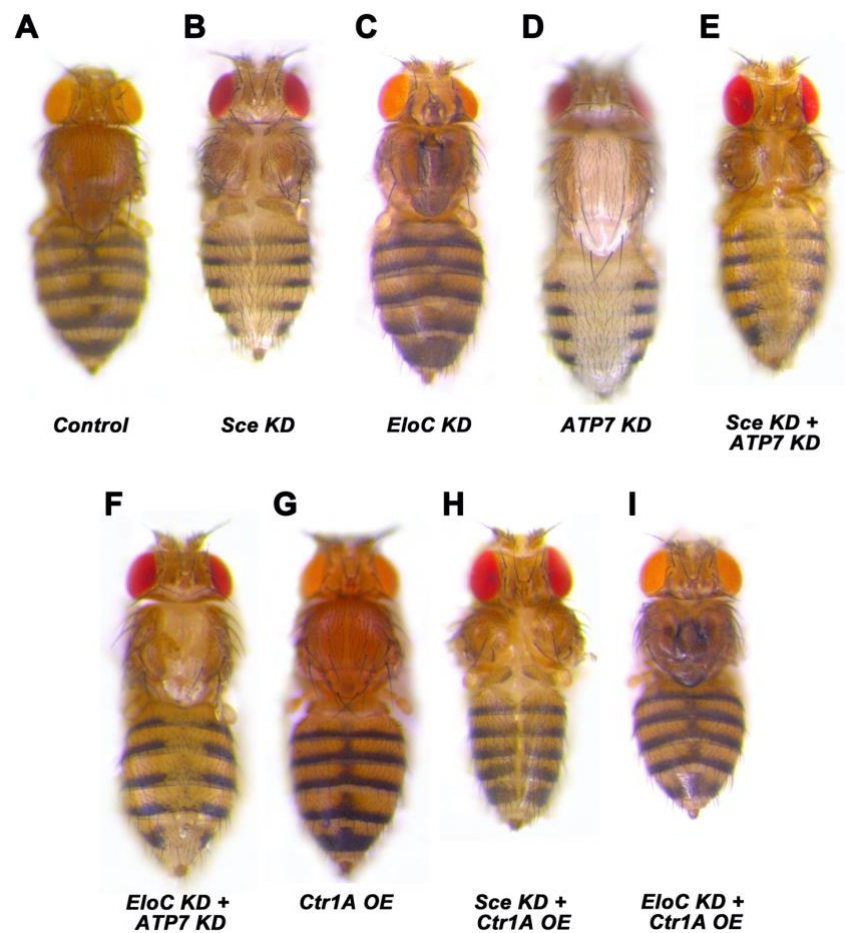
Fig.4 *Phenotype produced by knockdown of Sce or EloC combined with ATP7 knockdown or Ctr1A overexpression.* A-H) Dorsal views of adult female *Drosophila* containing the *Pnr-Gal4* driver together with the following transgenes: A) no transgene (*w^1118^*); B) *UAS-Sce^RNAi^*; C) *UAS-EloC^RNAi^*; D) *UAS-ATP7^RNAi^*; E) *UAS-Sce^RNAi^ + UAS-ATP7^RNAi^*; F) *UAS-EloC^RNAi^ +UAS-ATP7^RNAi^*; G) *UAS-Ctr1A*; H) *UAS-Sce^RNAi^ + UAS-Ctr1A*; I) *UAS-EloC^RNAi^ + UAS-Ctr1A*.

Abbreviations: KD, knockdown; OE, overexpression. All images were captured using a 3.2× objective lens and are representative of n > 20 for each genotype.

Next, we investigated whether knockdown of *Sce* or *EloC* could regulate intracellular copper levels by using *Ctr1B(prom)::eYFP* which is upregulated in copper deficient cells. No change in *Ctr1B(prom)::eYFP* expression was observed after *Sce* knockdown (Fig.5B) while knockdown of *EloC* led to the decrease of Ctr1B(prom)::eYFP which suggested the increase in copper levels (Fig.5C). Given that EloC might regulate copper levels, we tested the impact of copper levels on EloC activity by using *Mex-Gal4* which expresses genes in midgut. Here, we found the survival rate of EloC knockdown-expressing flies was higher than the control in high copper conditions (1mM CuCl$_2$ containing medium) while low copper conditions (300μM BCS containing medium) did not cause any effect, suggesting that *EloC* knockdown protects larvae from copper toxicity (Fig.5D). These results together suggested that EloC is involved in copper efflux. Therefore, we mainly focused on EloC in subsequent experiments.
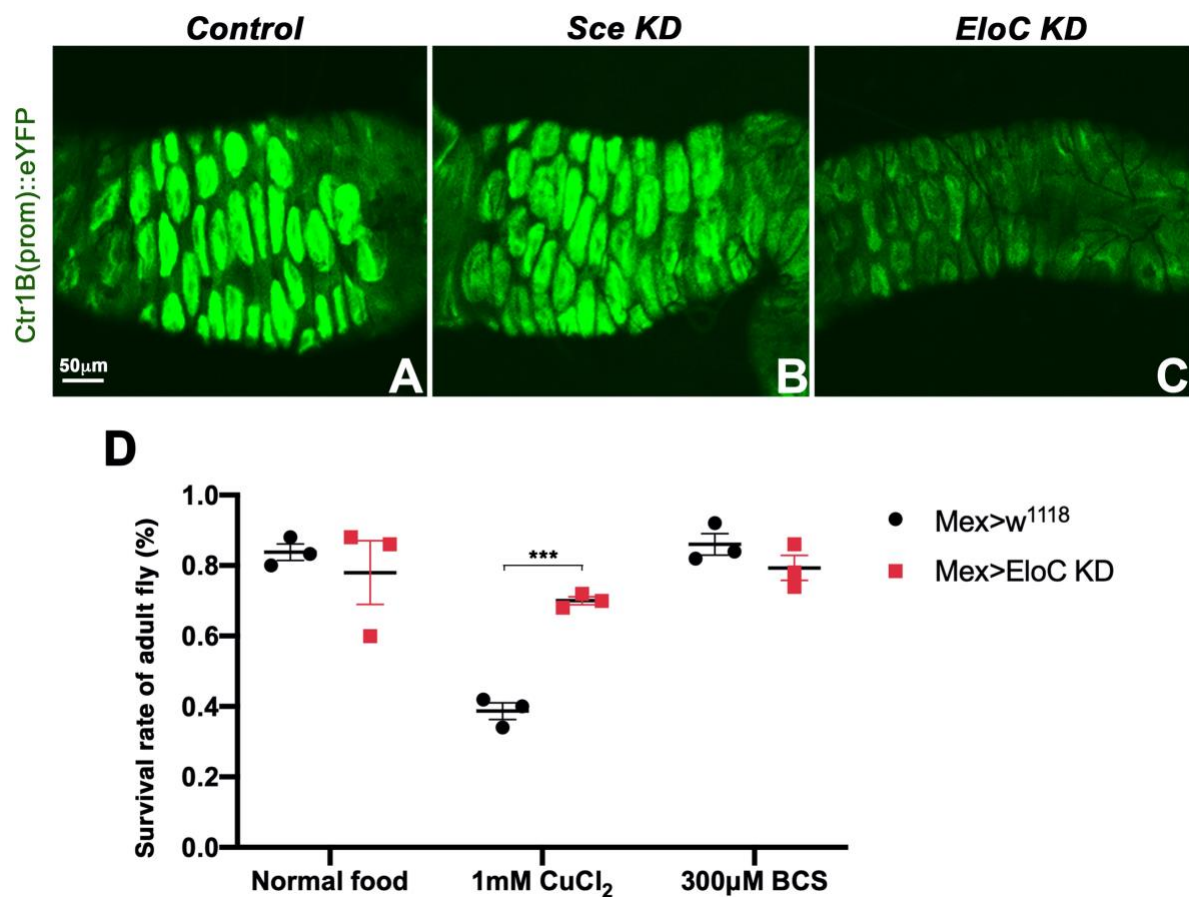

Fig.5 *EloC might regulate copper efflux*. Reporter gene *Ctr1B::eYFP* was used to assess copper levels under control of candidate gene modification in a dietary copper-deficient

environment. A-C) The midgut copper cell region of larvae raised under copper-deficient conditions with the following genotypes, all containing *HR-Gal4*: A) control group (*w^1118^*); B) *UAS-Sce^RNAi^*; C) *UAS-EloC^RNAi^*. D) Percentage survival from 1st instar larval stage to adulthood was assessed for each genotype on normal, 1 mM CuCl₂, and 300 μM BCS-supplemented food. Error bars represent mean ± S.E.M. Genotypes tested were *w^1118^* and *UAS-EloC^RNAi^* under the control of *Mex-Gal4*. *EloC* knockdown was able to provide significant rescue compared with the control on 1 mM CuCl₂ supplemented medium. Abbreviations: KD, knockdown. n = 3 for each genotype, ***$p < 0.001$. Scale bar: 50 μm in A–C.

4.3 Conclusion

In this chapter, 23 *Drosophila* orthologues of ATP7A interacting proteins possessing ubiquitin-protein transferase activity were selected and screened by using GAL4/UAS system combined with *RNAi* technique. Only those candidates which produced defects on the thorax and / or abdomen under the control of *Pnr-Gal4* were used in the subsequent experiments. With *En-Gal4* driven, knockdown of *Sce*, *EloC* and *Chi* caused complete ablation of the posterior wings. However, immunostaining against caspase 3 revealed an increase of caspase 3 only in *Sce* and *EloC* knockdown but not in *Chi* knockdown. Therefore, Sce and EloC were selected to investigate whether they could interact with ATP7 and Ctr1A. Rescue experiments failed to demonstrate whether Sce and EloC regulate ATP7 and Ctr1A like Slmb does. In order to investigate whether Sce and EloC participate in regulating copper levels, the copper reporter gene *Ctr1B(prom)::eYFP* was utilized. Here, we found that only *EloC* knockdown resulted in a decrease in the expression of *Ctr1B*. In addition, adult fly survival experiments showed that knockdown of *EloC* increased the fly survival rate in high copper conditions, suggesting that EloC is involved in maintaining copper homeostasis. Since EloC forms an E3 ubiquitin complex with Von Hippel-Lindau (Vhl), Cullin2 (Cul2) and RBX1 (Gossage et al., 2015), we investigated how the Vhl/EloC/Cul2 E3 ubiquitin ligase regulates copper homeostasis in Chapter 5.

Sce, an E3 ubiquitin-protein ligase, ubiquitinates histone H2A, thereby participating in histone code and gene regulation (Gutiérrez et al., 2012). In addition, Sce was also reported to play a critical role in somatic cell proliferation and differentiation during ovarian follicle formation (Narbonne et al., 2004), and promote epithelial-mesenchymal transition (Jefferies et al., 2020). In this study, we suspected that Sce might be involved in the posttranslational regulation of

copper transporter ATP7 since its mammalian homologue was identified to physically bind with ATP7A. Knockdown of *Sce* was found to generate copper deficient defects: thoracic cleft and abdominal hypopigmentation, while inducing apoptosis in wing discs. However, modifying *ATP7* expression failed to rescue the *Sce* knockdown defects, even though a partial rescue effect was observed by *Ctr1A* overexpression, suggesting that Sce might regulate copper levels via Ctr1A. Unfortunately, the results of copper detection by using copper reporter gene *Ctr1B(prom)::eYFP* showed no alteration of *Ctr1B* expression after Sce knockdown, indicating no change in copper levels. Given that *EloC* knockdown resulted in a decrease of *Ctr1B*, *EloC* was therefore selected for the subsequent experiment. Due the rescue effect of *Ctr1A* overexpression on *Sce* knockdown defects, we will be investigating whether Sce interact with Ctr1A in regulating copper homeostasis in the future.

References:

Burke, R., Commons, E., Camakaris, J., 2008. Expression and localisation of the essential copper transporter DmATP7 in Drosophila neuronal and intestinal tissues. Int J Biochem Cell Biol 40, 1850-1860.

Comstra, H.S., McArthy, J., Rudin-Rush, S., Hartwig, C., Gokhale, A., Zlatic, S.A., Blackburn, J.B., Werner, E., Petris, M., D'Souza, P., Panuwet, P., Barr, D.B., Lupashin, V., Vrailas-Mortimer, A., Faundez, V., 2017. The interactome of the copper transporter ATP7A belongs to a network of neurodevelopmental and neurodegeneration factors. Elife 6.

Gossage, L., Eisen, T., Maher, E.R., 2015. VHL, the story of a tumour suppressor gene. Nat Rev Cancer 15, 55-64.

Gutiérrez, L., Oktaba, K., Scheuermann, J.C., Gambetta, M.C., Ly-Hartig, N., Müller, J., 2012. The role of the histone H2A ubiquitinase Sce in Polycomb repression. Development 139, 117-127.

Jefferies, G., Somers, J., Lohrey, I., Chaturvedi, V., Calabria, J., Marshall, O.J., Southall, T.D., Saint, R., Murray, M.J., 2020. Maintenance of Cell Fate by the Polycomb Group Gene Sex Combs Extra Enables a Partial Epithelial Mesenchymal Transition in. G3 (Bethesda) 10, 4459-4471.

Linz, R., Lutsenko, S., 2007. Copper-transporting ATPases ATP7A and ATP7B: cousins, not twins. J Bioenerg Biomembr 39, 403-407.

Madsen, E., Gitlin, J.D., 2007. Copper and iron disorders of the brain. Annu Rev Neurosci 30, 317-337.

Narbonne, K., Besse, F., Brissard-Zahraoui, J., Pret, A.M., Busson, D., 2004. polyhomeotic is required for somatic cell proliferation and differentiation during ovarian follicle formation in Drosophila. Development 131, 1389-1400.

Norgate, M., Lee, E., Southon, A., Farlow, A., Batterham, P., Camakaris, J., Burke, R., 2006. Essential roles in development and pigmentation for the Drosophila copper transporter DmATP7. Mol Biol Cell 17, 475-484.

Petris, M.J., Mercer, J.F., Culvenor, J.G., Lockhart, P., Gleeson, P.A., Camakaris, J., 1996. Ligand-regulated transport of the Menkes copper P-type ATPase efflux pump from the Golgi

apparatus to the plasma membrane: a novel mechanism of regulated trafficking. EMBO J 15, 6084-6095.

Petris, M.J., Strausak, D., Mercer, J.F., 2000. The Menkes copper transporter is required for the activation of tyrosinase. Hum Mol Genet 9, 2845-2851.

Ray, M., Lakhotia, S.C., 2015. The commonly used eye-specific sev-GAL4 and GMR-GAL4 drivers in Drosophila melanogaster are expressed in tissues other than eyes also. J Genet 94, 407-416.

Squitti, R., Siotto, M., Arciello, M., Rossi, L., 2016. Non-ceruloplasmin bound copper and ATP7B gene variants in Alzheimer's disease. Metallomics 8, 863-873.

Tchaparian, E.H., Uriu-Adams, J.Y., Keen, C.L., Mitchell, A.E., Rucker, R.B., 2000. Lysyl oxidase and P-ATPase-7A expression during embryonic development in the rat. Arch Biochem Biophys 379, 71-77.

Wang, N., Leung, H.T., Mazalouskas, M.D., Watkins, G.R., Gomez, R.J., Wadzinski, B.E., 2012. Essential roles of the Tap42-regulated protein phosphatase 2A (PP2A) family in wing imaginal disc development of Drosophila melanogaster. PLoS One 7, e38569.

White-Cooper, H., 2012. Tissue, cell type and stage-specific ectopic gene expression and RNAi induction in the Drosophila testis. Spermatogenesis 2, 11-22.

Zhang, B., Binks, T., Burke, R., 2020. The E3 ubiquitin ligase Slimb/β-TrCP is required for normal copper homeostasis in Drosophila. Biochim Biophys Acta Mol Cell Res 1867, 118768.

CHAPTER 5: THE VHL E3 UBIQUITIN LIGASE COMPLEX REGULATES MELANIZATION VIA SIMA, CNC AND THE COPPER IMPORT PROTEIN CTR1A
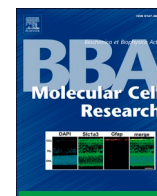
The Vhl E3 ubiquitin ligase complex regulates melanisation via sima, cnc and the copper import protein Ctr1A

Bichao Zhang, Lauren A Kirn, Richard Burke[*]

School of Biological Sciences, Monash University, Wellington Rd Clayton, 3800 VIC, Australia

A B S T R A C T

VHL encodes a tumour suppressor, which possesses E3 ubiquitin ligase activity in complex with EloC and Cul2. In tumour cells or in response to hypoxia, VHL activity is lost, causing accumulation of the transcription factor HIF-1alpha. In this study, we demonstrated that in *Drosophila,* Rpn9, a regulatory component of the 26 s proteasome, participates in the Vhl-induced proteasomal degradation of sima, the *Drosophila* orthologue of HIF-1alpha. Knockdown of *Vhl* induces increased melanisation in the adult fly thorax and concurrent decrease in pigmentation in the abdomen. Both these defects are rescued by knockdown of *sima* and partially by knockdown of *cnc*, which encodes the fly orthologue of the transcription factor Nrf2, the master regulator of oxidative stress response. We further show that *sima* overexpression and *Rpn9* knockdown both result in post-translational downregulation of the copper uptake transporter Ctr1A in the fly eye and that Ctr1A expression exacerbates *Vhl* knockdown defects in the thorax and rescues these defects in the abdomen. We conclude that Vhl negatively regulates both sima and cnc and that in the absence of Vhl, these transcription factors interact to regulate Ctr1A, copper uptake and consequently melanin formation. We propose a model whereby the co-regulatory relationship between sima and cnc flips between thorax and abdomen: in the thorax, sima is favoured leading to upregulation of Ctr1A; in the abdomen, cnc dominates, resulting in the post-translational downregulation of Ctr1A.

1. Introduction

Copper is an essential cofactor and/or structural component for several important cellular enzymes which participate in biological processes such as energy metabolism (e.g. cytochrome *c* oxidase), defence against oxidative stress (e.g. Zn, Cu-superoxide dismutase) and iron metabolism (e.g. ceruloplasmin) [1–3]. An excess of copper is toxic to cells due to its potential to catalyse the generation of reactive oxygen species [4], and therefore transport of copper and cellular copper content are tightly regulated. Many of the components involved in copper homeostasis are well characterized at the molecular level. These include transporters that mediate copper uptake (CTR1) and efflux (ATP7A and ATP7B), molecules that sequester and store copper (MT and GSH) and specialized copper chaperone proteins (CCS, ATOX1 and COX17) that guide copper to organelles and copper-dependent cuproenzymes [5].

Von Hippel-Lindau (VHL) is a tumour suppressor protein which forms the VCB-CR complex together with transcription elongation factors C and B (ELOC and ELOB), Cullin2 (CUL2) and RBX1 [6]. This complex is involved in the proteasomal degradation of hypoxia-inducible factors (HIFs), transcription factors which regulate cellular responses to hypoxia [7,8]. Hypoxia has been found to stimulate copper uptake by increasing the expression of CTR1 through the HIF pathway [9–11]. However, extreme hypoxia inhibited Cu uptake [12]. ATP7A is also upregulated under hypoxia and HIF-2alpha can directly interact with *ATP7A* at the transcriptional level [13–15]. Furthermore, copper was hypothesized to be required for HIF-1alpha transcriptional activity [16,17].

Defective VHL-mediated proteolysis is a common feature of clear-cell renal cell carcinomas (ccRCCs), which can also be caused by TCEB1 mutations that abolish EloC-VHL binding, leading to HIF accumulation [18]. Other pathways and components recurrently mutated in ccRCC have also been identified, including the Keap1-Nrf2-Cul3 complex [19]. Keap1 is the substrate recognition subunit of a Cul3-based E3 ubiquitin ligase complex [20]. The transcription factor Nrf2 (Cap-n-collar (cnc) in *Drosophila*), activates genes in response to oxidative stress and is negatively regulated by Keap1 [21,22]. We have previously demonstrated that cnc is involved in regulating copper uptake via Ctr1A after downregulation of the Slmb (Supernumerary limbs) E3 ubiquitin ligase in

Drosophila [23].

Melanisation is an important innate immune response that involves both melanin formation and deposition [24]. Toxic metabolites, such as reactive oxygen species, are generated during melanin biosynthesis in order to harm pathogens [25]. The melanisation reaction is strictly regulated since excessive toxic metabolites could kill the host [26]. In *Drosophila*, DOPA and dopamine serve as the precursors of melanin [27]. *Drosophila* Tyrosine Hydroxylase (TH) catalyses the oxidation of tyrosine to DOPA which is then converted to dopamine by DOPA decarboxylase (Ddc) [25]. Some fractions of DOPA and dopamine are then converted into DOPA-melanin and dopamine-melanin [25]. In *Drosophila*, laccase 2, a multicopper oxidase, is thought to be responsible for this final catalytic conversion which results in the production of both brown and black pigment [28]. Furthermore, an examination of the metallomes of several *Drosophila* wild type and mutant strains found that copper content correlated with cuticle pigmentation levels [29]. Therefore, cellular copper levels may contribute to melanisation via modulation of laccase 2 activity.

In the present study, we found that knockdown of *Vhl* induced gain and loss of pigmentation on the adult *Drosophila* thorax and abdomen respectively and that these phenotypes were completely rescued by co-knockdown of *similar* (*sima*), which encodes the *Drosophila* orthologue of HIF-1alpha. Thoracic hyper-melanisation is a known response to oxidative stress while hypopigmentation can be caused by reduced Golgi copper levels [25,30]. Furthermore, we found that Vhl/sima interacts genetically with Keap1/cnc to regulate Ctr1A and that Rpn9, a component of the 26 s proteasome, participates in Vhl's targeting of sima. Therefore, we propose that the Vhl/EloC/Cul2 E3 ubiquitin complex regulates copper trafficking and subsequent melanisation via sima, cnc and ultimately Ctr1A.

2. Materials and methods

2.1. Drosophila stocks and maintenance

The following fly stocks were used: w^{1118} (BL (Bloomington *Drosophila* Stock Center, Bloomington, IN, USA) 3605), *Pannier* (*Pnr*)-*Gal4* (BL3039), *GMR-Gal4* (BL9146), *Mex-Gal4*, *TubP-GAL80ts/Cyo; Pnr-Gal4/TM6β* (BL67060) and Double balancer (*w; IF/CyO; MKRS/TM6β*). RNAi lines obtained from the Vienna *Drosophila* Resource Center include V108920 (*Vhl*), V15303 (*EloC*), V108159 (*ATP7*), V46758 (*Ctr1A*), and V108127 (*cnc*). Other RNAi lines were purchased from Bloomington *Drosophila* Stock Center, including BL50727 (*Vhl*), BL34988 (*Cul2*), BL67915 and BL34034 (*Rpn9*), BL33894 (*sima*), BL65875 (*ple*) and BL27030 (*Ddc*). Overexpression lines *UAS-hVHL::HA* (BL66300), *UAS-Ddc* (BL37540) and *UAS-sima* (BL9582) were obtained from the Bloomington *Drosophila* Stock Center while *UAS-Rpn9* (F001557), *UAS-Rpn9::HA* (F000756) and *UAS-cnc::HA* (F000602) were purchased from FlyORF. *pUAST-dNCtr1A::FLAG* (missing the first ~20 amino acids) has been described previously [23].

All *Drosophila* strains and crosses were maintained on standard medium at 25 °C unless stated otherwise. Standard medium was supplemented with either 300 μM bathocuproine disulfonate (BCS; Sigma-Aldrich, St. Louis, MO, USA, B1125) or 1 mM copper chloride (CuCl₂; Merck, Whitehouse station, NJ, USA, 751944) to make copper-deficient or copper supplemented food medium.

2.2. Temporal control of gene manipulation

The *tubP-GAL80ts/Cyo; Pnr-Gal4/TM6β* (BL67060) stock was used to perform temperature shift experiments to test phenotypic defects caused by overexpression of *sima* and *cnc*. Pnr-Gal4 activity was suppressed at low temperature (22 °C) and switched on at high temperature (29 °C). All crosses were maintained at 22 °C and transferred to a new vial every day in the afternoon. When progeny developed to early pupal stages, fly vials were transferred to 29 °C. The phenotypic defects caused by *sima*

and *cnc* overexpression were assessed in surviving adults.

2.3. Microscopy

Adult flies were anaesthetized using CO_2, then mounted directly onto white plasticine and monitored with a Leica MZ6 stereomicroscope. All images of adult fly phenotypes were recorded with a Leica DFC295 digital camera using Leica Application Suite (LAS) software. All adult fly images are representative of >10 individuals of that genotype / temperature, unless stated otherwise. Where mild variation existed between individuals of a particular genotype, images were chosen to represent the intermediate phenotype. Where considerable variation presented, examples of mild, moderate and severe phenotypes are all provided. All adult flies were imaged between 24 and 72 h of age.

2.4. Drosophila survival experiments

In all survival experiments, crosses were set up in a cage with >50 virgin females and 20–25 males. To assess adult survival, 50 1st instar larvae (=1 replicate) for each group were transferred onto standard medium or medium supplemented with 1 mM CuCl₂ or 300 μM BCS. Successful adult survival was classified as the ability of the adults to emerge from their pupal cases. The survival of each genotype was calculated as percentage of expected. $n \geq 3$ for each genotype/food type combination.

2.5. Western blot analysis

Five adult heads per sample were lysed in 25 μl of 1% Triton X-100 lysis buffer (50 mM Tris-HCl (pH 7.5), 100 mM NaCl, 1 mM EDTA, 1% Triton-X, 10% glycerol, complete EDTA-free protease inhibitor mixture (Roche Applied Science)). Equal volumes of lysate were separated by SDS-PAGE (Mini-PROTEAN® TGXTM Precast Gels Any kDTM, Bio-Rad, Hercules, CA, USA, 4569034). Ctr1A::Flag or cnc::HA was detected using mouse anti-Flag primary antibody (1:5000; Sigma-Aldrich, St. Louis, MO, USA, 3165) or rat anti-HA primary antibody (1:5000; Roche, Basel, Switzerland, 12,158,167,001) and HRP-conjugated anti-mouse (1:5000; Invitrogen, Carlsbad, CA, USA, A24518).) or anti-Rat secondary antibody (1:5000; Invitrogen, Carlsbad, CA, USA, A24549). Immunoblots were developed using ECL Prime (GE Healthcare, Chicago, IL, USA, RPN2232) and imaged using a chemiluminescence detector (Vilber Lourmat). Image J was used to quantify the grey value of each western blot band; in cases where the bands 'frowned' (i.e. were not straight), the entire band-containing region was included for quantification. Relative grey values were then calculated by dividing the grey value for each anti-Flag or anti-HA band by the grey value for the corresponding loading control (anti-Tubulin).

2.6. Real-time PCR

Total RNA was extracted using the Trizol plus RNA purification kit (Invitrogen, 12183018A), including DNase treatment. cDNA was transcribed from 1 μg of total RNA in a 20 μl reaction using AMV Reverse Transcriptase (Invitrogen, BIO-65042). Primers for real-time PCR were designed using Primer3 software; primer sequences are listed in Supp. Table.1.

QuantStudio 3 Real-Time PCR System (Applied Biosystems, Foster City, CA, USA) was applied to perform real-time PCR. cDNA was amplified in a 10 μl reaction containing 1 μM of each primer and 5 μl of 2 × SYBR Select Master Mix (Applied Biosystems, A25742). The amount of gene product in each sample was determined using ΔCT method. *Rpl23* was used as a housekeeping gene. The amount of gene product for each gene of interest was expressed relative to that of *Rpl23* to normalize for differences in total cDNA between samples.

2.7. Statistical analysis

All data were presented as mean ± S.E.M. An independent Student's *t*-test was applied using GraphPad Prism 7.0b (GraphPad, San Diego, CA, USA). *P* < 0.05 was considered as a statistically significant difference.

3. Results

3.1. Rpn9 participates in the negative regulation of sima by Vhl

To explore the influence the Vhl / EloC / Cul2 complex might have on the copper homeostasis machinery in *Drosophila*, the *Pannier (Pnr)-Gal4* line, was applied to test various UAS-RNAi knockdown constructs. *Pnr-Gal4* drives expression of UAS transgenes along the middle ~1/3rd of the dorsal midline in the adult thorax and abdomen (the area in
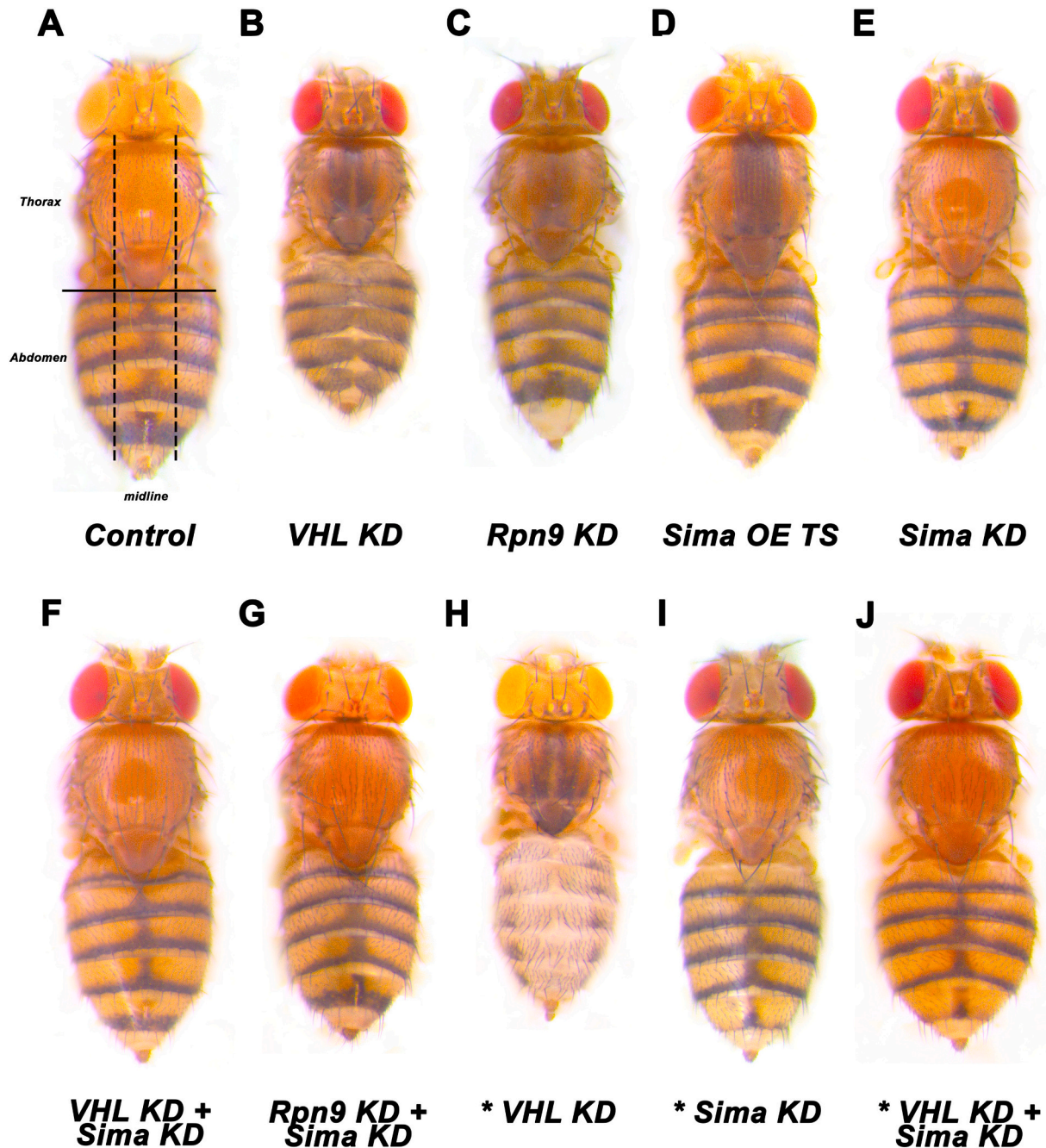

Fig. 1. Rpn9 participates in the proteasomal degradation of sima by Vhl. *sima* KD was applied to rescue the defects caused by *Vhl* or *Rpn9* knockdown. A-J) Dorsal views of adult female *Drosophila* containing *Pnr-Gal4* together with the following transgenes: A) no transgene (*w*^{1118} - dotted lines indicate the boundaries of the *Pnr-Gal4* expression domain); B) *UAS-Vhl*^{RNAi}; C) *UAS-Rpn9*^{RNAi}; D) *UAS-Sima*; E) *UAS-Sima*^{RNAi}; F) *UAS-Vhl*^{RNAi} + *UAS-Sima*^{RNAi}; G) *UAS-Rpn9*^{RNAi} + *UAS-sima*^{RNAi}; H) *UAS-Vhl*^{RNAi}; I) *UAS-Sima*^{RNAi}; J *UAS-Vhl*^{RNAi} + *UAS-Sima*^{RNAi}. * indicates 29 °C: A-G were raised at 25 °C, H-J at 29 °C. *Vhl RNAi* line in all figures is BL50727 unless stated. D) Since *sima* overexpression caused lethality under the control of *Pnr-Gal4* even at 18 °C, *tubP-GAL80ts; Pnr-Gal4 > UAS-sima* flies were shifted from 22 to 29 °C during pupal development, resulting in viable adults with thoracic hyperpigmentation. All images were captured using 3.2 × objective lens. Abbreviations: OE, overexpression; KD, knockdown; TS, temperature shift. Images are representative of *n* > 10 for each genotype / temperature combination.

between the dashed lines in Fig. 1A) and depletion of copper in these cells causes loss of normal pigmentation [30], with the wild type flanking tissue acting as a control for direct comparison. Knockdown of *Vhl* (*RNAi* lines BL50727 and V108920) under the control of *Pnr-Gal4* produced a moderate increase in pigmentation (hyperpigmentation) in the thorax (Fig. 1B and Supp. Fig. 1C). However, in the central *pannier* domain of the abdomen, black pigment was dispersed throughout each abdominal segment upon *Vhl* knockdown (Fig. 1B), in contrast to the restricted posterior localisation in control flies (Fig. 1A) and in flanking wild type tissue.

The Gal4 / UAS system generates higher expression / knockdown levels at higher temperatures [31] and when progeny were raised at 29 °C rather than the standard 25 °C, *Vhl* knockdown produced obvious hyperpigmentation on the thorax and contrasting hypopigmentation on the abdomen (Fig. 1H and Supp. Fig. 1D). Overexpression of *hVHL* had no phenotypic effect under *Pnr-Gal4* yet was able to compensate for the loss of endogenous *Vhl* by restoring cuticle pigmentation back to normal levels (Supp. Fig. 1A). Two additional components of the Vhl complex were also tested. Under *Cul2* (*RNAi* line BL34988, Supp. Fig. 1E) and *EloC* (*RNAi* line V15303, Supp. Fig. 1F) knockdown only thoracic hyperpigmentation was observed, with *EloC* knockdown displaying an additional moderate cleft on the thorax.

Since VHL is chiefly known as a negative regulator of HIF transcription factors, we next investigated whether sima, the fly ortholog of HIF1alpha, was mediating the pigmentation defects caused by loss of Vhl. *Vhl* knockdown defects were completely rescued by *sima* knockdown (*RNAi* line BL33894) at both 25 °C and 29 °C, while *sima* knockdown alone did not produce any defects on the thorax and abdomen at either temperature (Fig. 1E, F, I and J). This demonstrated that sima is the main substrate of Vhl in these cuticle-producing cells. *Sima* knockdown showed a partial rescue of the defects caused by *Cul2* (Supp. Fig. 1G) and *EloC* (Supp. Fig. 1H) knockdown.

As VHL downregulates HIF1alpha by ubiquitination and subsequent proteasomal degradation, we wanted to examine whether components of the proteasome were involved in the pigmentation defects caused by *Vhl* downregulation. Numerous proteasomal proteins have been found to physically interact with the copper efflux transporter ATP7A [15,32] so we tested knockdown of the *Drosophila* orthologues of each of these. In most cases, these gene knockdowns were lethal under *Pnr-Gal4* (data not shown). However, knockdown of *Rpn9* (*RNAi* line BL67915), which encodes a regulatory component of the 26 s proteasome, resulted in thoracic hyperpigmentation (Fig. 1C, 25 °C) or death (29 °C); these defects were rescued by *Rpn9* overexpression which caused no phenotypic defects by itself (Supp. Fig. 1B). Knockdown of *sima* had a complete rescue effect on *Rpn9* knockdown hyperpigmentation (Fig. 1G), indicating that normally, Rpn9 contributes to degradation of sima by Vhl.

Since *sima* knockdown completely rescued the defects produced by knockdown of both *Vhl* and *Rpn9*, we hypothesized that upregulation of sima was responsible for these defects. However, overexpression of *sima* (line BL9582) caused lethality under the control of *Pnr-Gal4* at all temperatures tested (18–29 °C). Therefore, temperature shift experiments were performed to determine the defects caused by *sima* overexpression. By shifting *Tub-Gal80ts; Pnr-Gal4 > UAS-sima* flies from 22 °C to 29 °C at the beginning of pupal development, viable adults displaying varying levels of thoracic hyperpigmentation were retrieved (Fig. 1D and Supp. Fig. 1I-L). These results suggested that upregulation of sima was responsible only for the induction of thoracic hyperpigmentation and that other substrates might be involved in generating abdominal hypopigmentation after *Vhl* knockdown at 29 °C.

3.2. ple/Ddc are involved in the melanisation induced by loss of Vhl/Rpn9

Drosophila Tyrosine Hydroxylase (TH, encoded by *ple*) and DOPA decarboxylase (DDC, encoded by *Ddc*) are rate-limiting factors in converting DOPA or dopamine into DOPA-melanin or dopamine-melanin,

the main constituents of the brown and black pigments in *Drosophila* cuticle (Fig. 2A) [25,26]. Knockdown of *ple* (*RNAi* line BL65875, Fig. 2C and Supp. Fig. 2C) or *Ddc* (*RNAi* line BL27030, Fig. 2H and Supp. Fig. 2G) under *Pnr-Gal4* control produced hypopigmentation both on the thorax and abdomen while no obvious defects were observed after overexpressing *Ddc* (Fig. 2F and Supp. Fig. 2E) at 29 °C and 25 °C. The thoracic hyperpigmentation produced by knockdown of *Vhl* was abolished by *ple* knockdown (Fig. 2E (29 °C) and Supp. Fig. 2D (25 °C)) but not by Ddc overexpression (Fig. 2G (29 °C) and Supp. Fig. 2F (25 °C)). At 29 °C, co-knockdown of *Vhl* and *Ddc* caused lethality (Fig. 2I) while *Ddc* knockdown abolished the thoracic hyperpigmentation generated by *Vhl* knockdown at 25 °C (Supp. Fig. 2H). Since *Rpn9* knockdown resulted in death at 29 °C, we tested the relationship between ple/Ddc and Rpn9 at 25 °C. Consistent with *Vhl* knockdown, knockdown of *ple* or *Ddc* abolished *Rpn9* knockdown hyperpigmentation (Supp. Fig. 2J and L), but overexpression of *Ddc* had no effect on the defects produced by *Rpn9* knockdown (Supp. Fig. 2K).

3.3. Keap1/cnc interact genetically with the Vhl/sima pathway

A second E3 Ubiquitin ligase, Keap1, has also been implicated in regulation of *Drosophila* copper levels due its negative regulation of cnc, a transcription factor that indirectly controls copper uptake [23]. Therefore, we investigated whether *Keap1* manipulation also affects adult pigmentation. Knockdown of *Keap1* (*RNAi* line V330323) produced abdominal hypopigmentation at 29 °C (Fig. 3B, no phenotypic defects observed at 25 °C (Supp. Fig. 3B)) which was completely rescued by downregulation of *cnc* (*RNAi* line V108127, Fig. 3E); *cnc* alone is not required for pigment formation (Fig. 3D (29 °C) and Supp. Fig. 3C (25 °C)). By performing temperature shift experiments, we found that *cnc* overexpression, normally lethal under *Pnr-Gal4* control, could generate abdominal hypopigmentation in surviving adults (Fig. 3C). *cnc* knockdown rescued *Vhl* knockdown defects completely at 25 °C (Supp. Fig. 3F) and partially at 29 °C (Fig. 3F and G). These results suggested that cnc might be a common substrate of both Keap1 and Vhl. In contrast, *cnc* knockdown caused lethality in combination with knockdown of *Rpn9*. As cnc and sima are both transcription factors negatively regulated by E3 ubiquitin ligases active in the fly cuticle-producing cells, they may be able compensate for each other's absence. However, co-knockdown of both *cnc* and *sima* under *Pnr-Gal4* control had no phenotypic impact (Supp. Fig. 3G).

3.4. Ctr1A expression modulates the effects of Vhl knockdown

In our previous study, knockdown of *cnc* was able to restore the post-translational downregulation of Ctr1A caused by inhibition of the E3 ubiquitin ligase Slmb [23]. Therefore, we hypothesized that *Vhl* knockdown defects may also be due to dysregulation of Ctr1A. At 25 °C, overexpression of Ctr1A had no discernible rescue effect on *Vhl* knockdown defects (Fig. 4B and D), although the thoracic hyperpigmentation was abolished by mild *Ctr1A* knockdown (Fig. 4F) and the abdominal hypopigmentation became more distinct (Fig. 4F). However, at 29 °C, overexpression of *Ctr1A* showed a marked interaction with *Vhl* knockdown (Fig. 4H-J), exacerbating the thoracic defects to generate a cleft while partially rescuing the abdominal hypopigmentation. In contrast, *Ctr1A* knockdown mitigated the *Vhl* knockdown thoracic hyperpigmentation but exacerbated the abdominal hypopigmentation (Fig. 4H, K and L). These results implied that *Ctr1A* plays a critical role in the changes in melanisation induced by *Vhl* knockdown.

3.5. Rpn9 and sima are involved in post-translational regulation of Ctr1A levels

Since Ctr1A participates in *Vhl* knockdown-induced melanisation in *Drosophila* (Fig. 4). we next tested the impact of *Vhl* knockdown on Ctr1A levels. *UAS-Ctr1A::Flag* transgenes were used to assess Ctr1A protein
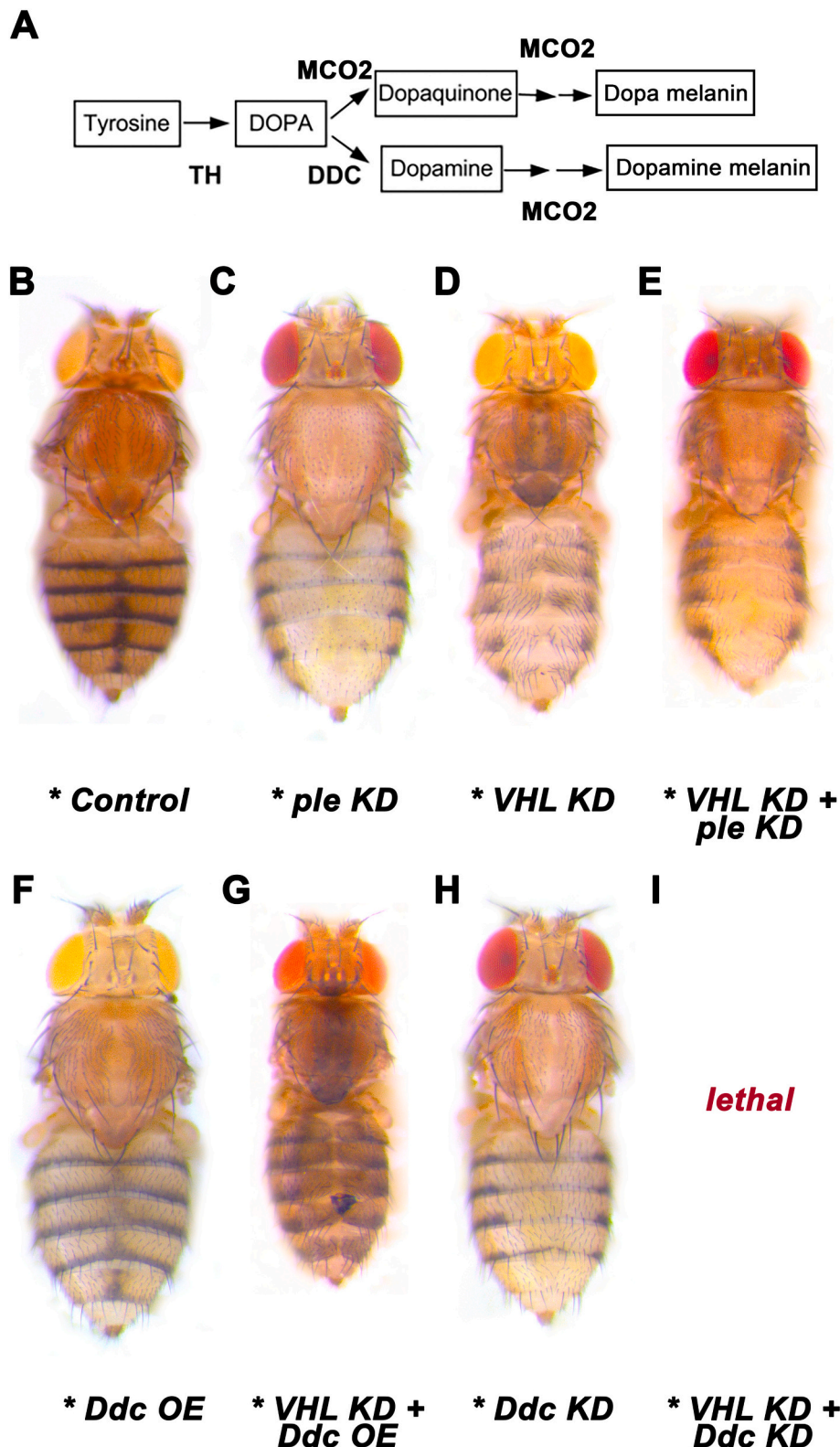
Fig. 2. TH and DDC are required for *Vhl*-knockdown induced melanisation. A) Melanin biosynthesis in *Drosophila*. Tyrosine is converted by Tyrosine Hydroxylase (TH, encoded by the *ple* gene) to DOPA, which is in turn catalysed to dopamine by DOPA decarboxylase (DDC) Some fractions of DOPA and dopamine are converted into DOPA-melanin and dopamine-melanin by MCO2 / laccase 2. B—I) Dorsal views of adult female *Drosophila* containing *Pnr-Gal4* together with the following transgenes (all at 29 °C): B) no transgene (w^{1118}); C) *UAS-ple^{RNAi}*; D) *UAS-Vhl^{RNAi}*; E) *UAS-Vhl^{RNAi} + UAS-ple^{RNAi}*; F) *UAS-Ddc*; G) *UAS-Vhl^{RNAi} + UAS-Ddc*; H) *UAS-Ddc^{RNAi}*; I) *UAS-Vhl^{RNAi} + UAS-Ddc^{RNAi}*. * indicates 29 °C. All images were captured using 3.2 × objective lens. Abbreviations: KD, knockdown; OE, overexpression. n > 10 for each genotype / temperature combination.

levels after *Vhl / Rpn9 / sima* manipulation. In lysates from homogenized adult thorax and abdomen, Ctr1A::Flag was not detectable when driven by *Pnr-Gal4* (Supp Fig. 4A). Therefore, real-time PCR was performed to investigate whether *Vhl* knockdown affects endogenous *Ctr1A* transcription in the thorax and abdomen. The expression of *Ctr1A* mRNA in the thorax was dramatically reduced after *Vhl* knockdown while no significant change was observed in the abdomen (Fig. 5).

We next turned to the adult eyes to test the expression of Ctr1A protein using *UAS-Ctr1A::Flag* transgenes. A significant decrease in Ctr1A protein levels was detected after *Rpn9* knockdown or *sima* overexpression driven by *GMR-Gal4* (Fig. 6A and B). Knockdown of *Vhl* had no effect on Ctr1A levels (Fig. 6A and B). However, a decrease in Ctr1A protein was observed after *EloC* knockdown but not *Cul2* (Supp Fig. 4B). Furthermore, we investigated whether Vhl could regulate cnc protein
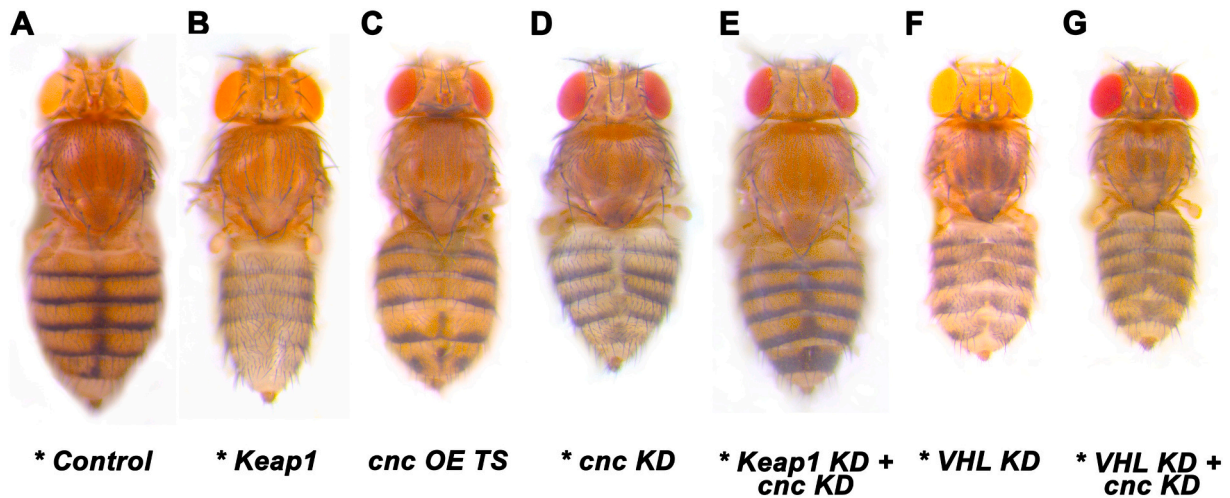
Fig. 3. Knockdown of *cnc* partially rescues *Vhl* knockdown defects. A-G) Dorsal views of adult female *Drosophila* containing *Pnr-Gal4* together with the following transgenes (all at 29 °C): A) no transgene (*w^1118^*); B) *UAS-Keap1^RNAi^*; C) *UAS-cnc*; D) *UAS-cnc^RNAi^*; E) *UAS-Keap1^RNAi^ + cnc^RNAi^*; F) *UAS-Vhl^RNAi^*; G) *UAS-Vhl^RNAi^ + cnc^RNAi^*. * indicates 29 °C. Since *cnc* overexpression caused lethality under the control of *Pnr-Gal4* even at 18 °C, *tubP-GAL80ts; Pnr-Gal4 > UAS-cnc* flies were shifted from 22 to 29 °C during pupal development, resulting in viable adults with abdominal hypopigmentation. All images were captured using 3.2 × objective lens and are representative of n > 10 for each genotype / temperature combination. Abbreviations: KD, knockdown; OE, overexpression; TS, temperature shift.

levels since *cnc* knockdown partially rescued the defects caused by *Vhl* knockdown. Neither *Vhl* knockdown nor *EloC* knockdown under the control of *GMR-Gal4*. resulted in a change in the expression of cnc produced by a *UAS-cnc::HA* transgene (Fig. 6C and D).

Since we observed no effect of *Vhl* knockdown on Ctr1A protein levels in the adult head, we turned to fly survival experiments to further test how Vhl might affect Ctr1A activity in another copper-responsive tissue, the larval midgut. Survival experiments were performed on flies raised from 1st larval instar on normal media or media supplemented with $CuCl_2$ or BCS, using the midgut-specific driver *Mex-Gal4* to manipulate target gene expression. No changes in survival rate on normal food and 300 μM BCS supplemented food were observed after knockdown of *Vhl*, *EloC* or *Rpn9* (Fig. 7). In contrast, *Vhl*, *EloC* and *Rpn9* knockdown all significantly increased the survival rate on 1 mM $CuCl_2$-containing medium (Fig. 7), indicating that all three manipulations protect larvae from copper toxicity. We hypothesized that *Rpn9 / Vhl / EloC* knockdown rescued survival rate on high copper by reducing intestinal copper uptake via a decrease in Ctr1A levels, as we have shown previously for *Slmb* knockdown [23]. This is consistent with the decrease in adult head Ctr1A levels under *Rpn9* knockdown, *sima* overexpression and *EloC* knockdown. However *Vhl* knockdown had no detectable impact on Ctr1A levels in the eye and we were unable to confirm Vhl's post-translational regulation of Ctr1A in other tissues as no Ctr1A::FLAG expression could be detected from larval midguts (*Mex-Gal4*), or from adult thoraces or abdomens (*Pnr-Gal4*) (Supp Fig. 4A).

Next, we investigated whether copper could affect *Vhl* and *Rpn9* transcription by performing real-time PCR using adult midguts of wild type flies raised in different copper conditions. The expression of *Vhl* and *Rpn9* was significantly reduced in 1 mM $CuCl_2$-containing medium (high copper condition) whereas no changes were observed in 300 μM BCS containing medium (low copper condition) (Fig. 8).

3.6. Rpn9 participates in regulating copper homeostasis

Our phenotypic gene interaction results strongly indicated that alteration of Ctr1A levels after *Vhl* knockdown was responsible for generating hyper- or hypo- pigmentation, implying that copper homeostasis was disrupted after *Vhl* knockdown. Therefore, we tested cellular copper levels by performing real-time PCR to measure expression of the copper-responsive chaperone gene *MtnB* after knockdown of *Vhl* and *Rpn9* under the control of *Mex-Gal4*. *MtnB* plays a critical role in

copper storage and detoxification [33]. It is upregulated in high copper conditions and downregulated in copper deficient conditions [23,34]. Examining mRNA extracted from adult midguts, *MtnB* was weakly upregulated in *Vhl* knockdown tissues but strong downregulated in *Rpn9* knockdown tissues (Fig. 9). The Rpn9 results mirrored the strong protective effect of *Rpn9* knockdown against copper-toxicity (Fig. 7), indicating reduced copper uptake into the midgut. The Vhl results were less conclusive and we cannot rule out regulation of additional copper homeostasis genes by Vhl.

3.7. Sima downregulates cnc transcription in the adult midgut

Finally, we asked if the putative targets of Vhl-mediated proteasomal degradation - sima and cnc - were able regulate each other or Ctr1A transcriptionally. While knockdown of either *sima* or *cnc* had negligible impact on transcript levels, *sima* over expression in the adult midgut strongly reduced *cnc* expression. The effect of *cnc* overexpression could not be assessed as it caused lethality (Fig. 10).

4. Discussion

VHL possesses E3 ubiquitin activity in complex with Cul2 and EloC and is classed as a tumour suppressor. In clear cell renal carcinomas (ccRCCs) for instance, VHL activity is suppressed, leading to the accumulation of HIF-1alpha which normally regulates the cellular response to hypoxia [18]. In this study, we found that knockdown of *Drosophila Vhl* in the epithelial cells that secrete adult cuticle had the opposite effect in two adjacent body segments. In the thorax, loss of *Vhl* resulted in hyperpigmentation whereas in the abdomen, *Vhl* knockdown caused hypopigmentation. Knockdown of *sima*, which encodes the *Drosophila* orthologue of HIF-1alpha, completely rescued both phenotypes, confirming that sima is a key target of Vhl-mediated ubiquitination and proteasomal degradation.

The hyperpigmentation generated by *Vhl* knockdown was also abolished after introducing knockdown of *ple*, which decreases melanin production due to decreased Tyrosine Hydroxylase activity. Therefore, we have demonstrated that loss of *Vhl* can induce melanisation. Furthermore, we propose that the effects of *Vhl* knockdown in both thorax and abdomen are ultimately mediated by the copper uptake transporter Ctr1A, albeit via different pathways. *Ctr1A* knockdown rescues the thoracic hyperpigmentation and exacerbates the abdominal
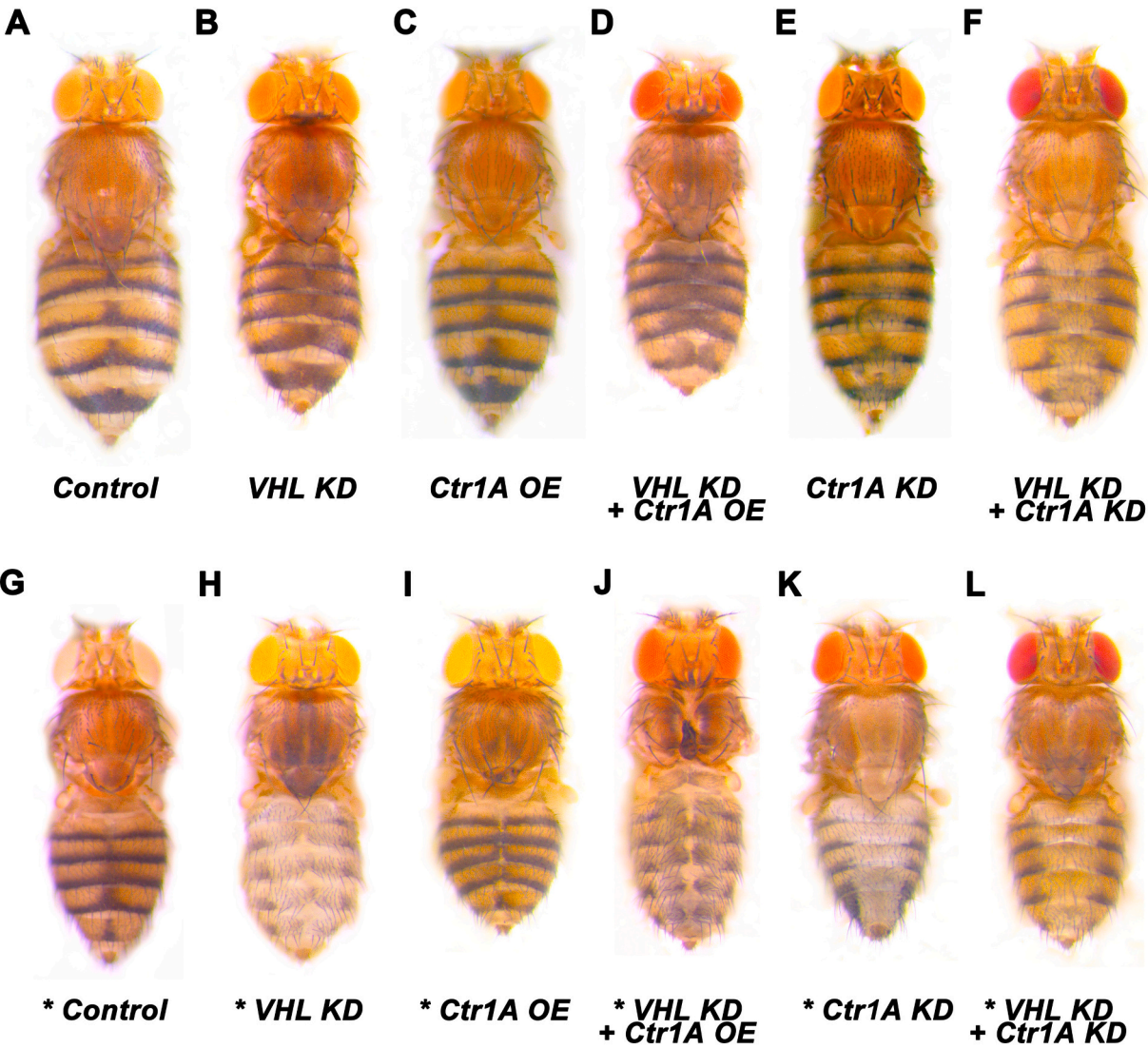
Fig. 4. Manipulation of *Ctr1A* rescues *Vhl* knockdown defects. A-L) Dorsal views of adult female *Drosophila* containing *Pnr-Gal4* with the following transgenes: A) no transgene (w^{1118}); B) *UAS-Vhl^{RNAi}*; C) *UAS-Ctr1A*; D) *UAS-Vhl^{RNAi}* + *UAS-Ctr1A*; E) *UAS-Ctr1A^{RNAi}*; F) *UAS-Vhl^{RNAi}* + *UAS-Ctr1A^{RNAi}*; G) no transgene (w^{1118}); H) *UAS-Vhl^{RNAi}*; I) *UAS-Ctr1A*: J) *UAS-Vhl^{RNAi}* + *UAS-Ctr1A*; K) *UAS-Ctr1A^{RNAi}*; L) *UAS-Vhl^{RNAi}* + *Ctr1A^{RNAi}*. * indicates 29 °C. A-F were raised at 25 °C, G-L at 29 °C. All images were captured using 3.2 × objective lens and are representative of n > 10 for each genotype / temperature combination Abbreviations: KD, knockdown; OE, overexpression.
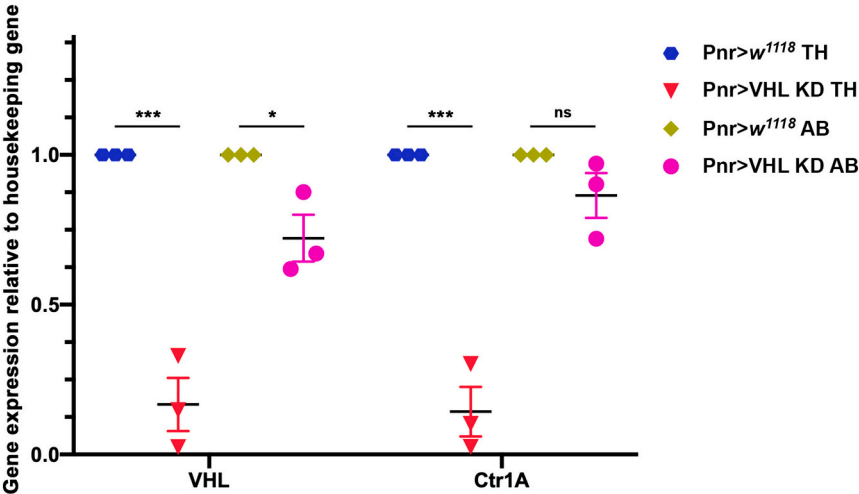
Fig. 5. Ctr1A expression levels in *Vhl*- knockdown thorax and abdomen. *Vhl* and *Ctr1A* mRNA levels were quantified by real-time PCR. Expression was normalized to that of *Rpl23* and expressed relative to the control group genotype, Pnr-Gal4 > w^{1118}. Data were 2^n-transformed and horizontal bars indicate the mean and S.E.M of the three replicates shown. Under the control of *Pnr-Gal4, Vhl* knockdown resulted in decrease in the expression of *Ctr1A* in the thorax but no change in the abdomen. Abbreviations: KD, knockdown; TH, thorax; AB, abdomen; ns, no significance. $n = 3$ for each genotype, *$p < 0.05$, ***$p < 0.001$.
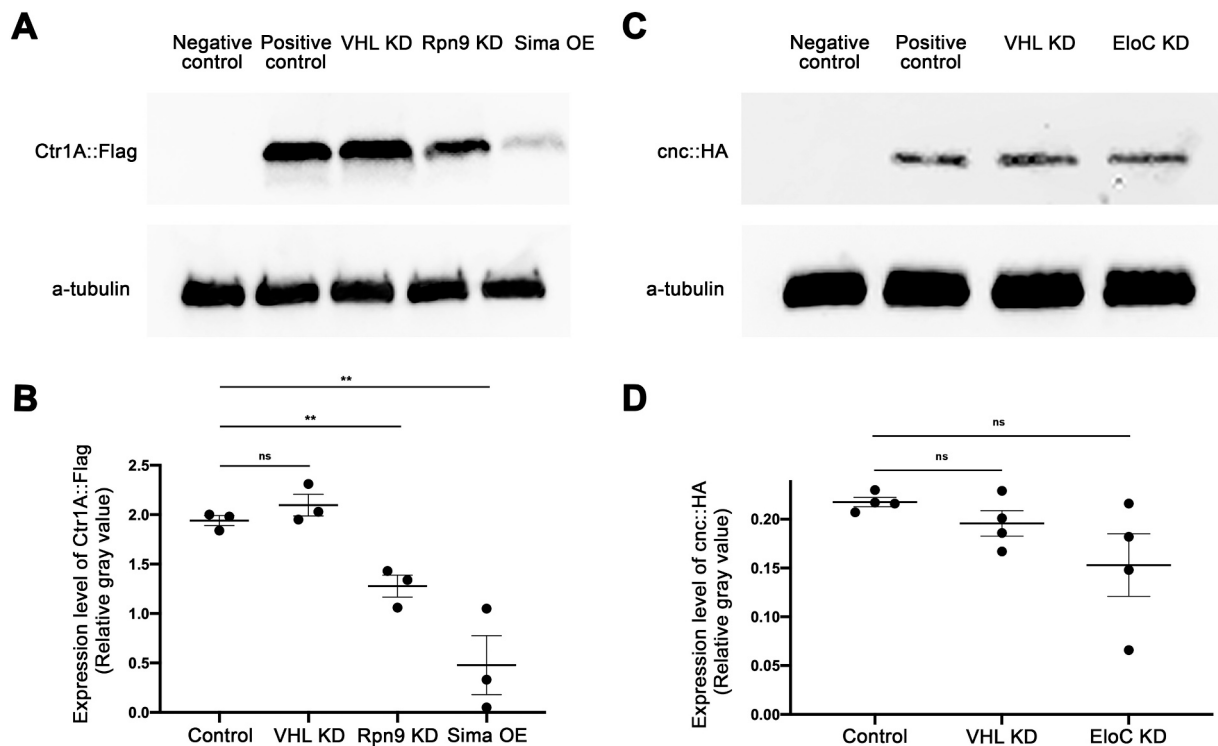
Fig. 6. *Rpn9* KD and *sima* OE both decrease Ctr1A levels. Western blots against Flag and HA epitopes to detect Ctr1A::Flag and cnc::HA expression respectively. A) Ctr1A::Flag expression in adult heads after manipulating *Vhl*, *Rpn9* and *sima* using *GMR-Gal4*. B) Quantification of Ctr1A::Flag levels from (A). C) cnc::HA expression in adult heads after manipulating *Vhl* and *EloC* using *GMR-Gal4*. D) Quantification of cnc::HA levels from (C). *Vhl* knockdown did not cause any change in the expression of Ctr1A and cnc. All western blot images are representative of ≥3 independent experiments. Abbreviations: KD, knockdown; OE, overexpression; ns, no significance. **$p < 0.01$.

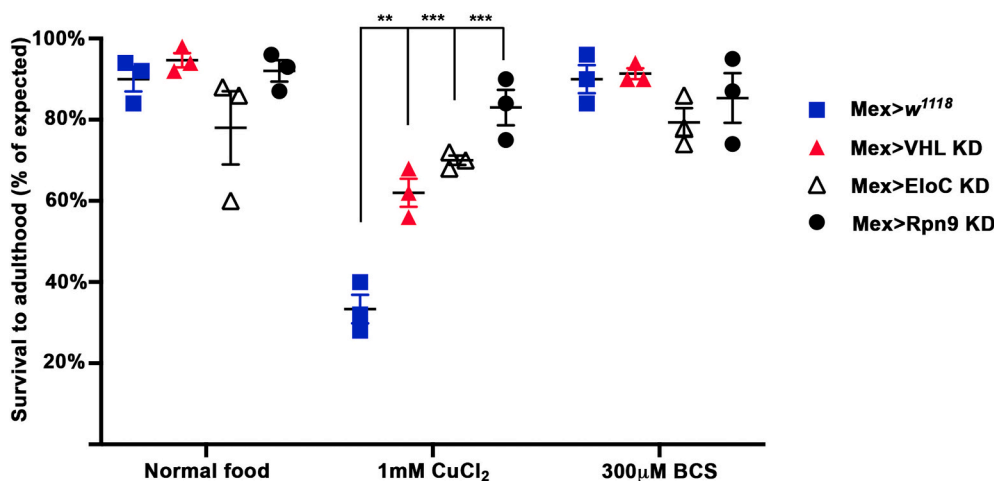
Fig. 7. Knockdown of *Vhl*, *EloC* and *Rpn9* increase survival rate in high copper conditions. Percentage survival from 1st instar larval stage to adulthood was assessed for each genotype on normal, 1 mM $CuCl_2$ and 300 μm BCS-supplemented food. Error bars represent mean ± S.E.M. Genotypes tested were w^{1118}, *UAS- Vhl^{RNAi}*, *UAS-EloC^{RNAi}* and *UAS-Rpn9^{RNAi}* under the control of *Mex-Gal4*. A rescue of survival rate was observed in *Vhl-*, *EloC-* and *Rpn9-* knockdown flies raised on 1 mM $CuCl_2$ supplemented medium. Abbreviations: KD, knockdown. n = 3 for each genotype, **$p < 0.01$, ***$p < 0.001$.

hypopigmentation whereas Ctr1A overexpression aggravates the thoracic hyperpigmentation and attenuates the abdominal hypopigmentation.

To account for the contrasting effects of *Vhl* knockdown in thorax versus abdomen, we propose a model (Fig. 11) where there are two major, competing inputs into Ctr1A activity. First, the transcription factor cnc indirectly inhibits Ctr1A via posttranslational regulation, as we have shown previously [23]. Second, sima induces Ctr1A activity, as has been shown for mammalian HIF1alpha and CTR1. Vhl may inhibit both sima and cnc, which we predict are both inactive in healthy tissues; knockdown of either transcription factor alone or both together has no phenotypic impact. According to our model, the difference between the

two tissues lies in which of the two regulatory pathways dominates; cnc rules in the abdomen and sima is ascendant in the thorax. This is exemplified by our *cnc* and *sima* over expression results; excess sima causes thoracic hyperpigmentation whereas more cnc causes abdominal hypopigmentation.

The picture is complicated, however, by the fact that sima in particular can function in both tissues; knockdown rescues the effects of *Vhl* knockdown in thorax AND abdomen. How then do these two tissues differ? We believe this may be a due to contrasting co-regulatory relationships between cnc and sima. In the abdomen, our model predicts that sima induces *cnc* while cnc represses *sima*. Loss of *Vhl* would upregulate both cnc and sima – then the equilibrium shifts in cnc's
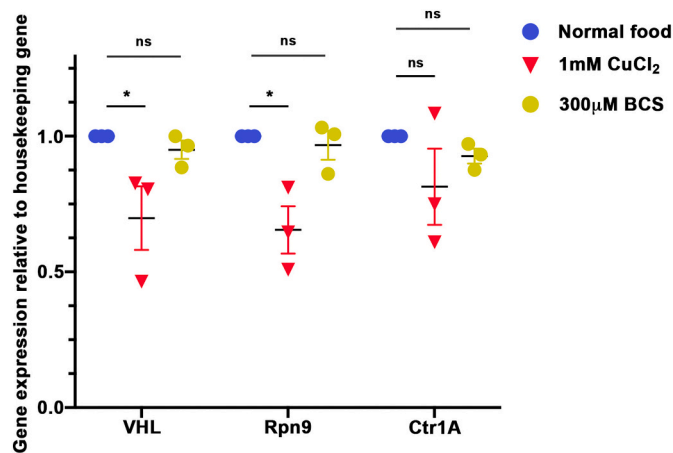
8

Fig. 8. *Vhl*, *Rpn9* and *Ctr1A* transcription levels in different copper conditions. *Vhl*, *Rpn9* and *Ctr1A* mRNA levels in the adult midgut of w^{1118} flies were quantified by real-time PCR. Expression was normalized to that of *Rpl23* and expressed relative to the control group genotype, w^{1118} on normal food. Data were 2^n-transformed and horizontal bars indicate the mean and S.E.M of the three replicates shown. Abbreviations: KD, knockdown; ns, no significance. n = 3 for each genotype, $*p < 0.05$.

favour, leading to Ctr1A degradation and loss of pigmentation. Both induction by sima and release of Vhl inhibition are needed to boost cnc levels to the point where Ctr1A is degraded, explaining why knockdown of either *cnc* OR *sima* can rescue *Vhl* knockdown. This situation may also exist in the eye where both sima and cnc overexpression lead to the posttranslational downregulation of Ctr1A.

In the thorax, we propose that the relationship between cnc and sima is reversed; sima represses *cnc* while cnc induces *sima*. Again, *Vhl* knockdown relieves both transcription factors but this time the equilibrium shifts towards sima, resulting in the activation of Ctr1A and subsequent hyperpigmentation. And similar to the abdomen, both induction by cnc and release of Vhl inhibition are needed to boost sima levels to the point where Ctr1A is upregulated. Our QPCR data from the adult midgut show that at least in one tissue, sima expression can potently inhibit *cnc* transcription.

Since HIF1alpha has been shown to transcriptionally activate CTR1 in mammalian cells, the simplest explanation for the thoracic hyperpigmentation would be that similarly, sima induces Ctr1A transcriptionally. However, our QPCR results from the thorax clearly show the exact opposite; transcriptional *down*regulation of Ctr1A upon *Vhl*

knockdown. Given our evidence that forced over expression of Ctr1A exacerbates the thoracic defects caused by *Vhl* knockdown, we propose that the observed inhibition of Ctr1A transcription is in fact a secondary, negative feedback response to posttranslational upregulation of Ctr1A by sima; excess copper import through Ctr1A triggers a compensatory shutdown of Ctr1A production. Assessing transcription levels in the thorax and abdomen is complicated by the presence of multiple different tissues. Future studies to test this model will need to assess the activity of cnc and sima-responsive reporter genes during the late pupal development of the thorax and abdomen. It is interesting to note that in ccRCCs, both the VHL / HIF1alpha and Keap1 / Nrf2 pathways are disrupted [19], supporting our model of dynamic interaction between sima and cnc.

As Rpn9 is a constitutive regulatory component of the 26 s proteasome, reduction in Rpn9 levels is predicted to affect many proteasomal degradation pathways, leading to accumulation of normally downregulated proteins. Thus, like *Vhl* knockdown, *Rpn9* knockdown is predicted to activate both sima and cnc, yet only thoracic hyperpigmentation is observed, with abdominal pigmentation left intact. We propose that since cnc-mediated downregulation of Ctr1A involves proteasomal degradation, this response would be mitigated upon *Rpn9* knockdown, leaving abdominal Ctr1A / pigmentation intact while thoracic Ctr1A / hyperpigmentation is still induced by sima regulation. *Sima* knockdown restores *Rpn9*-knockdown thoracic hyperpigmentation back to normal by negating the initial sima upregulation.

The lethality caused by co-knockdown of *cnc* and *Rpn9* is striking. We propose that reduction in proteasomal activity caused by *Rpn9* knockdown induces an oxidative stress response, as hinted at by the thoracic hyperpigmentation. As the master regulator of oxidative stress response, cnc likely initiates numerous protective responses to such stress. Knockdown of *cnc* would blunt this defence mechanism, leading to the death of the organism. *Sima* knockdown does not have this effect, possibly because sima's action is more specifically targeted to hypoxic responses.

In general, we propose that multiple E3 ubiquitin ligase complexes converge to co-regulate cnc and sima, which in turn are mutually interdependent and coordinate both transcriptional and posttranslational responses. We have focussed on the response of the copper transporter Ctr1A and postulate that this in turn modulates pigmentation levels, possibly through the activity of laccase 2, a multicopper oxidase thought to be required for the production of both brown and black pigment [28]. However, sima and cnc have many other target genes which are presumably also impacted by loss of Vhl or Rpn9.

The regulatory input of several E3 ubiquitin ligases may be a mechanism by which sima and cnc activities can be coordinated to
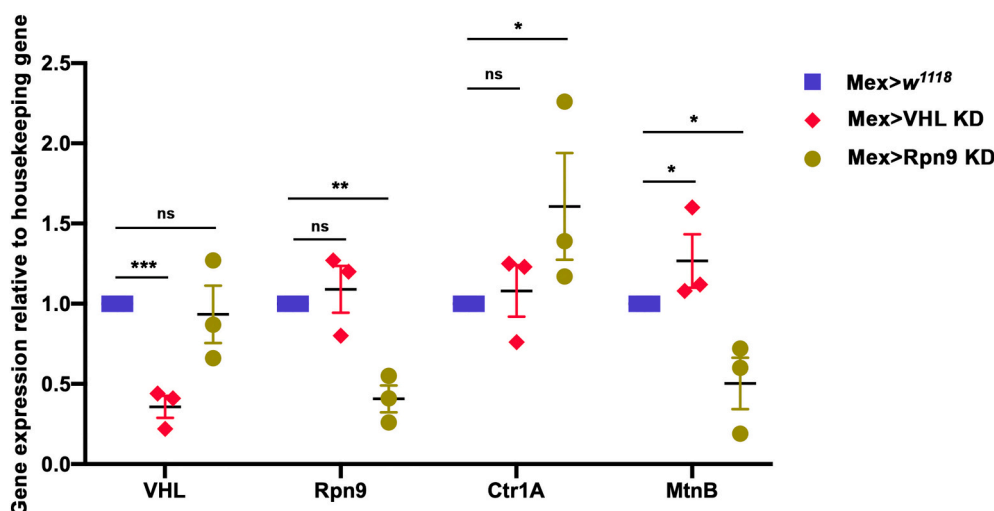
Fig. 9. Gene expression levels in *Vhl*- and *Rpn9*- knockdown midguts. *Vhl*, *Rpn9*, *Ctr1A* and *MtnB* mRNA levels were quantified by real-time PCR. Expression was normalized to that of *Rpl23* and expressed relative to the control group genotype, Mex > w^{1118}. Data were 2^n-transformed and horizontal bars indicate the mean and S.E.M of the three replicates shown. Under the control of *Mex-Gal4*, *Vhl* knockdown reduced *Vhl* levels and *Rpn9* knockdown reduced *Rpn9* levels, confirming efficacy of the RNAi lines used. Knockdown of *Vhl* and *Rpn9* significantly affected *MtnB* expression. Abbreviations: KD, knockdown; ns, no significance. n = 3 for each genotype, $*p < 0.05$, $**p < 0.01$, $***p < 0.001$.
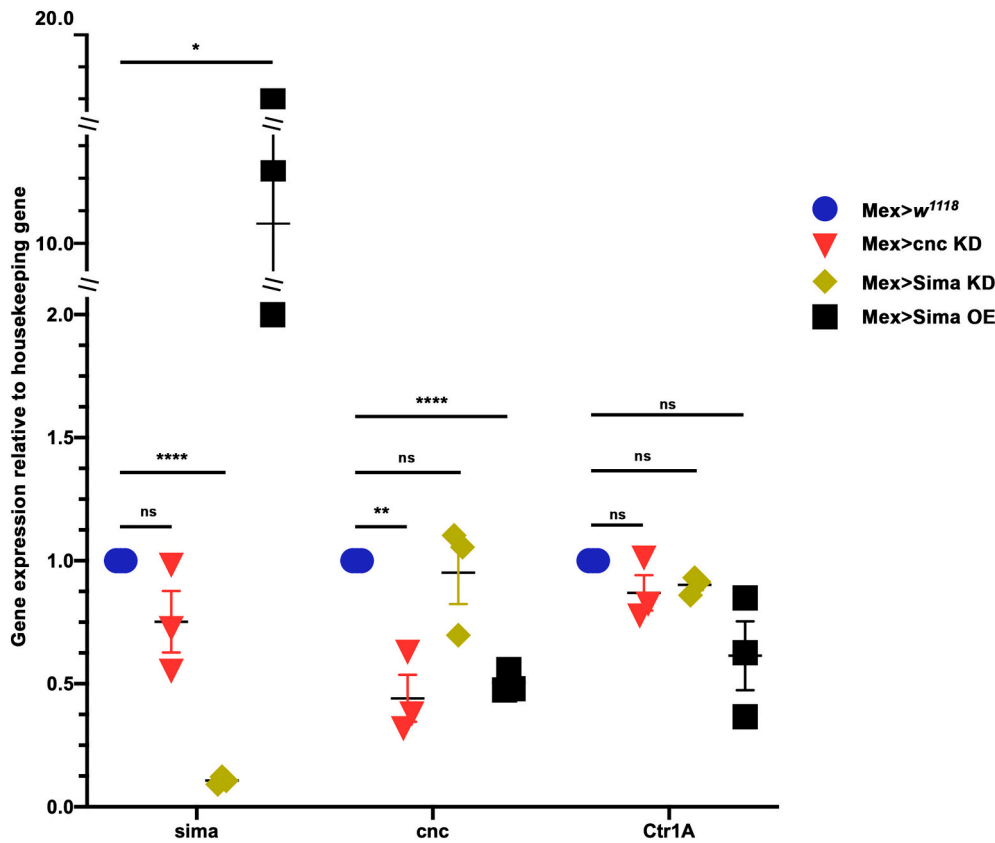
Fig. 10. Gene expression levels in *cnc*- and *sima*- knockdown or sima overexpression midguts. *Sima, cnc* and *Ctr1A* mRNA levels were quantified by real-time PCR. Expression was normalized to that of *Rpl23* and expressed relative to the control group genotype, Mex > w^{1118}. Data were 2^n-transformed and horizontal bars indicate the mean and S.E.M of the three replicates shown. Under the control of *Mex-Gal4, sima* knockdown reduced *sima* levels and *cnc* knockdown reduced *cnc* levels, confirming efficacy of the RNAi lines used. Abbreviations: KD, knockdown; ns, no significance. n = 3 for each genotype, *p > 0.05, **p < 0.01, ****p < 0.0001.
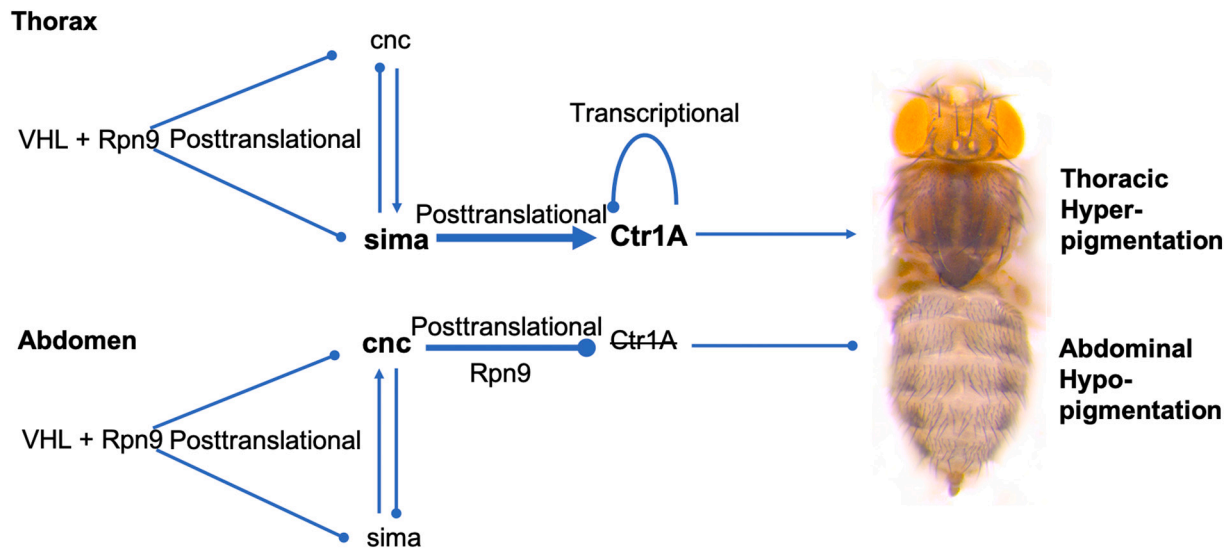
Fig. 11. Model summarizing how Vhl may regulate cnc and sima to control pigmentation levels through post-translational control of Ctr1A. Filled circles represent negative regulation, arrows represent positive regulation.

respond to multiple sources of stress. In our previous report on the role of the E3 Slmb in regulating Ctr1A via cnc, we speculated that excess copper, a known inducer of oxidative stress, may trigger cnc to reduce Ctr1A levels in order to restore cellular copper balance. Keap1 similarly releases its inhibition of Nrf2 / cnc upon exposure to reactive oxygen species, allowing a cnc-mediated defence to be mounted. And Vhl is renowned for its ability to respond to hypoxia via HIF gene upregulation, inducing angiogenesis which requires high cellular copper levels (reviewed in Fukai et al. [35]).

The opposite effects of *Vhl* knockdown on pigmentation in thorax versus abdomen are intriguing. Although not specifically mentioned, a similar dichotomy can be observed with activation of the p38 pathway which directly regulates transcription of *ple* and *Ddc* [25]. Single gene knockdown is a highly invasive and 'unnatural' manipulation, so the results we observe do not necessarily reflect a biologically relevant process. However, it is interesting to speculate that the effect of *Vhl* knockdown may involve a relocation of available pigment or pigment precursors from the abdomen to the thorax. It will be fascinating to test

whether such a redistribution can be observed under organism-wide hypoxic, oxidative or immune stress. Ultimately, we wish to monitor the in vivo activity of Vhl, Keap1, Slmb, sima and cnc to determine how each responds to real-life stressors and how their activity is coordinated to effect a robust defence response.

CRediT authorship contribution statement

Bichao Zhang: Conceptualization, Methodology, Investigation, Writing – original draft, Visualization. **Lauren Kirn:** Methodology, Investigation. **Richard Burke:** Conceptualization, Investigation, Writing – original draft, Supervision, Project administration, Funding acquisition.

Declaration of competing interest

None.

Appendix A. Supplementary data

Supplementary data to this article can be found online at https://doi.org/10.1016/j.bbamcr.2021.119022.

References

[1] N.E. Hellman, J.D. Gitlin, Ceruloplasmin metabolism and function, Annu. Rev. Nutr. 22 (2002) 439–458.

[2] J.J. Perry, D.S. Shin, E.D. Getzoff, J.A. Tainer, The structural biochemistry of the superoxide dismutases, Biochim. Biophys. Acta 1804 (2010) 245–262.

[3] D.M. Popovic, I.V. Leontyev, D.G. Beech, A.A. Stuchebrukhov, Similarity of cytochrome c oxidases in different organisms, Proteins 78 (2010) 2691–2698.

[4] C. Saporito-Magriñá, R. Musacco-Sebio, J.M. Acosta, S. Bajicoff, P. Paredes-Fleitas, S. Reynoso, A. Boveris, M.G. Repetto, Copper(II) and iron(III) ions inhibit respiration and increase free radical-mediated phospholipid peroxidation in rat liver mitochondria: effect of antioxidants, J. Inorg. Biochem. 172 (2017) 94–99.

[5] S. Lutsenko, Human copper homeostasis: a network of interconnected pathways, Curr. Opin. Chem. Biol. 14 (2010) 211–217.

[6] L. Gossage, T. Eisen, E.R. Maher, VHL, the story of a tumour suppressor gene, Nat. Rev. Cancer 15 (2015) 55–64.

[7] M. Ivan, K. Kondo, H. Yang, W. Kim, J. Valiando, M. Ohh, A. Salic, J.M. Asara, W. S. Lane, W.G. Kaelin, HIFalpha targeted for VHL-mediated destruction by proline hydroxylation: implications for O2 sensing, Science 292 (2001) 464–468.

[8] P. Jaakkola, D.R. Mole, Y.M. Tian, M.I. Wilson, J. Gielbert, S.J. Gaskell, A. von Kriegsheim, H.F. Hebestreit, M. Mukherji, C.J. Schofield, P.H. Maxwell, C.W. Pugh, P.J. Ratcliffe, Targeting of HIF-alpha to the von Hippel-Lindau ubiquitylation complex by O2-regulated prolyl hydroxylation, Science 292 (2001) 468–472.

[9] K. Pourvali, P. Matak, G.O. Latunde-Dada, S. Solomou, M. Mastrogiannaki, C. Peyssonnaux, P.A. Sharp, Basal expression of copper transporter 1 in intestinal epithelial cells is regulated by hypoxia-inducible factor 2α, FEBS Lett. 586 (2012) 2423–2427.

[10] C. White, T. Kambe, Y.G. Fulcher, S.W. Sachdev, A.I. Bush, K. Fritsche, J. Lee, T. P. Quinn, M.J. Petris, Copper transport into the secretory pathway is regulated by oxygen in macrophages, J. Cell Sci. 122 (2009) 1315–1321.

[11] Y. Xia, L. Liu, Q. Bai, Q. Long, J. Wang, W. Xi, J. Xu, J. Guo, Prognostic value of copper transporter 1 expression in patients with clear cell renal cell carcinoma, Oncol. Lett. 14 (2017) 5791–5800.

[12] S.R. Nadella, C.C. Hung, C.M. Wood, Mechanistic characterization of gastric copper transport in rainbow trout, J. Comp. Physiol. B. 181 (2011) 27–41.

[13] Xie, L., Collins, J.F., 2011. Transcriptional regulation of the Menkes copper ATPase (Atp7a) gene by hypoxia-inducible factor (HIF2{alpha}) in intestinal epithelial cells. Am. J. Phys. Cell Phys. 300, C1298–1305.

[14] L. Xie, J.F. Collins, Transcription factors Sp1 and Hif2α mediate induction of the copper-transporting ATPase (Atp7a) gene in intestinal epithelial cells during hypoxia, J. Biol. Chem. 288 (2013) 23943–23952.

[15] Zimnicka, A.M., Tang, H., Guo, Q., Kuhr, F.K., Oh, M.J., Wan, J., Chen, J., Smith, K. A., Fraidenburg, D.R., Choudhury, M.S., Levitan, I., Machado, R.F., Kaplan, J.H., Yuan, J.X., 2014. Upregulated copper transporters in hypoxia-induced pulmonary hypertension. PLoS One 9, e90544.

[16] W. Feng, F. Ye, W. Xue, Z. Zhou, Y.J. Kang, Copper regulation of hypoxia-inducible factor-1 activity, Mol. Pharmacol. 75 (2009) 174–182.

[17] L. Zheng, P. Han, J. Liu, R. Li, W. Yin, T. Wang, W. Zhang, Y.J. Kang, Role of copper in regression of cardiac hypertrophy, Pharmacol. Ther. 148 (2015) 66–84.

[18] A.A. Batavia, P. Schraml, H. Moch, Clear cell renal cell carcinoma with wild-type von Hippel-Lindau gene: a non-existent or new tumour entity? Histopathology 74 (2019) 60–67.

[19] Y. Sato, T. Yoshizato, Y. Shiraishi, S. Maekawa, Y. Okuno, T. Kamura, T. Shimamura, A. Sato-Otsubo, G. Nagae, H. Suzuki, Y. Nagata, K. Yoshida, A. Kon, Y. Suzuki, K. Chiba, H. Tanaka, A. Niida, A. Fujimoto, T. Tsunoda, T. Morikawa, D. Maeda, H. Kume, S. Sugano, M. Fukayama, H. Aburatani, M. Sanada, S. Miyano, Y. Homma, S. Ogawa, Integrated molecular analysis of clear-cell renal cell carcinoma, Nat. Genet. 45 (2013) 860–867.

[20] L. Kinch, N.V. Grishin, J. Brugarolas, Succination of Keap1 and activation of Nrf2-dependent antioxidant pathways in FH-deficient papillary renal cell carcinoma type 2, Cancer Cell 20 (2011) 418–420.

[21] J.G. Spiers, C. Breda, S. Robinson, F. Giorgini, J.R. Steinert, Nrf2/Keap1 mediated redox signaling supports synaptic function and longevity and impacts on circadian activity, Front. Mol. Neurosci. 12 (2019) 86.

[22] G.P. Sykiotis, D. Bohmann, Keap1/Nrf2 signaling regulates oxidative stress tolerance and lifespan in Drosophila, Dev. Cell 14 (2008) 76–85.

[23] Zhang, B., Binks, T., Burke, R., 2020. The E3 ubiquitin ligase Slimb/β-TrCP is required for normal copper homeostasis in Drosophila. Biochim Biophys Acta Mol Cell Res 1867, 118768.

[24] H. Yassine, L. Kamareddine, M.A. Osta, The mosquito melanization response is implicated in defense against the entomopathogenic fungus Beauveria bassiana, PLoS Pathog. 8 (2012), e1003029.

[25] Y. Sekine, S. Takagahara, R. Hatanaka, T. Watanabe, H. Oguchi, T. Noguchi, I. Naguro, K. Kobayashi, M. Tsunoda, T. Funatsu, H. Nomura, T. Toyoda, N. Matsuki, E. Kuranaga, M. Miura, K. Takeda, H. Ichijo, p38 MAPKs regulate the expression of genes in the dopamine synthesis pathway through phosphorylation of NR4A nuclear receptors, J. Cell Sci. 124 (2011) 3006–3016.

[26] H. Tang, Regulation and function of the melanization reaction in Drosophila, Fly (Austin) 3 (2009) 105–111.

[27] P.J. Wittkopp, S.B. Carroll, A. Kopp, Evolution in black and white: genetic control of pigment patterns in Drosophila, Trends Genet. 19 (2003) 495–504.

[28] F. Riedel, D. Vorkel, S. Eaton, Megalin-dependent yellow endocytosis restricts melanization in the Drosophila cuticle, Development 138 (2011) 149–158.

[29] J. Vasquez-Procopio, S. Rajpurohit, F. Missirlis, Cuticle darkening correlates with increased body copper content in Drosophila melanogaster, Biometals 33 (2020) 293–303.

[30] T. Binks, J.C. Lye, J. Camakaris, R. Burke, Tissue-specific interplay between copper uptake and efflux in Drosophila, J. Biol. Inorg. Chem. 15 (2010) 621–628.

[31] J.B. Duffy, GAL4 system in Drosophila: a fly geneticist's Swiss army knife, Genesis 34 (2002) 1–15.

[32] H.S. Comstra, J. McArthy, S. Rudin-Rush, C. Hartwig, A. Gokhale, S.A. Zlatic, J. B. Blackburn, E. Werner, M. Petris, P. D'Souza, P. Panuwet, D.B. Barr, V. Lupashin, A. Vrailas-Mortimer, V. Faundez, The interactome of the copper transporter ATP7A belongs to a network of neurodevelopmental and neurodegeneration factors, Elife 6 (2017).

[33] K. Balamurugan, D. Egli, H. Hua, R. Rajaram, G. Seisenbacher, O. Georgiev, W. Schaffner, Copper homeostasis in Drosophila by complex interplay of import, storage and behavioral avoidance, EMBO J. 26 (2007) 1035–1044.

[34] A. Southon, R. Burke, M. Norgate, P. Batterham, J. Camakaris, Copper homoeostasis in Drosophila melanogaster S2 cells, Biochem. J. 383 (2004) 303–309.

[35] T. Fukai, M. Ushio-Fukai, J.H. Kaplan, Copper transporters and copper chaperones: roles in cardiovascular physiology and disease, Am. J. Phys. Cell Phys. 315 (2018) C186–C201.

Supplementary Material

Gene name	Forward primer	Reverse primer
Rpl23	GACAACACCGGAGCCAAGAACC	GTTTGCGCTGCCGAATAACCAC
Vhl	CGGATCAGCTGGTTGACGTA	CCGTGGATAATCCTCCGTGG
Rpn9	ATGTCCAATCCTCAGCCTAATGT	TGGTCAGCTCATTCCAGAGTTT
Ctr1A	GACCACGCCCATCACAGTG	GATCAGGTCGAACATGGAAGC
MtnB	GGTTTGCAAGGGTTGTGGAA	CAGTTGTCCCCGCACTTTTG
Sima	GCCCCAAAAACCAATCTCACG	CAGCCGAGAGTTCCATGAATATC
cnc	CTGCATCGTCATGTCTTCCAGT	AGCAAGTAGACGGAGCCAT

Supp. Table. 1 Sequences of primers used for real-time PCR
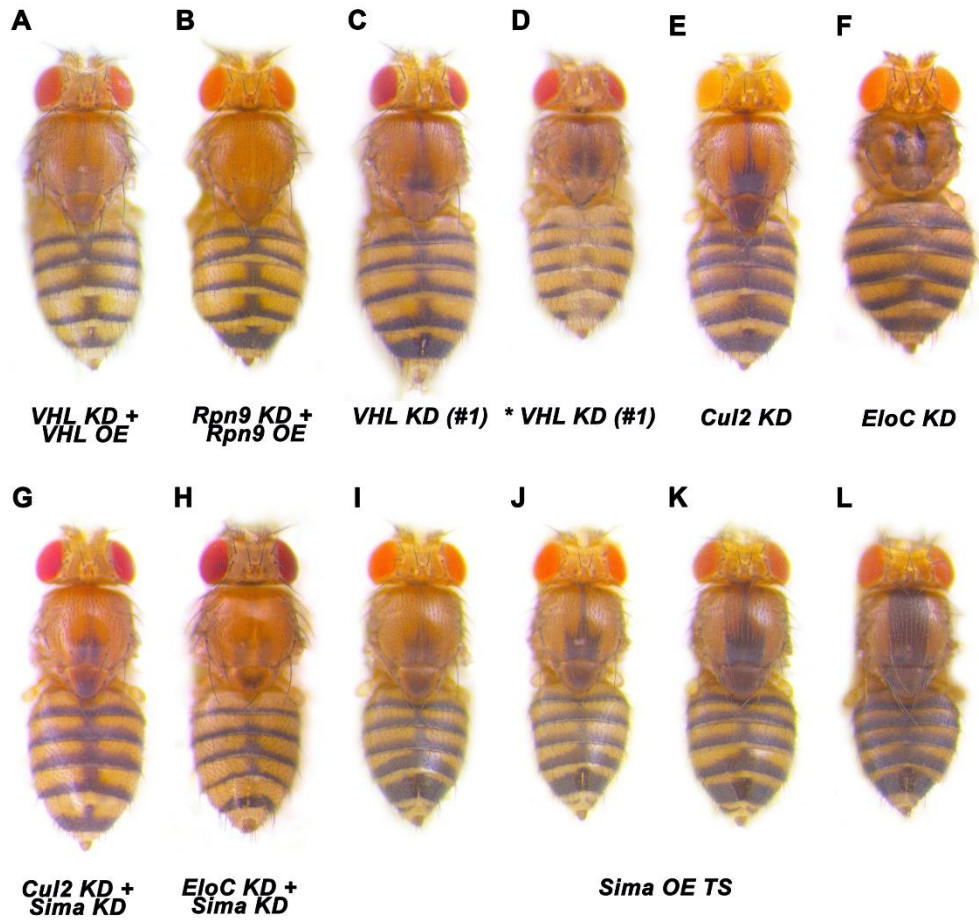
Supp. Fig. 1 Rpn9 participates in the proteasomal degradation of sima by the Vhl / EloC / Cul2 complex. A-L) Dorsal views of adult female *Drosophila* containing *Pnr-Gal4* together with the following transgenes: A) *UAS-Vhl^{RNAi} + UAS-Vhl*; B) *UAS-Rpn9^{RNAi} + UAS-Rpn9*; C) *UAS-Vhl^{RNAi}* (#1); D) *UAS-Vhl^{RNAi}* (#1); E) *UAS-Cul2^{RNAi}*; F) *UAS-EloC^{RNAi}*; G) *UAS-Cul2^{RNAi} + UAS-sima^{RNAi}*; H) *UAS-EloC^{RNAi} + UAS-Sima^{RNAi}*. * indicates 29°C and #1 stands for new *Vhl RNAi* line (V108920). I-L) Varying levels of thoracic hyperpigmentation produced by sima overexpression at 29°C. All images were captured using 3.2 × objective lens. Abbreviations: OE, overexpression; KD, knockdown; TS, temperature shift. Images are representative of n>10 for each genotype / temperature combination.
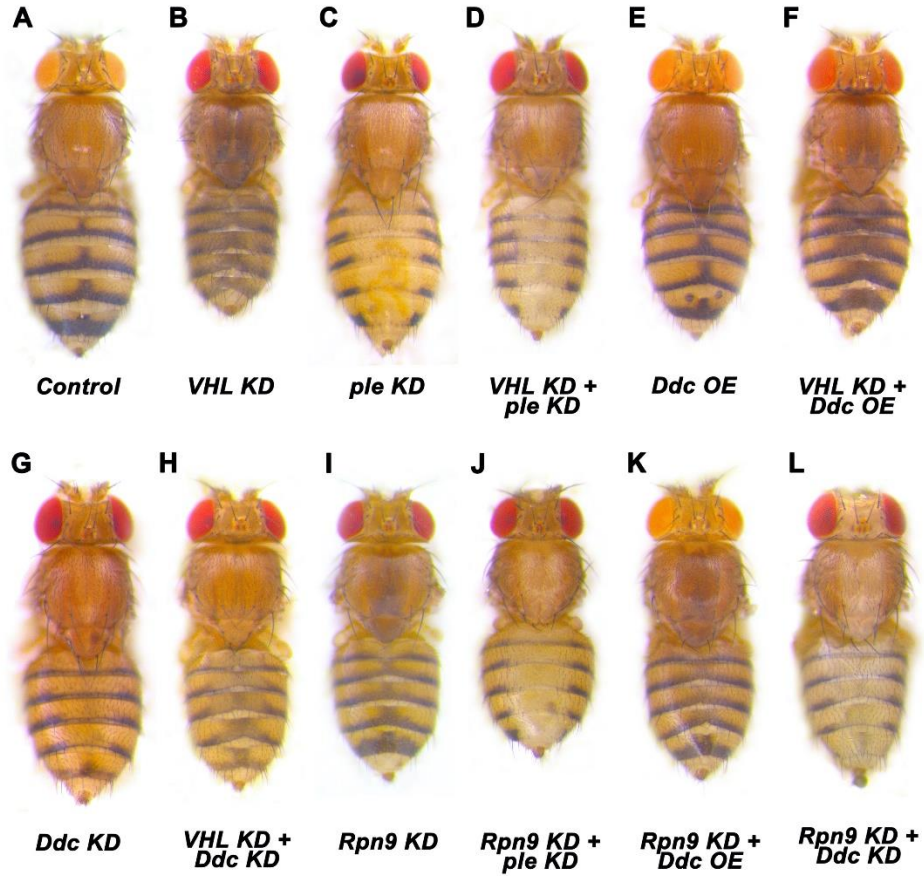
Supp. Fig. 2 TH and DDC are required for *Vhl*-knockdown induced melanisation. A-L) Dorsal views of adult female *Drosophila* containing *Pnr-Gal4* together with the following transgenes (all at 25°C): A) no transgene (w^{1118}); B) *UAS-Vhl^{RNAi}*; C) *UAS-ple^{RNAi}*; D) *UAS-Vhl^{RNAi} + UAS-ple^{RNAi}*; E) *UAS-Ddc*; F) *UAS-Vhl^{RNAi} + UAS-Ddc*; G) *UAS-Ddc^{RNAi}*; H) *UAS-Vhl^{RNAi} + UAS-Ddc^{RNAi}*; I) *UAS-Rpn9^{RNAi}*; J) *UAS-Rpn9^{RNAi} + UAS-ple^{RNAi}*; K) *UAS-Rpn9^{RNAi} + UAS-Ddc*; L) *UAS-Rpn9^{RNAi} + UAS-Ddc^{RNAi}*. All images were captured using 3.2 × objective lens. Abbreviations: KD, knockdown; OE, overexpression. n>10 for each genotype.
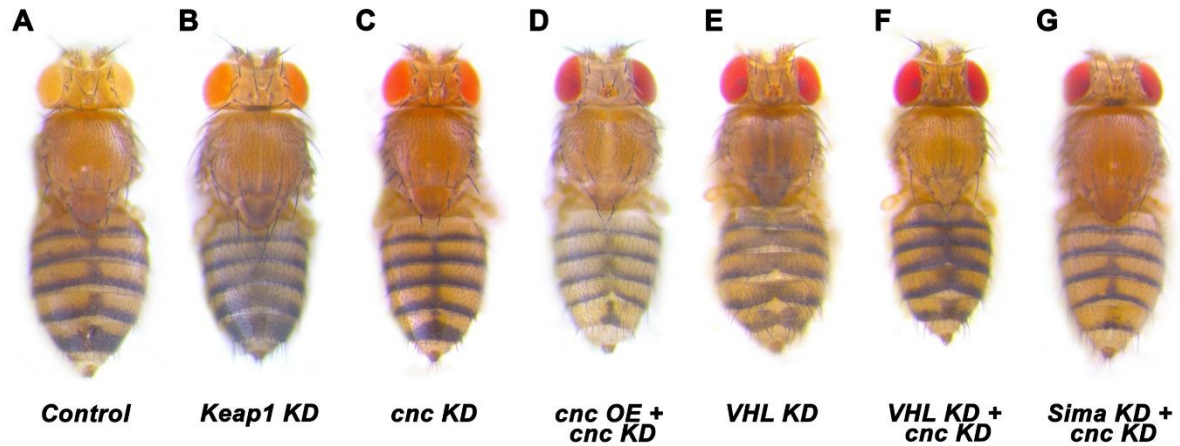
Supp. Fig. 3 Knockdown of *cnc* rescues *Vhl* knockdown defects. A-G) Dorsal views of adult female *Drosophila* containing *Pnr-Gal4* together with the following transgenes (all at 25°C): A) no transgene (*w^1118^*); B) *UAS-Keap1^RNAi^*; C) *UAS-cnc^RNAi^*; D) *UAS-cnc + UAS-cnc^RNAi^*; E) *UAS-Vhl^RNAi^*; F) *UAS-Vhl^RNAi^ + cnc^RNAi^*; G) *UAS-Sima^RNAi^ + cnc^RNAi^*. All images were captured using 3.2 × objective lens and are representative of n>10 for each genotype. Abbreviations: KD, knockdown; OE, overexpression.
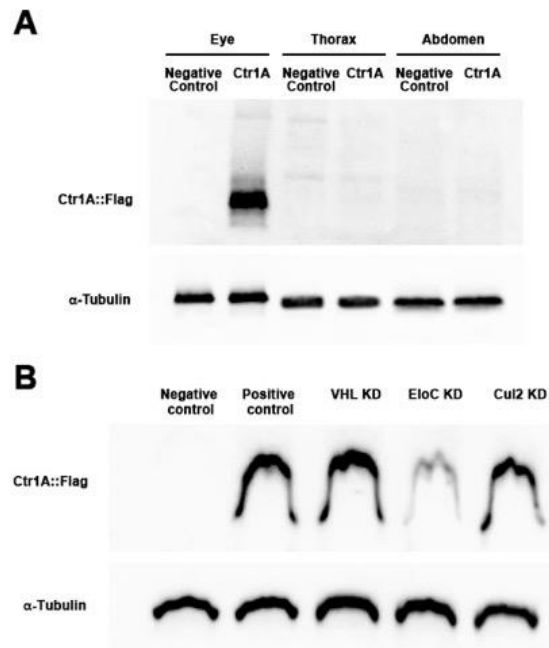
Supp. Fig. 4 Ctr1A::Flag expression in different tissues under the knockdown of target genes. Western blots against the Flag epitope to detect Ctr1A::Flag expression. A) Ctr1A::Flag expression in adult eyes, thorax and abdomen of Ctr1A overexpressing flies. Ctr1A::Flag was highly expressed in adult eyes under *GMR-Gal4* control, but not detectable in thorax and abdomen under *Pnr-Gal4* control. B) Ctr1A::Flag expression in adult eyes after knockdown of *Vhl*, *EloC* and *Cul2*. A decrease in Ctr1A expression was detected after *EloC* knockdown while knockdown of *Vhl* and *Cul2* showed no impact in Ctr1A expression. Abbreviations: KD, knockdown; OE, overexpression.

CHAPTER 6: THE ROLE OF THE COPPER BINDING E2 UBIQUITIN-CONJUGATING ENZYME UBCD1 IN DEVELOPMENT

A copper binding site on UBE2D2 / UbcD1 is essential for *Drosophila* development

6.1 Background

Copper is important for cell growth and neuronal differentiation (Turski and Thiele, 2009). It has been reported that cellular copper promotes polyubiquitination and accelerates protein degradation in mammalian cells (Opazo et al., 2021). Our collaborators Carlos Opazo and Ashley Bush (The University of Melbourne) revealed that Cu^+ dramatically promoted the activity of UBE2D2 by binding to an evolutionarily ancient CXXXC motif (Opazo et al., 2021). UBE2D2, one of 40 mammalian E2 ubiquitin conjugating enzymes, is involved in ubiquitin mediated proteolysis (Saville et al., 2004). Structural inspection of UBE2D2 identified two putative Cu^+ binding regions: one comprised of a group of three cysteines (Cys21, Cys107 and Cys111) with a possible involvement of Met38, and the other of His32 and His55 (Fig.1, the areas circled with red square are copper binding domain). The $C_{107}XXXC_{111}$ sequence is a consensus Cu^+-binding motif (Banci et al., 2007). Opazo *et al* demonstrated that Cys107 and Cys111 residues were critical for Cu-enhanced UBE2D2 conjugation activity by using a site-directed mutagenesis strategy. Cu^+-binding affinity of UBE2D2 was dramatically attenuated after mutation either at Cys107 or Cys111 site. The Cys111 thiol is exposed to the protein surface and is solvent accessible, whereas the Cys107 thiol is buried by Ub and is not accessible to solvent. Given the information of the structural model, we focused on the role of Cys111. This study aimed to investigate the biological relevance of the Cys111 residue of UBE2D2 *in vivo*. Therefore, we turned to the fruit fly *Drosophila*.

Fig.1 *Solution structure of UBE2D2.* The areas circled with red square are the two copper binding domains. Coloured spheres represent putative sub-pM affinity Cu+-binding sites, and sidechains of conserved Cys/Met residues are shown as sticks (Opazo et al., 2021).

The *Drosophila* UBE2D2 orthologue, UbcD1 (aka Effete) shows a remarkable 95% identity with UBE2D2, including conservation of the copper binding C107 and C111 residues (Fig.2). UbcD1 has known roles in: 1) promoting apoptosis, where it interacts with the anti-apoptotic E3 ubiquitin ligase DIAP1 (XIAP in mammals) (Ryoo et al., 2002; Yeh and Bratton, 2013); 2) neuronal dendrite pruning, where it promotes auto-ubiquitination / degradation of DIAP1 (Kuo et al., 2006), and its loss causes mislocalization of TDP-43 (Rumpf et al., 2014); and 3) Hedgehog pathway signalling, where it interacts with the E3 ubiquitin ligase Slmb (BTRC in mammals) to promote partial degradation of the transcription factor Ci (Pan et al., 2017).

Fig.2 *Amino acid sequence alignment of mammalian UBE2D2 and Drosophila UbcD1.* The result of sequence alignment shows that the similarity of these two is approximate to 97% and the identity scores 95%. The copper binding residues, C107 and C111, are conserved in UbcD1.

In this study, two transgenic stocks: *UAS-UBE2D2 WT* (wild type) and *UAS-UBE2D2 C111S* (mutant), were generated and then applied to *UbcD1* rescue experiments to test whether mutations in Cys111 could compromise UBE2D2 activity in *Drosophila*. Since UbcD1 has the highly conserved copper binding regions, we tested the relationship between UbcD1 and copper. Next, we also investigated the role of UbcD1 during *Drosophila* development through gain-of-function or loss-of-function experiments. In order to identify which partners or substrates UbcD1 might work with, a recombinant compound transgenic stock (UbcD1 hypomorph stock) was generated for the UbcD1 candidates screening. Finally, this study demonstrated that the copper binding region is essential for UBE2D2 / UbcD1 activity and UbcD1 might regulate copper homeostasis by controlling the stability of copper transporter proteins. Our results suggested that UbcD1 might regulate melanization through one or more E3 ubiquitin ligases and / or the 26 proteasome and may participate in apoptosis in *Drosophila*.

6.2 Results

6.2.1 UBE2D2 transgenic stocks

In order to characterize the role of the copper binding domain of UBE2D2 in its *in vivo* activity, *UAS-UBE2D2 WT and UAS-UBE2D2 C111S* transgenic stocks were generated by subcloning both human cDNAs into the *upstart Drosophila* expression vector then injecting these constructs into *Drosophila* embryos expressing PhiC31 integrase and containing the ZH-51C attP integration site (Groth et al., 2004). Positive transgenic stocks were identified on the basis of the red-eyed phenotype. These stocks then allowed the expression of wild type and mutated UBE2D2 proteins respectively under the control of appropriate *GAL4* driver lines. In *UAS-UBE2D2 C111S* transgenic flies, the high-affinity copper binding residue C111 of the UBE2D2 protein was mutated to S111. We postulated that the mutation in C111 site could compromise UBE2D2 activity.

In *Drosophila,* no distinguishable phenotypic defects were observed after overexpressing *UBE2D2 WT* and *UBE2D2 C111S* under the control of *tub-Gal4* which expresses genes ubiquitously (Fig.3A). Next, Real-Time PCR was performed to test whether *UBE2D2 WT* and *UBE2D2 C111S* were successfully expressed in transgenic stocks. Examining mRNA extracted from entire adult flies, we detected a remarkably high level of *UBE2D2* in *UBE2D2 WT* and

UBE2D2 C111S-expressing tissues, indicating that *UAS-UBE2D2 WT* and *-UBE2D2 C111S* transgenic stocks were successfully established (Fig.3B). Additionally, *UBE2D2* expression levels were equivalent in these two groups (Fig.3B). Therefore, *UAS-UBE2D2 WT* and *UAS-UBE2D2 C111S* transgenic stocks were subsequently used to investigate the role of the copper binding residue C111 in UBE2D2 activity by performing rescue experiments in *Drosophila*.
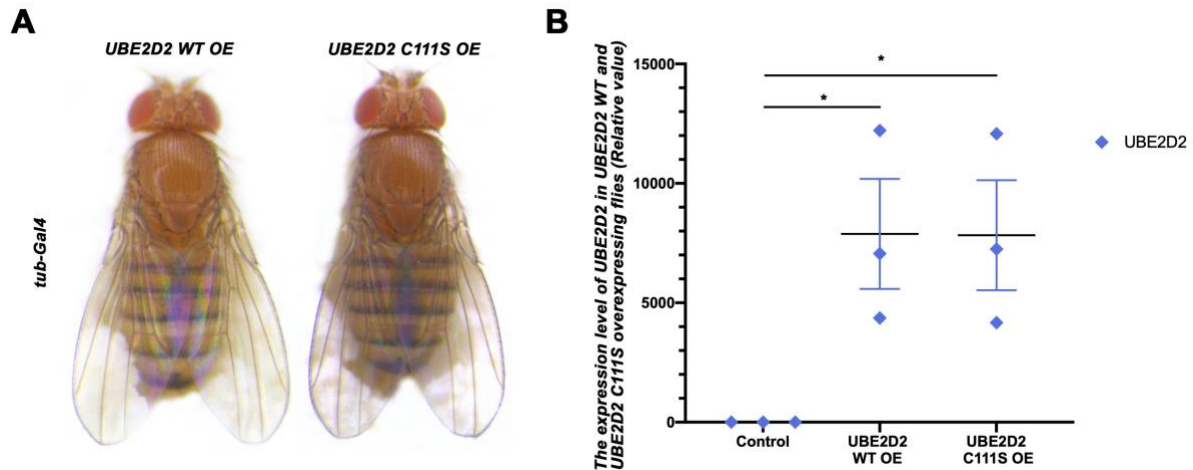

Fig.3 *UAS-UBE2D2 WT* **and** *UAS-UBE2D2 C111S* **transgenic flies.** A) Dorsal views of female *Drosophila* after the overexpression of *UBE2D2 WT* (left) and *UBE2D2 C111S* (right) under the control of *tub-Gal4* which expresses genes ubiquitously. B) Quantification of *UBE2D2* mRNA levels in *UAS-UBE2D2 WT* and *-UBE2D2 C111S* transgenic flies. In order to test whether *UAS-UBE2D2 WT* and *-UBE2D2 C111S* transgenic flies were successfully generated, qPCR was performed to assess the expression of *UBE2D2*. Data were $2^{\triangle CT}$-transformed and horizontal bars indicate the mean and S.E.M of the three replicates shown. UBE2D2 was expressed at equivalent levels in *UBE2D2 WT* and *UBE2D2 C111S*-expressing flies. Abbreviation: OE, overexpression. *$p>0.05$.

6.2.2 Phenotypic defects caused by UbcD1 knockdown

UbcD1, the *Drosophila* homologue of mammalian UBE2D2, is remarkably conserved, showing 95% identical amino acid residues to UBE2D2. The role of UbcD1 during *Drosophila* development was investigated using *RNAi* knockdown combined with the GAL4/UAS system. All of the *GAL4* drivers used in this study are listed in Table 1, including their expression pattern. UbcD1 was reported to be involved in apoptosis via interacting with the anti-apoptotic E3 ubiquitin ligase DIAP1 (Ryoo et al., 2002). This is consistent with our study, where we observed

a lethal phenotype when *UbcD1* was knocked down ubiquitously, in all neurons, or in the posterior compartment of the wing imaginal discs under the control of *tub-Gal4*, *Elav-Gal4* and *En-Gal4* respectively (Table 1). It is worth of noting that there was a slight difference between them. *UbcD1* knockdown flies under the control of *tub-Gal4* died at the 2nd instar while those driven by *Elav-Gal4* and *En-Gal4* died at the early pupal stage.

	GAL4 driver					
	tub-Gal4	*Elav-Gal4*	*En-Gal4*	*Pnr-Gal4*	*Ey-Gal4*	*GMR-Gal4*
Expression pattern	Ubiquitous	All neurons	Posterior compartment of wings	Dorsal midline	Eye discs	Eye discs
UbcD1 KD	Die at the 2nd larval instar	Die at the early pupal stage		Thoracic cleft	Headless phenotype	Rough eyes
UbcD1 OE	No phenotypic defects					
UBE2D2-WT OE	No phenotypic defects					
UBE2D2-C111S OE	No phenotypic defects					

Table 1 ***Phenotypes produced by the targeted knockdown of UbcD1 and overexpression of UbcD1, UBE2D2 WT and UBE2D2 C111S.*** All of experiments were performed at 25 degrees except those under the control of *GMR-Gal4* where the knockdown phenotype was only observed at 29 degrees. Abbreviation: KD, knockdown; OE, overexpression.

Knockdown of *UbcD*1 was also observed to produce other phenotypic defects under the control of *Pnr-Gal4*, *Ey-Gal4* and *GMR-Gal4* (Table 1). As shown in Fig.4, a thoracic cleft with dark pigmentation was generated after *UbcD1* knockdown under the control of *Pnr-Gal4*, which drives gene expression in the *Drosophila* dorsal midline. With *Ey-Gal4*, *UbcD1* knockdown caused a severe defect – a headless phenotype (Fig.4). The fly head was completely missing, and the fly was not able to survive to eclosion. At 29 degrees, knockdown of *UbcD1* under *GMR-Gal4* control produced rough eyes, which was not observed at 25 degrees (Fig.4). However, no phenotypic defects were detected after overexpressing *UbcD1*, *UBE2D2 WT* and *UBE2D2 C111S* under the control of all six *GAL4* drivers (Table 1 and Fig.4).
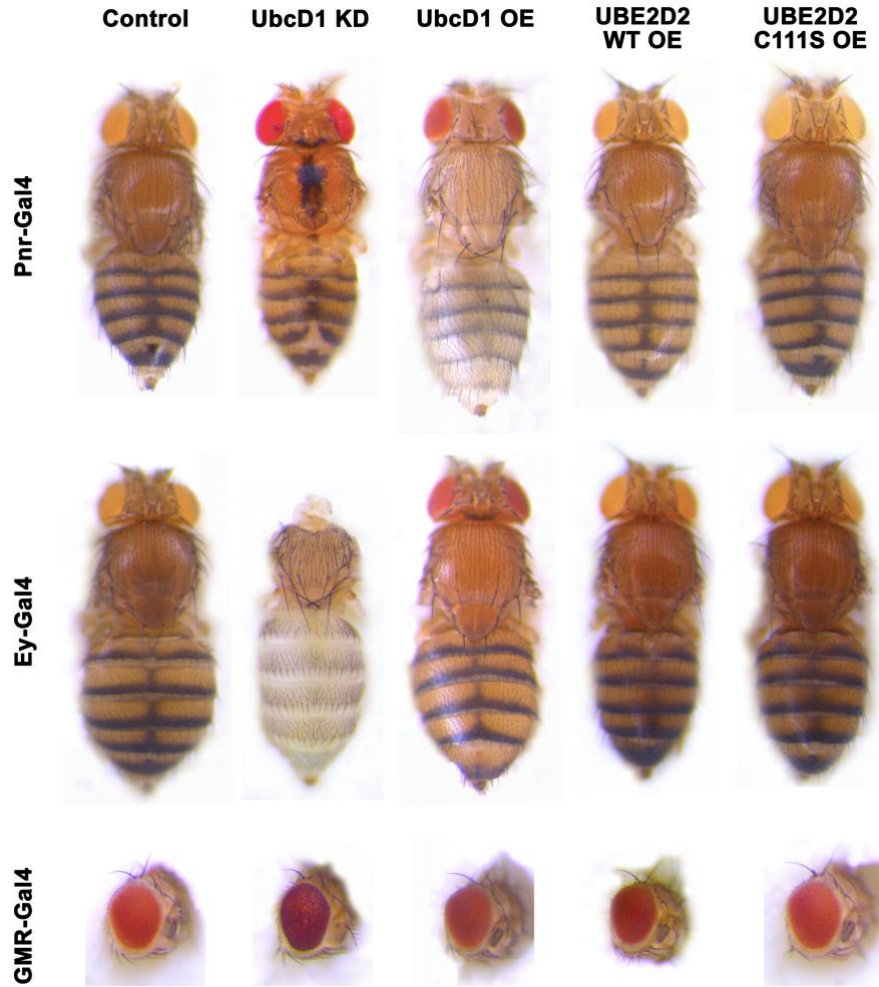
Fig.4 *UbcD1 knockdown caused a series of defects under the control of three different GAL4 drivers.* First, second and third rows show the female *Drosophila* phenotype caused by control (*w[1118]*), *UbcD1* knockdown (*UAS-UbcD1[RNAi]*), *UbcD1* overexpression (*UAS-UbcD1*), *UBE2D2 WT* overexpression (*UAS-UBE2D2 WT*) and *UBE2D2 C111S* (*UAS-UBE2D2 C111S*) under the control of *Pnr-Gal4*, *Ey-Gal4* and *GMR-Gal4* respectively. Flies in the third row were raised at 29 degrees, and the rest were raised at 25 degrees. Abbreviation: KD, knockdown; OE, overexpression.

6.2.3 Mutation in the copper binding region causes partial loss of UBE2D2 activity

In order to confirm that the copper binding region is essential for UBE2D2 activity *in vivo*, the *UAS-UBE2D2 WT* and *UAS-UBE2D2 C111S* transgenes were tested for their ability to rescue *UbcD1* knockdown phenotypes. With *tub-Gal4* driven, *UbcD1* knockdown caused death at 2nd instar, which was partially rescued by *UBE2D2 WT* expression (rescued to pupal stage) but not by *UBE2D2 C111S* expression (Fig.5A). In addition, the rough eye phenotype caused by

UbcD1 knockdown driven by *GMR-Gal4* at 29 degrees was only rescued by expressing *UBE2D2 WT* (Fig.5A). Furthermore, only *UAS-UBE2D2 WT* was found to partially rescue the headless phenotype caused by *UbcD1* knockdown under the control of *Ey-Gal4* (head rescued but still die at pupal stage) (Fig.5A). These results together demonstrated that mutation of the copper binding site causes the loss of UBE2D2 activity.
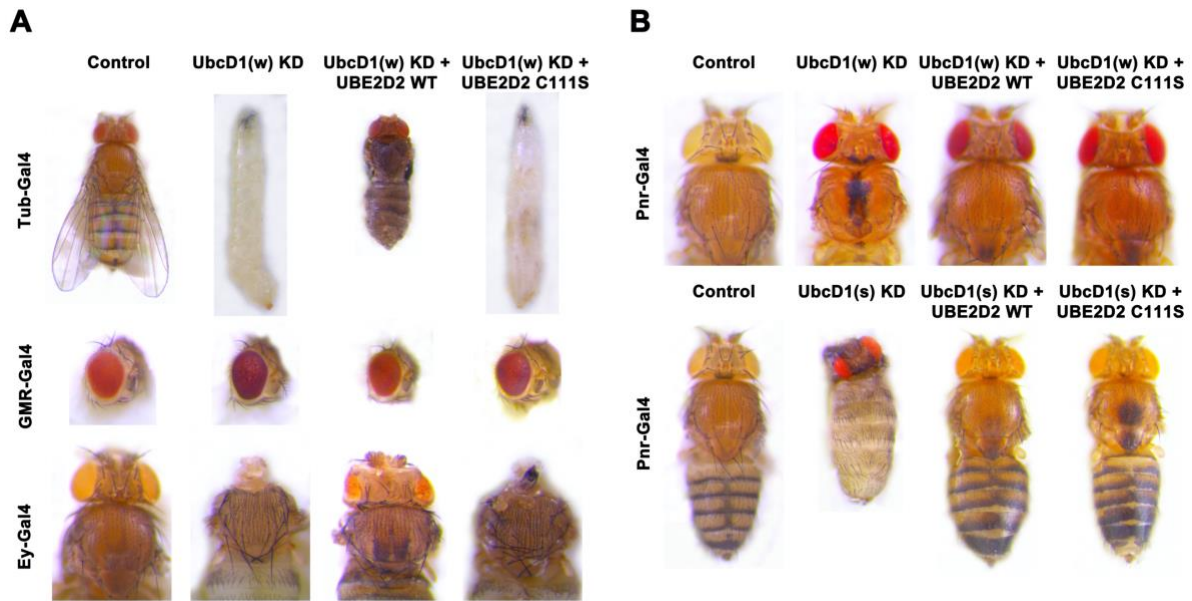

Fig.5 *Mutation of the copper binding region causes partial loss of UBE2D2 activity*. In order to investigate whether mutation of the copper binding residue C111 site could compromise UBE2D2 activity, both *UAS-UBE2D2 WT* and *UAS-UBE2D2 C111S* were used to rescue *UbcD1* knockdown defects. Two *UbcD1 RNAi* lines were used: one weak (w, BL35431) and the other strong (s, V26011). A) female *Drosophila* phenotypes of w^{1118}, *UAS-UbcD1^{wRNAi}*, *UAS-UbcD1^{wRNAi} + UAS-UBE2D2 WT*, and *UAS-UbcD1^{wRNAi} + UAS-UBE2D2 C111S* (from left to right) under the control of *tub-Gal4*, *GMR-Gal4* and *Ey-Gal4* (from top to bottom). Only *UAS-UBE2D2 WT* showed a partial or complete rescue of the phenotypic defects caused by weak *UbcD1* knockdown. B) female *Drosophila* phenotype of weak (w) and strong (s) *UbcD1* knockdown under the control of *Pnr-Gal4*: First row, w^{1118}, *UAS-UbcD1^{wRNAi}*, *UAS-UbcD1^{wRNAi} + UAS-UBE2D2 WT*, and *UAS-UbcD1^{wRNAi} + UAS-UBE2D2 C111S*; Second row, w^{1118}, *UAS-UbcD1^{sRNAi}*, *UAS-UbcD1^{sRNAi} + UAS-UBE2D2 WT*, and *UAS-UbcD1^{sRNAi} + UAS-UBE2D2 C111S*. Even though rescue of the weak *UbcD1 RNAi* was observed with *UAS-UBE2D2 C111S* under the control of *Pnr-Gal4*, only *UAS-UBE2D2 WT* showed a complete rescue effect of the defects produced by both weak and strong *UbcD1 RNAi*, indicating that

UBE2D2 C111S retains partial but not full activity. Abbreviation: KD, knockdown; w, weak; s, strong.

Contrary to the results with the other three *GAL4* drivers, the phenotypic defects caused by *UbcD1* knockdown under the control of *Pnr-Gal4* could be rescued by both *UAS-UBE2D2 WT* and *UAS-UBE2D2 C111S* (Fig.5B). As these initial experiments employed a weaker (w) *UbcD1 RNAi* line, we repeated the rescue experiment with a second, stronger (s) line. Weak *UbcD1* knockdown produced a thoracic cleft, which could be rescued by overexpression of both *UBE2D2 WT* and *UBE2D2 C111S* (Fig.5B). In contrast, the strong *UbcD1* knockdown caused a complete ablation of the thorax which was fully rescued by *UBE2D2 WT* overexpression while *UBE2D2 C111S* overexpression showed a partial rescue effect, with strong hyperpigmentation remaining on the thorax (Fig.5B). These results suggested that UBE2D2 C111S still possesses partial activity. Therefore, we proposed that mutation of the C111 residue causes a partial loss of UBE2D2 activity.

Since UBE2D2/UbcD1 is a cuproprotein, we investigated whether *UbcD1* knockdown defects were influenced by copper levels. However, high copper (1 mM $CuCl_2$-containing medium) or low copper (300 μM BCS-containing medium) dietary conditions failed to rescue or exacerbate the defects caused by knockdown of *UbcD1* under the control of *tub-Gal4*, *Elav-Gal4*, *Pnr-Gal4*, *Ey-Gal4* and *GMR-Gal4* (data not shown). Additionally, UbcD1 overexpression did not produce any discernable defects in flies raised in high or low copper conditions.

We still could not rule out the possibility that dietary copper content could modulate UbcD1 activity; flies raised on high or low dietary copper conditions may be capable of maintaining their internal copper homeostasis by regulating copper intake. In order to further examine the role of UbcD1 in copper homeostasis, we turned to the midgut-specific driver *Mex-Gal4*, since the epithelial cells of the midgut are directly in contact with the fly media. On normal food, around 60% flies could survive to adulthood after *UbcD1* knockdown, slightly lower than the control survival rate of ~80% (Fig.6A). The survival rate of *Mex>UbcD1* knockdown animals dropped to zero on $CuCl_2$-containing medium, and this heightened copper sensitivity could be rescued by both *UBE2D2 WT* and *UBE2D2 C111S* co-expression. Indeed, the survival rate of these two rescue groups was higher than that of the control in high copper conditions. These data suggested that UbcD1 in the midgut normally protects larvae from copper toxicity.

Western blot analysis, using exogenous expression of FLAG epitope-tagged versions of Ctr1A and ATP7 in the adult eye under *GMR-Gal4* control, showed that both these copper transporters were post-translationally downregulated upon *UbcD1* knockdown (Fig.6B). These results together suggested that UbcD1 might be required for a general protective response to high copper levels.
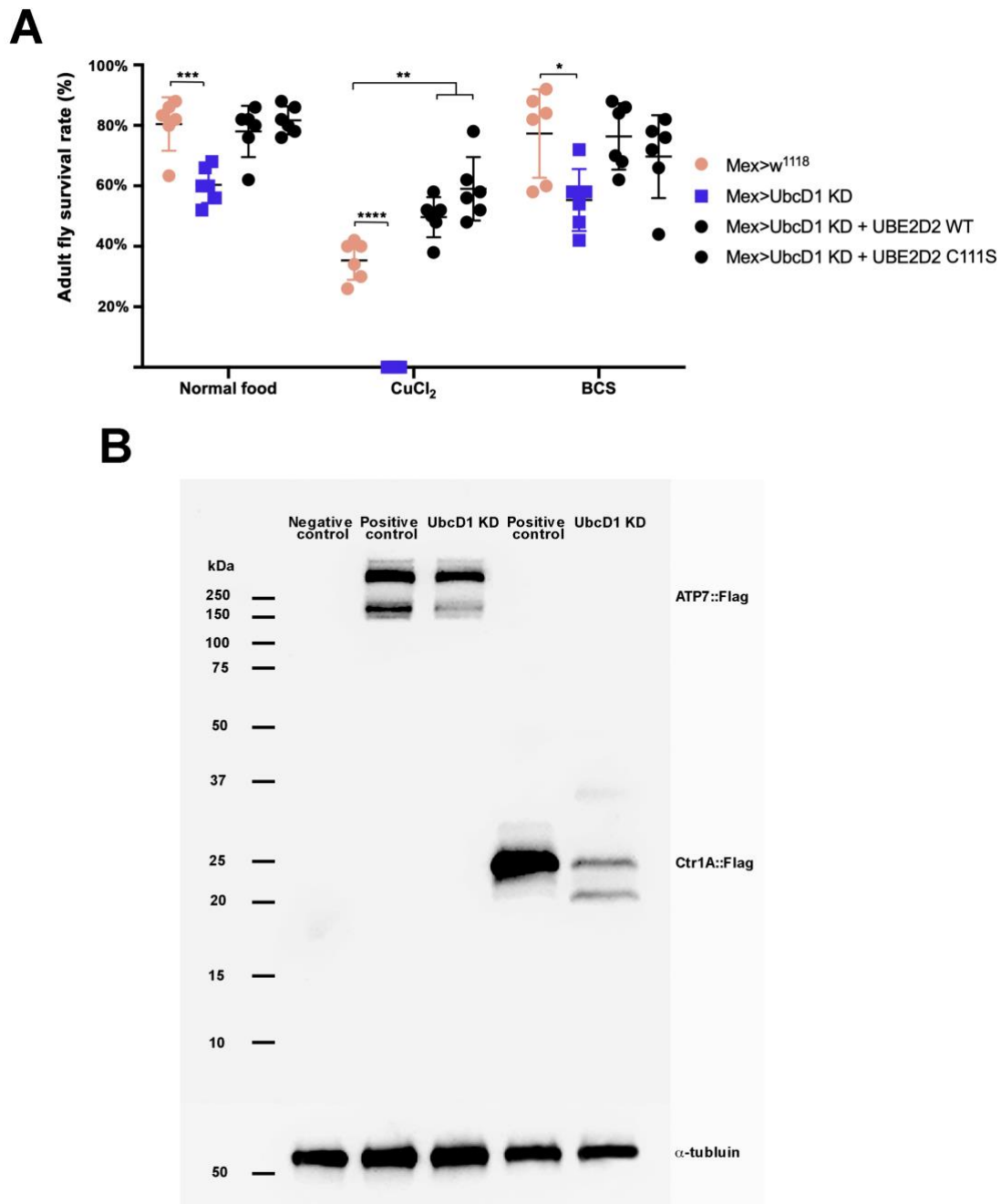

Fig.6 *UbcD1 protects larvae from copper toxicity*. A) Quantification of adult fly survival rate after *UbcD1* knockdown under different copper conditions. Percentage survival from 1st instar

larval stage to adulthood was assessed for each genotype on normal, 1 mM $CuCl_2$ and 300 μm BCS-supplemented food. Error bars represent mean ± S.E.M. Genotypes tested were w^{1118}, *UAS-UbcD1*^{wRNAi}, *UAS-UbcD1*^{wRNAi} + *UAS-UBE2D2 WT* and UAS-UbcD1^{wRNAi} + *UAS-UBE2D2 C111S* under the control of *Mex-Gal4*. n = 6 for each genotype, *p<0.05, **$p < 0.01$, ***$p < 0.001$, ****p<0.0001. B) ATP7::Flag and Ctr1A::Flag expression in adult heads after *UbcD1* knockdown using *GMR-Gal4*. Knockdown of *UbcD1* caused a decrease in the expression of ATP7 and Ctr1A. Abbreviations: KD, knockdown.

6.2.4 UbcD1 plays a critical role in apoptosis in Drosophila

In the nervous system, the ubiquitin proteasome system is involved in the remodelling of neuronal processes. Kuo *et al* reported that mutation in the E2 ubiquitin-conjugating enzyme UbcD1 caused dendrite pruning defects (Kuo et al., 2006). In this study, knockdown of *UbcD1* in all neurons using *Elav-Gal4* caused lethality at early pupal stages. However, immunostaining against caspase 3 revealed that no increase in caspase 3 expression was detected after knockdown of *UbcD1* (data not shown).

UbcD1 knockdown under the control of *Ey-Gal4* caused a complete ablation of the head structures (Fig.7B), with just the mouthparts left connected to the thorax. Dissection of these pharate adults revealed that the brain was still present but smaller, with aberrant morphology and now located in thorax (Fig.7B). The reduction in head size was rescued by *UAS-UBE2D2 WT* but not *UAS-UBE2D2 C111S* (Fig. 5A), demonstrating that *UbcD1* knockdown was responsible for the alteration. Furthermore, elevated active caspase 3 levels were detected in the pharate adult brains of *Ey>UbcD1 RNAi*-expressing flies (Fig.7C). Together, these results demonstrated that *UbcD1* knockdown-induced apoptosis which then altered the brain size and morphology. *UbcD1* knockdown was also found to cause cell death in wing imaginal discs under the control of *En-Gal4* which drives expression in posterior compartment of the wing. As shown in Fig.7D, the entire wing disc greatly decreased in size upon knockdown of *UbcD1*.
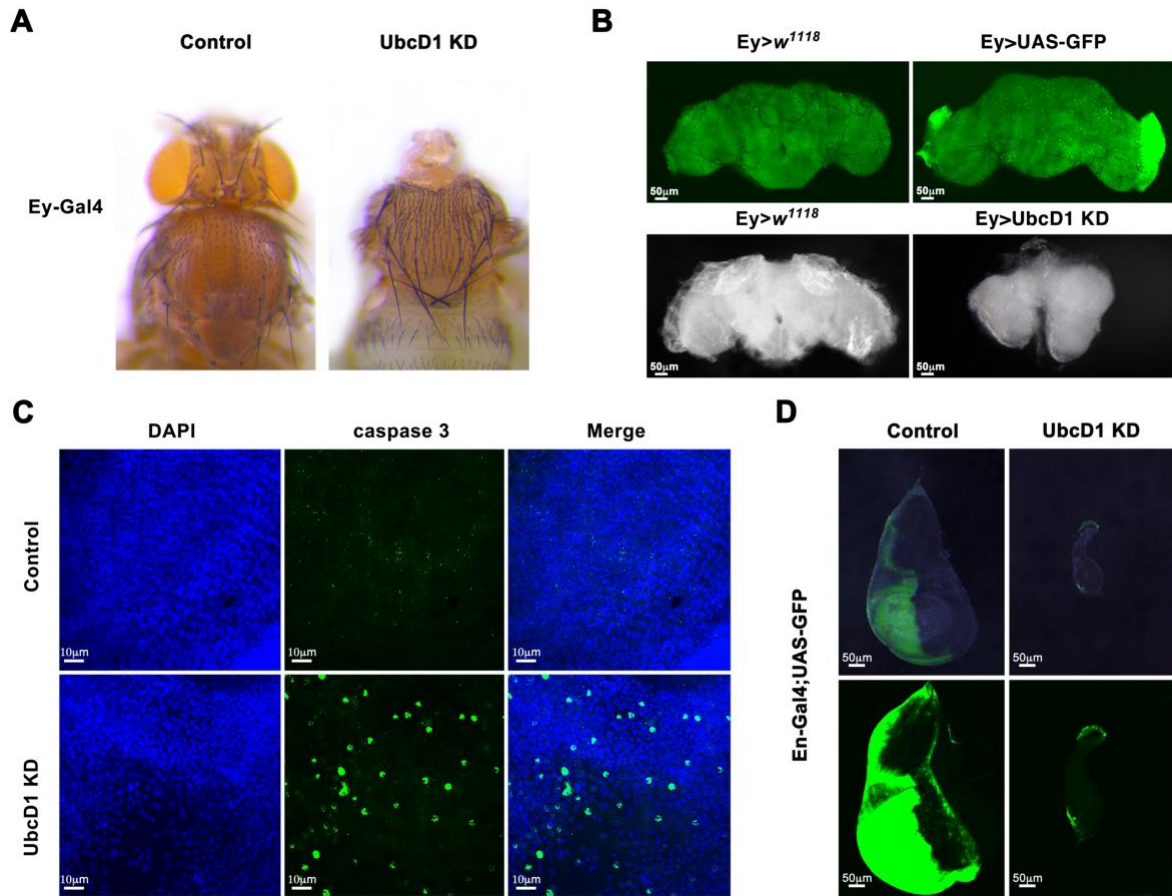
Fig.7 *UbcD1 knockdown induces apoptosis in Drosophila.* A) Dorsal views of adult female *Drosophila* of control (*w^1118^*) and *UbcD1* knockdown (*UAS-UbcD1^RNAi^*) driven by *Ey-Gal4*. *UbcD1* knockdown produced a headless phenotype, whereby the brain still existed but was displaced into thorax. B) first row: expression pattern of *Ey-Gal4* in the adult fly brain, GFP (small, bright green spots) shows the *Ey-Gal4*-expressing area; second row: brain morphology of control (*w^1118^*) and *UbcD1* knockdown (*UAS-UbcD1^RNAi^*) driven by *Ey-Gal4*. The brain morphology was altered after knockdown of *UbcD1*. C) Immunostaining against active caspase 3 was performed to detect cell death in the pharate adult brain after *UbcD1* knockdown under the control of *Ey-Gal4*: DAPI (blue) and caspase 3 (green). An increase in caspase 3 expression was detected after *UbcD1* knockdown. D) Wing discs were visualized after *UbcD1* knockdown using *En-Gal4*. Green fluorescence indicates where *En-Gal4* expresses. Knockdown of *UbcD1* led to the absence of the posterior compartment of the wing disc (green area) and an overall reduction in wing disc size. Scale bar: 50μm in B and D, 10μm in C. Abbreviation: KD, knockdown.

6.2.5 Drosophila p38 pathway is involved in UbcD1-induced melanization via regulating Ddc/ple

To try and identify possible substrates of UBE2D2/UbcD1, a compound transgenic stock was generated; *UAS-UBE2D2-C111S / CyO; Pnr-Gal4, UAS-UbcD1^{sRNAi} / TM6B*. This stock effectively has hypomorphic UbcD1/UBE2D2 activity in the *Pnr* domain since the C111S mutation reduces the rescue ability of UBE2D2, resulting in a strong thoracic hyperpigmentation phenotype (Fig.8B). UbcD1 hypomorph defects could be rescued by both UAS-UBE2D2 WT and UAS-UBE2D2 C111S, suggesting that mutation in the C111 residue just decreases UBE2D2 activity (Fig.8C and D); adding more of this mutant protein is sufficient to restore full function. This *UbcD1* hypomorph was then used to test whether manipulation of candidate downstream genes could rescue or exacerbate the loss of UbcD1 activity.

In order to test whether the UbcD1 hypomorph defects were influenced by copper levels, we manipulated copper uptake or copper transport by overexpressing Ctr1A (copper transporter regulating copper uptake in *Drosophila*) and suppressing Atox1 (copper chaperone responsible for transporting copper to ATP7 in *Drosophila*), respectively. Consistent with our anticipation, no rescue or additive effect was observed, presumably since UBE2D2 C111S protein was not capable of binding additional copper in order to increase its activity (Fig.8E and F).

Control *UbcD1 hypomorph* *UBE2D2 WT OE* * *UBE2D2 C111S OE* * *Ctr1A OE* * *Atox1 KD* *

Fig.8 *Ambient copper levels do not affect UbcD1-induced pigmentation.* A-F) Dorsal views of adult female *Drosophila* containing different transgenes. A) *Pnr-Gal4 with no transgene w^{1118}* B) *UAS-UBE2D2 C111S/+; Pnr-Gal4::UAS-UbcD1^{sRNAi}/+* (UbcD1 hypomorph). C-D) UbcD1 recombinant together with the following transgenes: C) *UAS-UBE2D2 WT*; D) *UAS-UBE2D2 C111S*; E) *UAS-Ctr1A*; F) *UAS-Atox1^{RNAi}*. * indicates the stock contains *UAS-UBE2D2 C111S/+; Pnr-Gal4::UAS-UbcD1^{sRNAi}/+*. A-F were captured using the 4.0× objective lens. Abbreviations: KD, knockdown; OE, overexpression. n>10 for each genotype.

When activated, the *Drosophila* p38 MAPK pathway was reported to induce hyperpigmentation (Sekine et al., 2011) similar to that observed in our *UbcD1* hypomorph. Therefore, we examined whether components of this pathway participated in the generation of the *UbcD1* hypomorph thoracic hyperpigmentation, by crossing in *RNAi* constructs for each. Knockdown of *p38a* showed a partial rescue effect; the black pigment in the marginal area disappeared (the area marked by white asterisks in Fig.9C). We also tested a *Drosophila* MAP2K gene, *licorne* (*lic*), which phosphorylates p38a (Han et al., 1998). Consistent with the *p38a* knockdown, *lic* knockdown also mitigated the thoracic hyperpigmentation (Fig.9D). Sekine et al revealed that Hr38 is required for p38-induced pigmentation (Sekine et al., 2011). *Hr38* knockdown caused a partial rescue of UbcD1 hypomorph thoracic hyperpigmentation (Fig.9E) similar to that seen with *p38a* knockdown. Knockdown of *Slim*, which encodes an E3 ubiquitin ligase that activates the p38 MAPK signalling pathway (Sekine et al., 2011), also resulted in a partial rescue of the defects of the UbcD1 hypomorph stock (Fig.9F). No phenotypic defects were observed after knockdown of *p38a*, *lic*, *Hr38* and *Slim* alone (data not shown). Together, these results suggested that the p38 pathway is involved in the hyperpigmentation induced upon loss of UbcD1 activity.

Black and brown pigments in *Drosophila* cuticle are comprised of DOPA- and dopamine-melanin (Wittkopp et al., 2003). Tyrosine hydroxylase (encoded by ple) catalyses the oxidation of tyrosine to DOPA which is then converted to dopamine by DOPA decarboxylase (Ddc). Some fractions of DOPA and dopamine are converted into DOPA and dopamine melanin respectively by the MCO2/laccase2 (Fig.9I). Knocking down *Ddc* produced hypopigmentation alone and with the UbcD1 hypomorph (Fig.9G and H), suggesting that *Ddc* participates in the melanization induced by loss of UbcD1 function. Sekine *et al* demonstrated that *Drosophila* p38 induces Ddc through post-translational activation of Hr38 (Sekine et al., 2011). Therefore, UbcD1 might regulate Ddc via the p38 signalling pathway.
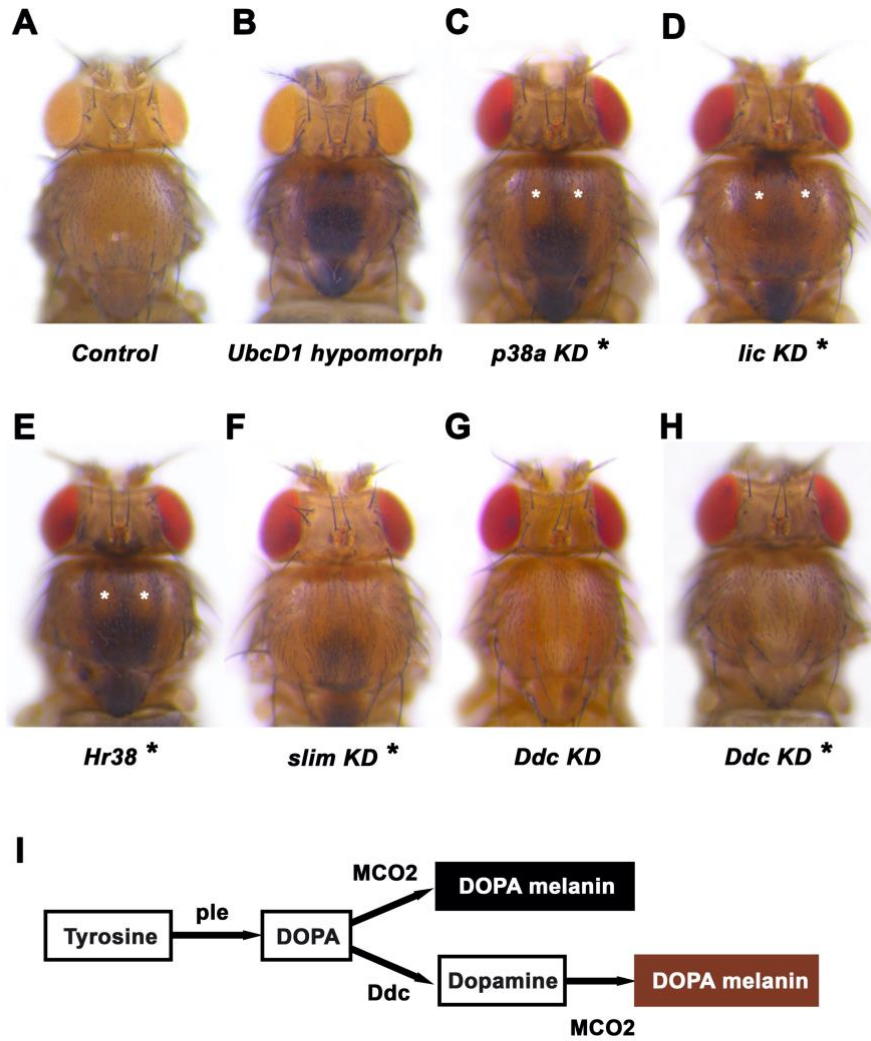
Fig.9 *Drosophila p38 MAPK pathway is required for UbcD1 mediated melanization.* A-H) Dorsal views of adult female *Drosophila* containing different transgenes. A) *Pnr-Gal4 with no transgene w^{1118},* B) *UAS-UBE2D2 C111S/+; Pnr-Gal4, UAS-UbcD1^{sRNAi}/+* (UbcD1 hypomorph), G) *UAS-Ddc^{RNAi}.* C-F and H) UbcD1 hypomorph together with the following transgenes: C) *UAS-p38^{RNAi};* D) *UAS-lic^{RNAi};* E) *UAS-Hr38^{RNAi};* F) *UAS-slim^{RNAi};* H) *UAS-Ddc^{RNAi}.* * indicates the stock contains *UAS-UBE2D2 C111S/+; Pnr-Gal4::UAS-UbcD1^{sRNAi}/+.* I) A model of the *Drosophila* melanin biosynthesis pathway. Knockdown of *p38a*, *lic*, *Hr38* and *slim*, or Ddc overexpression under the *Pnr-Gal4* did not generate any discernible defects (data not shown). A-H were captured using the 4.0× objective lens. Abbreviations: KD, knockdown; s, strong. n>10 for each genotype.

6.3 Discussion and Conclusion

Our collaborators Carlos Opazo and Ashley Bush identified that the E2 ubiquitin conjugase UBE2D2 possesses two putative copper binding regions and that the Cys111 residue in the first such domain was essential for copper enhanced UBE2D2 activity *in vitro*. In order to investigate whether mutation in Cys111 could compromise UBE2D2 activity *in vivo*, *UAS-UBE2D2 WT* and *UAS-UBE2D2 C111S* transgenic stocks were applied to rescue the defects produced by knockdown of *UbcD1* (*Drosophila* orthologue of UBE2D2) under the control of *tub-Gal4*, *GMR-Gal4*, *Ey-Gal4* and *Pnr-Gal4*. Consistent with our hypothesis, we showed that mutation in Cys111 reduced but did not ablate UBE2D2 activity, demonstrating that this copper binding region is essential for optimal UBE2D2 activity.

Interestingly, we showed that midgut specific knockdown of *UbcD1* makes developing larvae acutely sensitive to increased dietary copper levels, suggesting that copper binding to UbcD1 may normally trigger a protective response to copper toxicity, an idea supported by the observation that both Ctr1A and ATP7 are strongly downregulated at the posttranslational level upon *UbcD1* knockdown.

Previous evidence has indicated that UbcD1 participates in apoptosis by interacting with the E3 ubiquitin ligase DIAP1 (Ryoo et al., 2002). We demonstrated a reduction in brain size after suppressing *UbcD1* under the control of *Ey-Gal4* and showed that these defects were due to apoptosis, by performing immunofluorescent staining against caspase 3 in the adult brain. Knockdown of *UbcD1* also caused the loss of posterior wing disc cells under the control of *En-Gal4*. Knockdown of *UbcD1* in neurons caused pupal lethality, however in this case no increase of caspase 3 was detected in the larval brain. The absence of detectable apoptosis under pan-neuronal *UbcD1* knockdown might be due to the earlier developmental stage at which the apoptosis assay was conducted. It is possible that *UbcD1* knockdown does not initiate apoptosis in brain until late larval / early pupal stages and therefore no caspase 3 signal was detected. Therefore, consistent with Ryoo et al's report, our study also showed that *UbcD1* knockdown induces apoptosis in multiple cell types, indicating it is normally essential for the viability of many cells. *Drosophila* inhibitor of apoptosis 1 (DIAP1) has been reported to mediate the ubiquitination of caspases, thereby possessing anti-apoptotic function (Goyal et al., 2000). UbcD1 / reaper (reaper is a key activator of apoptosis in *Drosophila*) could stimulate DIAP1 auto-ubiquitination, thereby promoting its own degradation (Ryoo et al., 2002). If this is the

case, knockdown of *UbcD1* should have inhibited apoptosis, which is in contrast with our results, implying that other signalling pathways might be involved. Pan *et al* demonstrated that UbcD1 regulates Hedgehog signalling via Slmb mediated Ci degradation (Pan et al., 2017). However, our previous study revealed that overexpression or knockdown of *Slmb* in neurons did not produce any phenotypic defects (Zhang et al., 2020), indicating that Hedgehog signalling pathway is not involved in *UbcD1* knockdown-induced neuronal apoptosis. A recent paper showed that UbcD1 might also possess anti-apoptotic function since UbcD1/DIAP1 was shown to mediate the polyubiquitylation of Grim (a caspase substrate) which resulted in an increased Grim turnover (Yeh and Bratton, 2013). It will be interesting to investigate whether Grim is involved in *UbcD1* knockdown-induced apoptosis during neurodevelopment.

In order to identify partners and substrates of UBE2D2/UbcD1 and cellular pathways controlled by this E2, a recombinant compound transgenic stock representing a UBE2D2 hypomorphic allele was generated, showing a strong thoracic hyperpigmentation phenotype. The p38 signalling pathway has previously been shown to participate in pigmentation (Sekine et al., 2011). Our genetic interaction experiments showed that knockdown of members of the p38 pathway, in particular *slim*, caused a partial rescue effect of the thoracic hyperpigmentation of the UbcD1 hypomorph, suggesting that this pathway is required for the increased pigmentation caused by loss of UbcD1. In mammals, NR4A2 (HR38 in *Drosophila*) has been shown to regulate the expression of ple and Ddc which are important in the synthesis and storage of dopamine in central dopaminergic neurons (Jankovic et al., 2005; Perlmann and Wallén-Mackenzie, 2004). Dopamine could be converted to melanin by the MCO2/laccase2 (Wittkopp et al., 2003). Sekine *et al* reported that the p38 pathway transcriptionally regulates Ddc and ple through Hr38 (Sekine et al., 2011) in flies too. Similarly, we found that the hyperpigmentation of the UbcD1 hypomorph could be attenuated by *Ddc* knockdown, suggesting that UbcD1 might regulate melanization via Ddc through the p38 signalling pathway (Fig.10). In *Drosophila*, laccase2, a multicopper oxidase, is equivalent to mammalian tyrosinase, responsible for the production of melanin (Riedel et al., 2011) and it has been reported that copper content was correlated with cuticle pigmentation levels (Vasquez-Procopio et al., 2020). Therefore, we propose that UbcD1 might participate in melanin synthesis by regulating the activity of laccase2 / MCO2 through control of cellular copper levels (Fig.10).
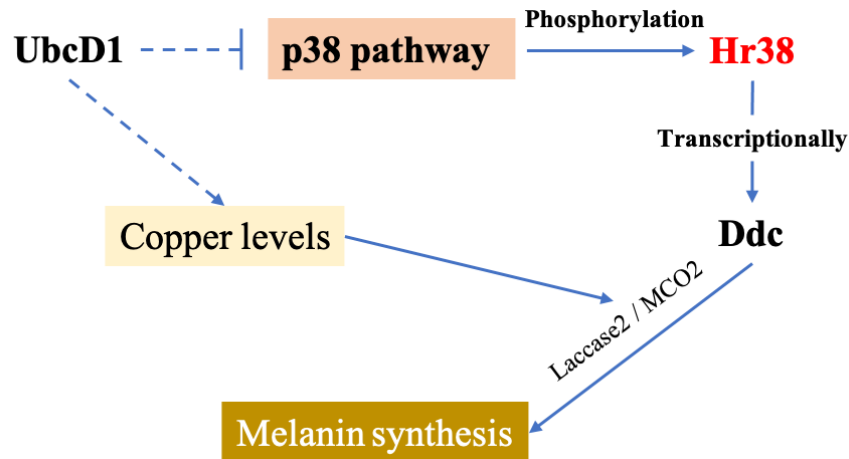
Fig.10 Schematic graph of how UbcD1 may regulate the synthesis of melanin

Our data revealed that inhibition of E3 ubiquitin ligase Slim partially rescued the defects of the UbcD1 hypomorph, suggesting that other E3s might also participate in UbcD1's regulation of melanization. The UbcD1 hypomorph stock was also used for screening several E3 ubiquitin ligases and proteasomal components which might interact with UBE2D2/UbcD1 (data not shown). Among them, we found that Cul3 (scaffold component of several E3 ubiquitin ligases) and Rpn9 (26S proteasome) might participate with UbcD1 in the proteasomal degradation of UbcD1's substrates. One of Rpn9's substrates, sima, was also demonstrated to be involved in UbcD1-induced melanization, suggesting that Cul3/Rpn9/sima are in the same pathway (Fig.11). Since none of these candidates could completely rescue the defects of UbcD1 hypomorph stock, more E3s and proteasomal components need to be investigated.
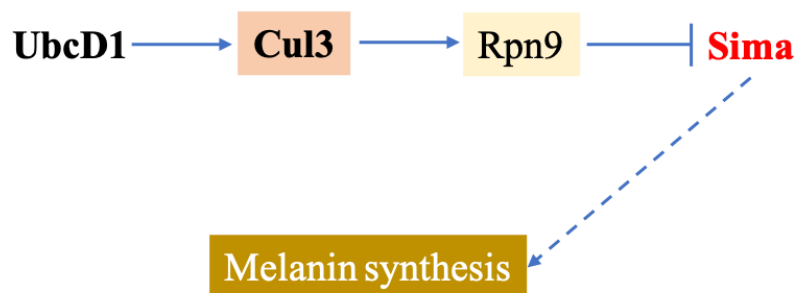

Fig.11 Schematic graph of UbcD1 / Cul3 / Rpn9 / Sima pathway

Melanization is an important immune defence, using toxic intermediates such as reactive oxygen species generated during melanin synthesis to kill pathogens (Cerenius and Söderhäll, 2004). In the nervous system, neurons such as the dopaminergic neurons of the *substantia nigra*

and noradrenergic neurons of the *locus coeruleus* produce neuromelanin (Fedorow et al., 2005). In Parkinson's disease, neuromelanin‑containing neurons preferentially degenerate (Vila, 2019). Our results demonstrated that *UbcD1* knockdown upregulated melanization and induced apoptosis in the nervous system. Therefore, we hypothesize that knockdown of *UbcD1* might induce the generation of melanin in neurons, thereby causing the cell death. In order to test this hypothesis, we next will be investigating how UbcD1 mediated melanization affects neurodevelopment, especially whether melanization is associated with neuronal death. In addition, many reports showed that copper homeostasis is essential for the brain function and our results revealed that UbcD1 might participate in regulating cellular copper levels. Therefore, we will be exploring the relationship between UbcD1 and copper homeostasis in regulating melanization during neurodevelopment and then elucidating the associated mechanism.

References:

Banci, L., Bertini, I., Ciofi-Baffoni, S., Leontari, I., Martinelli, M., Palumaa, P., Sillard, R., Wang, S., 2007. Human Sco1 functional studies and pathological implications of the P174L mutant. Proc Natl Acad Sci U S A 104, 15-20.

Cerenius, L., Söderhäll, K., 2004. The prophenoloxidase-activating system in invertebrates. Immunol Rev 198, 116-126.

Fedorow, H., Tribl, F., Halliday, G., Gerlach, M., Riederer, P., Double, K.L., 2005. Neuromelanin in human dopamine neurons: comparison with peripheral melanins and relevance to Parkinson's disease. Prog Neurobiol 75, 109-124.

Goyal, L., McCall, K., Agapite, J., Hartwieg, E., Steller, H., 2000. Induction of apoptosis by Drosophila reaper, hid and grim through inhibition of IAP function. EMBO J 19, 589-597.

Groth, A.C., Fish, M., Nusse, R., Calos, M.P., 2004. Construction of transgenic Drosophila by using the site-specific integrase from phage phiC31. Genetics 166, 1775-1782.

Han, Z.S., Enslen, H., Hu, X., Meng, X., Wu, I.H., Barrett, T., Davis, R.J., Ip, Y.T., 1998. A conserved p38 mitogen-activated protein kinase pathway regulates Drosophila immunity gene expression. Mol Cell Biol 18, 3527-3539.

Jankovic, J., Chen, S., Le, W.D., 2005. The role of Nurr1 in the development of dopaminergic neurons and Parkinson's disease. Prog Neurobiol 77, 128-138.

Kuo, C.T., Zhu, S., Younger, S., Jan, L.Y., Jan, Y.N., 2006. Identification of E2/E3 ubiquitinating enzymes and caspase activity regulating Drosophila sensory neuron dendrite pruning. Neuron 51, 283-290.

Opazo, C.M., Lotan, A., Xiao, Z., Zhang, B., Greenough, M.A., Lim, C.M., Trytell, H., Ramirez, A., Ukuwela, A.A., Mawal, C.H., McKenna, J., Saunders, D.N., Burke, R., Gooley, P.R., Bush, A.I., 2021. Copper singaling promotes proteostasis and animal development via allosteric activation of ubiquitin E2 conjugates. bioExiv, doi.org/10.1101/2021.1102.1115.431211.

Pan, C., Xiong, Y., Lv, X., Xia, Y., Zhang, S., Chen, H., Fan, J., Wu, W., Liu, F., Wu, H., Zhou, Z., Zhang, L., Zhao, Y., 2017. UbcD1 regulates Hedgehog signaling by directly modulating Ci ubiquitination and processing. EMBO Rep 18, 1922-1934.

Perlmann, T., Wallén-Mackenzie, A., 2004. Nurr1, an orphan nuclear receptor with essential functions in developing dopamine cells. Cell Tissue Res 318, 45-52.

Riedel, F., Vorkel, D., Eaton, S., 2011. Megalin-dependent yellow endocytosis restricts melanization in the Drosophila cuticle. Development 138, 149-158.

Rumpf, S., Bagley, J.A., Thompson-Peer, K.L., Zhu, S., Gorczyca, D., Beckstead, R.B., Jan, L.Y., Jan, Y.N., 2014. Drosophila Valosin-Containing Protein is required for dendrite pruning through a regulatory role in mRNA metabolism. Proc Natl Acad Sci U S A 111, 7331-7336.

Ryoo, H.D., Bergmann, A., Gonen, H., Ciechanover, A., Steller, H., 2002. Regulation of Drosophila IAP1 degradation and apoptosis by reaper and ubcD1. Nat Cell Biol 4, 432-438.

Saville, M.K., Sparks, A., Xirodimas, D.P., Wardrop, J., Stevenson, L.F., Bourdon, J.C., Woods, Y.L., Lane, D.P., 2004. Regulation of p53 by the ubiquitin-conjugating enzymes UbcH5B/C in vivo. J Biol Chem 279, 42169-42181.

Sekine, Y., Takagahara, S., Hatanaka, R., Watanabe, T., Oguchi, H., Noguchi, T., Naguro, I., Kobayashi, K., Tsunoda, M., Funatsu, T., Nomura, H., Toyoda, T., Matsuki, N., Kuranaga, E., Miura, M., Takeda, K., Ichijo, H., 2011. p38 MAPKs regulate the expression of genes in the dopamine synthesis pathway through phosphorylation of NR4A nuclear receptors. J Cell Sci 124, 3006-3016.

Turski, M.L., Thiele, D.J., 2009. New roles for copper metabolism in cell proliferation, signaling, and disease. J Biol Chem 284, 717-721.

Vasquez-Procopio, J., Rajpurohit, S., Missirlis, F., 2020. Cuticle darkening correlates with increased body copper content in Drosophila melanogaster. Biometals 33, 293-303.

Vila, M., 2019. Neuromelanin, aging, and neuronal vulnerability in Parkinson's disease. Mov Disord 34, 1440-1451.

Wittkopp, P.J., Carroll, S.B., Kopp, A., 2003. Evolution in black and white: genetic control of pigment patterns in Drosophila. Trends Genet 19, 495-504.

Yeh, T.C., Bratton, S.B., 2013. Caspase-dependent regulation of the ubiquitin-proteasome system through direct substrate targeting. Proc Natl Acad Sci U S A 110, 14284-14289.

Zhang, B., Binks, T., Burke, R., 2020. The E3 ubiquitin ligase Slimb/β-TrCP is required for normal copper homeostasis in Drosophila. Biochim Biophys Acta Mol Cell Res 1867, 118768.

CHAPTER 7: FINAL DISCUSSION AND FUTURE DIRECTIONS

7.1 Copper homeostasis and the Ubiquitin proteasome system

Accumulating evidence has revealed that the ubiquitin proteasome system (UPS) is involved in copper homeostasis while in turn intracellular copper levels affect the activity of the UPS. In this study, many components of the UPS (such as an E2 ubiquitin conjugase, E3 ubiquitin ligases and 26 proteasome subunits) have been tested to investigate whether they participate in regulating copper homeostasis. Interestingly, some of these candidates produced copper deficiency or excess defects after knockdown, suggesting that they might regulate intracellular copper levels. For instance, it was demonstrated that suppression of the E3 ubiquitin ligase Slmb caused a decrease in copper levels via inhibition of copper uptake (Zhang et al., 2020). *Cnc* encodes a transcription factor responsible for regulating the activation of genes induced by oxidative stress (Sykiotis and Bohmann, 2008). Here, we found that knockdown of *cnc* could rescue the decrease of copper import protein caused by *Slmb* downregulation, indicating that cnc was involved in Slmb mediated copper uptake. In addition, suppression of *Slmb* could protect larvae from the toxicity of excess copper, further demonstrating that Slmb regulates copper uptake and finally alters intracellular copper levels. However, a feedback loop might exist where cellular copper levels maintain Slmb activity. Homeodomain-interacting protein kinase (HipK, a serine/threonine kinase) has been shown to inhibit Slmb mediated ubiquitination (Swarup and Verheyen, 2011). Unpublished genetic interaction experiments by our group showed that downregulation of *HipK* partially rescues the defects of *Slmb* knockdown and copper is reported to play a role in phosphorylation of some kinases (Turski et al., 2012). Therefore, we postulate that copper might affect Slmb activity by mediating the phosphorylation of HipK.

Another E3 we particularly investigated is Vhl, which forms an E3 ubiquitin complex together with EloC and Cul2 (Gossage et al., 2015). Unlike Slmb, Vhl appears to regulate cellular copper levels distinctly in different tissues in *Drosophila*. Knockdown of *Vhl* produced thoracic hyperpigmentation and abdominal hypopigmentation, which could be rescued by decreasing or increasing intracellular copper levels respectively, suggesting that copper levels are elevated in the thorax and reduced in the abdomen. In renal carcinoma cells, Vhl has been reported to regulate the proteasomal degradation of the transcription factor Hif-1α (Ivan et al., 2001). Knockdown of *Sima*, which encodes the *Drosophila* orthologue of human Hif-1α, showed a rescue effect to *Vhl* knockdown defects, indicating that Vhl regulates copper homeostasis via Sima. However, only thoracic hyperpigmentation was observed in *Sima*-overexpressing flies,

implying that other transcription factors might be responsible for the generation of the abdominal hypopigmentation seen upon *Vhl* knockdown. In our previous study, cnc was demonstrated to regulate copper uptake and cause abdominal hypopigmentation when upregulated (Zhang et al., 2020). Consistent with our assumption, downregulation of *cnc* rescued the abdominal hypopigmentation of *Vhl* suppression. We hence concluded that Vhl might indirectly regulate copper levels via posttranslational regulation of different transcription factors in different tissues. In turn, the expression of Vhl was subject to copper levels. Real-time PCR results revealed that the expression of *Vhl* mRNA was significantly reduced in high copper conditions. We hypothesized that the reduction of Vhl was due to the oxidative stress generated by excess copper, resembling what hypoxia does to Vhl. It will be particularly interesting to determine whether a feedback loop exists whereby copper levels regulate Slmb / Vhl activity.

UBE2D2, an E2 ubiquitin conjugating enzyme, is a cuproprotein whose activity can be enhanced by copper (Opazo et al., 2021). UbcD1, the *Drosophila* orthologue of UBE2D2, shows 95% identity to its mammalian counterpart and has conserved copper binding regions. Since our western blot results showed that suppression of *UbcD1* caused a decrease in copper transporters, UbcD1 is predicted to also regulate cellular copper levels. Furthermore, downregulation of *sima* (the substrate of Vhl) partially rescued *UbcD1* knockdown defects, implying that UbcD1 interacts with Vhl in the proteasomal degradation of Sima (Fig.1). In Chapter 5, we demonstrated that Vhl / Sima regulates copper uptake via copper transporters. Therefore, we postulate that UbcD1 might regulate copper homeostasis via Vhl (Fig.1). Additionally, rescue experiments revealed that UbcD1 could interact with other E3s, including Cul3, Bre1, poe and Keap1. Future research will be investigating how they interact in regulating copper homeostasis.
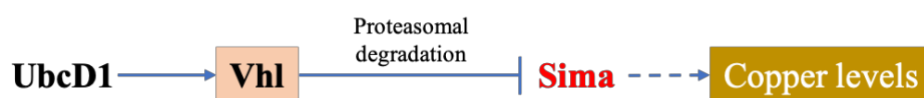

Fig.1 Schematic graph of a proposed UbcD1 / Vhl / Sima pathway

7.2 Copper transporters / Copper chaperones and the Ubiquitin proteasome system

The maintenance of cellular copper homeostasis involves numerous components, including transporters that mediate copper uptake (e.g., CTR1) and efflux (e.g., ATP7A and ATP7B), biomolecules that sequester and store copper (e.g., metallothioneins and glutathione), and copper chaperones that guide copper to copper-dependent enzymes (e.g., Atox1, CCS, Cox11, Sco1 and Sco2) (Kim et al., 2008; Nose et al., 2006; Petris et al., 2000; Rae et al., 1999; Scheiber et al., 2013). In this study, we demonstrated that Slmb, Vhl and UbcD1 regulate intracellular copper levels by controlling the levels of copper transporter proteins.

7.2.1 ATP7 and ubiquitin proteasome system

Copper transporter ATP7, the *Drosophila* orthologue of mammalian ATP7A and ATP7B, is responsible for delivering copper to copper dependent enzymes in the *trans*-Golgi network (TGN). In previous study, we observed that flies lacking ATP7 died at the early larval stage due to copper deficiency (Norgate et al., 2006). In polarized mammalian cells, ATP7A could be translocated from the TGN to the basolateral membrane for exporting excess copper when in high copper conditions (Petris et al., 1996). Here, we demonstrated for the first time in *Drosophila* that copper levels could affect ATP7 intracellular localization (Zhang et al., 2020) in a manner similar to that seen for mammalian ATP7A.

Since *Slmb* knockdown produced similar defects to those caused by *ATP7* overexpression, Slmb was selected to investigate whether it interacts with ATP7 to regulate copper levels. The partial rescue effect of *ATP7* knockdown to *Slmb* knockdown defects initially made us believe that Slmb post-translationally regulates ATP7. Additionally, a decrease in copper levels was observed in both *ATP7* overexpression and *Slmb* suppression, which supported our hypothesis. However, the results of survival experiments refuted our hypothesis since two different impacts to fly survival rate in high copper conditions were detected after *ATP7* upregulation and *Slmb* downregulation. Overexpression of *ATP7* caused larval lethality in high copper conditions whereas the survival rate of adult flies was increased by *Slmb* suppression, suggesting a difference in the mechanism causing the reduction of copper levels. ATP7 plays a critical role in copper efflux (Petris et al., 1996), and therefore we inferred that Slmb might regulate copper influx via copper transporter Ctr1A instead (discussed later). Suppression of *ATP7* inhibited copper efflux thus increasing cytosolic copper levels, which could explain why *Slmb* knockdown defects were partially rescued. In short, Slmb appeared to not directly interact with ATP7 in regulating cellular copper levels.

Comstra *et al* identified 541 ATP7A interacting proteins and some of them are involved in the ubiquitin proteasome system (Comstra et al., 2017). In order to screen for those which could post-translationally regulate ATP7, *Drosophila* orthologues of ATP7A-interacting candidates were examined by using the GAL4/UAS system combined with *RNAi* technique. EloC was selected from this targeted genetic screen for further investigation due to its knockdown phenotype. However, genetic interaction experiments and western blot could not convincingly demonstrate a role for EloC in the degradation of ATP7. Since EloC combines with Vhl to form an E3 ubiquitin complex (Aso et al., 2000), we also investigated the interaction between Vhl and ATP7. Vhl promotes proteasomal degradation of the hypoxia inducible factor (Hif-1α, encoded by *Sima* in flies) during normoxia (Shmueli et al., 2014). In rat intestinal epithelial cells, the transcription factor Hif-2α mediates induction of ATP7A during hypoxia (Xie and Collins, 2011, 2013). In addition, activation of Hif-1 signaling ameliorates liver steatosis in ATP7B deficient zebrafish, suggesting that Hif-1 upregulates ATP7B (Mi et al., 2020).

Given previous evidence that VHL's substrates regulated mammalian ATP7A and ATP7B, we postulated that Vhl might interact with ATP7 via Sima in *Drosophila*. In this study, we found that *Vhl* knockdown generated abdominal hypopigmentation which could be rescued by upregulating copper levels. Our hypothesis about the generation of hypopigmentation is that copper deficiency in the TGN leads to the inhibition of cuproenzyme laccase 2 (the fly equivalent of tyrosinase) activity, which then results in the reduction of melanin production (Binks et al., 2010; Zhang et al., 2020). ATP7 is normally localized to the TGN where it may be responsible for transporting copper to laccase2 (Burke et al., 2008; Norgate et al., 2006). It is translocated to the cell membrane for copper efflux in copper overload conditions (Zhang et al., 2020). One possibility is that the decrease of copper levels causing abdominal hypopigmentation is due to accumulation of ATP7 after knockdown of *Vhl*; excess *ATP7* expression could cause the forced export of intracellular copper leading to cytoplasmic deficiency. However, suppressing *ATP7* failed to rescue the abdominal hypopigmentation due to the fact that copper trafficking to the *trans*-Golgi network is inhibited by downregulation of *ATP7,* which likewise causes hypopigmentation. So, we are unable to demonstrate whether Vhl could regulate *ATP7* expression in abdomen. Additionally, *Sima* overexpression generated hyperpigmentation rather than hypopigmentation, a result that was not consistent with the hypothesis that Sima regulates ATP7. In chapter 5, our results revealed that Vhl in fact regulates copper levels in the abdomen through the transcription factor cnc. Upregulation of

cnc was reported to decrease ATP7 (Zhang et al., 2020), suggesting that Vhl might indirectly regulate ATP7 via cnc in the abdomen.

In survival experiments, we observed that knockdown of *UbcD1* caused larval lethality in high copper condition, similar to *ATP7* overexpression, suggesting that UbcD1 might regulate copper efflux via ATP7. However, western blot results revealed a decrease in the ATP7 protein levels after *UbcD1* downregulation, indicating that UbcD1 does not direct the proteasomal degradation of ATP7. So far, none of our E2, E3 and 26S proteasome candidates have been shown to regulate the proteasomal degradation of ATP7.

7.2.2 Ctr1A and ubiquitin proteasome system

Copper transporter CTR1 is localized at the apical membrane and is responsible for copper uptake from the diet (Nose et al., 2010). In yeast, the E3 ubiquitin ligase Rsp5 participates in the proteasomal degradation of CTR1, which then decreases cellular copper levels due to the reduction of copper uptake (Liu et al., 2007). Ctr1A and Ctr1B are orthologous to mammalian CTR1 (Southon et al., 2013). Ctr1A plays a major role in cellular copper uptake, with Ctr1B complementing Ctr1A's action in certain cell types (Binks et al., 2010). In this study, we demonstrated that Slmb, Vhl and UbcD1 indirectly regulate copper import protein Ctr1A via proteasomal degradation. A model was made to clarify how UbcD1, Vhl and Slmb might interact to control copper levels via Ctr1A (Fig.2).
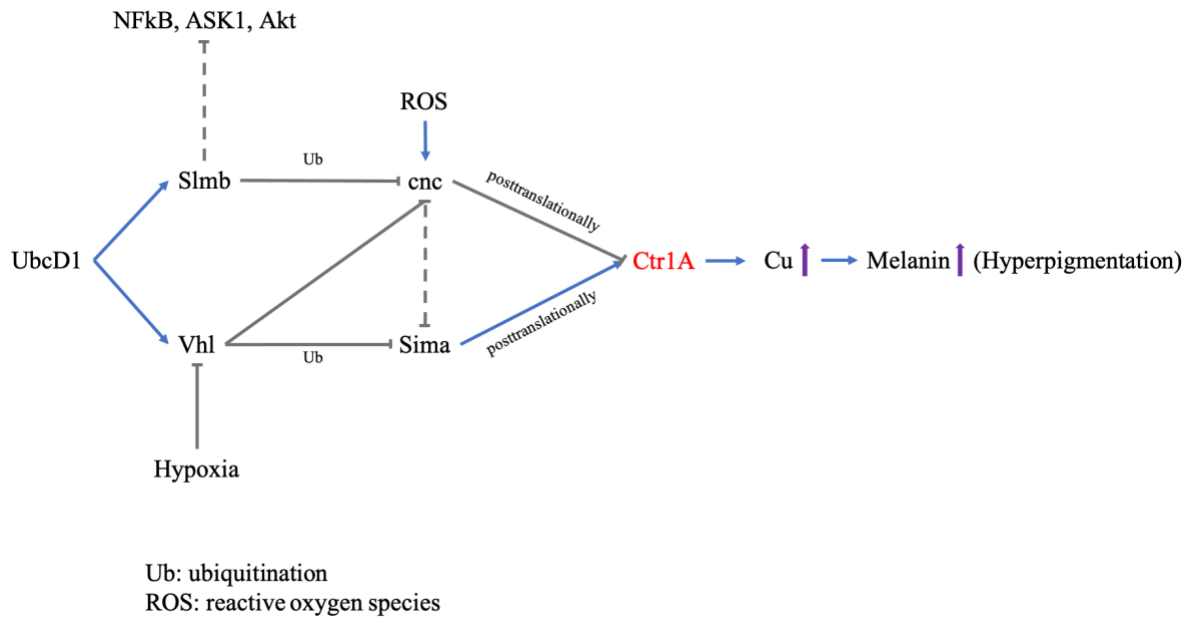
NFkB, ASK1, Akt

ROS

Slmb — cnc

Ub

posttranslationally

UbcD1

Ctr1A → Cu ↕ → Melanin ↕ (Hyperpigmentation)

Vhl — Sima

Ub

posttranslationally

Hypoxia

Ub: ubiquitination
ROS: reactive oxygen species

Fig.2 Schematic graph of how UbcD1, Vhl and Slmb might regulate Ctr1A

We showed that Slmb regulates Ctr1A via the transcription factor cnc (Zhang et al., 2020). cnc is a substrate of Slmb/BTRC and is considered the master regulator of the oxidative stress response (Hayes et al., 2015). Under the normal condition, cnc / Nrf2 is maintained at a very low level. However, the level of cnc / Nrf2 strikingly increases in response to redox stressors. Given the role of copper in the generation of reactive oxygen species, we postulated that cnc might participate in copper homeostasis in order to modulate ROS levels. In chapter 3, downregulation of *cnc* was observed to rescue the decrease of Ctr1A caused by *Slmb* knockdown. Additionally, western blot results showed that both Slmb and cnc post-translationally regulated Ctr1A, indicating that Slmb interacts with cnc in regulating Ctr1A (Fig.2). Since cnc encodes a transcription factor, we propose that cnc indirectly regulates Ctr1A expression. Analysis of known Nrf2(cnc) targets reveals some potential candidates for Ctr1A regulation: UBE2D2, PSMA3 and PSMD4 (Lacher et al., 2015). UbcD1, the *Drosophila* orthologue of UBE2D2, has been demonstrated to participate in Hedgehog signaling pathway via Slmb-mediated degradation of Ci (Pan et al., 2017). Here, we examined UbcD1. However, overexpression of *UbcD1* did not produce any discernable defects while suppression of *UbcD1* resulted in a decrease in Ctr1A expression, indicating that UbcD1 normally promotes the stability of Ctr1A rather than directing its proteasomal degradation. Thus, identification of cnc targets directly promoting Ctr1A degradation is a high priority. We found that *cnc* overexpression just produced abdominal hypopigmentation without thoracic cleft, suggesting

that additional Slmb targets might be involved in generating the thoracic cleft caused by *Slmb* knockdown. Many Slmb/BTRC substrates have been identified, including NFkB, ASK1 and Akt that are all implicated in copper homeostasis (Crouch et al., 2009; Kenneth et al., 2014; Wang et al., 2009). It will be particularly interesting to investigate whether these candidates could be involved in the generation of thoracic cleft after *Slmb* downregulation and how they interact in regulating intracellular copper levels.

This study demonstrated that Vhl regulates Ctr1A distinctly in different tissues of *Drosophila*. Vhl has been reported to regulate the proteasomal degradation of Hif-1α in response to hypoxia (Batavia et al., 2019). In hypoxic condition, the expression of CTR1 was post-translationally upregulated via the Hif pathway (White et al., 2009; Xia et al., 2017). In this study, the thoracic hyperpigmentation and abdominal hypopigmentation of *Vhl* knockdown-expressing flies were rescued by downregulation and upregulation of Ctr1A respectively, suggesting that suppressing *Vhl* increased Ctr1A in thorax while decreasing Ctr1A in abdomen. Downregulation of *Sima* could completely rescue *Vhl* knockdown defects, implying that Sima is involved in regulating Ctr1A, which is consistent with Xia et al's report. However, only thoracic hyperpigmentation was observed in *Sima*-overexpressing flies. This indicated that other Vhl substrates might play a dominant role in causing the decrease of Ctr1A in abdomen. Copper uptake was increased under hypoxia (Fitzgerald et al., 2016) while extreme hypoxia inhibited copper uptake (Nadella et al., 2011), suggesting that hypoxia could activate at least two different pathways in regulating copper uptake. We found that when upregulated, cnc produced abdominal hypopigmentation via downregulation of Ctr1A and that downregulation of *cnc* rescued the abdominal hypopigmentation caused by *Vhl* knockdown. Therefore, Vhl might regulate Ctr1A via Sima in the thorax and cnc in the abdomen (Fig.2). Additionally, suppression of Vhl in adult fly eyes failed to cause a change in the expression of Ctr1A while overexpression of Sima and cnc decreased Ctr1A, further supporting that Vhl regulates cellular copper levels via activating different pathways in different tissues.

7.2.3 Copper chaperones and ubiquitin proteasome system

A group of copper chaperones including Atox1 and CCS play critical roles in the intracellular trafficking of copper. CCS is primarily localized in the cytosol and is responsible for transporting copper to copper dependent cytosolic enzymes (Culotta et al., 1997; Prohaska et al., 2003). It was reported that CCS delivers copper to the E3 ubiquitin ligase XIAP in

mammals and that CCS itself could be ubiquitinated by XIAP (Brady et al., 2010). DIAP, the *Drosophila* orthologue of XIAP, can be post-translationally regulated by UbcD1 together with Reaper (Yeh and Bratton, 2013). Combining these results leads to the possibility that UbcD1 might indirectly regulate CCS via DIAP in the fly. In future studies, we will be testing this idea by performing immunoprecipitation to detect whether knockdown of *UbcD1* could affect the ubiquitination of DIAP and CCS.

The chaperone Atox1 has been demonstrated to deliver copper to copper transporters ATP7A and ATP7B in the TGN (Scheiber et al., 2013). However, knockdown of *Atox1* in this study did not produce *ATP7* knockdown-like defects. Actually, no discernible defects were observed after *Atox1* knockdown even under the control of the ubiquitous *tub-Gal4*. There are two possibilities for it: 1) our Atox1 *RNAi* lines do not work; 2) other chaperones might compensate for Atox1's loss. We favour the latter since Atox1 deficient flies were reported to develop normally (Hua et al., 2011). Our study could not prove whether UbcD1 post-translationally regulates Atox1 because knockdown of *Atox1* did not show rescue or additive effect to *UbcD1* knockdown defects. Future experiments to determine whether UbcD1 mediates ubiquitination of Atox1 would involve the immunoprecipitation of Atox-1 in wild type and UbcD1-knockdown tissues followed by anti-ubiquitin immunoblotting to determine the level of Atox1 ubiquitination in the presence / absence of UbcD1

7.3 Copper transporters, the UPS and Melanization

Melanin, a cuticle pigment, is generated during melanization which is regulated by many enzymes such as TH (encoded by *ple*), Ddc, laccase 2 (Sekine et al., 2011). Laccase 2, a multicopper oxidase, is thought to be responsible for converting Dopa and Dopamine to Dopa melanin (black pigment) and Dopamine melanin (brown pigment) respectively (Riedel et al., 2011; Wittkopp et al., 2003). We observed that *UbcD1* and *Vhl* result in dark cuticle (also known as hyperpigmentation) when downregulated, suggesting that the production of melanin increases (upregulation of melanization). Due to the fact that UbcD1 and Vhl regulate intracellular copper levels via copper transporter Ctr1A, we propose that they participate in the generation of melanin by influencing laccase 2 activity through available copper levels. To clarify how UbcD1, Vhl and Slmb might interact to control copper levels and melanization, we propose a model (Fig.3).
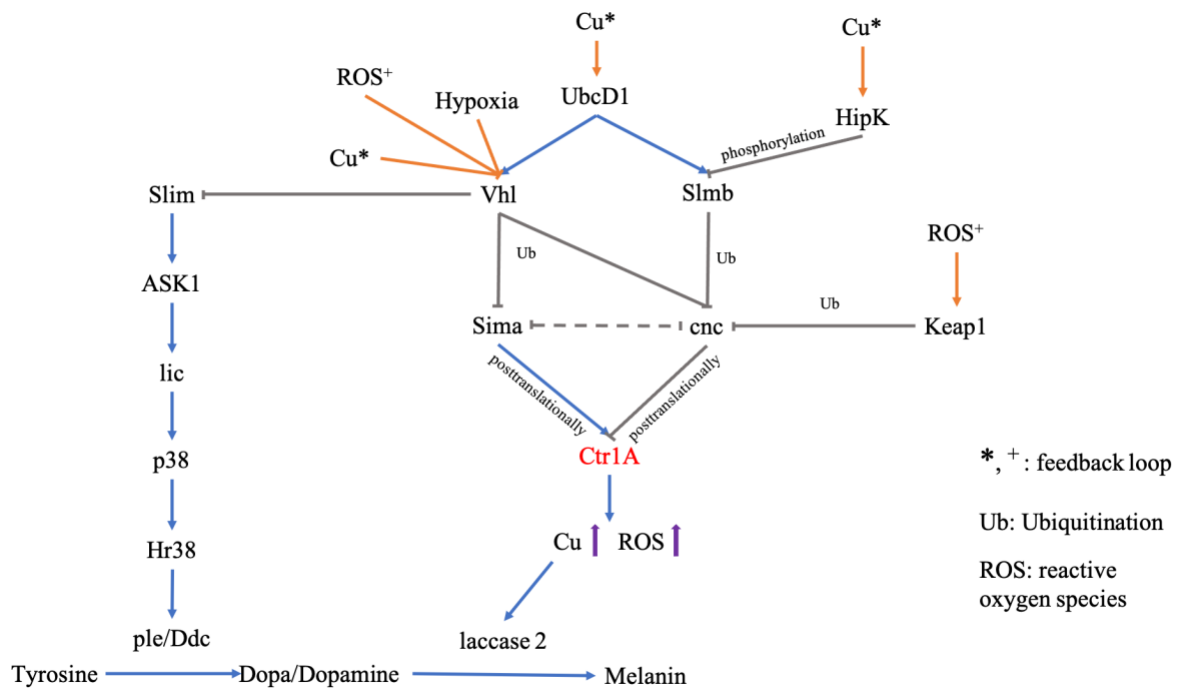
Fig.3 Schematic graph of the proposed UbcD1 / Vhl / Slmb pathway. The E2 ubiquitin conjugating enzyme UbcD1 may participate in the posttranslational regulation of the transcription factors Sima and cnc via the E3 ubiquitin ligases Vhl and Slmb, respectively. Sima and cnc might mutually repress each other. Furthermore, Sima positively stimulates the expression of copper transporter Ctr1A, while Ctr1A is negatively regulated by cnc which also could be ubiquitinated by E3 ubiquitin ligase Keap1. Given that Ctr1A plays a critical role in copper uptake, upregulation of Ctr1A leads to the increase of copper levels and reactive oxygen species which in turn affects the activity of UbcD1, Vhl and Slmb in a feedback loop. Vhl was also found to regulate melanization via the p38 signalling pathway. Additionally, the activity of laccase 2 (responsible for converting Dopa/Dopamine to melanin) is subject to copper levels. Blue line: positive effect; Grey line: negative effect; Dashed line; indirect effect; Orange line: feedback effect.

UbcD1 is one of 40 E2 ubiquitin conjugating enzymes and could interact with many E3 ubiquitin ligases (Pan et al., 2017; Ryoo et al., 2002; Saville et al., 2004; Valimberti et al., 2015). Downregulation of *Vhl* was found to exacerbate the thoracic hyperpigmentation of *UbcD1* knockdown while *Sima* suppression showed a partial rescue effect, suggesting that Vhl and Sima are involved in this increased melanization (Fig.3). In *Drosophila*, UbcD1 was reported to participate in hedgehog signalling pathway via Slmb (Pan et al., 2017). We have demonstrated that Slmb is needed for melanization via regulating cnc (Zhang et al., 2020).

Thus, we predict that UbcD1 might also regulate the Slmb / cnc pathway (Fig.3). UbcD1 also plays a critical role in several other biological processes. For example, it was reported to promote apoptosis via Reaper-mediated degradation of DIAP1 (Ryoo et al., 2002). Interestingly, Kuo *et al* found that UbcD1 might interact with DIAP1 in regulating *Drosophila* sensory neuron dendrite pruning (Kuo et al., 2006). Additionally, UbcD1 participates in the maintenance of germline stem cells via mediating the degradation of Cyclin A in *Drosophila* (Chen et al., 2009). These indicate that UbcD1 plays multiple roles in *Drosophila* development.

Sekine *et al* demonstrated that the p38 MAPK signalling pathway participates in pigmentation via ple/Ddc (Sekine et al., 2011). Our genetic interaction experiments showed that the defects of *UbcD1* knockdown could be partially rescued by downregulation of several components of the p38 MAPK pathway (such as *Slim*, *lic*, *p38*, *Hr38*), suggesting that this pathway might be also involved in *UbcD1* knockdown-induced hyperpigmentation (Fig.3). Furthermore, the p38 MAPK pathway was also reported to stabilize Hif-1α in human brain-derived micro-vessel endothelial cells under normoxia (Kim et al., 2014). In these cells, inhibition of p38 MAPK could attenuate radiation-induced stabilization of Hif-1α through destabilization of Vhl. We therefore postulate that p38 MAPK pathway might also regulate intracellular copper levels via Sima. We are currently testing whether downregulation of components of p38 MAPK has a rescue effect to the defects of *Vhl* knockdown or *Sima* overexpression.

UbcD1 is a cuproprotein and its mammalian orthologue UBE2D2 was demonstrated to lose partial activity when mutated in its copper binding region (Opazo et al., 2021), implying that UbcD1 activity might normally be subject to copper levels. For Vhl and Slmb, a feedback loop might also exist. Real-time PCR results revealed that high copper levels transcriptionally downregulated *Vhl*, suggesting that excess copper generates oxidative stresses which, like hypoxia, inhibits Vhl expression or activity (Fig.3). HipK, a serine / threonine protein kinase, is responsible for stabilizing the WNT signalling protein Armadillo (the *Drosophila* orthologue of β-catenin) by inhibiting Slmb mediated degradation (Swarup and Verheyen, 2011). We hypothesize that copper might regulate Slmb activity by promoting HipK phosphorylation (Fig.3).

7.4 Future directions

Copper homeostasis and the UPS are essential for neurodevelopment, and can lead to neurodegenerative diseases when dysregulated (Luza et al., 2020; Mathys and White, 2017). An increasing body of evidence indicates that the accumulation of Aβ / α-Syn and tau hyperphosphorylation in Alzheimer's disease (AD) and Parkinson's disease (PD) are associated with copper dyshomeostasis and UPS inhibition (Cook and Petrucelli, 2009; Hong et al., 2014; James et al., 2017; Montes et al., 2014), suggesting that copper homeostasis and the UPS work synergistically to maintain nervous system function. Therefore, elucidating the mechanisms by which of these two systems interact could possibly provide novel therapeutic strategies for the treatment of neurodegenerative diseases. In this study, we investigated one E2 and several E3s and 26s proteasomal components and demonstrated that some of them could influence copper homeostasis via regulation of the copper transporters Ctr1A and ATP7. The role of these candidates in neurodevelopment was tested as well. Here, we found that downregulation of *UbcD1* in neurons produced dramatic phenotypic defects such as a headless phenotype and abnormality of brain size and morphology, indicating that UbcD1 plays a critical role in neurodevelopment. It will be very interesting to investigate the mechanism of how UbcD1 functions during neurodevelopment.

Our study showed that knockdown of *UbcD1* resulted in neuronal death, in contrast to previous reports (Goyal et al., 2000; Ryoo et al., 2002). Therefore, it will be critical to fully characterise the mechanism of *UbcD1* knockdown-induced apoptosis. Neuromelanin is generated by some neuronal subsets, such as the dopaminergic neurons of *substantia nigra* and noradrenergic neurons of *locus coeruleus* (Fedorow et al., 2005). In PD, melanized dopaminergic neurons are vulnerable to neurodegeneration (Martin-Bastida et al., 2017). Naoi *et al* reported that neuromelanin selectively induces apoptosis in dopaminergic SH-SY5Y cells (Naoi et al., 2008). Phenotypic inspection revealed that *UbcD1* knockdown upregulates melanization in the thorax. Thus, we predict that *UbcD1* knockdown might induce melanization and then lead to neuronal death. Firstly, we will be investigating whether *UbcD1* knockdown upregulates melanization in fly brains by detecting neuromelanin or the melanization associated genes (such as *ple*, *Ddc*, *lasscase 2*, *p38*, *Hr38*) through performing western blot, real time PCR or immunostaining. In order to confirm that neuronal death caused by UbcD1 knockdown is due to the upregulation of neuromelanin, melanization associated genes will be manipulated in the brain to mimic or rescue *UbcD1* knockdown defects. Since just some certain neurons produce neuromelanin, we will be exploring whether apoptosis induced by knockdown of *UbcD1* restrictively occurs in some particular neuronal subsets by doing double staining immunohistochemistry against

caspase 3 and neuronal markers in *UbcD1* knockdown fly brains or suppressing UbcD1 in certain type of neurons using specific neuronal *GAL4* drivers.

Copper dyshomeostasis is involved in the development of AD and PD. Neuromelanin is thought to be associated to the cell death of dopaminergic neurons in PD (Naoi et al., 2008). Interestingly, the activity of enzymes (such as tyrosinase in mammals, laccase 2 in *Drosophila*) for generating melanin is subject to copper levels (Riedel et al., 2011). Additionally, UbcD1 activity might be affected by copper levels. Hence, it will be necessary to elucidate the interaction between copper and UbcD1 in melanization during neurodevelopment. This will be addressed from two aspects: 1) the impact of UbcD1 mediated melanization on copper levels; 2) the impact of copper levels on UbcD1 mediated melanization. In regard to the first aspect, copper levels will be detected after manipulating the expression of UbcD1 or melanization associated genes by using reporter genes Ctr1B-EYFP and MtnB-EYFP. In order to investigate how copper levels influence UbcD1 mediated melanization, we will be detecting the expression of neuromelanin and melanization associated genes by using western blot, real time PCR or immunohistochemistry after manipulating copper transporter Ctr1A expression in UbcD1 deficient fly brains or culturing *UbcD1* knockdown neurons in high copper or low copper containing medium.

Mutation of some components of the UPS have been reported to cause neurodegenerative diseases, such as Parkin in PD (Lücking et al., 2000). We are curious about whether UbcD1 is involved in the development of AD or PD. Therefore, we will be using established fly models of AD and PD to find out whether UbcD1, neuromelanin or melanization associated genes are affected, by performing western blot, real time PCR or immunohistochemistry in AD or PD fly brains. It is also worth trying to manipulate *UbcD1* or melanization associated genes to rescue AD or PD flies' phenotype.

There are also some interesting questions about Slmb and Vhl we are planning to resolve. In Chapter 3, we proposed that Slmb might also interact with NFkB, ASK1 or Akt in regulating copper homeostasis. Next, we will be testing the interaction of Slmb with NFkB, ASK1 or Akt by doing rescue experiments. Furthermore, western blot or real time PCR will be conducted to investigate whether Slmb regulates the expression of NFkB, ASK1 or Akt. Vhl was demonstrated to regulate Ctr1A via Sima in the thorax and cnc in the abdomen. This raises a question about whether Sima and cnc could co-regulate each other in these two tissues. In order to further investigate the mechanism of Vhl regulating copper homeostasis, it will be essential

to characterize the interaction of Sima and cnc in different tissues. One possible way is to overexpress Sima or cnc in thorax or abdomen respectively to detect the expression of thoracic cnc and abdominal Sima by using genomic reporter genes available for both these transcitpion factors.

7.5 Final conclusion

This study has confirmed that the ubiquitin proteasome system can participate in copper homeostasis via posttranslational regulation of copper transporters. Here, we demonstrated that E3 ubiquitin ligases Slmb and Vhl indirectly control cellular copper levels by inhibiting function of the transcription factors Sima and cnc, which in turn regulate the stability Ctr1A protein. We also showed that the E2 ubiquitin conjugating enzyme UBE2D2 / UbcD1 requires copper binding for its optimal activity and that reduced UbcD1 activity causes a hypermelanization phenotype similar to that induced by loss of Vhl or gain of Sima activity. Combined, these data reveal a complex regulatory network that may allow the ubiquitin proteasome system to sense and respond to multiple inputs including cellular copper levels, oxygen status and ROS levels, in part by altering copper import and efflux. Further elucidation of these interactions might illuminate the causes of several human neurodegenerative diseases and hopefully reveal potential targets for therapeutic intervention.

References:

Aso, T., Yamazaki, K., Aigaki, T., Kitajima, S., 2000. Drosophila von Hippel-Lindau tumor suppressor complex possesses E3 ubiquitin ligase activity. Biochem Biophys Res Commun 276, 355-361.

Batavia, A.A., Schraml, P., Moch, H., 2019. Clear cell renal cell carcinoma with wild-type von Hippel-Lindau gene: a non-existent or new tumour entity? Histopathology 74, 60-67.

Binks, T., Lye, J.C., Camakaris, J., Burke, R., 2010. Tissue-specific interplay between copper uptake and efflux in Drosophila. J Biol Inorg Chem 15, 621-628.

Brady, G.F., Galban, S., Liu, X., Basrur, V., Gitlin, J.D., Elenitoba-Johnson, K.S., Wilson, T.E., Duckett, C.S., 2010. Regulation of the copper chaperone CCS by XIAP-mediated ubiquitination. Molecular and cellular biology 30, 1923-1936.

Burke, R., Commons, E., Camakaris, J., 2008. Expression and localisation of the essential copper transporter DmATP7 in Drosophila neuronal and intestinal tissues. Int J Biochem Cell Biol 40, 1850-1860.

Chen, D., Wang, Q., Huang, H., Xia, L., Jiang, X., Kan, L., Sun, Q., 2009. Effete-mediated degradation of Cyclin A is essential for the maintenance of germline stem cells in Drosophila. Development 136, 4133-4142.

Comstra, H.S., McArthy, J., Rudin-Rush, S., Hartwig, C., Gokhale, A., Zlatic, S.A., Blackburn, J.B., Werner, E., Petris, M., D'Souza, P., Panuwet, P., Barr, D.B., Lupashin, V., Vrailas-Mortimer, A., Faundez, V., 2017. The interactome of the copper transporter ATP7A belongs to a network of neurodevelopmental and neurodegeneration factors. Elife 6.

Cook, C., Petrucelli, L., 2009. A critical evaluation of the ubiquitin-proteasome system in Parkinson's disease. Biochim Biophys Acta 1792, 664-675.

Crouch, P.J., Hung, L.W., Adlard, P.A., Cortes, M., Lal, V., Filiz, G., Perez, K.A., Nurjono, M., Caragounis, A., Du, T., Laughton, K., Volitakis, I., Bush, A.I., Li, Q.X., Masters, C.L., Cappai, R., Cherny, R.A., Donnelly, P.S., White, A.R., Barnham, K.J., 2009. Increasing Cu bioavailability inhibits Abeta oligomers and tau phosphorylation. Proceedings of the National Academy of Sciences of the United States of America 106, 381-386.

Culotta, V.C., Klomp, L.W., Strain, J., Casareno, R.L., Krems, B., Gitlin, J.D., 1997. The copper chaperone for superoxide dismutase. J Biol Chem 272, 23469-23472.

Fedorow, H., Tribl, F., Halliday, G., Gerlach, M., Riederer, P., Double, K.L., 2005. Neuromelanin in human dopamine neurons: comparison with peripheral melanins and relevance to Parkinson's disease. Prog Neurobiol 75, 109-124.

Fitzgerald, J.A., Jameson, H.M., Fowler, V.H., Bond, G.L., Bickley, L.K., Webster, T.M., Bury, N.R., Wilson, R.J., Santos, E.M., 2016. Hypoxia Suppressed Copper Toxicity during Early Development in Zebrafish Embryos in a Process Mediated by the Activation of the HIF Signaling Pathway. Environ Sci Technol 50, 4502-4512.

Gossage, L., Eisen, T., Maher, E.R., 2015. VHL, the story of a tumour suppressor gene. Nat Rev Cancer 15, 55-64.

Goyal, L., McCall, K., Agapite, J., Hartwieg, E., Steller, H., 2000. Induction of apoptosis by Drosophila reaper, hid and grim through inhibition of IAP function. EMBO J 19, 589-597.

Hayes, J.D., Chowdhry, S., Dinkova-Kostova, A.T., Sutherland, C., 2015. Dual regulation of transcription factor Nrf2 by Keap1 and by the combined actions of β-TrCP and GSK-3. Biochem Soc Trans 43, 611-620.

Hong, L., Huang, H.C., Jiang, Z.F., 2014. Relationship between amyloid-beta and the ubiquitin-proteasome system in Alzheimer's disease. Neurol Res 36, 276-282.

Hua, H., Gunther, V., Georgiev, O., Schaffner, W., 2011. Distorted copper homeostasis with decreased sensitivity to cisplatin upon chaperone Atox1 deletion in Drosophila. Biometals 24, 445-453.

Ivan, M., Kondo, K., Yang, H., Kim, W., Valiando, J., Ohh, M., Salic, A., Asara, J.M., Lane, W.S., Kaelin , W.G., 2001. HIFalpha targeted for VHL-mediated destruction by proline hydroxylation: implications for O2 sensing. Science 292, 464-468.

James, S.A., Churches, Q.I., de Jonge, M.D., Birchall, I.E., Streltsov, V., McColl, G., Adlard, P.A., Hare, D.J., 2017. Iron, Copper, and Zinc Concentration in Aβ Plaques in the APP/PS1 Mouse Model of Alzheimer's Disease Correlates with Metal Levels in the Surrounding Neuropil. ACS Chem Neurosci 8, 629-637.

Kenneth, N.S., Hucks, G.E., Jr., Kocab, A.J., McCollom, A.L., Duckett, C.S., 2014. Copper is a potent inhibitor of both the canonical and non-canonical NFkappaB pathways. Cell Cycle 13, 1006-1014.

Kim, B.E., Nevitt, T., Thiele, D.J., 2008. Mechanisms for copper acquisition, distribution and regulation. Nat Chem Biol 4, 176-185.

Kim, Y.H., Yoo, K.C., Cui, Y.H., Uddin, N., Lim, E.J., Kim, M.J., Nam, S.Y., Kim, I.G., Suh, Y., Lee, S.J., 2014. Radiation promotes malignant progression of glioma cells through HIF-1alpha stabilization. Cancer Lett 354, 132-141.

Kuo, C.T., Zhu, S., Younger, S., Jan, L.Y., Jan, Y.N., 2006. Identification of E2/E3 ubiquitinating enzymes and caspase activity regulating Drosophila sensory neuron dendrite pruning. Neuron 51, 283-290.

Lacher, S.E., Lee, J.S., Wang, X., Campbell, M.R., Bell, D.A., Slattery, M., 2015. Beyond antioxidant genes in the ancient Nrf2 regulatory network. Free Radic Biol Med 88, 452-465.

Liu, J., Sitaram, A., Burd, C.G., 2007. Regulation of copper-dependent endocytosis and vacuolar degradation of the yeast copper transporter, Ctr1p, by the Rsp5 ubiquitin ligase. Traffic 8, 1375-1384.

Luza, S., Opazo, C.M., Bousman, C.A., Pantelis, C., Bush, A.I., Everall, I.P., 2020. The ubiquitin proteasome system and schizophrenia. Lancet Psychiatry 7, 528-537.

Lücking, C.B., Dürr, A., Bonifati, V., Vaughan, J., De Michele, G., Gasser, T., Harhangi, B.S., Meco, G., Denèfle, P., Wood, N.W., Agid, Y., Brice, A., Group, F.P.s.D.G.S., Disease, E.C.o.G.S.i.P.s., 2000. Association between early-onset Parkinson's disease and mutations in the parkin gene. N Engl J Med 342, 1560-1567.

Martin-Bastida, A., Pietracupa, S., Piccini, P., 2017. Neuromelanin in parkinsonian disorders: an update. Int J Neurosci 127, 1116-1123.

Mathys, Z.K., White, A.R., 2017. Copper and Alzheimer's Disease. Adv Neurobiol 18, 199-216.

Mi, X., Li, Z., Yan, J., Li, Y., Zheng, J., Zhuang, Z., Yang, W., Gong, L., Shi, J., 2020. Activation of HIF-1 signaling ameliorates liver steatosis in zebrafish atp7b deficiency (Wilson's disease) models. Biochim Biophys Acta Mol Basis Dis 1866, 165842.

Montes, S., Rivera-Mancia, S., Diaz-Ruiz, A., Tristan-Lopez, L., Rios, C., 2014. Copper and copper proteins in Parkinson's disease. Oxid Med Cell Longev 2014, 147251.

Nadella, S.R., Hung, C.C., Wood, C.M., 2011. Mechanistic characterization of gastric copper transport in rainbow trout. J Comp Physiol B 181, 27-41.

Naoi, M., Maruyama, W., Yi, H., Yamaoka, Y., Shamoto-Nagai, M., Akao, Y., Gerlach, M., Tanaka, M., Riederer, P., 2008. Neuromelanin selectively induces apoptosis in dopaminergic SH-SY5Y cells by deglutathionylation in mitochondria: involvement of the protein and melanin component. J Neurochem 105, 2489-2500.

Norgate, M., Lee, E., Southon, A., Farlow, A., Batterham, P., Camakaris, J., Burke, R., 2006. Essential roles in development and pigmentation for the Drosophila copper transporter DmATP7. Mol Biol Cell 17, 475-484.

Nose, Y., Kim, B.E., Thiele, D.J., 2006. Ctr1 drives intestinal copper absorption and is essential for growth, iron metabolism, and neonatal cardiac function. Cell Metab 4, 235-244.

Nose, Y., Wood, L.K., Kim, B.E., Prohaska, J.R., Fry, R.S., Spears, J.W., Thiele, D.J., 2010. Ctr1 is an apical copper transporter in mammalian intestinal epithelial cells in vivo that is controlled at the level of protein stability. J Biol Chem 285, 32385-32392.

Opazo, C.M., Lotan, A., Xiao, Z., Zhang, B., Greenough, M.A., Lim, C.M., Trytell, H., Ramirez, A., Ukuwela, A.A., Mawal, C.H., McKenna, J., Saunders, D.N., Burke, R., Gooley, P.R., Bush, A.I., 2021. Copper singaling promotes proteostasis and animal development via allosteric activation of ubiquitin E2 conjugates. bioExiv, doi.org/10.1101/2021.1102.1115.431211.

Pan, C., Xiong, Y., Lv, X., Xia, Y., Zhang, S., Chen, H., Fan, J., Wu, W., Liu, F., Wu, H., Zhou, Z., Zhang, L., Zhao, Y., 2017. UbcD1 regulates Hedgehog signaling by directly modulating Ci ubiquitination and processing. EMBO Rep 18, 1922-1934.

Petris, M.J., Mercer, J.F., Culvenor, J.G., Lockhart, P., Gleeson, P.A., Camakaris, J., 1996. Ligand-regulated transport of the Menkes copper P-type ATPase efflux pump from the Golgi apparatus to the plasma membrane: a novel mechanism of regulated trafficking. Embo J 15, 6084-6095.

Petris, M.J., Strausak, D., Mercer, J.F., 2000. The Menkes copper transporter is required for the activation of tyrosinase. Hum Mol Genet 9, 2845-2851.

Prohaska, J.R., Broderius, M., Brokate, B., 2003. Metallochaperone for Cu,Zn-superoxide dismutase (CCS) protein but not mRNA is higher in organs from copper-deficient mice and rats. Arch Biochem Biophys 417, 227-234.

Rae, T.D., Schmidt, P.J., Pufahl, R.A., Culotta, V.C., O'Halloran, T.V., 1999. Undetectable intracellular free copper: the requirement of a copper chaperone for superoxide dismutase. Science 284, 805-808.

Riedel, F., Vorkel, D., Eaton, S., 2011. Megalin-dependent yellow endocytosis restricts melanization in the Drosophila cuticle. Development 138, 149-158.

Ryoo, H.D., Bergmann, A., Gonen, H., Ciechanover, A., Steller, H., 2002. Regulation of Drosophila IAP1 degradation and apoptosis by reaper and ubcD1. Nature cell biology 4, 432-438.

Saville, M.K., Sparks, A., Xirodimas, D.P., Wardrop, J., Stevenson, L.F., Bourdon, J.C., Woods, Y.L., Lane, D.P., 2004. Regulation of p53 by the ubiquitin-conjugating enzymes UbcH5B/C in vivo. J Biol Chem 279, 42169-42181.

Scheiber, I., Dringen, R., Mercer, J.F., 2013. Copper: effects of deficiency and overload. Met Ions Life Sci 13, 359-387.

Sekine, Y., Takagahara, S., Hatanaka, R., Watanabe, T., Oguchi, H., Noguchi, T., Naguro, I., Kobayashi, K., Tsunoda, M., Funatsu, T., Nomura, H., Toyoda, T., Matsuki, N., Kuranaga, E., Miura, M., Takeda, K., Ichijo, H., 2011. p38 MAPKs regulate the expression of genes in the dopamine synthesis pathway through phosphorylation of NR4A nuclear receptors. J Cell Sci 124, 3006-3016.

Shmueli, M.D., Schnaider, L., Herzog, G., Gazit, E., Segal, D., 2014. Computational and experimental characterization of dVHL establish a Drosophila model of VHL syndrome. PLoS One 9, e109864.

Southon, A., Burke, R., Camakaris, J., 2013. What can flies tell us about copper homeostasis? Metallomics 5, 1346-1356.

Swarup, S., Verheyen, E.M., 2011. Drosophila homeodomain-interacting protein kinase inhibits the Skp1-Cul1-F-box E3 ligase complex to dually promote Wingless and Hedgehog signaling. Proceedings of the National Academy of Sciences of the United States of America 108, 9887-9892.

Sykiotis, G.P., Bohmann, D., 2008. Keap1/Nrf2 signaling regulates oxidative stress tolerance and lifespan in Drosophila. Dev Cell 14, 76-85.

Turski, M.L., Brady, D.C., Kim, H.J., Kim, B.E., Nose, Y., Counter, C.M., Winge, D.R., Thiele, D.J., 2012. A novel role for copper in Ras/mitogen-activated protein kinase signaling. Mol Cell Biol 32, 1284-1295.

Valimberti, I., Tiberti, M., Lambrughi, M., Sarcevic, B., Papaleo, E., 2015. E2 superfamily of ubiquitin-conjugating enzymes: constitutively active or activated through phosphorylation in the catalytic cleft. Sci Rep 5, 14849.

Wang, S., Wu, L., Wang, Y., Luo, X., Lu, Y., 2009. Copper-induced germline apoptosis in Caenorhabditis elegans: the independent roles of DNA damage response signaling and the dependent roles of MAPK cascades. Chem Biol Interact 180, 151-157.

White, C., Kambe, T., Fulcher, Y.G., Sachdev, S.W., Bush, A.I., Fritsche, K., Lee, J., Quinn, T.P., Petris, M.J., 2009. Copper transport into the secretory pathway is regulated by oxygen in macrophages. J Cell Sci 122, 1315-1321.

Wittkopp, P.J., Carroll, S.B., Kopp, A., 2003. Evolution in black and white: genetic control of pigment patterns in Drosophila. Trends Genet 19, 495-504.

Xia, Y., Liu, L., Bai, Q., Long, Q., Wang, J., Xi, W., Xu, J., Guo, J., 2017. Prognostic value of copper transporter 1 expression in patients with clear cell renal cell carcinoma. Oncol Lett 14, 5791-5800.

Xie, L., Collins, J.F., 2011. Transcriptional regulation of the Menkes copper ATPase (Atp7a) gene by hypoxia-inducible factor (HIF2{alpha}) in intestinal epithelial cells. Am J Physiol Cell Physiol 300, C1298-1305.

Xie, L., Collins, J.F., 2013. Transcription factors Sp1 and Hif2α mediate induction of the copper-transporting ATPase (Atp7a) gene in intestinal epithelial cells during hypoxia. J Biol Chem 288, 23943-23952.

Yeh, T.C., Bratton, S.B., 2013. Caspase-dependent regulation of the ubiquitin-proteasome system through direct substrate targeting. Proceedings of the National Academy of Sciences of the United States of America 110, 14284-14289.

Zhang, B., Binks, T., Burke, R., 2020. The E3 ubiquitin ligase Slimb/β-TrCP is required for normal copper homeostasis in Drosophila. Biochim Biophys Acta Mol Cell Res 1867, 118768.